

**POLITECNICO DI TORINO**

Collegio di Ingegneria Energetica

**Corso di Laurea Magistrale  
in  
in Ingegneria Energetica e Nucleare**

Tesi di Laurea Magistrale

**Influence of feed concentration and  
residence time on the efficiency and gas  
yield of Supercritical Water Gasification of  
Glycerol**



**Relatori**

prof. Massimo Santarelli

prof. Tapio Wasterlund

**Candidato**

Fabrizio Marinelli

Luglio 2018



## ABSTRACT

The experiments discussed in this thesis have been performed in the Department of Chemical Engineering, Process & Systems Engineering Laboratory, at Åbo Akademi University in Turku.

Supercritical Water Gasification of glycerol has been carried out on a laboratory scale at 600 °C and 250 bar, by setting three levels of feed concentration (2.5, 5 and 10%) and three levels of volume flow rate of nitrogen (125, 250 and 375 ml/min). The latter, which is inversely proportional to the residence time, is used to push the biomass solution into the reactor. The choice of these parameters was a consequence of the previous experiments made in the same laboratory and of a careful bibliographic survey. The experiments, indeed, were performed in order to study the influence of feed concentration and residence time on the efficiency and gas yield of SCWG of glycerol, as the effect of temperature and pressure has already been widely investigated.

Besides, the aim of this thesis is also to evaluate the effect of heterogeneous catalysis on the gasification process, by using two different types of reactors: SS 316 (without catalytic properties), and the catalytic INCONEL 625.

The outputs of the process investigated in this thesis are the volume concentration of hydrogen, carbon dioxide, methane, carbon monoxide, ethane and ethylene of the syngas produced; the gasification and cold gas efficiencies and the gas yields.

Eventually, a simplified design of experiments of the volume concentration of the hydrogen has been performed in order to have a qualitative overview of the effects of the input parameters.



## *ACKNOWLEDGEMENTS*

I would first like to express my sincere gratitude to Professors Massimo Santarelli, Tapio Wasterlund and Cataldo De Blasio, whom gave me the wonderful opportunity to work at the Department of Process Design and System Engineering at Åbo Akademi University, a stimulating and rich in competent, kind and friendly people environment. Special thanks go to my instructor Professor Cataldo De Blasio, a friend and a mentor who supported and helped me for the entire period of my thesis.

In addition, I want to thank all the people working at the Department, for their friendliness and availability in helping me with both the academic and bureaucratic issues. In this regard, a special mention goes to Annika Fougsted, the most thoughtful, generous and capable secretary I became acquainted with.

Heartfelt thanks go to my friends in Turin and my best friends in Palermo, whom have supported me during my studies and outside of university.

Finally yet importantly, my warmest and most grateful thanks go to my family, whom has been supporting and motivating me for my entire life and whose help has been fundamental in order to accomplish my goals.



# Contents

<b>Abstract</b>	<b>iii</b>
<b>Acknowledgements</b>	<b>v</b>
<b>Contents</b>	<b>vii</b>
<b>List of Figures</b>	<b>xi</b>
<b>List of Tables</b>	<b>xv</b>
<b>List of Abbreviations</b>	<b>xvii</b>
<b>1 Introduction</b>	<b>1</b>
1.1 World energy overview and European strategy .....	1
1.2 Biomass .....	4
1.2.1 Biomass as a renewable source .....	4
1.2.2 Components of biomass .....	5
1.2.3 Role of biomass in the European strategies .....	7
1.3 Conversion processes of biomass .....	8
1.4 Hydrothermal processes .....	9
1.4.1 Hydrothermal liquefaction .....	10
1.4.2 Hydrothermal gasification .....	10
<b>2 Supercritical water</b>	<b>14</b>
2.1 Supercritical state .....	14
2.2 Supercritical water .....	15
2.2.1 Properties of supercritical water .....	17
2.3 Role of water in supercritical water gasification .....	23
2.3.1 Water as a reactant/product .....	24
2.3.2 Water as a catalyst .....	24
2.3.3 Water as a solvent .....	25
<b>3 Supercritical water gasification</b>	<b>26</b>
3.1 Model compounds .....	26

3.2	Reaction pathways . . . . .	27
3.2.1	Cellulose reaction pathways . . . . .	27
3.2.2	Hemicellulose reaction pathways . . . . .	30
3.2.3	Lignin reaction pathways . . . . .	31
3.2.4	Protein reaction pathways . . . . .	31
3.2.5	Organic acid and other intermediate compounds reaction pathways . . . . .	32
3.2.6	Gas-phase reactions . . . . .	33
3.2.7	Reaction pathways of SCWG of glycerol . . . . .	33
3.3	Influence of biomass composition . . . . .	34
3.3.1	Cellulose and hemicellulose influence . . . . .	34
3.3.2	Lignin influence . . . . .	34
3.3.3	Proteins influence . . . . .	35
3.3.4	Lipids influence . . . . .	36
3.3.5	Salts influence . . . . .	36
3.4	Catalysis . . . . .	36
3.5	Influence of operation conditions . . . . .	37
3.6	Influence of the type of reactor . . . . .	38
3.7	Challenges . . . . .	40
<b>4</b>	<b>Experimental setup</b>	<b>41</b>
4.1	SCWG plant and equipment . . . . .	41
4.1.1	Comparison with the previous configuration . . . . .	42
4.2	Nitrogen tank . . . . .	43
4.3	Mass flow controller . . . . .	44
4.4	Pipes and valves . . . . .	45
4.5	Pump . . . . .	47
4.6	Feed cylinders . . . . .	48
4.7	Reactors . . . . .	50
4.8	Heating system . . . . .	52
4.9	Cooling system . . . . .	53
4.10	Pressure and temperature sensors . . . . .	54
4.11	Collection of effluents and sampling . . . . .	55
4.12	Energy measurement . . . . .	56

4.13	Monitoring system and data acquisition . . . . .	56
<b>5</b>	<b>Analytical equipment</b>	<b>59</b>
5.1	Gas chromatography . . . . .	59
5.1.1	Data elaboration . . . . .	61
5.1.2	Calibration . . . . .	63
5.2	Elemental analysis . . . . .	67
5.3	Bomb calorimeter . . . . .	68
<b>6</b>	<b>Glycerol</b>	<b>71</b>
6.1	Chemical and physical properties of glycerol . . . . .	71
6.2	Production . . . . .	74
6.2.1	Transesterification . . . . .	74
6.2.2	Saponification . . . . .	76
6.2.3	Hydrolysis . . . . .	77
6.2.4	High-pressure splitting . . . . .	78
6.2.5	Glycerol via propylene . . . . .	79
6.3	Purification of crude glycerol . . . . .	80
6.4	Industrial applications . . . . .	80
6.5	Transformation to value-added products . . . . .	81
<b>7</b>	<b>Data elaboration and results</b>	<b>88</b>
7.1	Experimental procedure . . . . .	88
7.2	Data elaboration . . . . .	90
7.2.1	Mass balance . . . . .	92
7.2.2	Gas yield . . . . .	93
7.2.3	Efficiency of conversion . . . . .	94
7.2.4	Lower and Higher Heating Values . . . . .	95
7.2.5	Cold gas efficiency . . . . .	96
7.3	Results . . . . .	97
7.3.1	Stainless steel 316 at 2,5 %wt and 375 ml/min . . . . .	97
7.3.2	Stainless steel 316 at 2,5 %wt and 250 ml/min . . . . .	100
7.3.3	Stainless steel 316 at 2,5 %wt and 125 ml/min . . . . .	101

7.3.4	Stainless steel 316 at 5 %wt and 375 ml/min	102
7.3.5	Stainless steel 316 at 5 %wt and 250 ml/min	104
7.3.6	Stainless steel 316 at 5 %wt and 125 ml/min	105
7.3.7	Stainless steel 316 at 10 %wt and 375 ml/min	106
7.3.8	Stainless steel 316 at 10 %wt and 250 ml/min	108
7.3.9	Stainless steel 316 at 10 %wt and 125 ml/min	109
7.3.10	INCONEL 625 at 2,5 %wt and 375 ml/min	110
7.3.11	INCONEL 625 at 2,5 %wt and 250 ml/min	112
7.3.12	INCONEL 625 at 2,5 %wt and 125 ml/min	113
7.3.13	INCONEL 625 at 5 %wt and 375 ml/min	114
7.3.14	INCONEL 625 at 5 %wt and 250 ml/min	116
7.3.15	INCONEL 625 at 5 %wt and 125 ml/min	117
7.3.16	INCONEL 625 at 10 %wt and 375 ml/min	118
7.3.17	INCONEL 625 at 10 %wt and 250 ml/min	120
7.3.18	INCONEL 625 at 10 %wt and 125 ml/min	121
7.4	Effect of concentration	122
7.5	Effect of residence time	126
7.6	Effect of catalyst	130
<b>8</b>	<b>Design of Experiment</b>	<b>131</b>
8.1	Effects for the SS316 reactor	131
8.2	Effects for the INCONEL 625 reactor	134
<b>9</b>	<b>Conclusions</b>	<b>137</b>
9.1	Future analysis	138
	<b>Bibliography</b>	<b>139</b>

# List of Figures

1.1	World energy consumption in million tonnes oil equivalent from 1991 to 2016 . . . .	2
1.2	Percentage of regional consumption in 2016 . . . . .	2
1.3	Structure of cellulose . . . . .	5
1.4	Structure of xylene . . . . .	6
1.5	Basic monomers of lignin . . . . .	6
1.6	Primary energy production from renewable sources . . . . .	7
1.7	Gas yield of hydrothermal gasification of biomass as a function of temperature . . .	12
1.8	Gas yield of hydrothermal gasification of biomass as a function of concentration . .	12
2.1	State diagram of water as a function of temperature and pressure . . . . .	15
2.2	Diagram of water as function of pressure and temperature . . . . .	16
2.3	Thermophysical properties of water as function of temperature at four different pressures . . . . .	18
2.4	Ionic product in logarithmic scale as a function of temperature . . . . .	21
3.1	Pyrolysis and hydrolysis of cellobiose in sub- and near-critical conditions . . . . .	28
3.2	Pyrolysis and hydrolysis of cellobiose in sub- and near-critical conditions . . . . .	28
3.3	Glyceraldehyde and dihydroxyacetone degradation in subcritical and supercritical water conditions . . . . .	29
3.4	Fructose and glucose pathways . . . . .	29
3.5	Reaction pathways of D-xylose in supercritical conditions . . . . .	30
3.6	Reaction pathways of guaiacol in supercritical conditions . . . . .	31
3.7	Reaction pathways of aspartic acid in supercritical conditions . . . . .	32
3.8	Reaction pathways of organic acids and other organic compounds in sub- and supercritical conditions . . . . .	32
3.9	Simplified reaction pathways of SCWG of glycerol . . . . .	33
4.1	SCWG plant in laboratory scale . . . . .	41
4.2	SCWG plant layout . . . . .	42
4.3	SCWG plant layout (previous setup) . . . . .	43
4.4	Nitrogen tank . . . . .	44
4.5	Mass flow controller . . . . .	44
4.6	Thermal sensor . . . . .	45
4.7	Ball valves disposition . . . . .	46
4.8	View section of the valve . . . . .	46
4.9	Backpressure valve . . . . .	47
4.10	Pump . . . . .	47
4.11	Characteristic curve of the pump . . . . .	48
4.12	Feed cylinders . . . . .	49
4.13	Stainless steel reactor (on top) and Inconel 625 reactor (on bottom) . . . . .	50
4.14	Section of the reactor . . . . .	51
4.15	Heating system . . . . .	53
4.16	Cooling system . . . . .	54
4.17	Pressure sensor . . . . .	54
4.18	Collection system . . . . .	55
4.19	Electricity meter . . . . .	56

4.20 Graphical interface for the temperature and pressure monitoring . . . . .	57
4.21 Graphical interfaces for the regulation and control of the volume flow rate . . . . .	57
5.1 Claurus 500 GC gas chromatograph . . . . .	59
5.2 Scheme of a typical gas chromatograph . . . . .	60
5.3 Example of chromatogram provided by the Claurus 500 GC . . . . .	62
5.4 Report with numerical values of time and area provided by the dedicated software	62
5.5 Chromatogram of bottle 1 . . . . .	64
5.6 Chromatogram of bottle 2 . . . . .	64
5.7 Chromatogram of bottle 3 . . . . .	64
5.8 Chromatogram of bottle 4 . . . . .	65
5.9 Chromatogram of bottle 5 . . . . .	65
5.10 Chromatogram of bottle 6 . . . . .	66
5.11 Flash EA1100 . . . . .	68
5.12 1341 Oxygen Bomb Calorimeter with the electronic control unit and the ignition unit	69
. . . . .	70
5.13 Section of bomb calorimeter (left) and main components of bomb calorimeter (right)	70
. . . . .	72
6.1 Glycerol solution used in this thesis . . . . .	72
6.2 Molecular structure of glycerol . . . . .	72
6.3 Transesterification reaction . . . . .	74
6.4 Flow diagram of a homogeneous biodiesel production. . . . .	75
6.5 Flow diagram of a heterogeneous process for biodiesel production. . . . .	76
6.6 Saponification reaction. . . . .	76
6.7 Flow diagram of saponification process. . . . .	77
6.8 Hydrolysis reaction. . . . .	78
6.9 Flow diagram of a splitting column . . . . .	78
6.10 Propylene chlorination. . . . .	79
6.11 Glycerol production via propylene . . . . .	79
6.12 Possible derivatives of glycerol. . . . .	81
6.13 Production of hydrogen via steam reforming of glycerol. . . . .	82
6.14 Production of acrolein via dehydration of glycerol. . . . .	82
6.15 Production of propylene glycol via hydrogenolysis of glycerol. . . . .	83
6.16 Oxidation of glycerol. . . . .	84
6.17 Etherification of glycerol. . . . .	84
6.18 Etherification of glycerol to glycerol esters. . . . .	85
6.19 Conversion of glycerol into ECH. . . . .	85
6.20 Conversion of glycerol and furfural into dioxolane and dioxane. . . . .	86
6.21 Transesterification of glycerol with dimethyl carbonate. . . . .	86
7.1 Pressure trend as a function of temperature during the experiment. . . . .	89
7.2 Volumetric concentration of syngas for each bag for SS316, 2,5 %wt and 375 ml/min	99
. . . . .	99
7.3 Volumetric concentration of syngas for each bag for SS316, 2,5 %wt and 250 ml/min	100
. . . . .	100
7.4 Volumetric concentration of syngas for each bag for SS316, 2,5 %wt and 125 ml/min	101
. . . . .	101
7.5 Volumetric concentration of syngas for each bag for SS316, 5 %wt and 250 ml/min	103
. . . . .	103

7.6 Volumetric concentration of syngas for each bag for SS316, 5 %wt and 250 ml/min	104
7.7 Volumetric concentration of syngas for each bag for SS316, 5 %wt and 125 ml/min	105
7.8 Volumetric concentration of syngas for each bag for SS316, 10 %wt and 375 ml/min	107
7.9 Volumetric concentration of syngas for each bag for SS316 at 10 %wt and 250 ml/min	108
7.10 Volumetric concentration of syngas for each bag for SS316 at 10 %wt and 125 ml/min.	108
7.11 Volumetric concentration of syngas for each bag for INCONEL 625 at 2.5 %wt and 375 ml/min.	111
7.12 Volumetric concentration of syngas for each bag for INCONEL 625 at 2.5 %wt and 250 ml/min.	112
7.13 Volumetric concentration of syngas for each bag for INCONEL 625 at 2.5 %wt and 125 ml/min.	113
7.14 Volumetric concentration of syngas for each bag for INCONEL 625 at 5 %wt and 375 ml/min.	115
7.15 Volumetric concentration of syngas for each bag for INCONEL 625 at 5 %wt and 250 ml/min.	116
7.16 Volumetric concentration of syngas for each bag for INCONEL 625 at 5 %wt and 125 ml/min.	117
7.17 Volumetric concentration of syngas for each bag for INCONEL 625 at 10 %wt and 375 ml/min.	119
7.18 Volumetric concentration of syngas for each bag for INCONEL 625 at 10 %wt and 250 ml/min.	120
7.19 Volumetric concentration of syngas for each bag for INCONEL 625 at 10 %wt and 125 ml/min.	121
7.20 Composition of syngas as a function of concentrations and at fixed volume flow rate for SS316 and INCONEL 625.	123
7.21 Gas yield as a function of concentrations and at fixed volume flow rate for SS316 and INCONEL 625.	124
7.22 Gasification efficiencies as a function of concentrations and at fixed volume flow rate for SS316 and INCONEL 625.	125
7.23 Composition of syngas as a function of volume flow rates at fixed concentration for SS316 and INCONEL 625.	127
7.24 Gas yield of syngas as a function of volume flow rates at fixed concentration for SS316 and INCONEL 625.	128
7.25 Gasification efficiencies as a function of volume flow rates at fixed concentration for SS316 and INCONEL 625.	129
7.26 Cold Gas Efficiency for SS316 and INCONEL 625.	129
7.27 LHV for SS316 and INCONEL 625.	129
8.1 Effect of residence time (left) and feed concentration (right) on $H_2$ volume concentration.	132
8.2 Residence time-feed concentration interaction (left) and feed concentration-residence time interaction (right) for SS316.	133
8.3 Pareto chart of effects for SS316.	134

8.4 Effect of residence time (left) and feed concentration (right) on $H_2$ volume concentration. . . . .	135
8.5 Residence time-feed concentration interaction (left) and feed concentration-residence time interaction (right) for INCONEL. . . . .	136
8.6 Pareto chart of effects for INCONEL. . . . .	136

# List of Tables

2.1 Peak values of specific heat at different pseudocritical temperatures and pressure. .	19
2.2 Specific heat at critical temperatures, pseudocritical and super critical temperatures and at critical and supercritical pressures . . . . .	19
4.1 Components and materials of the reactors. . . . .	51
4.2 Features, advantages, disadvantages and elemental composition of stainless steel 316 and Inconel 625 . . . . .	51
5.1 Gas samples with known concentration for the calibration. . . . .	63
5.2 Areas and proportionality constant for bottle 1. . . . .	66
5.3 Areas and proportionality constant for bottle 2. . . . .	66
5.4 Areas and proportionality constant for bottle 3. . . . .	66
5.5 Areas and proportionality constant for bottle 4. . . . .	66
5.6 Areas and proportionality constant for bottle 5. . . . .	67
5.7 Areas and proportionality constant for bottle 6. . . . .	67
5.8 Constant of proportionality for every compound. . . . .	67
6.1 Solubility of glycerol in various organic solvents. . . . .	73
6.2 Physicochemical properties and toxicity data of glycerol. . . . .	73
7.1 Lower heating values of compounds. . . . .	96
7.2 Main input parameters for SS316, 2,5 %wt and 375 ml/min. . . . .	97
7.3 Densities and specific volumes at 25°C and 250 bar. . . . .	98
7.4 Composition and gas yield for SS316, 2,5 %wt and 375 ml/min. . . . .	99
7.5 Efficiencies and LHV for SS316, 2,5 %wt and 375 ml/min. . . . .	99
7.6 Main input parameters for SS316, 2,5 %wt and 250 ml/min. . . . .	100
7.7 Composition and gas yield for SS316, 2,5 %wt and 250 ml/min. . . . .	100
7.8 Efficiencies and LHV for SS316, 2,5 %wt and 250 ml/min. . . . .	101
7.9 Main input parameters for SS316, 2,5 %wt and 125 ml/min. . . . .	101
7.10 Composition and gas yield for SS316, 2,5 %wt and 125 ml/min. . . . .	102
7.11 Efficiencies and LHV for SS316, 2,5 %wt and 250 ml/min. . . . .	102
7.12 Main input parameters for SS316, at 5 %wt and 375 ml/min. . . . .	102
7.13 Composition and gas yield for SS316 at 5 %wt and 375 ml/min. . . . .	103
7.14 Efficiencies and LHV for SS316 at 5 %wt and 375 ml/min. . . . .	103
7.15 Main input parameters for SS316, at 5 %wt and 250 ml/min. . . . .	104
7.16 Composition and gas yield for SS316 at 5 %wt and 250 ml/min. . . . .	104
7.17 Efficiencies and LHV for SS316 at 5 %wt and 250 ml/min. . . . .	105
7.18 Main input parameters for SS316, at 5 %wt and 125 ml/min. . . . .	105
7.19 Composition and gas yield for SS316 at 5 %wt and 125 ml/min. . . . .	106
7.20 Efficiencies and LHV for SS316 at 5 %wt and 125 ml/min. . . . .	106
7.21 Main input parameters for SS316, at 10 %wt and 375 ml/min. . . . .	106
7.22 Composition and gas yield for SS316 at 10 %wt and 375 ml/min. . . . .	107
7.23 Efficiencies and LHV for SS316 at 10 %wt and 375 ml/min. . . . .	107
7.24 Main input parameters for SS316, at 10 %wt and 250 ml/min. . . . .	108
7.25 Composition and gas yield for SS316 at 10 %wt and 250 ml/min. . . . .	108
7.26 Efficiencies and LHV for SS316 at 10 %wt and 250 ml/min. . . . .	109
7.27 Main input parameters for SS316, at 10 %wt and 125 ml/min. . . . .	109

7.28	Composition and gas yield for SS316 at 10 %wt and 125 ml/min. . . . .	110
7.29	Efficiencies and LHV for SS316 at 10 %wt and 125 ml/min. . . . .	110
7.30	Main input parameters for INCONEL 625, at 2.5 %wt and 375 ml/min. . . . .	110
7.31	Composition and gas yield for INCONEL 625 at 2.5 %wt and 375 ml/min. . . . .	111
7.32	Efficiencies and LHV for INCONEL 625 at 2.5 %wt and 375 ml/min. . . . .	111
7.33	Main input parameters for INCONEL 625, at 2.5 %wt and 250 ml/min. . . . .	112
7.34	Composition and gas yield for INCONEL 625 at 2.5 %wt and 250 ml/min. . . . .	112
7.35	Efficiencies and LHV for INCONEL 625 at 2.5 %wt and 250 ml/min. . . . .	113
7.36	Main input parameters for INCONEL 625, at 2.5 %wt and 125 ml/min. . . . .	113
7.37	Composition and gas yield for INCONEL 625 at 2.5 %wt and 125 ml/min. . . . .	114
7.38	Efficiencies and LHV for INCONEL 625 at 2.5 %wt and 125 ml/min. . . . .	114
7.39	Main input parameters for INCONEL 625, at 5 %wt and 375 ml/min. . . . .	114
7.40	Composition and gas yield for INCONEL 625 at 5 %wt and 375 ml/min. . . . .	115
7.41	Efficiencies and LHV for INCONEL 625 at 5 %wt and 375 ml/min. . . . .	115
7.42	Main input parameters for INCONEL 625, at 5 %wt and 250 ml/min. . . . .	116
7.43	Composition and gas yield for INCONEL 625 at 5 %wt and 250 ml/min. . . . .	116
7.44	Efficiencies and LHV for INCONEL 625 at 5 %wt and 250 ml/min. . . . .	117
7.45	Main input parameters for INCONEL 625, at 5 %wt and 125 ml/min. . . . .	117
7.46	Composition and gas yield for INCONEL 625 at 5 %wt and 125 ml/min. . . . .	118
7.47	Efficiencies and LHV for INCONEL 625 at 5 %wt and 125 ml/min. . . . .	118
7.48	Main input parameters for INCONEL 625, at 10 %wt and 375 ml/min. . . . .	118
7.49	Composition and gas yield for INCONEL 625 at 10 %wt and 375 ml/min. . . . .	119
7.50	Efficiencies and LHV for INCONEL 625 at 10 %wt and 375 ml/min. . . . .	119
7.51	Main input parameters for INCONEL 625, at 10 %wt and 250 ml/min. . . . .	120
7.52	Composition and gas yield for INCONEL 625 at 10 %wt and 250 ml/min. . . . .	120
7.53	Composition and gas yield for INCONEL 625 at 10 %wt and 250 ml/min. . . . .	121
7.54	Main input parameters for INCONEL 625, at 10 %wt and 125 ml/min. . . . .	121
7.55	Composition and gas yield for INCONEL 625 at 10 %wt and 125 ml/min. . . . .	122
7.56	Composition and gas yield for INCONEL 625 at 10 %wt and 125 ml/min. . . . .	122
8.1	Data for SS316 . . . . .	131
8.2	Data for INCONEL 625. . . . .	134

# List of Abbreviations

<b>HTL</b>	Hydrothermal Liquefaction
<b>SCWG</b>	Supercritical Water Gasification
<b>WGS</b>	Water-gas Shift
<b>GHG</b>	Greenhouses Gases
<b>GC</b>	Gas Chromatograph
<b>CSTR</b>	Continuous-flow Stirred-Tank Reactor
<b>HDPE</b>	High-Density Polyethylene
<b>MFC</b>	Mass Flow Controller
<b>GSC</b>	Gas-Solid Chromatography
<b>GLC</b>	Gas-Liquid Chromatography
<b>FID</b>	Flame Ionization Detector
<b>ECD</b>	Electron-Capture Detector
<b>TCD</b>	Thermal Conductivity Detector
<b>PID</b>	Photoionization Detector
<b>VOC</b>	Volatile Organic Compound
<b>DHA</b>	Dihydroxyacetone
<b>GA</b>	Glyceric Acid
<b>MA</b>	Mesoxalic Acid
<b>TA</b>	Tartronic Acid
<b>GTBE</b>	Glycerol Tertiary Butyl Ether
<b>MTBE</b>	Methyl Tertiary Butyl Ether
<b>ECH</b>	Epichlorohydrin
<b>BPV</b>	Ball Pressure Valve
<b>HHV</b>	Higher Heating Value
<b>LHV</b>	Lower Heating Value
<b>DoE</b>	Design of Experiments

# 1. Introduction

The aim of this thesis is to assess the influence of the feed concentration and the residence time on the efficiencies and gas yields of a supercritical water gasification (SCWG) of a glycerol solution.

In this chapter, an overview regarding the political European strategy, in the field of renewable sources, will be provided. Moreover, the composition and the role of biomass as a renewable source will be discussed. Finally, the conversion procedures along with the state of the art of technologies being involved will be examined, focusing the attention on hydrothermal treatments to which supercritical water gasification belongs.

In the second chapter all the properties of supercritical water will be examined, focusing the attention in those important for supercritical water gasification.

In the third chapter SCWG will be fully examined, describing in detail the mechanisms of the process, the principle reactions, the state of the art technology along with the possible configurations and how it is affected by the operating parameters and eventual catalysts. The concept of model compound will be introduced, focusing the attention on glycerol, used as a simpler model compound of cellulose than glucose. Eventually, challenges and solutions for an industrial scale-up will be investigated.

In the fourth and fifth chapters, all the equipment and the analytical instruments present in the laboratory are examined, describing the structure and the functions of every component.

The sixth chapter is devoted to an examination of the feedstock used in this thesis, along with the production, industrial application, purification and transformation processes to value-added products.

The seventh chapter shows all the methods for data elaboration and the results obtained by the experiments. All the numerical and graphical results of the whole set of experiments are provided, making a comparison between them and between the results presented in the literature.

Finally, the last chapter is about a merely qualitative Design of Experiments with two levels and two quantitative and continuous factors (feed concentration and residence time), in order to analyse how both variables affect the volume concentration of  $H_2$  (response variable), so as to try to predict the outcome of SCWG of glycerol in terms of  $H_2$  production.

## *1.1. World energy overview and European strategy*

The industrial revolution of the 18<sup>th</sup> century led human beings to a widespread use of fossil fuels.

Since the second half of the 20<sup>th</sup> century, the world started a more and more increasing exploitation of huge quantities of fossil fuels, thus, reducing tremendously the global energy resources.

Furthermore, fossil sources are located in various regions of the world, having different and unstable government policies, which in turn results in making its price and supply unstable and unsettled.

Lastly, the combustion of fossil fuels produces several pollutants, including CO<sub>2</sub> which is regarded as being the main pollutant responsible for the global warming of our planet.

The unbridled consumption of coal, natural gas and oil, with the uncertainty of their price, along with the growing global warming, show the strict necessity to turn to the use of renewable and clean energy sources. The latter are identified, by definition, as any natural resource that can be renewed in the same or less amount of time that it takes to draw the supply down.

The graph 1.1 shows the trend of world energy consumption over the last 25 years.

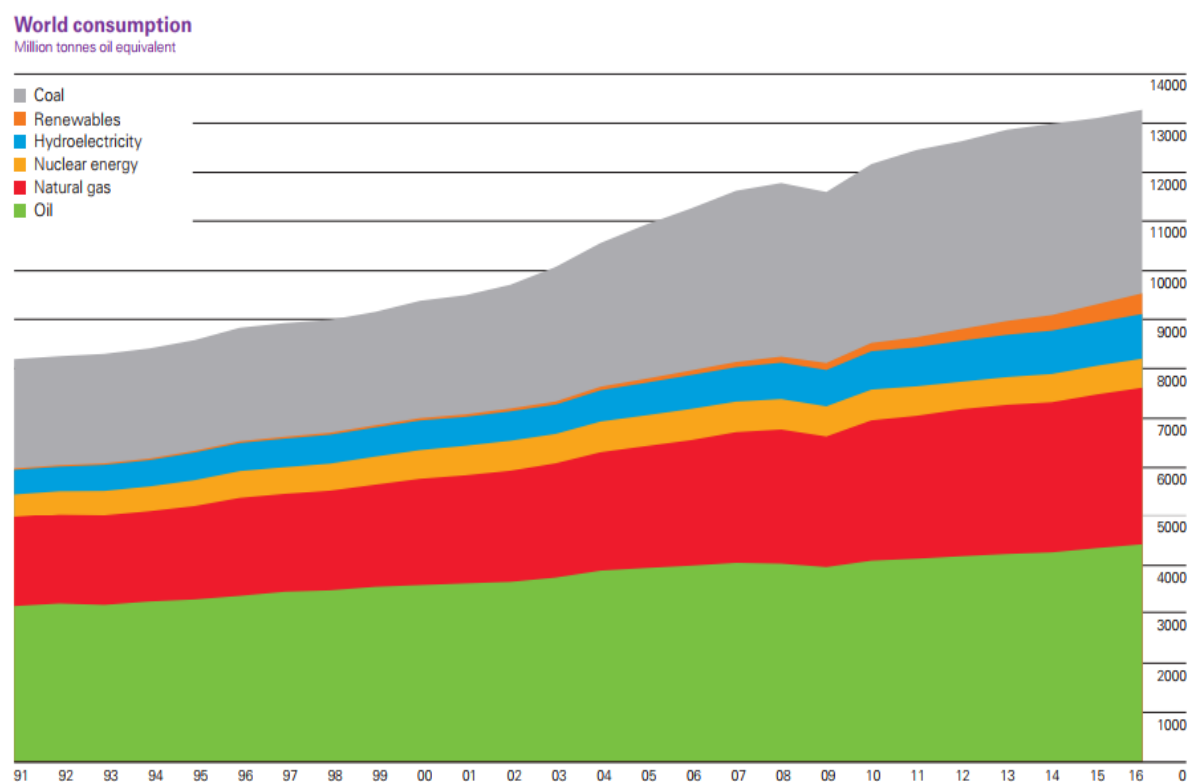


**Figure 1.1** – World energy consumption in million tonnes oil equivalent from 1991 to 2016 [1].

The shape of the graph demonstrates that the share of fossil fuels in 2016 is still quite high, in spite of the rapid increase of renewable sources. In particular, oil represents the most used fuel in the world, followed by carbon and natural gas.

The graph 1.2 provides an overview of the regional consumption of energy.

**Regional consumption by fuel 2016**  
Percentage

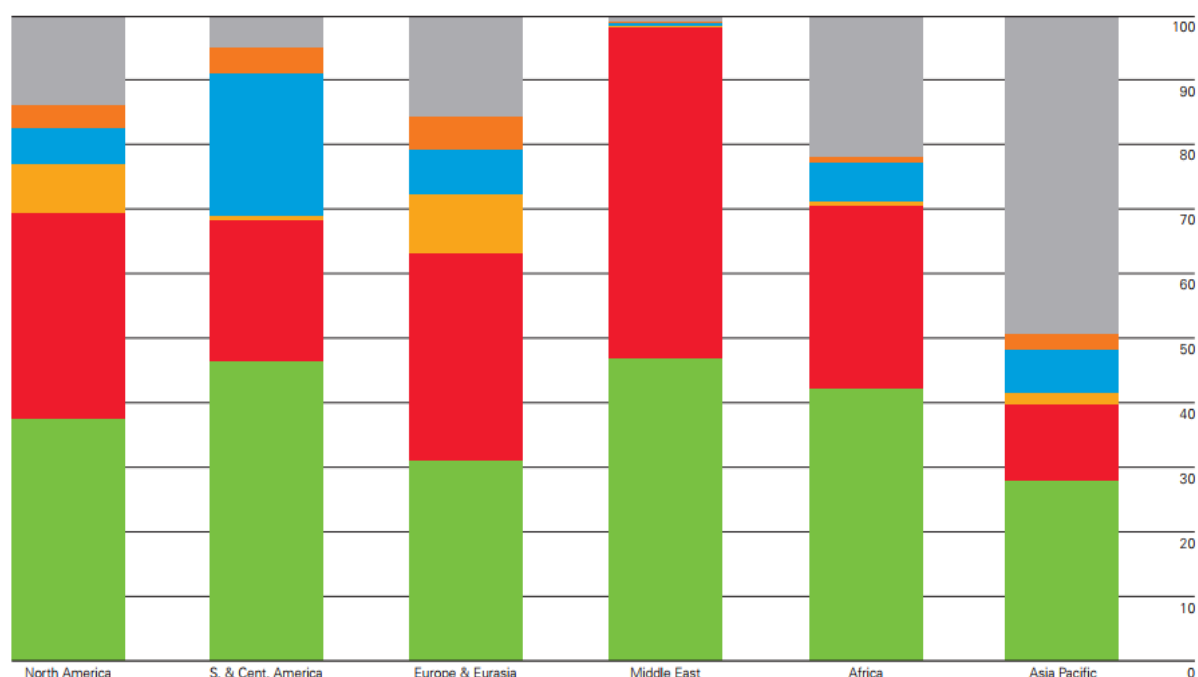


**Figure 1.2** –Percentage of regional consumption in 2016 [1].

As can be seen, oil remains the main fuel available in The Middle East, Africa and the Americas, while natural gas is predominant in the Middle East, Europe & Eurasia. Coal is the main fuel in the Asian Pacific region, accounting for 49% of the regional energy consumption, while renewable sources are mainly used in Americas and Europe & Eurasia.

In order to ensure a sustainable energy consumption, by means of reducing the greenhouse effect caused by gas emissions and fossil fuel dependence, The European Union has developed energy strategies [2].

The aim of these strategies is also to guarantee long-term energy supplies and ensure that energy providers operate in competitive markets to warrant affordable prices in every sector. In order to pursue these objectives, the EU has established targets for 2020, 2030, and 2050.

The 2020 energy strategy refers to a period of time that goes from 2010 to 2020 and, by taking as reference the year 1990, its objective is to reduce the greenhouse emission by at least 20% by 2020, to increase the share of renewable sources to 20% or more and to gain energy savings up to at least 20%. Moreover, a share of 10% of renewable sources must be achieved by all EU Countries to be used in their transportation sector.

In order to attain these objectives, the European strategy intends to:

- Accelerate investments in order to get more efficient buildings also improving the transport and manufacture sectors;
- Implement the “Strategic Energy Technology”, i.e. a strategy made to improve the development of low carbon technologies.
- Enhance the relations with external energy suppliers and energy transit countries.

-Make a pan European energy market, by building the necessary infrastructures (pipelines, transmission lines etc.).

-Protecting consumer rights and enhancing safety standards in the energy sector.

The 2030 energy strategy covers the period ranging from 2020 to 2030. It aims to reduce the greenhouses emissions by 40 %, to achieve a share of renewable sources of 27% or more and to reach energy savings of at least 27%. In order to fulfil these goals, the European strategy program suggests reforming an EU emissions trading scheme, to generate new indicators for the security and competitiveness of the energy system and to think about a new governance system based on national scale plans to obtain a sustainable, competitive and secure energy.

Finally, the goals of the 2050 energy strategy aims at achieving a reduction of 80-95% of greenhouse emissions. In order to pursue these goals, The European Commission's 2011 Energy Roadmap suggests to increase the efficiency of the energy systems and improve nuclear, renewable and carbon capture and storage systems.

According to the European Commission, the GHG (greenhouse gases) emission has been reduced by 22% in 2015, thus fulfilling ahead of time the target imposed [3].

Looking at the progress made in the renewable sector instead, the share of the renewable sources in the gross final energy consumption in 2014 was 16% and 16.7% in 2015, both values were above the indicative estimates. The largest growth is in the electricity sector with a share of 28.8% in 2015, while the lowest growth rate registered is in the transport sector, with a share of 6.7%. The heating and cooling sector shows a share of 18.6%, using as main source solid biomass, whose contribution was estimated to be about 82% [4].

According to the report issued by The Commission of the European Parliament and the Council [3], the final energy consumption in Europe decreased by 7% between 2005 and 2013, while the primary energy consumption was reduced by 8% in the same period. However, the European Commission predicts an overall reduction of energy savings of about 18-19% in 2020, so below the target imposed.

## **1.2. Biomass**

Biomass is defined as organic material of non-fossil origin, including organic waste, which can be converted into energy through combustion, either directly or via derived products.

Plants absorb carbon dioxide and water from the surrounding environment turning them into organic material, by means of solar energy and nutrients taken from the soil.

Common examples of biomass include crops for energy, crop residues (e.g., corn stover), food crops, wood waste and by-products (both mill residues and noncommercial biomass in the woods), and animal manure.

Examples of derived products from waste streams are the conversion of waste oil into biodiesel, organic household waste and animal manure into biogas and plant or plant waste products into biofuel [5]. In the last years, biomass has included also food waste, algae, construction debris, municipal solid waste and yard waste.

### 1.2.1. *Biomass as a renewable source*

There are different kinds of renewable sources. The first one is the solar energy, the most important energy source for the earth, which allows us to produce energy by means of technologies that exploit directly or indirectly the solar irradiation: photovoltaic and solar systems. Another source is the hydraulic energy, acquired from watercourses and basins by way of hydroelectric plants (the oceanic energy falls under this category). A further form of energy is the geothermal energy, which is the thermal energy present in the subsoil resulting mostly from the radioactive decay of the substances, which are below the earth's crust. An additional energy source is the wind, which is possible to turn into electrical power using wind turbines. Eventually, one source with a high utilization potential and one of the most studied is biomass, since it is guaranteed as long as the solar energy and the presence of water in the organic substratum are available.

Biomass is extensively available and it may be obtained at a minimal cost. Moreover, the use of biomass for energy purposes does not worsen the greenhouses effect, since the amount of carbon dioxide released in the atmosphere as a result of combustion or natural decomposition process, is equivalent to the same amount absorbed for the growth of biomass itself.

On the other hand, others argue claiming that biomass has a limited use as an energy source since it is not effortlessly available as a year-round feedstock; it is located at dispersed sites, it could be costly to transport, lacks long-term performance data, needs expensive energy conversion technologies and might not match quality specifications for electric generators [6].

### 1.2.2. *Components of biomass*

Biomass is a heterogeneous mixture of organic substances and a small quantity of inorganic substances. It is mainly composed of carbon, hydrogen and a high oxygen content compared to the fossil fuels. The typical composition of a dry biomass is made up of 30-60% of carbon, 30-40% of oxygen and 5-6% of hydrogen being determined by the ash content [7]. The amount of nitrogen, chlorine and sulfur is less than 1% and it depends on the type of biomass [8]. Inorganic components are contained in the ash.

The average chemical composition of lignocellulosic structures is made up of 25-30% of lignin and 75% of carbohydrates, which are molecules of sugars joined to make long polymeric chains, while lipids, carbohydrates and proteins constitute algal biomasses.

The most important carbohydrates in lignocellulosic materials are cellulose and hemicellulose. Cellulose and hemicellulose provide resistance, structural and mechanical strength to the plant, while lignin acts as a binding force between the fibers, maintaining the stability of these structures.

**Cellulose**, represented by the formula  $(C_6H_{10}O_5)_n$ , is a natural polysaccharide with a high molecular weight and a high degree of polymerization. It provides the support structure to biomass and it constitutes 50% of the material's cell wall. It is insoluble in water at ambient temperature but it is partially soluble at 302°C and entirely soluble at 330°C under subcritical conditions [9]. Figure 1.3 shows the chemical composition of cellulose.

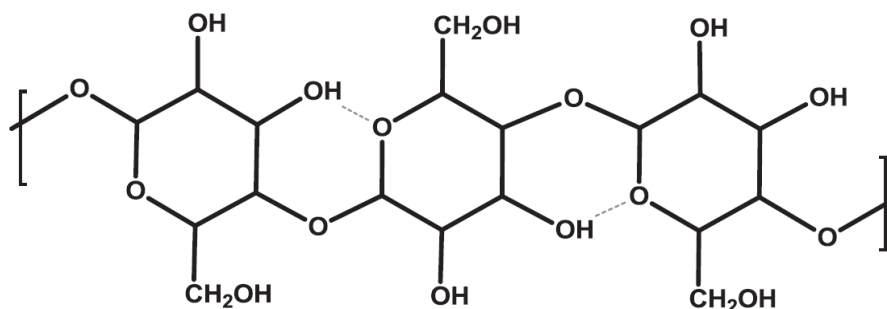


Figure 1.3 – Structure of cellulose

**Hemicellulose** is a complex polysaccharide placed, along with cellulose, in the cell wall. It has a lower polymerization degree than cellulose and it is soluble in diluted alkaline solutions. The branched structure of hemicellulose change remarkably whether biomass is woody or herbaceous. In general, the former type has a quantity of hemicellulose greater than the latter.

Hemicellulose is not composed by different monomer units repeated, but from several sugars among which some have five atoms of carbon (xylan) while others have six atoms of carbons (glucan, mannan, galacturonic acid). Chains are composed by 50-200 monomer units in which xylan is the most abundant. Figure 1.4 shows the molecular structure of xylan.

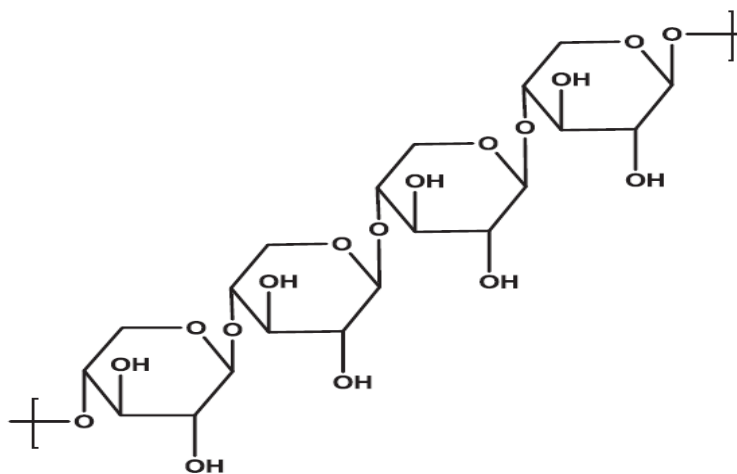
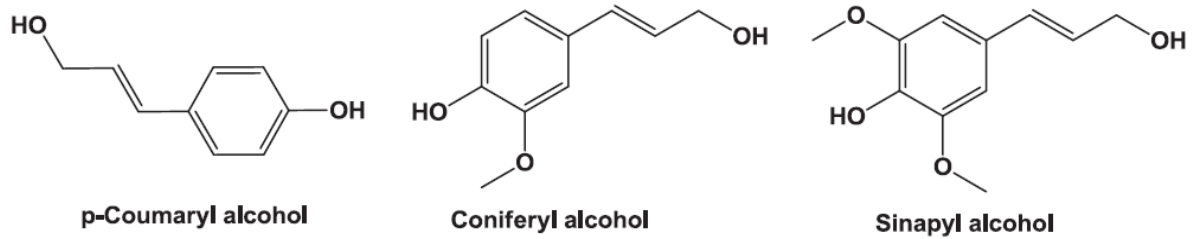


Figure 1.4 – Structure of xylan.

**Lignin** is a complex natural molecule composed of different phenylpropane units, and along with polysaccharide, it represents the organic structure present in plants. The quantity of this molecule changes considerably from one species to another, while it is basically constant within a single type. For example, gymnosperms (conifers) have a lignin content varying from 27% to 37%, while angiosperms have a content of lignin ranging from 16% to 29%. Moreover, lignin performs fundamental functions for the life of plants, in particular, its main function is to reduce the permeability of water acting on every exchange process of minerals and nutrients. Figure 1.5 shows the basic monomers of lignin.



**Figure 1.5** – Basic monomers of lignin.

Wet biomass such as algae are composed mainly by fats and proteins.

**Lipids/fats** are immiscible and hydrophobic non-polar compounds in ambient conditions. They become polar with a change of temperature.

**Proteins/amino acids** are composed by several heterogeneous chains of peptide, which are the main component of algal biomass.

### 1.2.3. Role of biomass in the European strategies

Biomass is generally used as a source to produce electrical and thermal energy, as a fuel for transportation and as a raw material for the production of chemicals.

The graph 1.3 shows the trend of world primary production of energy obtained from renewable sources from 1990 to 2015 [10].

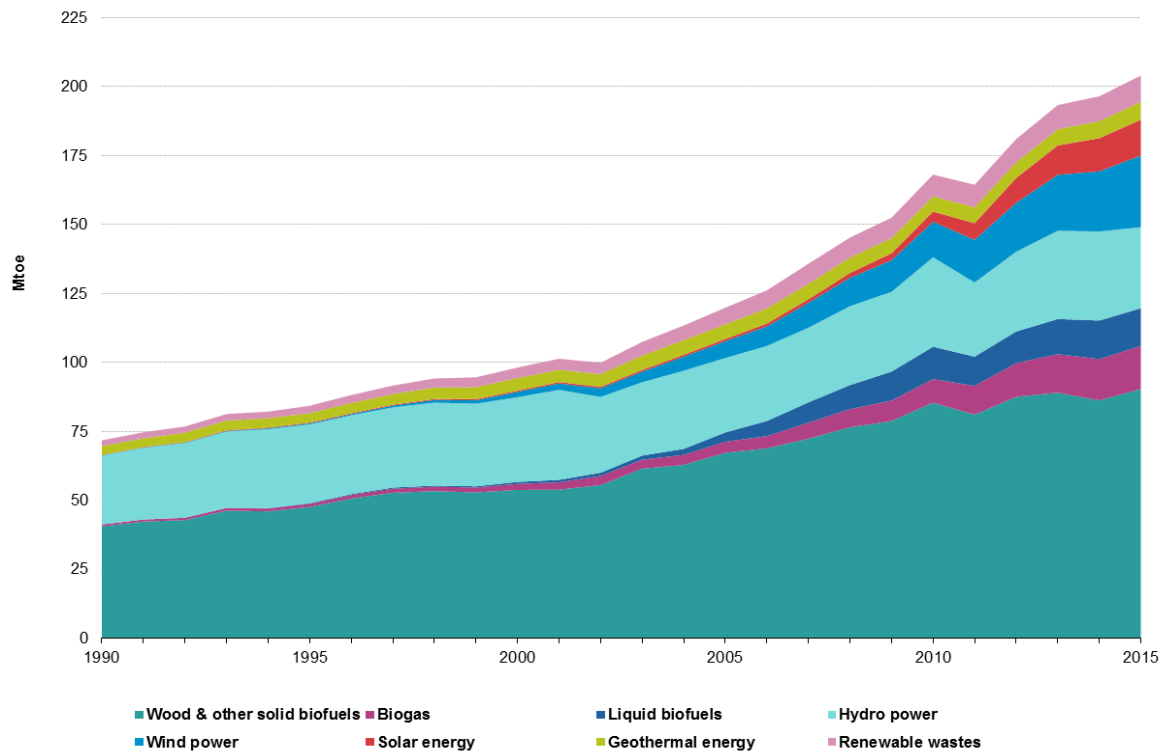


**Figure 1.6** – Primary energy production from renewable sources [10].

According to the diagram, wood and other solid biofuels are the largest contributors to the mix of renewable sources. Hydropower accounted for a high share in 1990, however, its increase rate since then has been slower with respect to other sources as, for example, wind power, liquid biofuels and solar energy, which, by the way, in 2015 have a role in the production from renewable sources comparable to the hydropower.

As it has already been mentioned, solid biomass is the largest contributor to renewable heating and cooling production (82%). In the electricity generation, whereas, the use of biomass has increased from 9 Mtoe in 2010 to 13 Mtoe in 2015, while the combination of biogases and bio-liquids reached the rate of 7% of electricity production. Finally, biofuels play an important role in the transport sector, accounting for 88% [11].

### **1.3. Conversion processes of biomass**

There are many pathways by which biomass feedstock could be converted into useful renewable energy. A wide range of wastes, residues and crops grown for energy purposes could be used directly as fuel for heating, cooling and electricity production or, otherwise, they could be converted into gas or liquid fuels for transportation or as a replacement for fossil fuels.

The conversion processes of biomass can be gathered basically into 4 groups: physical, biochemical, chemical and thermochemical processes.

The **physical conversion** is essentially a mechanical pressing process of high oil content grains (rapeseeds, sunflowers, soy). The final result is a combustible oil and proteins which can be used in the feed industry. The vegetable oil obtained can be used directly as fuel for diesel engines slightly modified or can be further processed to make it similar to the diesel fuel.

The **biochemical conversion** of biomass is a natural procedure performed by bacterial enzymes and microorganisms and it can be divided into three processes: anaerobic digestion, aerobic digestion and alcoholic fermentation.

The **anaerobic digestion** is a conversion process made by bacteria that occurs in an environment lacking oxygen. The microorganisms take oxygen from biomass breaking complex organic substances (proteins, fats and carbohydrates), contained in vegetal and animal by-products, producing a gas made up by methane for 50-70% and by carbon dioxide.

The **aerobic digestion** is a metabolism made by bacteria in an environment with the presence of oxygen. These microorganisms turn complex substances into simpler ones, releasing  $CO_2$  and  $H_2O$  producing in this process a high rise in temperature of the substratum, in proportion to the metabolic activity. The heat produced can be exploited using heat exchangers.

Finally, the **alcoholic fermentation** is a microaerophilic conversion through which carbohydrates contained in vegetals are converted into ethanol through the following reaction:



The **chemical conversion** consists mainly in an acid degradation that produces pentoses, hexoses and lignin-processing well known possibilities in chemical processing [12].

The **thermochemical process**, eventually, allows the production of traditional and modern liquid fuels for transportation and it also provides the upgrading or synthesis of products [13].

The thermochemical conversion of vegetal biomass into energy or by-products can be obtained through different processes, such as combustion, pyrolysis and gasification.

**Combustion** is the most traditional process, by which biomass burns to carbon dioxide ( $CO_2$ ) and water vapour ( $H_2O$ ). In order to make the process efficient, a water reduction in biomass is needed. Hence, the humidity of vegetal biomass has to be reduced from the initial value of 60-70% to 10-12%.

**Pyrolysis** is a thermal degradation of biomass by means of heat in severe shortage of oxygen. The temperature of the substance is raised to 200-700 °C, sometimes introducing a proper amount of oxygen that produces a partial combustion, which, in turn leads to an increase of temperature itself. The process can be applied to every organic material as long as it has a low water content (less than 15%). The final outcomes of the pyrolysis are gases, liquids and solids in a percentage depending on the biomass type and the reaction parameters such as temperature, residence time, heating rate, presence of a catalyst.

The process generates a condensable (liquid) and a non-condensable gas. The former, known as tar, pyrolytic oil or bio-oil, is a high energy density liquid obtained by the decomposition of hemicellulose, cellulose and lignin, which includes oxygenated hydrocarbons. It can be converted in distillates such as gasoline, it can replace petroleum oil or it can be converted into chemicals through purification and separation processes.

The non-condensable gases are those with a low molecular weight such as  $CO$ ,  $CO_2$ ,  $CH_4$  and  $H_2$ .

The solid product, called char, is composed mainly by carbon, oxygen and hydrogen and by a less amount of inorganic matter with respect to fossil fuels.

Finally, the **gasification** is a physical chemical process through which a solid fuel is turned into a gaseous one. The process consists in an incomplete oxidation of carbonaceous compounds brought to high temperature (around 1000°C) in an environment lacking oxygen. The outcome is a gas called syngas, composed of nitrogen, hydrogen, methane, carbon monoxide and other gases, which can be used directly in internal combustion engines employed for energy production.

An important thermochemical conversion is the **hydrothermal process**, which includes hydrothermal liquefaction and gasification, in which water is not a component needed to be disposed of, but a reactant itself.

#### **1.4. Hydrothermal processes**

Hydrothermal processing is an important thermochemical conversion used to produce valuable products or biofuels from biomass. It is defined as a thermochemical

transformation performed at high temperatures (200-600°C) and high pressure (50-400 bar), in super or near critical water conditions. These processes have remarkable advantages with respect to traditional processes, because of the high energy obtainable and the higher separation efficiency. Besides, hydrothermal conversion allows to use biomass with high moisture content without the necessity of a pre-drying [14]. Furthermore, the application of this process to a biomass with a moisture content less than 30% and in supercritical condition, needs less amount of energy than that needed for pre-drying the biomass [15].

By contrast, hydrothermal processing needs large water handling equipment [16] more complex and costly reactors are needed [17] and it is complicated to manage the separation and extraction procedures on industrial scale. Another disadvantage of the process is the difficulty to compute the gas yields because of the complexity of mass balance due to the variability of hydrothermal media [18].

As in pyrolysis tar and char are produced by this process along with gases. The proportion of these products depend on the type of biomass used and the reaction parameters.

Depending on the operation parameters, it is possible to have three different processes. Under 520 K hydrothermal carbonization takes place. It is a relatively new method, which produces a fuel called hydrochar, having similar properties as low rank coal. Hydrothermal liquefaction occurs at temperatures ranging between 520 K and 647 K. Above these temperatures, the process is defined as hydrothermal gasification [19]. The last two are the basic hydrothermal processes which will be described in the following paragraphs.

#### ***1.4.1. Hydrothermal liquefaction***

Hydrothermal liquefaction (HTL) is a process used to convert biomass in liquid fuels with high-energy content and high efficiencies. It consists in breaking down the complex molecules of biomass to liquid components in a hot and pressurized water environment. The water can be in subcritical or supercritical conditions depending on the values of temperature and pressure. In this way, as already stated above, the water is a solvent and there is no need to pre-dry the biomass. Another fact worth noticing is that the process can be run at lower temperatures than pyrolysis [20].

As already mentioned, biomass presents a complex structure, made of lignin, carbohydrates, proteins and lipids. As stated above, the reactions taking place in the process are complex as well. The main steps of hydrothermal liquefaction are depolymerisation, decomposition and recombination [19].

In the first step macromolecules of biomass dissolve. Temperature and pressure turn the structure of the long chain polymers into shorter chains of hydrocarbons.

Decomposition turns macromolecules into oligomers and monomers by hydrolysis. In this step, biomass loses water molecule (dehydration), carbon dioxide molecules (decarboxylation) and amino acids (deamination).

Finally, because of a lack of hydrogen compounds or an excess of free radicals, a recombination and repolymerization of reactive fragments occurs, to form high molecular weight char compounds called coke [21].

The HTL does not need a catalyst, since the reaction is, basically, a pyrolysis in hot water. By contrast, some researches have demonstrated the advantages of using some catalysts. In particular, the alkali modifies the ionic medium supporting base-catalyzed reactions which

generate aromatic oils, instead of acid polymerization reactions which, on the other hand, generate solid products [19].

The crude oil produced is a mixture of oxygenated compounds with a high range of molecular weight such as alcohols, phenols, cyclic ketones, acids, methoxy-phenols and more condensed compounds such as naphthols and benzofurans [19].

#### **1.4.2. Hydrothermal gasification**

Hydrothermal gasification is a conversion of biomass into gases and liquids, in pressurized hot water in sub or supercritical conditions.

The process is more efficient than traditional gasification and water is not only a solvent but also a reactant itself. Therefore, there is no need to pre-dry the biomass before processing it and this allows a better exploitation of biomass residues such as those from the paper industry, food production or sewage sludge.

Another advantage, thanks to a fast hydrolysis, is that the degradation of polymeric structure is rapid as well, leading to an increase of kinetics of further reactions, allowing a production of gases at lower temperatures compared to dry processes [22]. Furthermore, this treatment produces less tar and coke thanks to the high solubility of intermediates, especially with supercritical water.

Another fact worth noticing is that hydrothermal gasification has a higher carbon efficiency since a lower quantity of organic matter is found in water [19].

Lastly, the presence of chlorine and other inorganic compounds in dry biomass causes corrosion problems. In hydrothermal gasification, by contrast, inorganic compounds settle into the aqueous phase, which leads to having less corrosion. On the other hand, the problem is how to separate cheaply these inorganic compounds from water.

Despite all these advantages, a serious disadvantage hinders the progress of this technology. Because of the big amount of water, heating it up can be energetically costly. Hence, the use of hydrothermal gasification is justified if the heat exchanger is efficient enough so that the energy content of biomass is bigger than the energy needed to heat it up. Luckily, state-of-the-art high-pressure heat exchangers are efficient and compact.

Additionally, especially for supercritical water gasification, materials have to withstand high temperatures and pressures, so that the investment costs can be excessive.

Reaction parameters determine the type of the process. With a temperature between 215 and 265°C, “aqueous phase reforming” occurs [23], through which compounds from biomass as glycol, glucose, sorbitol, glycerol and methanol, gasify to form hydrogen and carbon dioxide with the presence of a heterogeneous catalyst.

With a temperature close to the critical point and with the presence of a heterogeneous catalyst, a “catalysed near-critical gasification” occurs [24]. The water’s temperature can be 350°C in liquid phase or 400°C in supercritical conditions. In this process, the main products are methane and carbon dioxide. The presence of a catalyst allows operating at a lower temperature so that investment costs can be reduced.

Finally, above the critical point of water, the process is called *supercritical water gasification* (SCWG). There is no need to use a catalyst but it is possible to use a carbon [25] or a solid catalyst in order to increase the kinetics.

The main gaseous products are methane and hydrogen, along with carbon monoxide and dioxide. Figure 1.7 shows the dependence of the composition on gas temperature.

It is possible to notice that, in order to produce a gas rich in hydrogen, it is required a temperature above 500°C without catalysts or by using a non-metallic one. A gas rich in methane can be obtained, by contrast, operating between the critical temperature and 500°C by using a catalyst.

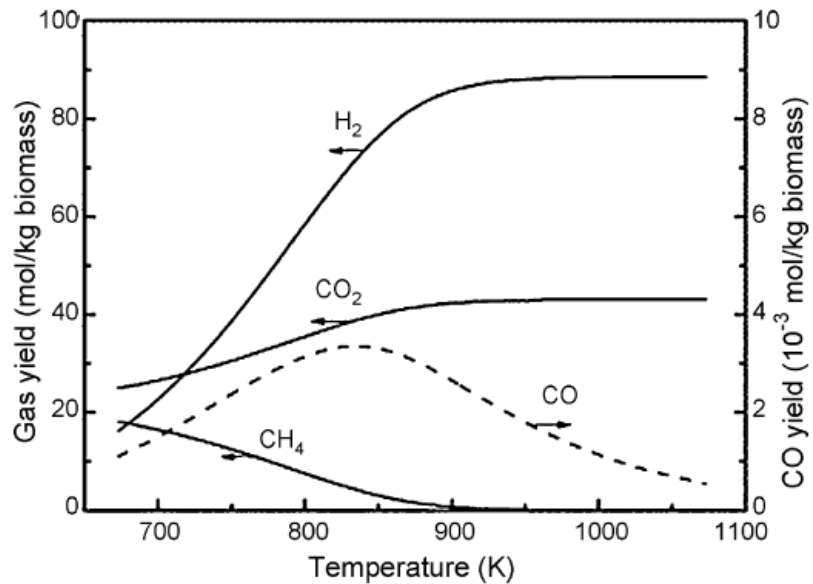


**Figure 1.7** – Gas yield of hydrothermal gasification of biomass as a function of temperature [22].

Figure 1.8 shows, instead, the dependence on the concentration of biomass.

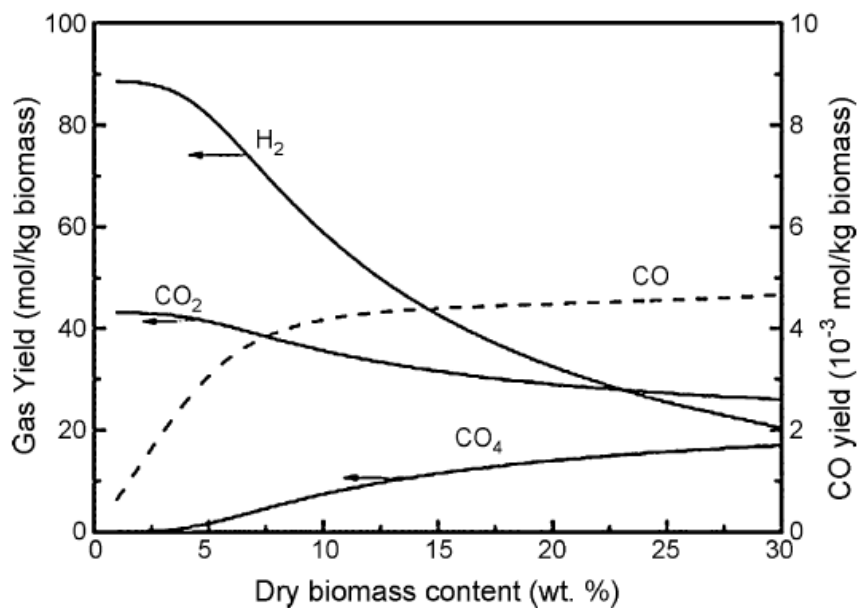


**Figure 1.8** – Gas yield of hydrothermal gasification of biomass as a function of concentration [22].

If a bigger amount of hydrogen is required, a lower dry biomass content is needed and vice versa for methane.

Reactions in hydrothermal gasification are complicated due to the complexity of the biomass' structure itself. During the process, biomass breaks down into lower weight molecules by hydrolysis. Other reactions such as thermal decomposition, methanation and water gas shift take place. Pyrolysis and water gas shift produce hydrogen at high temperatures (500-800°C) [7]. Catalysts are not needed in supercritical conditions, despite the necessity in subcritical conditions in which nickel, rhodium, rubidium and alkaline salts are generally used. [22].

The presence of lignin leads to a greater formation of biochar and a lower gas yield since it breaks down to form formaldehyde. The latter condensate with alkyl phenols that, consequently, polymerize to form higher weight compounds, in which formaldehyde acts as cross-linking agent [7].

In the following chapter, the properties of supercritical water will be investigated, in order to better understand the supercritical water gasification process.

## 2. Supercritical water

Supercritical water gasification is a hydrothermal conversion with water in supercritical conditions. In this state, water has properties which differ markedly from those at ambient conditions, in particular, it shows some advantages that make itself a good candidate as a medium, reactant and catalyst in supercritical gasification.

In this chapter, all these properties will be investigated, focusing the attention on those important for supercritical water gasification.

### 2.1. *Supercritical state*

A fluid is supercritical when its temperature is above the critical temperature and its pressure is higher than the critical pressure.

A supercritical fluid is a substance in a state with physical and chemical characteristics in the between of a liquid (such as density) and a gas (e.g. viscosity). Above the critical point, there is a single phase with no surface, since the absence of liquid and gas bonds. This characteristic can be suitable for reactions with permanent gases (for example oxidation or hydration) since it eliminates inter-phase mass transport limitations.

A substance, when in a supercritical state, has a particular internal structure with properties far different from the ambient condition. Because of the high pressure, the atoms are close to each other as in the liquid state. The temperature, on the other hand, increases the kinetic energy of particles, which win the attractive forces and, thus, making the fluid similar to a gas.

A supercritical fluid can behave as a gas or as a liquid depending on the temperatures and pressures. An increase in density corresponds to a rise of miscibility and since the density is related to the pressure, the solubility increases with it.

The relation with temperature is more complicated. In particular, around the critical point, there is a marked variation of solubility. Generally, at constant pressure, solubility increases with temperature, but near to the critical point, the solubility often decreases intensely with a slight increase in temperature. Once this region is exceeded, the solubility returns to increase with temperature.

Thanks to these advantageous properties, supercritical fluids are used in many applications, for example as industrial solvents, instead of organic solvents, in extractions thanks to the low viscosity and the high diffusivity that make the operation fast. As P.E. Savage claims [26], the reaction product could be separated easily from the supercritical reaction medium simply by returning to conditions below the critical point, while in traditional processes a distillation or liquid-liquid extraction is needed.

Supercritical water is a good medium for hydrothermal gasification since its properties improve at this state. Below, the advantages of using supercritical water are examined, underlining, in particular, the benefits in the supercritical water gasification.

## 2.2. *Supercritical water*

As mentioned above, the critical point is identified by a critical temperature and a critical pressure. Below this point liquid and gaseous phase are separated. Liquid density decreases as temperature increases and vice versa for vapour, getting closer and closer until they become equivalent when the critical point is reached, where the state of saturated liquid and vapour coincide.

Figure 2.1 illustrates the state diagram of water as a function of temperature and pressure.

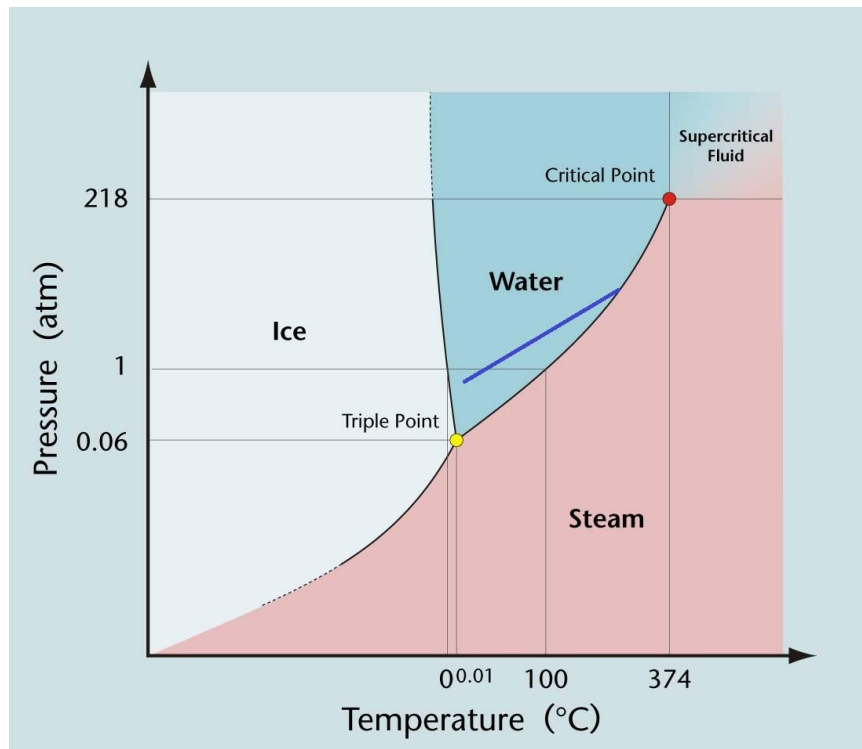


**Figure 2.1** – State diagram of water as a function of temperature and pressure.

This diagram is called *phase diagram* because all the three phases are present, separated by three lines: the sublimation line, dividing the solid phase by the vapour phase; the evaporation line, dividing the liquid phase by the vapour phase; the liquefaction or fusion line, separating the liquid phase by the solid phase.

The triple point is the point where these three lines intersect. It is constituted by the temperature and pressure values at which the three phases of water (solid, liquid and vapour) coexist.

When the temperature is higher than the critical temperature, while the pressure is lower than the critical pressure, the fluid is called “superheated fluid”. Vice versa, if the pressure is higher than the critical pressure, while the temperature is lower than the critical temperature, the fluid is called *compressed fluid*.

The evaporation line ends at the critical point since beyond it there is no distinction between the two phases.

As can be seen, the critical temperature of water is 374.14 °C, the critical pressure is around 218 atm and the critical specific volume is  $0.003155 \frac{m^3}{kg}$ .

Beyond the critical point, the change of state does not occur separately because the specific volume increases continuously and in every instant only one phase exists. Supercritical water is a gaseous phase characterized by liquid density. The region close to the critical point is called near-critical region. Here the properties of water show a significant variation.

Finally, the points at a certain pressure with the maximum value of specific heat are called *pseudo-critical points*. The pseudo critical line is the union of these points, as shown in figure 2.2.

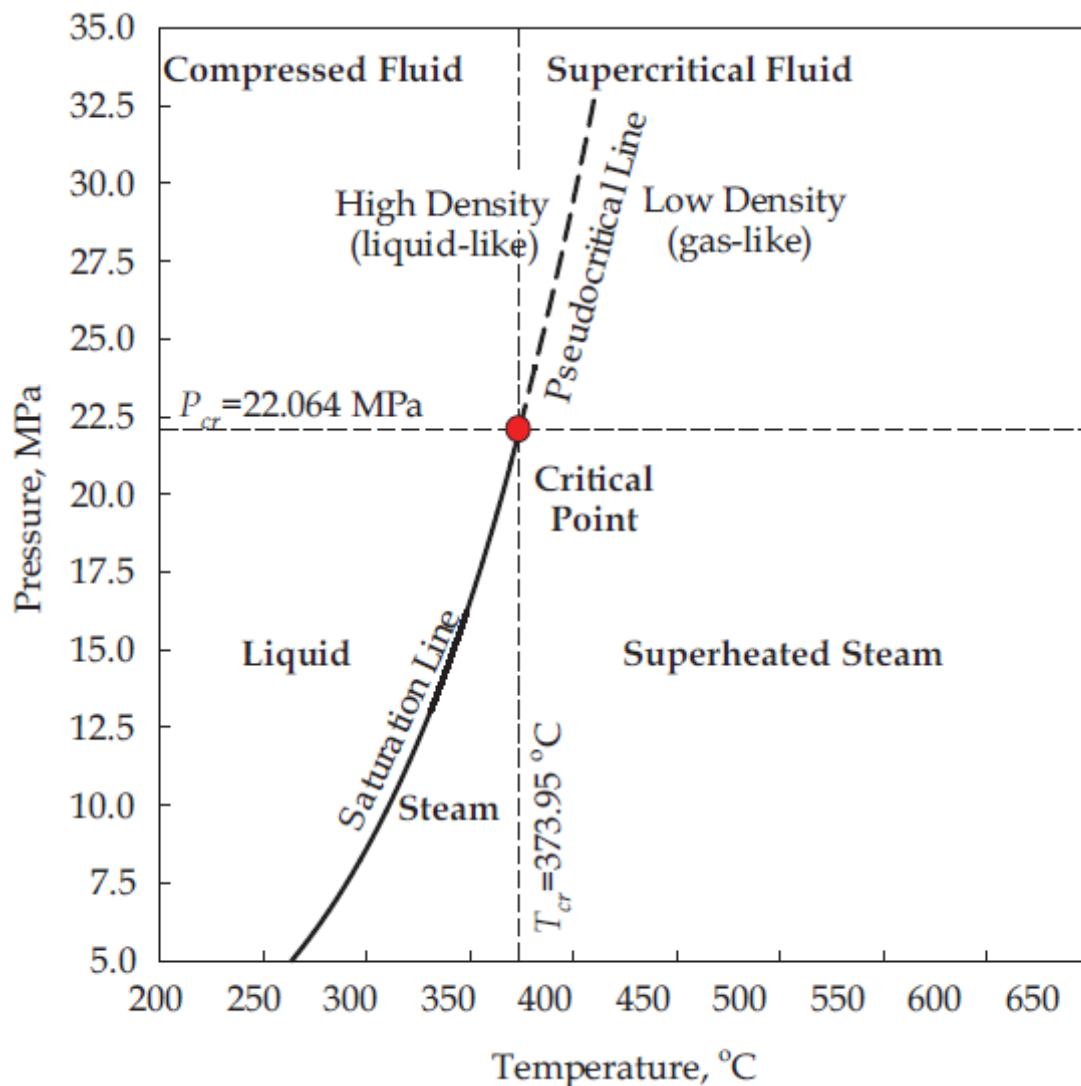


**Figure 2.2** – Diagram of water as a function of pressure and temperature [27].

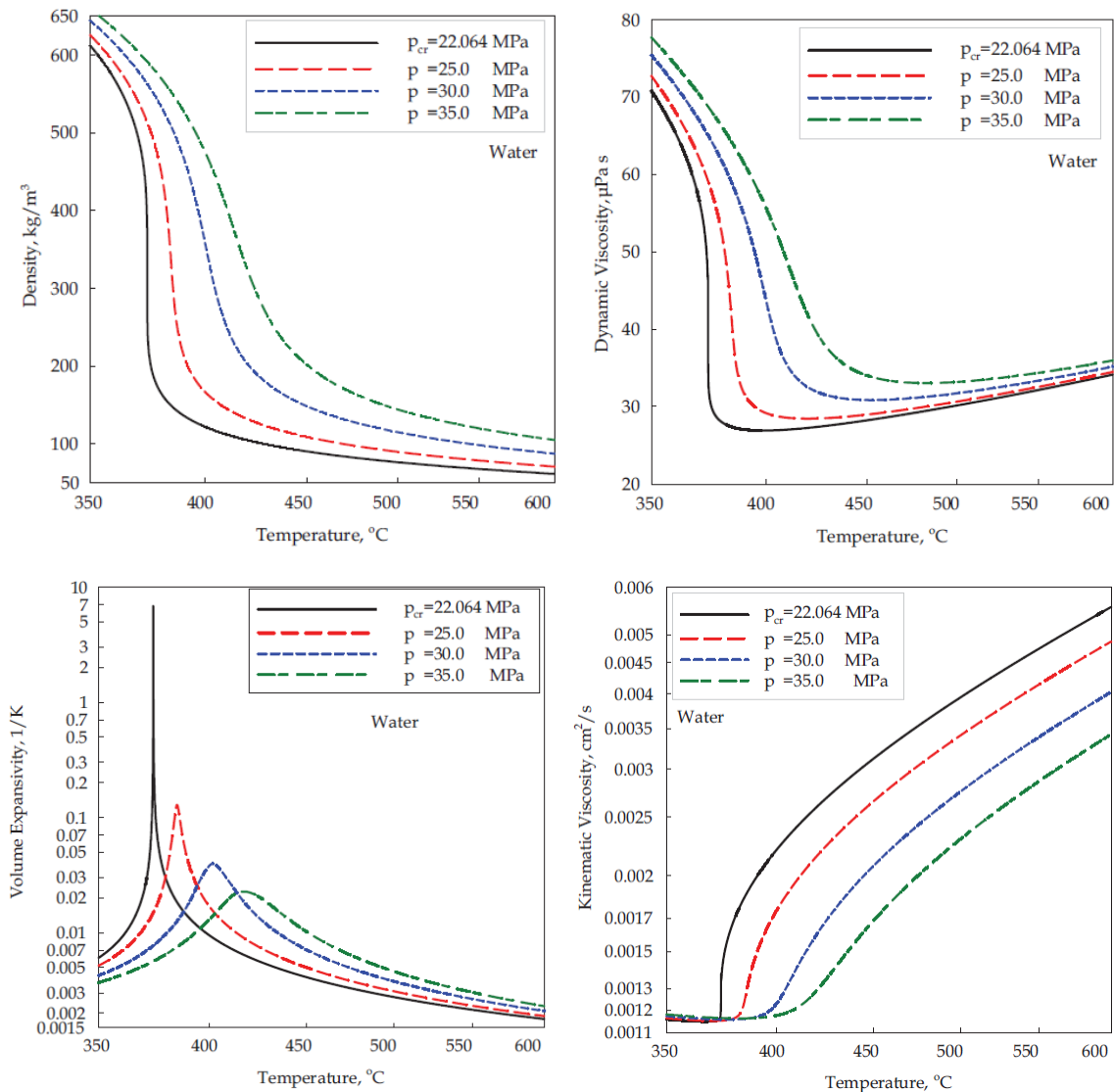
Crossing the pseudocritical line from left to right does not cause a discontinuous change of the properties of water as it happens under the critical point when a liquid turns to vapour, but the properties change continuously, making supercritical water a single phase.

### 2.2.1. Properties of supercritical water

The properties of water change with temperature and pressure, so that supercritical water has characteristics markedly different from those at liquid or gaseous phase. These differences make water interesting in the industrial or chemical sector.

#### Thermophysical properties

Thermophysical properties, for example, show significant variations in the critical and pseudo-critical region. Figure 2.3 portrays the variations of the basic thermophysical properties as a function of temperature at the critical and three supercritical pressures [28].



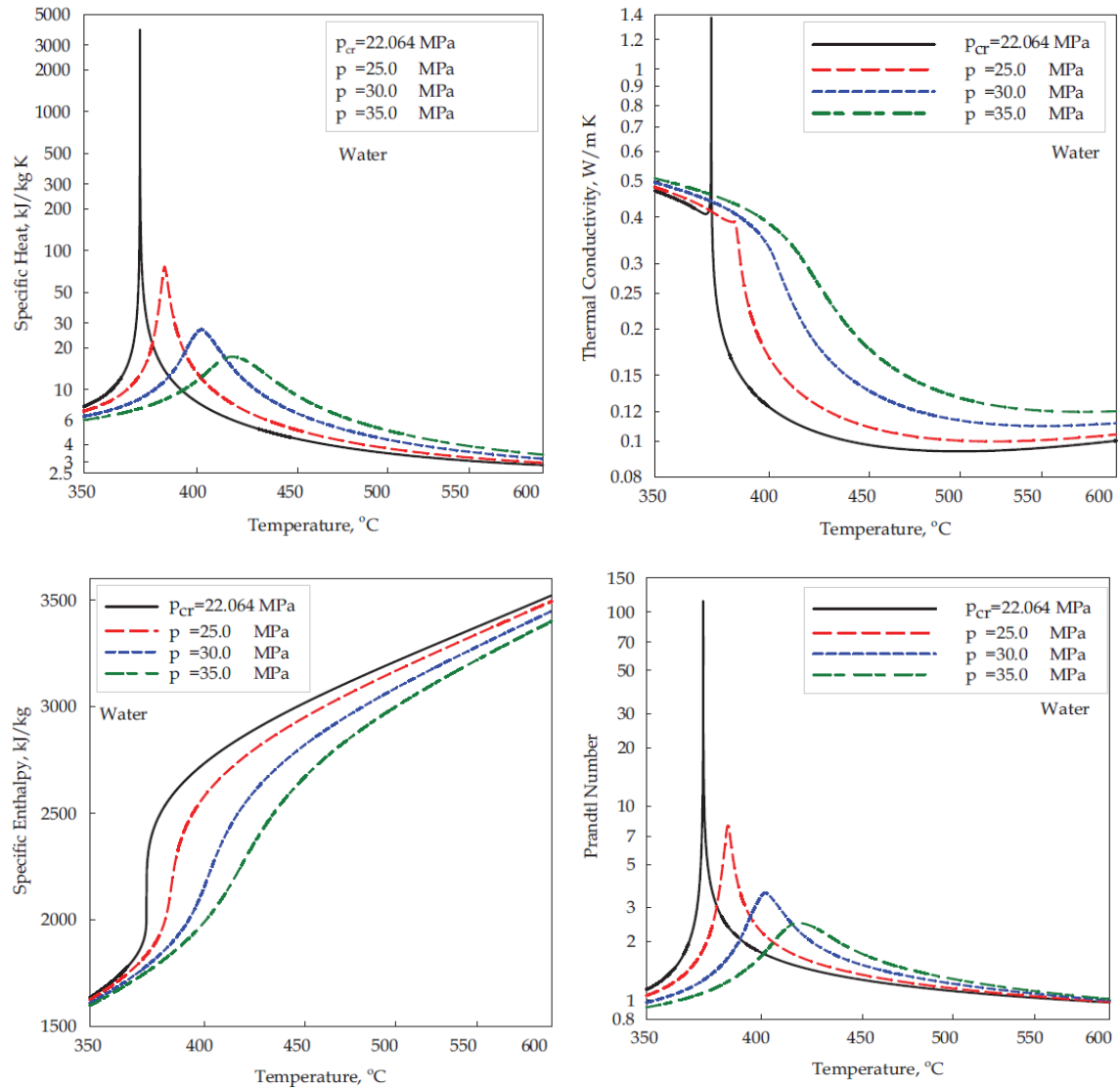


**Figure 2.3** – Thermophysical properties of water as a function of temperature at four different pressures [27].

It is possible to notice that in the near-critical region the variations of the parameters are more marked, while beyond this region, in the nearby of the pseudo critical points, the curve is less steep.

The first two figures illustrate the density and the dynamic viscosity. At the supercritical pressure and within a small range around the critical temperature, both parameters undergo a significant reduction, it is indeed an almost vertical line. A lower viscosity provides a higher diffusion coefficient, leading to high reaction rates.

On the contrary, kinematic viscosity and specific enthalpy increase strongly in the critical region.

The variations of all these parameters are less pronounced as pressure increases.

Finally, volume expansivity, specific heat, thermal conductivity and Prandtl number show a peak at the critical point, which decreases as the pressure increases, turning into a bell-shaped curve at higher pressures.

Kinematic viscosity, thermal conductivity and density, reach the minimum value right after the critical and pseudo-critical points.

Table 2.1 displays the peak values of specific heat at different pseudocritical temperatures and pressures. Table 2.2 shows the peak values of specific heat, volume expansivity and thermal conductivity at different pseudocritical temperature and pressures.

Pressure, MPa	Pseudocritical temperature, °C	Peak value of specific heat, kJ/kg·K
23	377.5	284.3
24	381.2	121.9
25	384.9	76.4
26	388.5	55.7
27	392.0	43.9
28	395.4	36.3
29	398.7	30.9
30	401.9	27.0
31	405.0	24.1
32	408.1	21.7
33	411.0	19.9
34	413.9	18.4
35	416.7	17.2

**Table 2.1** – Peak values of specific heat at different pseudocritical temperatures and pressure [27].

Pressure, MPa	Pseudocritical temperature, °C	Temperature, °C	Specific heat, kJ/kg·K	Volume expansivity, 1/K	Thermal conductivity, W/m·K
$p_{cr}=22.064$	$t_{cr}=374.1$	-	$\infty$	$\infty$	$\infty$
22.5	375.6	-	690.6	1.252	0.711
23.0	-	377.4	-	-	0.538
	377.5	-	284.3	0.508	-
23.5	-	379.2	-	-	0.468
	-	379.3	-	0.304	-
	379.4	-	171.9	-	-
24.0	-	381.0	-	-	0.429
	381.2	-	121.9	0.212	-
24.5	-	382.6	-	-	0.405
	-	383.0	-	0.161	-
	383.1	-	93.98	-	-
25.0	-	384.0	-	-	0.389
	384.9	-	76.44	-	-
	-	385.0	-	0.128	-
25.5	386.7	-	64.44	0.107	no peak
26.0	388.5	-	55.73	0.090	0.355
27.0	392.0	-	43.93	0.069	0.340
28.0	395.4	-	36.29	0.056	0.329
29.0	398.7	-	30.95	0.046	0.321
30.0	401.9	-	27.03	0.039	0.316

**Table 2.2** – Specific heat at critical temperatures, pseudocritical and super critical temperatures and at critical and supercritical pressures [27].

It is possible to notice that the maximum values of volume expansivity and thermal conductivity may not correspond to the pseudocritical temperatures.

First of all the macroscopic properties as miscibility, dielectric constant, ionic product and transport properties will be investigated. Lastly, the microscopic properties as collision frequencies, dipole moment and hydrogen bonds will be examined as well.

## Miscibility

At ambient conditions ( $T=25^{\circ}\text{C}$  and  $p=0.1\text{ MPa}$ ), water is a good solvent for salts, thanks to the high value of the relative dielectric constant ( $78.5$  at  $997\frac{\text{Kg}}{\text{m}^3}$ ) [28], while, in these conditions, miscibility is low for hydrocarbons and gases.

Near to the critical point, the dielectric constant decreases down to the range of 10 [29], increasing the solubility of organic compounds. The dielectric constant continues to decrease as the temperature increases. Therefore, in the supercritical state, water is a bad solvent for ionic species like salts but it is entirely miscible with many organic compounds, which makes water an excellent medium for supercritical gasification.

## Dielectric constant

Electric permittivity is a constant of proportionality between electric displacement and electric field intensity. In a vacuum, this constant is equal to  $8,85 \times 10^{-12}$  farad per meter ( $\frac{\text{F}}{\text{m}}$ ).

In engineering applications, permittivity is frequently expressed in relative terms. The relative permittivity  $\epsilon$ , also called dielectric constant, is the ratio of the permittivity of a substance and the permittivity of free space and it represents a measure of the polarity of the solvent. Thus, the relative dielectric permittivity controls the solvent behaviour and the ionic dissociation of salts. In particular, the polarity of a transition state, during a reaction, could be higher or lower than the polarity of the initial state. A higher dielectric constant corresponds to a lower activation energy, which means that the polarity of the transition state is higher than the initial state and that the reaction rate increases. Thus, by varying temperatures and pressures on which dielectric constant depends, the reaction rates may be controlled [30].

Uematsu and Frank proposed an empirical equation that shows the relationship between the dielectric constant, the temperature and the pressure [31]:

$$\epsilon = 1 + \left(\frac{A_1}{T}\right)\rho + \left(\frac{A_2}{T} + A_3 + A_4T\right)\rho^2 + \left(\frac{A_5}{T} + A_6T + A_7T^2\right)\rho^3 + \left(\frac{A_8}{T^2} + \frac{A_9}{T} + A_{10}\right)\rho^4 \quad (2.1)$$

where  $A_i$  is a fitting parameter and  $T$  is a normalized temperature.

By increasing the temperature  $\epsilon$  decreases, while it increases proportionally to the density. At ambient conditions, the permittivity of water is high ( $\epsilon \cong 80$ ) due to the effect of hydrogen bonds, which make water a polar solvent. By contrast, in the supercritical region, at high

density and in a large range,  $\epsilon = 10-25$  [32]. The last values are high enough to allow water to dissolve and ionize electrolytes, but in addition, with this permittivity water is miscible with non-polar compounds being able to dissolve many organic compounds with fast reactions and appearing as a single homogeneous phase compound. At the critical point  $\epsilon \cong 6$ .

### Ionic product

The ionic product is the product of molar concentrations of ions obtained by self-dissociation of a chemical compound. The ionic product of water is  $K_w = [H_3O^+][OH^-]$  or, based on the simplified equilibrium  $K_w = [H^+][OH^-]$ .  $K_w$  is just an equilibrium constant.

The ionic product increases slightly with temperature in the subcritical region since the self-dissociation of water is endothermic. The ionic product, in this region, can reach a value of  $K_w = 10^{-11}$  in the range of 200-300 °C [30]. Around the critical point, the ionic product raises leading to an increase of the electric conductivity. Beyond the critical point, on the other hand, it increases with pressure but decreases considerably with temperature, since at higher temperature the dielectric constant and the density of water are low. Therefore, the solvation and stabilization capability of water for ionic species decrease, which causes a reduction of the ionic product.

Figure 2.5 shows the variation of the ionic product as a function of temperature.

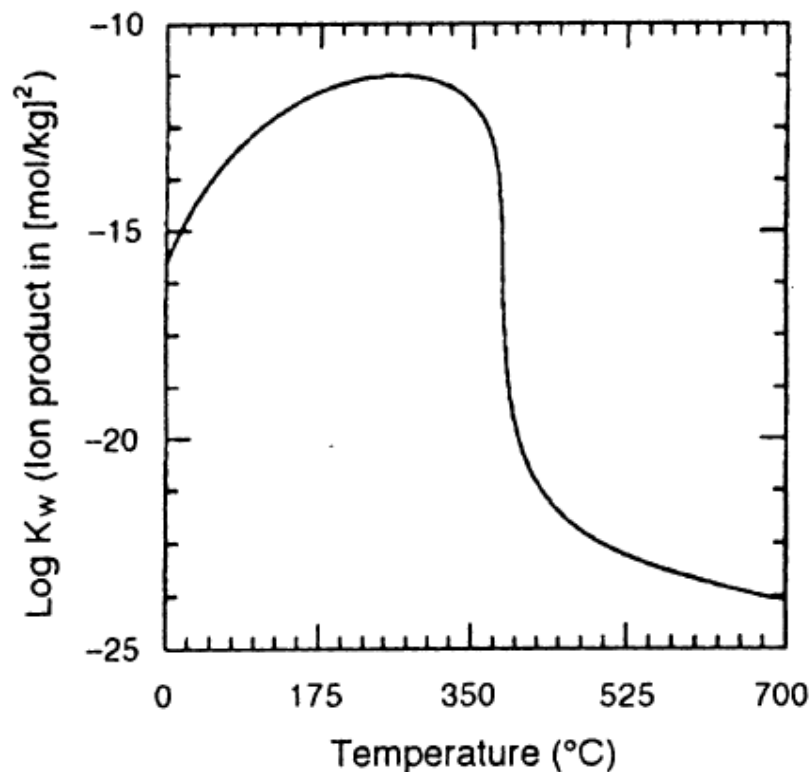


Figure 2.4 – Ionic product in the logarithmic scale as a function of temperature [31].

The drastic reduction of the ionic product above the critical point promotes the radical-based reaction, necessary to form gases. Thus, the shift from ionic-based reactions to radical-based reactions makes the supercritical water a suitable solvent for gasification reactions.

In the supercritical and subcritical region at high pressures, the ionic product might be several orders of magnitude higher than the value at ambient conditions. In the range where  $K_w$  is high, there is a large availability of  $H_3O^+$  and  $OH^-$  ions, which allows to use water as a base or acid catalyst precursor [30].

### **Transport properties**

The rate of chemical reactions is also influenced by the transport properties. As previously mentioned, the viscosity is low in the supercritical region, while diffusion rates are high. As a result of these properties, supercritical water is a very good reaction medium for fast, homogeneous and efficient reactions and for processes where heterogeneous catalysts are used since the high diffusion rates avoid mass transfer limitations, while the high miscibility prevents coke formation or poisoning of the catalyst [30].

From a microscopic point of view, important properties worth noticing are the hydrogen bonds, the collision frequencies and the dipole moment.

### **Hydrogen Bonds**

At normal conditions, water is made of a three-dimensional structure of hydrogen bonds. The lifetime of a hydrogen bond, along with the number of molecules of water connected to clusters through the hydrogen bonds, decrease if the temperature increases and the density decreases [30]. Bonded and non-bonded water molecules are together present at low densities as well, thanks to the thermodynamic stability constraints [33]. Experimental measures guarantee that these bonds are still present in dense supercritical water. In these conditions, at temperatures equal or higher than 500°C, molecular simulations showed that the number of water molecules connected to clusters by hydrogen bonds is five or fewer times smaller. As a result, at the critical temperature, the energy of the hydrogen bonds is fairly higher than the thermal energy. The hydrogen-bonded is made probably of small clusters, however, due to a broad distribution, a small number of clusters (more than 20 molecules) is present as well. These heterogeneous differences are more pronounced in the near-critical region.

The reduction of the number of water molecules connected by hydrogen bonds, along with the drop of the lifetime of the hydrogen bonds, lead to an increase of mobility of water molecules. This causes, in turn, an increase of diffusivity and a change of energy transfer between very fast reacting solutes and solvent, since the barrier for translation and rotation motions is reduced.

## Collision frequencies

Supercritical water is water at high pressure and temperature. The higher the pressure, the higher is the reaction rates of small free radicals, until the “high-pressure plateau” value is reached. Above this point, the rate falls down because of the enhanced energy equilibration rate due to an increase in the collision frequency [34].

Conversely, water molecules at high pressure cause a so-called cage effect that slows down some reactions of high molecular-mass (e.g. reactions occurring during pyrolysis) [35]. This is a consequence of the higher collision frequencies of the reactant with water molecules than with another reactant.

## Dipole moment

The water molecule has a permanent dipole moment, which means that it is very reactive in several reactions [30]. This property is important to determine the dielectric properties and the chemical behaviour of fluids and their capacity to dissolve certain compounds.

The dipole moment of a separate particle in a fluid depends on the electric field induced by the surrounding molecules. Measures and computer simulations suggest that this electric field enhances the dipole moment of a hydrogen-bonded molecule [32].

The dipole moment distribution in supercritical water is different from the dipole moment distribution at ambient conditions since it depends on the spatial configuration of hydrogen bonds [36]. At ambient conditions, the network of the hydrogen bonds is infinite and continuous, while at supercritical conditions the structure of water is made of separated clusters with finite sizes [37].

In supercritical water, the clusters are regularly destroyed and restored and the molecules pass from the unbound into the bound state. As a result, water shows local density and local dipole moment fluctuations, which cause an increase in reaction rates in supercritical water [38].

### ***2.3. Role of water in supercritical water gasification***

As mentioned above, supercritical water is an excellent medium for the supercritical water gasification, since it participates to the process as a reactant and as a catalyst as well. Besides, in this chapter it has been fully investigated how the properties of water change and how it is possible to control them by changing the working parameters, as temperature and pressure.

In supercritical gasification, thanks to its properties, water performs three functions:

- Reactant, because water participates in the gasification reactions.
- Catalyst, because water increases the rate of some chemical reactions involved in the gasification process.

- Medium, since the organic compound is mixed with water beforehand, which acts as diluent and solvent.

Nevertheless, supercritical water is an aggressive reaction medium. In the presence of halogenoids ions and under certain conditions, water may strongly corrode the reactor material [39]. Moreover, under those conditions, many heterogeneous catalysts may have a low stability [40].

### **2.3.1. Water as a reactant/product**

Water may participate in different reactions as a reactant or a product. In supercritical gasification, water takes part for example in the hydrolysis reaction. The latter is a chemical reaction in which the cleavage of chemical bonds by addition of water occurs, causing a fast demolition of the structure of biomass [41]. For example, in the supercritical gasification of biomass, hydrolysis is the reaction through which the polymeric structure of cellulose and hemicellulose collapses to produce sugars, while lignin decomposes into phenolic compounds.

Additionally, water can act as a hydrogen source, supplying hydrogen atoms in chain-terminating reactions, thus avoiding the formation of high molecular weight species in pyrolysis [31].

Moreover, supercritical water reacts with carbon monoxide obtained by biomass conversion, producing hydrogen and carbon dioxide. This reaction is called water-gas shift and leads to an increase of hydrogen yield compared to syngas produced by a dry process [41].

Finally, another reaction involving water is the methanation reaction.

### **2.3.2. Water as a catalyst**

Water can participate in several reactions as a catalyst. As mentioned previously, supercritical water at high pressure has a high  $K_w$ , which means a high concentration of the  $H^+$  and  $OH^-$  ions. As a result, many acid or base-catalysed reactions are promoted by supercritical water. Moreover, the high thermal energy of supercritical water compensates for the lower concentrations of  $H^+$  and  $OH^-$  ions. However, the concentrations of aforementioned ions from self-ionization is high enough to make unnecessary the use of strong mineral acids or base as catalysts, which would be necessary at ambient conditions [31].

Another reaction catalysed by supercritical water is hydrolysis. This reaction, generally, is catalysed by either acid or base in the presence of added catalysts. Nevertheless, experimental data showed that acid catalysis by  $H^+$  ions, produced by self-ionizations, is prevalent.

Lastly, hydrolysis products can act as an acid catalyst, like the carboxylic acids, or as a base catalyst, like the ammonia.

### 2.3.3. *Water as a solvent*

Intermediate products of biomass degradation have double bonds and can re-polymerize producing char and tar. Supercritical water, as a medium, is able to dissolve substances and dilute the solution, reducing the char and tar formation. Moreover, the presence of water in a solution increases the collision frequencies of organic molecules with water molecules, lowering the probability of organic particles to interact with other similar particles. In this way, the coke formation is reduced, since the molecules that could polymerize have a lower probability to meet.

In addition, the degradation of tar is improved, since the reactions catalysed by the  $H^+$  and  $OH^-$  ions are, in most cases, splitting reactions.

### 3. Supercritical water gasification

Supercritical water gasification (SCWG) is a hydrothermal gasification process carried out with water in supercritical condition. The pressure is higher than reforming and dry gasification, but the temperature is lower.

In the first chapter, all the advantages and disadvantages related to the utilization of a hydrothermal gasification have been investigated. One of the main advantages is that it allows to use wet biomass with a water content ranging from 50% up to 80%, enabling, in this way, the use of residues from agriculture, food and beverage industry and by-products of bioenergy production [42]. The energy required for heating up the water can be recovered by using a compact heat exchanger.

In this chapter this technology will be fully examined, describing in detail the mechanisms of the process, the state of the art technology along with the possible configurations and how it is affected by the operating parameters and eventual catalysts.

All the principle reactions taking place in this thermochemical conversion will be listed. In order to do so, the concept of model compound will be introduced, focusing our attention on glycerol, used as a simpler model compound of cellulose than glucose.

Eventually, challenges and solutions for an industrial scale-up will be investigated.

#### 3.1. Model compounds

The reactions taking place in SCWG depend on the components of biomass (cellulose, hemicellulose, lignin, ash, proteins and lipids), operating conditions, catalysts and type of reactor.

Because of the intricate structure of lignocellulosic materials along with the complexity of chemical and physical interactions in presence of supercritical fluids, it is hard to find a single pathway that makes possible a detailed and exhaustive description of the reaction mechanisms. Therefore, in order to study the possible reactions occurring in this process, a model compound is used.

Examples of model compounds that can be used are methanol, ethanol, cellulose, glucose (hydrolysis product of cellulose), hemicellulose, lignin and aromatic compounds like phenols.

SCWG of methanol, for example, produces gases rich with  $H_2$  and with low concentrations of  $CO$  and  $CO_2$  [43]. The maximum concentration of  $H_2$  as a function of residence time is due to the direct decomposition of methanol and the water gas shift reaction (3.3). The subsequent decrease is a result of the incidence of the methanation reaction [44], while the slowness of water gas shift reaction (WGSR) at low temperatures is probably the reason why the concentration of  $CO$  is high, meaning that the activation energy is higher than the decomposition of methanol.

Di Leo and Savage [45] suggested a scheme providing for steam reforming of methanol:



SCWG of ethanol, with temperatures between 400 and 500°C, produces a gas composed of  $H_2$ ,  $CH_4$ ,  $CO$ ,  $CO_2$  and small amounts of ethylene and ethane. Acetaldehyde is the only component detected in the liquid phase [46]. In absence of catalysts, the first reaction, as shown below, is the dehydrogenation of ethanol and acetaldehyde, followed by the decomposition to  $CH_4$ ,  $CO$  and subsequent water gas shift reaction:



Hydrolysis of cellulose and hemicellulose is fairly fast and complete with suitable operating conditions, meaning that its primary reaction products are acceptable model compounds.

Glucose is a good model compound, since cellulose is made of linearly linked glucose units attached to each other. Nevertheless, glucose conversion is still too complex. For this reason, glycerol, which is the model compound used in this work, can represent a good alternative. Moreover, glycerol is a good feedstock for gasification, since it is a by-product of biodiesel production [42].

## **3.2. Reaction pathways**

In this paragraph, an overview of the possible reaction pathways in supercritical conditions will be given. Different model compounds have been chosen in order to describe the reaction pathways of the main components of biomass, leading to the intermediate compounds.

Finally, gas-phase reactions that produce the final products will be investigated as well.

### **3.2.1. Cellulose reaction pathways**

Kabyemela et al. [47] conducted some experiments by using cellobiose as model compound for cellulose, since it has glycosidic bonds similar to those of cellulose.

In sub- and near-critical conditions, cellobiose produces simpler organic compounds through reactions in series and parallel. As illustrated in figure 3.1, first, cellobiose depolymerizes in three different ways: via pyrolysis to glucosyl-glycolaldehyde and erythrose ( $k_2$ ), or glucosyl-erythrose and glycolaldehyde ( $k_1$ ) and via hydrolysis to glucose ( $k_H$ ).

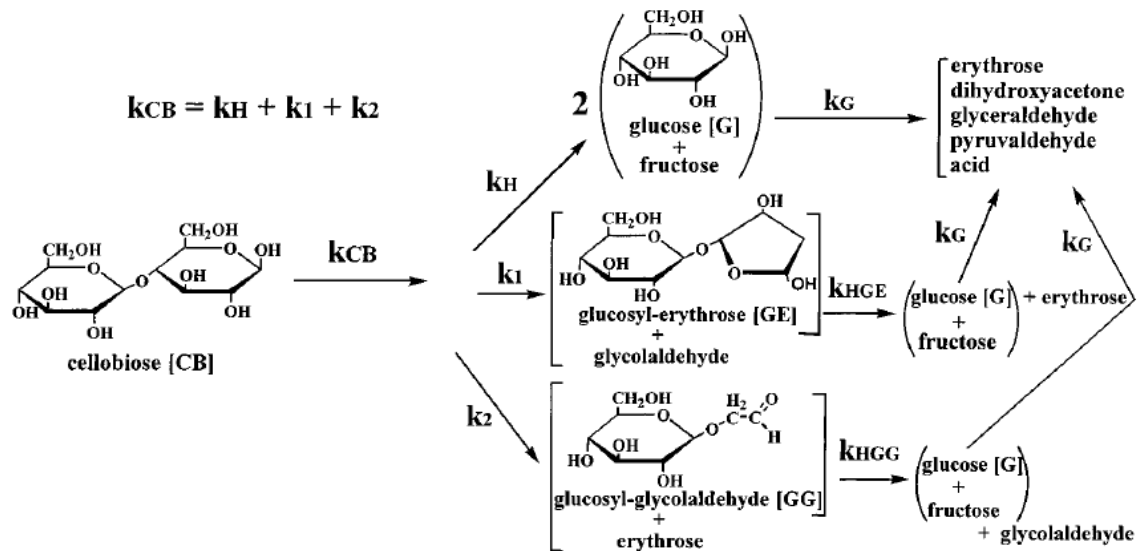
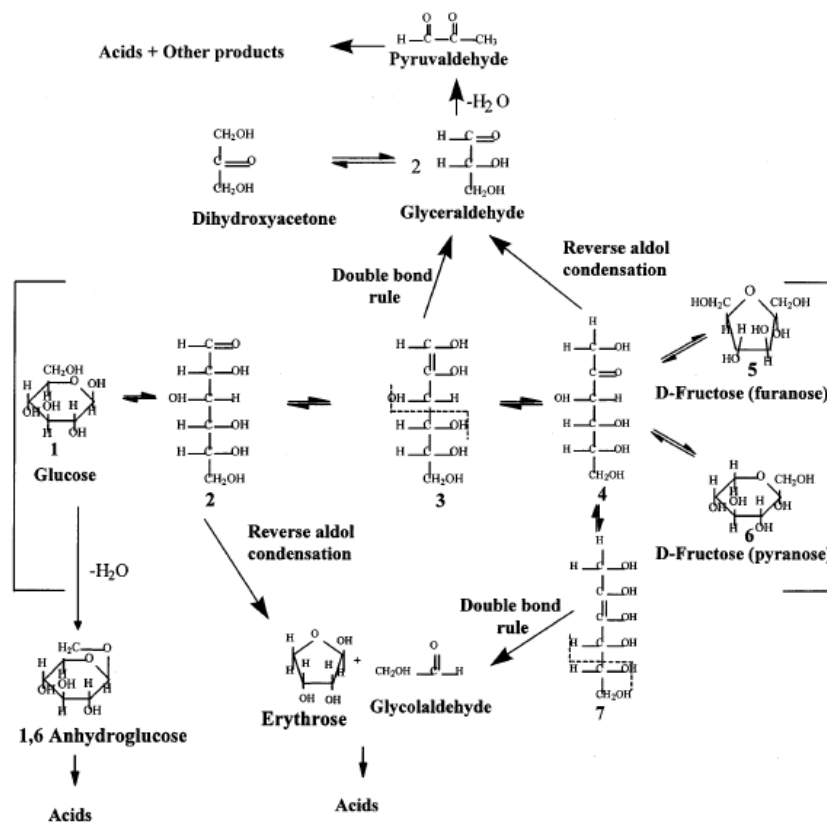
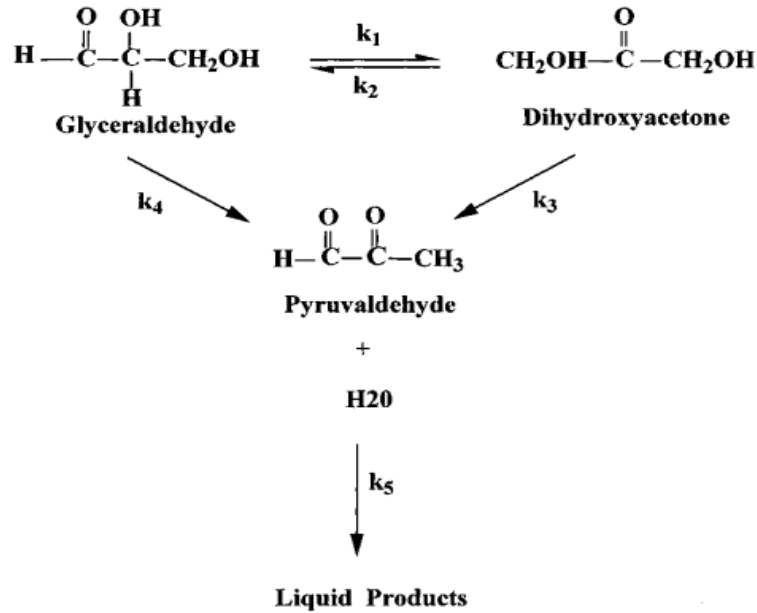


Figure 3.2 shows the mechanism of glucose decomposition in sub- and super-critical conditions.



Glucose isomerizes to fructose, dehydrates to 1,6-anhydroglucose under hydrothermal conditions and decomposes to erythrose and glyceraldehyde [48].

A two-way isomerization reaction involves glyceraldehyde and dihydroxyacetone [49]. Pyruvaldehyde is a dehydration product of the isomer compounds (figure 3.3).



**Figure 3.3** – Glyceraldehyde and dihydroxyacetone degradation in subcritical and supercritical water conditions [49].

Eventually, fructose decomposes into glyceraldehyde, 5-HMF and furfural [50].

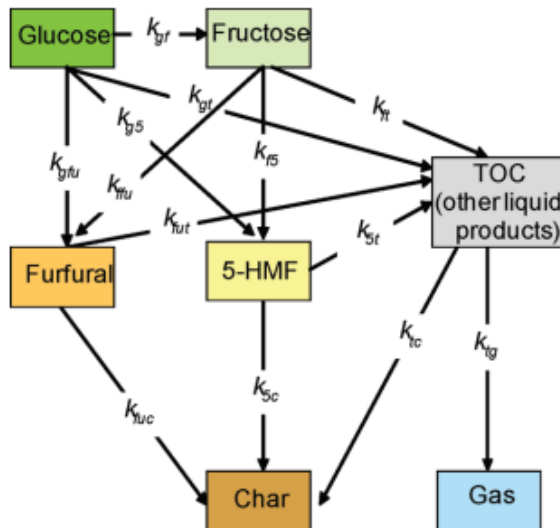


**Figure 3.4** – Fructose and glucose pathways [50].

### 3.2.2. Hemicellulose reaction pathways

In order to model the hemicellulose, D-xylose has been chosen by Jing and Lü [51], since it is the main hydrolysis product of hemicellulose.

According to the authors, in supercritical conditions xylose dehydrates to furfural or it reacts via a retro-aldol condensation to form glyceraldehyde and methyl formate [52]. Glyceraldehyde decomposes to acrylic acid that is reduced by  $H_2$  to propanoic acid, while methyl formate decomposes fast to acetic acid. Propanoic and acetic acid are stoichiometrically gasified to  $H_2$  and  $CO$ . Propanoic acid could further be gasified to ethane and  $CO_2$ . Furfural, by contrast, can decompose in three ways. The first possibility is the direct gasification to  $CO$ ,  $H_2$ ,  $CH_4$ , and  $CO_2$ . In the second option, furfural reacts to form maple lactone, which is gasified to  $CO$ ,  $H_2$ , and  $CH_4$ . Lastly, furfural breaks down to WSHS, which is gasified to  $CO$  and  $H_2$ .

Water gas shift and methanation are assumed to be at thermodynamic equilibrium.

Figure 3.5 shows the possible pathways of D-xylose.

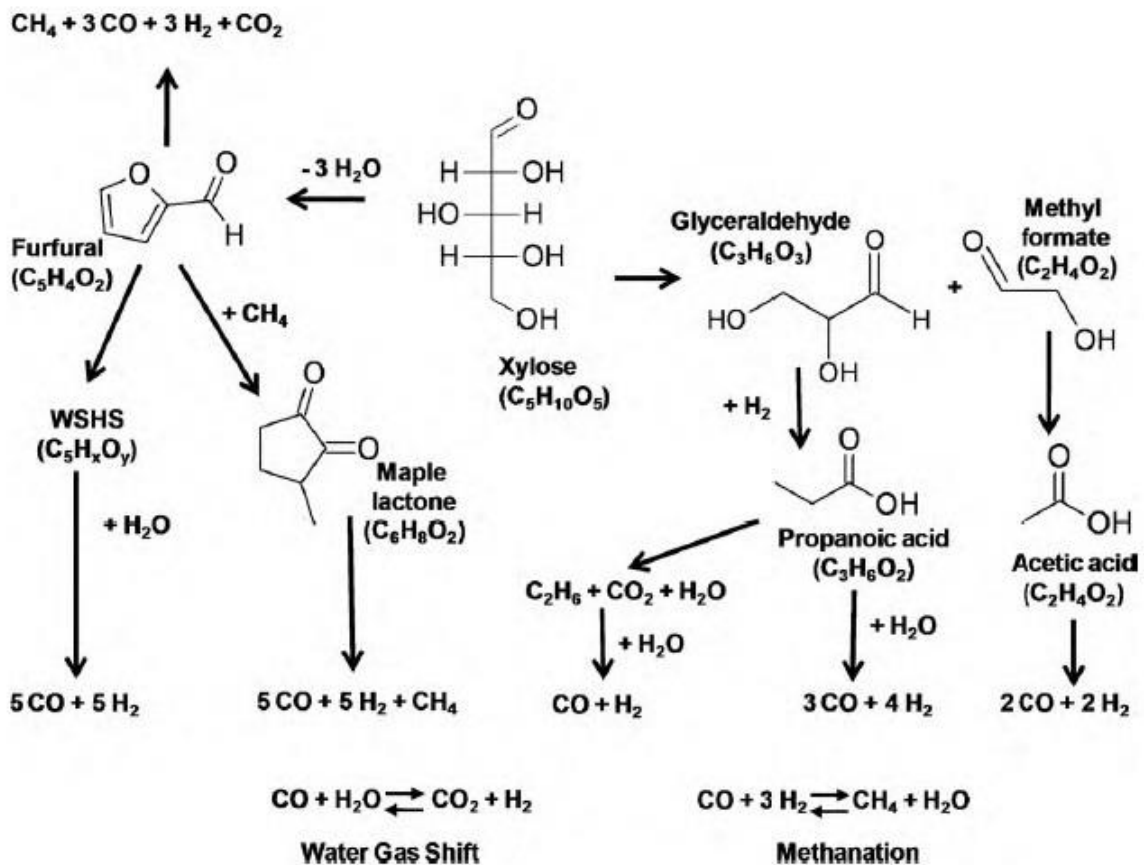


Figure 3.5 – Reaction pathways of D-xylose in supercritical conditions [50].

### 3.2.3. Lignin reaction pathways

Yong and Matsumura [53] proposed guaiacol as a model compound of lignin, because of its similar attached groups and chemical structure.

As shown in figure 3.6, intermediates of guaiacol are catechol, o-cresol, m-cresol, phenol and phenolic-derived compounds, typically indicated as TOC.

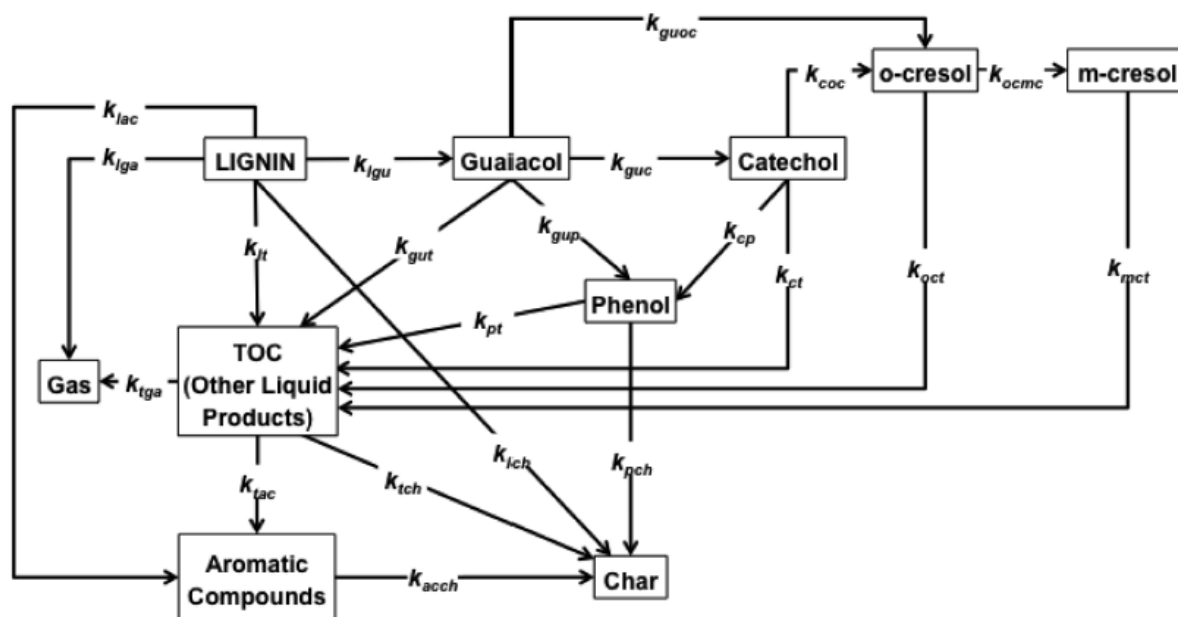


Figure 3.6 – Reaction pathways of guaiacol in supercritical conditions [53].

It can be seen that gases can both be produced directly from lignin or from intermediates, through the cleavage of either bond in methoxyl groups and aromatic rings. Char formation is due mostly to re-polymerization of phenols.

### 3.2.4. Protein reaction pathways

Alanine and glycine are the most investigated amino acids under hydrothermal conditions. Nevertheless, aspartic acid might be a more suitable model compound because it has a higher number of carbon atoms in its molecular structure [54].

Figure 3.7 illustrates the reaction mechanism of aspartic acid in supercritical water. Alanine and glycine decomposition is present too, producing gases along with the intermediate compounds, as ethylamine and methylamine, from amino acids decomposition.

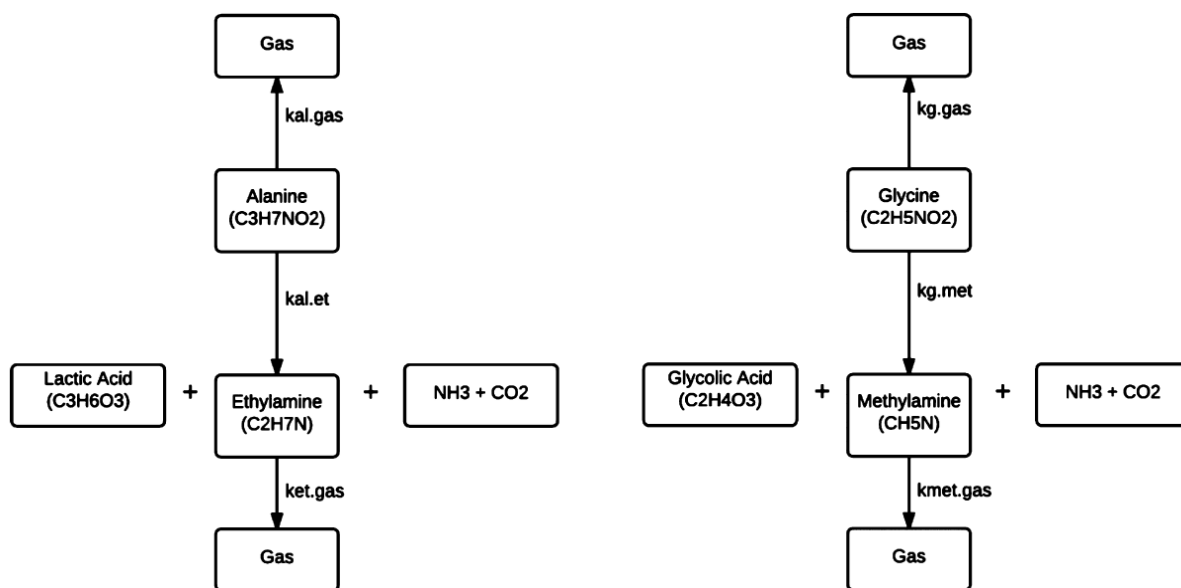


Figure 3.7 – Reaction pathways of aspartic acid in supercritical conditions [54].

### 3.2.5. Organic acid and other intermediate compounds reaction pathways

Figure 3.8 shows the reaction pathways of various organic acids and other intermediate organic compounds, which are further gasified under hydrothermal conditions.

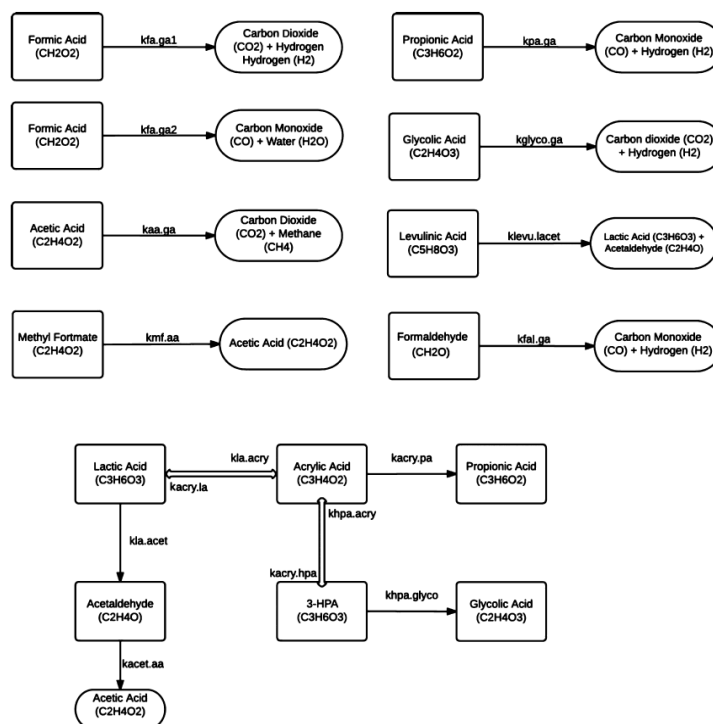


Figure 3.8 – Reaction pathways of organic acids and other organic compounds in sub- and supercritical conditions [54].

### 3.2.6. Gas-phase reactions

The final products of SCWG of biomass are low molecular weight compounds, mainly  $H_2$ ,  $CO_2$ ,  $CH_4$  and  $CO$ . The latter, under supercritical conditions, reacts with water to form  $CO_2$  and  $H_2$  through the water-gas shift reaction (3.3).

According to the Le Châtelier principle, because of the large amount of water, the equilibrium of the water-gas shift reaction is shifted towards the right-hand side [55]. The result is a low concentration of  $CO$ . Because of the endothermic nature of this reaction,  $H_2$  is favored at temperature definitively higher than the critical point of water. Moreover, since the reaction is slow, it can be catalyzed by alkali metals [56].

Another reaction occurring is the methanation reaction (3.7):



However, the methane formation is affected mainly by the gasification reactions of intermediates and guaiacol, while the contribution of the methanation reaction can be neglected. Therefore, a typical hydrogenation catalyst, as nickel or other noble metals, is needed so as to increase the reaction rate.

### 3.2.7. Reaction pathways of SCWG of glycerol

Guo et al. [57], proposed a scheme of reaction pathways taking place in SCWG of glycerol, as shown in figure 3.9.

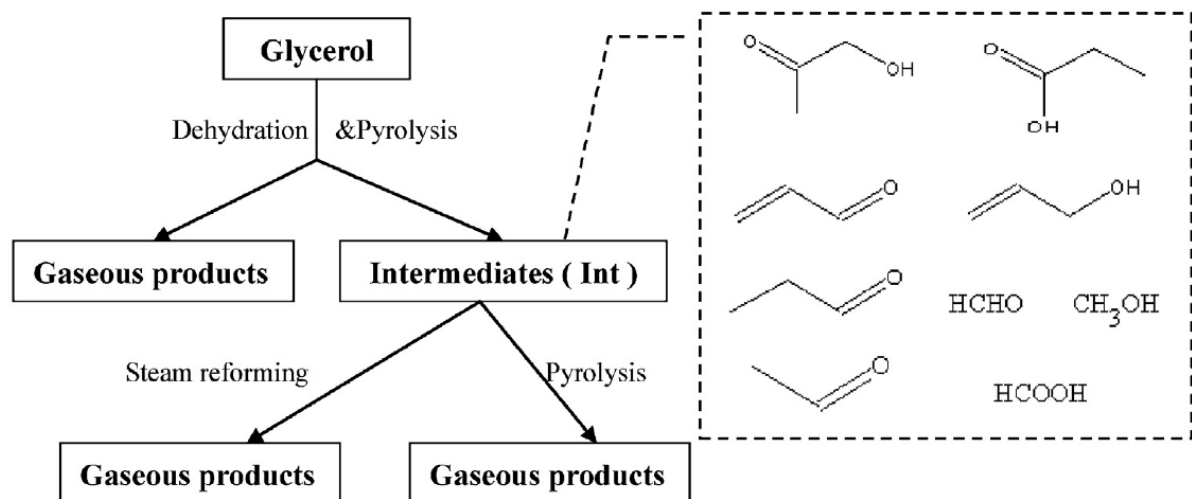


Figure 3.9 – Simplified reaction pathways of SCWG of glycerol [57].

Possible intermediates coming from the SCWG of glycerol are water-soluble products like acetaldehyde, propionaldehyde, acrolein, ally alcohol, hydroxyacetone, propanoic acid, methanol, formic acid, formaldehyde and unreacted glycerol, as evidenced by the experiments made by May et al. [58] and Bühler et al. [59].

Guo et al. [57] noticed that when glycerol was mixed with preheated water and further heated in the reactor, dehydration and pyrolysis took place. When the temperature was high enough, dehydrated three carbon atoms compounds (e.g. hydroxyacetone) were pyrolyzed, producing one and two carbon atoms compounds (e.g. acetaldehyde and formaldehyde). Moreover, glycerol C-C bonds could break in this phase, producing some gas as  $H_2$ ,  $CO$  and  $CO_2$ .

The intermediates produced gases undergoing steam reforming or pyrolysis reactions. Only a little amount of molecular fragments can be directly steam reformed easily.

Eventually, WGSR and methanation reactions occurred between the gases produced.

### ***3.3. Influence of biomass composition***

As outlined in the first chapter, lignocellulosic biomass is made approximately 40-55% of cellulose, 15-35% of hemicellulose and 20-40% of lignin.

The composition of biomass is a determining parameter since it affects the reaction pathways and the composition of the final product. Lignin or ash and protein content, for example, can increase or decrease the hydrogen yield.

This paragraph examines how the different components affect the final products of supercritical water gasification of biomass.

#### ***3.3.1. Cellulose and hemicellulose influence***

Yoshida et al. [60] demonstrate that cellulose supports the hydrogen production more than hemicellulose (modelled with xylan). A possible reason is that cellulose has a larger hydrogen content. According to the authors, there is no interaction between these two components, but they react with lignin by giving hydrogen for lignin splitting.

#### ***3.3.2. Lignin influence***

Different authors conducted studies with mixtures of lignin, xylan and cellulose. By using this mixture, it has been confirmed a decrease of the gas yield than using the same mixture without lignin. In particular, both  $H_2$  and  $CH_4$  yields are lower than expected from experiments with the pure components. This suggests that degradation intermediates from cellulose and xylan react with lignin reducing the  $H_2$  yield.

Firstly, low molecular weight fractions (e.g. phenolic compounds and formaldehyde) are produced by hydrolysis of the main structure of lignin. Then, these compounds polymerize into heavier compounds leading to char formation [55].

The type of lignin is important as well, different studies demonstrated that the char amount of hardwood is lower than the char production of softwood.

### 3.3.3. *Proteins influence*

In studies of model compounds containing proteins, a lower gas yield has been observed. Kruse et al. [61] performed an experiment in supercritical conditions with phyto, a real biomass rich in carbohydrates, and zoo, a real biomass rich in proteins. The latter showed lower gas yields and severe corrosion of the reactor. This suggests the formation of free radical scavengers via a Maillard reaction. Free radical scavengers are quite stable, not reactive enough to start a free radical chain reaction, which, thus, reduce the gas yield. Amines, formed by the degradation of proteins and splitting of carbohydrates, react with each other producing heterocyclic compounds that easily form stable free radical cations acting as free radical scavengers.

### 3.3.4. *Lipids influence*

There are few studies about the influence of lipids in SCWG of biomass. Holliday et al. [62] made some experiments by using three types of vegetable oils in sub- and supercritical conditions.

In supercritical water, thermal degradation to fatty acids via decomposition, pyrolysis or polymerization occurred. Free radical splitting can be considered as the main decomposition mechanism, leading to the production of many different compounds.

### 3.3.5. *Salts influence*

Matsumura et al. [63] studied the influence of an alkali salt ( $Na_2CO_3$ ) on the degradation of cellulose. They found that with an alkali salt the degradation of cellulose begins at lower temperatures. Besides, the degradation of sugars is promoted, leading to higher yields of gas and oil. Finally, coke formation from oil is inhibited, which means higher oil yields. Without sodium carbonate, the main product was char, while in the presence of it the main product was oil.

The most important aspect is that alkali salts catalyse the WGS reaction [64].

Several studies, conducted by using different types of reactors (batch, tubular, CSTR), investigated the influence of  $K_2CO_3$  and  $KHCO_3$  in supercritical conditions [42]. The authors observed higher yields of  $CO_2$  and  $H_2$  and low quantities of  $CO$  were present after the reaction. In addition, the gas yield increased, while the char/coke yield decreased. They detected a slightly increase of yields of phenols and a little decrease of the amount of furfurals produced, probably because in this acid-catalyzed reaction,  $KHCO_3$  acts as a basic compound reducing the reaction rate.

### 3.4. Catalysis

In order to make SCWG feasible, the reduction of its energy demand is required. Catalysts can be used to reduce the temperature and pressure needed to sustain the reaction. They are required to gasify reactive intermediates produced by hydrolysis and dehydration of the feedstock. Gasification of intermediates needs to be fast enough to avoid the formation of polymeric materials and reducing, in this way, the production of char.

A good catalyst is supposed to break the carbon-carbon bonds and disassociate water to produce reactive  $O$  and  $OH$  on its active surface. These radicals, by bounding with adsorbed fragments of organic compounds, produce  $CO$  and  $CO_2$ , while the adsorbed H atoms combine to produce  $H_2$ . Besides, a good catalyst is supposed to support the achievement of chemical equilibrium for WGS reactions and hydrogenation of  $CO$  and  $CO_2$  to  $CH_4$  and  $H_2O$  [65].

Catalysts are used to increase both the rate of a chemical reaction (activity) and to guide the distribution of products towards the desired composition (selectivity). They can be either heterogeneous or homogeneous.

In SCWG the walls and the corrosion products of the reactor (metallic ions like  $Ni$ ,  $Fe$  and  $Cr$ ) can act as heterogeneous catalysts, while alkaline salts present in the real biomass can act as homogeneous catalysts [66].

The basic behaviour of alkaline catalysts increases the rate of some reactions involved in gasification. With  $NaCO_3$ , for example, cellulose degradation begins at  $180^\circ C$ , accelerating the formation of liquid products from cellulose [67].

Alkaline salts promote the breakage of C-C bonds [68] and reduce the production of char increasing the gasification efficiency [69].  $K_2CO_3$ ,  $KHCO_3$ ,  $KOH$  and  $NaOH$  attack severely monomers and dimers of carbohydrates such as glucose, fructose and cellobiose [70]. Once gases have been produced, basic species support water gas shift reaction, increasing the yields of  $H_2$  and the total gas yield.

A drawback of alkaline homogeneous catalysts is the subsequent separation of them by the products, making the process less sustainable from the economic point of view [71].

Heterogeneous catalysts tested in SCWG of biomass are metals such as nickel, ruthenium and rhodium and carbonaceous materials.

Nickel-based catalysts are widely used since their performance is comparable to that of noble metals, but the price is fairly lower [72]. Moreover, nickel supports the hydrogenation reaction and the formation of  $H_2$  and  $CO$  from biomass.  $H_2$ , in turn, can produce  $CH_4$  and  $CO_2$  via methanation. Nickel catalyst suppresses tar formation and promotes the WGS, methanation and hydrogenation reactions, leading to a higher gasification efficiency, in particular of  $H_2$ ,  $CH_4$  and  $CO_2$  [72, 73].

Despite all these advantages, nickel-based catalysts have a drawback. Tar products or carbon deposition deactivate them, overall if it is an alumina supported catalyst [72]. Li et al. [74] demonstrated that, in SCWG of glucose, this problem could be resolved by producing high quantities of  $H_2$ , using co-precipitated  $NiMgAl$  catalysts, which avoid the formation of char that is responsible of the deterioration of the catalyst.

Noble metals such as rhodium, ruthenium and palladium have shown great performances with respect to hydrogen production in SCWG of biomass [75]. Ruthenium supports

hydrogenation reaction leading in this way to a lower  $H_2$  gas yield [76]. This catalyst has showed a higher activity than nickel and other metals as rhodium, palladium and platinum. This is probably due to the high activity of ruthenium in breaking C-C bonds [77], obtaining the gasification of active intermediates such as formaldehyde, which otherwise participate to cross-linking reactions with phenolic compounds to produce solid products [78].

Carbonaceous materials have been tested because of their high surface area, low costs, stability in supercritical water and fewer corrosion problems than metallic catalysts.

Xu et al. [43] studied the effects of spruce wood charcoal, coal activated carbon, macadamia shell charcoal and coconut shell activated carbon in supercritical water. They observed that the presence of a carbonaceous material increased the carbon gasification efficiency independently of its surface area. Nonetheless, with the higher surface area, the  $H_2$  yield was lower, since higher surfaces do not support WGS reactions.

A suitable combination of different catalysts might be more effective in SCWG of biomass. Chakinala et al. [79] gasified alga *Chlorella Vulgaris* with a mixture of ruthenium and  $TiO_2$ . A total conversion was possible at 600°C and only two minutes of residence time.

### **3.5. Influence of operation conditions**

The operation conditions influence considerably the thermodynamics and kinetics of SCGW process. The main parameters affecting the reaction are temperature, pressure, concentration of biomass and residence time.

Lu et al. [80] stated that the hydrogen production is affected, in order of influence, by these parameters: temperature, pressure, feedstock concentration and residence time.

Temperature has a strong effect on distribution products and kinetics. At high temperatures, decomposition is fast, solids tend to be consumed, while the formation of liquids and oils reach a maximum with a subsequent production of gases [81]. Moreover, the steam reforming of methane is shifted towards higher hydrogen gas yields, to the detriment of methane.

SCWG of glucose showed that, by increasing the temperature above 650°C,  $H_2$  and  $CO_2$  yields soared, while the CO yield decreased due to the WGS reaction [77]. The  $CH_4$ , instead, was independent.

Kruse and Dahmen [83] confirm that at high temperatures, the hydrogen production is higher, on the contrary, at low temperatures methane is preferred. Nevertheless, if the concentration is kept low, the production of hydrogen can be enhanced at low temperatures due to Le Châtelier principle.

The effect of the pressure can also be described by the Le Châtelier law at equilibrium conditions. The compression of the mixture shift the reactions towards the side with fewer molecules, while the expansion of the mixture shifts the reactions towards the side with more molecules.

Moreover, the dependence of gas yields on pressure is less evident than temperature. Increasing the pressure, the  $H_2$  yield decreases, while the  $CH_4$  yield increases, according to the Le Châtelier principle.

The effect of the pressure is in the molecular interactions, which depend on the density of water as well. Density influences the interaction of catalysts and reactants. At high water

densities, the breakage of lignin is supported with a consequent production of oil and gas, probably due to the hydrolysis [20].

It is assumed that a higher presence of water molecules in the volume unit, supports the formation of  $CH_4$  and  $CO_2$  from alkyl compounds [78, 83]. Moreover, Sato et al. [83] showed how the gasification efficiency decreases as the density increases above  $0,4 \frac{g}{cm^3}$ .

Concentration is an important parameter since by increasing it, often the gasification yield decreases. It plays a key role in the enhancement of selectivity. In low feedstock concentrations, the thermodynamic equilibrium is shifted towards the WGS reaction, since the content of water is high. On the other hand, the methane formation is favoured at low temperature, because of its exothermic behaviour.

Loppinet-Serani et al. [66] observed significant surges in the production of solids by increasing the concentration, sometimes with plugging events.

Kruse et al. [84] proved that high concentrations of biomass hinder the hydrogen production, promoting, instead, the phenol formation. However, for a commercial purpose, the process needs to be conducted at high concentrations, otherwise, it would be economically disadvantageous [85].

Residence time, along with temperature, provides information on the kinetics and, therefore, on the type of chemical reactions involved. In this work, in particular, the attention is focused on the influence of concentration and residence time of SCWG of glycerol.

Besides the operating conditions above investigated, another factor affecting the composition of the products is the heating rate. This is a significant parameter in SCWG, since it strongly affects the transition phase and, in case of slow heating, it favours heterogeneous conditions for hydrolysis. By increasing the heating rate, the critical point is fast overtaken, with a rapid dissolution of biomass and achievement of reaction conditions in pseudo homogeneous phase. This is the reason why the gas yields are higher with an increase in the heating rate [81].

Gasification of wood showed that low heating rates tend to support the formation of coke and char, with a production of  $CH_4$ , at the expense of  $H_2$  [70, 86]. In addition, in catalysed hydrothermal gasification, a reduction of catalyst deactivation is possible by increasing the heating rate.

Finally, homogeneous reactions have been observed in a diamond anvil cell with higher heating rates, while heterogeneous reactions with the interference of char and dissolved compounds occurred with lower heating rates [81].

### ***3.6. Influence of the type of reactor***

Most of the works present in the literature are conducted by means of batch and continuous tubular reactors.

The batch reactor is used in a discontinuous way, according to a definite sequence. Firstly, an initial loading of material at an initial time is required, the quantity of feedstock is determined so as to obtain the condition of pressure to be reached in the reactor according to the temperature of the system [87].

The reactor is then closed and heated up. Once the chemical reactions occurred, the reactor is turned off, opened, emptied and cleaned.

The reactor is usually equipped with a stirrer that guarantees the homogeneity of the mixture. The volumes of batch reactors are typically very small, with a large ratio surface/volume leading to an enhancement of the catalytic effect.

A batch reactor is preferred over continuous reactor when: the plant needs to work seasonally; the chemical reaction is very slow; fluids that can clog the reactor up are used; the reactor needs to produce a different range of products; the production is low and low flows of slurry are treated.

Another type of reactor is the CSTR (Continuous-flow Stirred-Tank Reactor). It is a continuous reactor made of a tank fed by a constant flow equipped with a stirrer.

The material of which the reactors are made have to be taken into account as well since, along with the corrosion degree, it affects the biomass decomposition in SCWG. Moreover, the material needs to endure high thermal stresses (creep resistance) and the tangential and radial stresses generated at high temperatures and pressures.

Mainly, the reactors for SCWG of biomass are made of Inconel (alloy of Ni, Fe and Cr), Hastelloy (alloy with molybdenum, chromium, iron and cobalt) and Stainless Steel like the grade 316, thanks to its corrosion resistance and mechanical properties [55].

Yu et al. [88] observed that in cellulose gasification, the hydrogen production with Inconel 625 was three times higher than the hydrogen production with Hastelloy, meaning that the WGS reaction is supported by the former material. However, corroded Hastelloy showed a slightly higher hydrogen yield, since it presents a higher catalytic activity.

Bjerre and Sørensen [89] compared different stainless steel reactors with different operation time in a process involving formic acid decomposition. Here, with the corroded reactor, a higher hydrogen production was observed as well. Indeed, seems that corrosion supports the catalysis of decarboxylation and WGS reaction. Yet, by investigating the influence of the surface-to-volume ratio of a Hastelloy C-276 on the reaction rate, it has been noticed that the effect of the reactor wall is negligible compared to the catalytic effect of water [90].

Castello et al. [91] confirmed the results of Yu et al. [88] by gasifying glucose and beech wood sawdust at different temperatures and residence times. With higher values of the latter parameter, the hydrogen production and selectivity in stainless steel was considerably higher than that of Inconel 625, while the methane production increased constantly in both reactors.

Ceramics have been studied by Richard et al. [92] because of their high chemical stability at extreme conditions. They proved that materials as Y-stabilized zirconia and alumina are not suitable for supercritical gasification and easily corrode under subcritical conditions. While SiC showed better performances. The latter was more stable in subcritical conditions, but still corroded in a supercritical environment. The authors state that graphite and glassy carbon, thanks to their low chemical reactivity and their resistance at high temperatures, are more appropriate. Nevertheless, they didn't take the mechanical stability into account.

### 3.7. Challenges

In spite of the advantages coming from the utilization of SCWG, there are still some challenges to overcome in order that such a technology can be placed in the market.

SCWG is not attractive for the industry mainly because of the very high processing costs. Therefore, only biomass with high disposal costs is an interesting feedstock [93].

Since this technology is too expensive, a possible use of it is in combination with other processes. It is possible for example integrating it in a bio-refinery process, with a solid fuel cell [94] or with a supercritical steam turbine. The latter, with an additional anaerobic digestion, turned out to be very promising from the  $CO_2$  footprint point of view [95].

An important point is the heat exchange for the energy efficiency, as already stated in the first chapter. Moreover, the heating rate should be high so as to avoid high char productions and to increase the gas yield. An interesting solution to this problem is to superheat only water by heat exchanger [96]. Afterwards, this water is mixed with biomass at the entrance of the reactor. By doing so, the biomass can have a high dry mass content.

Another important issue in the industry scale-up is the necessity to achieve high gas yields and high energy recover with high concentrations.

Biomass may include many different components and corrosion is a challenge for SCWG.

Kruizer et al. [97] studied the corrosion effect by using nickel, molybdenum, chromium and Inconel 625 at conditions similar to SCWG. They observed that nickel and molybdenum started to lose mass very quickly (only after 5 hours), as a consequence of the instability of the solid oxides in the high-temperature oxidizing solution. On the other hand, corruptions of Inconel 625 and chromium started at the grain boundaries. A reason, for Inconel 625, might be the presence of high concentrations of phosphorus and silicon.

Lastly, another problem is the salt deposition and plugging, especially in the combination with char. As already mentioned in the previous paragraphs, salts can be already present in biomass and act as homogeneous catalysts, promoting the hydrogen production. On the other hand, they can cause plugging, since, depending on the type of salts, the solubility is low in the supercritical water. The kinetics and geometry of the reactor can play a key role in the plugging phenomenon. Alkali salts, for example, can easily pass through a tube, while other salts do not [98].

Mostly, the salts are found in liquid effluent. It would be useful to separate salts from water and send them back to the fields, closing the nutrition cycle of biomass.

Kruse et al. [99] developed a salt-water system able to catch other salts and avoid plugging. The sodium and other alkali salts separated can be further used to produce fertilizers.

## 4. Experimental setup

The aim of the following chapter is to list and analyze all the instruments and equipment present in the laboratory.

A preliminary overview is provided concerning the general mechanisms of the process and the schematic of the plant.

A deep analysis is then carried out in order to describe the physical structure and the functions of every component, including also the related software and all the parameters of interest.

### 4.1. SCWG plant and equipment

The SCWG of the biomass is realized through a continuous tubular flow reactor. The laboratory-scale is located in Turku, at the Process Design and System Engineering Laboratory at the Åbo Akademi University.

The picture below shows the whole experimental setup (figure 4.1).

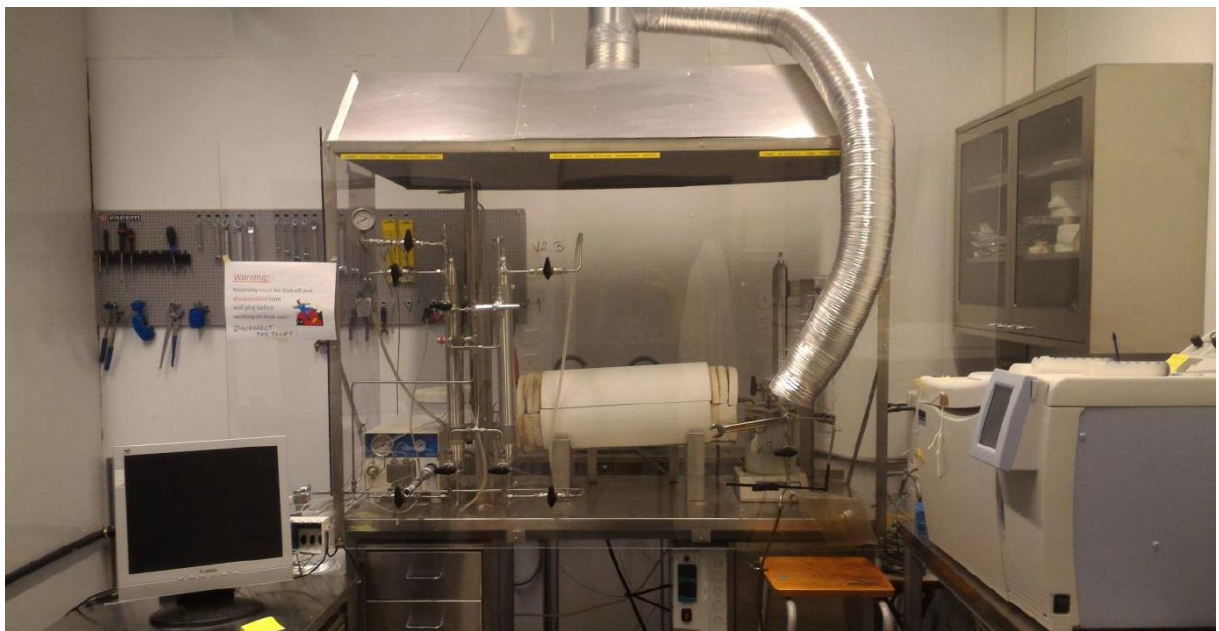


Fig. 4.1: SCWG plant in laboratory scale [courtesy of Process Design and System Engineering Department].

Biomass is mixed and stirred with water beforehand. The mixture is then introduced by means of a big syringe into the cylinder.

The earlier pressurized solution of biomass and water is introduced into a system at very high temperatures in order to reach the supercritical conditions, skipping the evaporation step and saving, therefore, the related latent energy.

The solution is pushed by pressurized nitrogen, with a constant flow rate guaranteed by a mass flow controller, which monitors and controls the nitrogen flow.

The outgoing stream is then cooled down in a bowl containing water at ambient condition in which the pipe is submerged.

A back-pressure valve, situated downstream of the cooling system, allows the stream to regulate its pressure.

Finally, the gas and liquid are collected into a plastic bag at ambient conditions.

A shield of Plexiglas, with a thickness of 6mm, has been installed in order to preserve the operator's conditions during the experiments.

Furthermore, an additional screen is present inside the room in order to control and monitor all the operating parameters in real time during the experiments. Besides, the software warns the operators if the safety operational limits are exceeded.

Figure 4.2 illustrates the plant layout, including the control devices and valves.

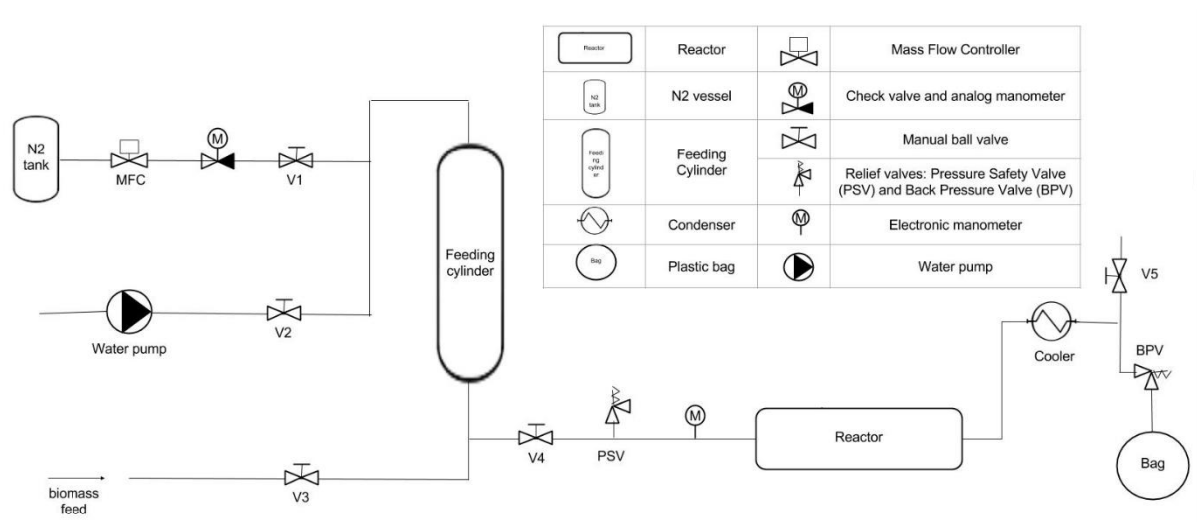


Fig. 4.2: SCWG plant layout [100].

#### 4.1.1. Comparison with the previous configuration

The previous experimental setup, with which Lucca [102], Magnano [103] and Saqlan [104] worked in the same laboratory, was slightly different. The plant worked without the nitrogen compression system, used in the current setup to push the feedstock into the reactor, and without the mass flow controller. Nevertheless, without these two little modifications, the operation mode was quite different as the reactor worked in semi-batch mode. In this way, the system allowed partial filling of reactants with the flexibility of further additions in time.

Figure 4.3 shows the layout of the previous setup. As it is possible to see, the lane dedicated to the nitrogen flow is missing, however, the role of the valves has not changed.

In the previous setup, the feedstock in the feeding vessel was pushed by the water pump at a higher pressure than the operating pressure.

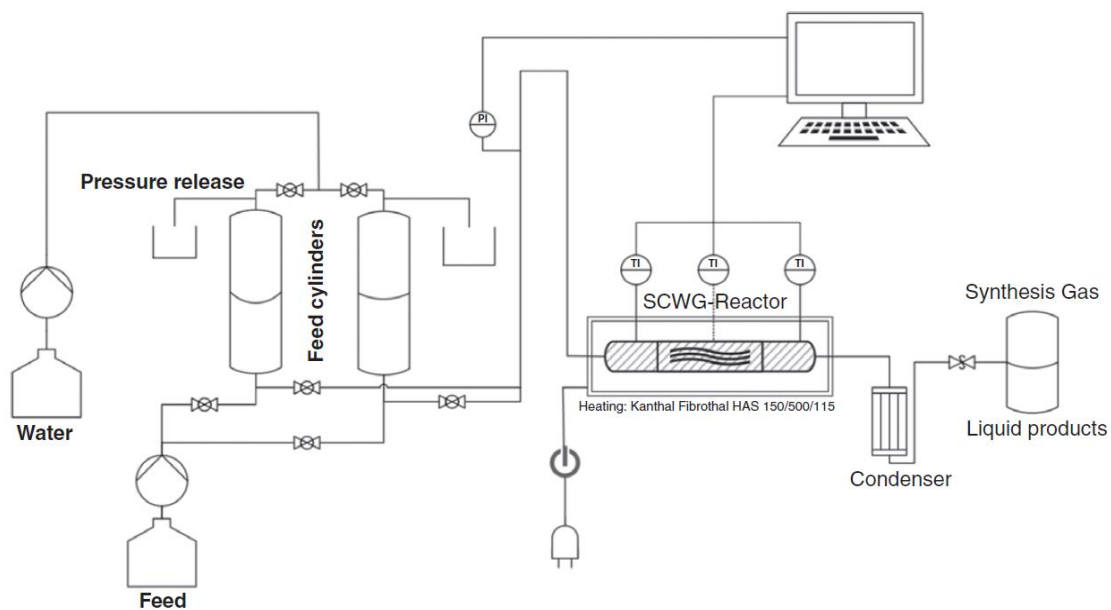


Fig. 4.3: SCWG plant layout (previous setup) [105].

## 4.2. Nitrogen tank

The nitrogen vessel used in the plant is a patented product, GENIE<sup>®</sup>, designed by AGA, a member of the Linde Group. It is a steel lined carbon fibre wrapped pressure vessel, with a nominal capacity of 20 l and a nominal pressure of 300 bar. It is encased in a tough, recyclable High-Density Polyethylene (HDPE) jacket and equipped with gas identification rings, a detachable wheelbase and a telescopic handle. An alarm sounds when contents are low. The tank is equipped with a regulation valve attached to the exit nozzle, so as to regulate the outlet pressure according to the user's request.

As illustrated in figure 4.4, on the top of the valve there are two manometers indicating the pressure levels. The left manometer displays the pressure of the gas inside the tank, while the right manometer shows the gas pressure in the output.

During the experiments, the regulation valve was set to provide an output pressure of 280 bar.



**Fig. 4.4:** Nitrogen tank.

### ***4.3. Mass flow controller***

The mass flow controller (figure 4.5) is the other modification applied to the previous setup in order to switch to a continuous operation mode as it fixes the mass flow rate of nitrogen.



**Fig. 4.5:** Mass flow controller.

The component used in this setup is the EL-FLOW mass controller F-231M, designed by the Bronkhorst High-Tech. This model is suitable for accurate measurements and control of flow ranges between 0,01-0,5 l<sub>n</sub>/min and 0,2-10 l<sub>n</sub>/min at high operating pressures (up to 400 bar).

In these experiments, the mass flow controller will be set at 0,125, 0,250 and 0,375 l<sub>n</sub>/min of nitrogen and, thanks to a normally closed control valve, with a pressure drop of just 6bar between inlet and outlet, which can respectively support 300bar and 294bar.

The mass flow controller consists of a thermal mass flow sensor, a precise control valve and a microprocessor-based pc-board with signal and Fieldbus conversion. As a function of a setpoint value, the flow controller swiftly adjusts the desired flow rate.

The control valve is a proportional, electromagnetic control valve with extremely fast and smooth control characteristics.

The kernel of the thermal mass flow controller is the sensor which consists of a stainless steel capillary tube with resistance thermometer elements.

As it is possible to see from figure 4.6, a part of the gas flows through this bypass sensor and is warmed up by heating elements.

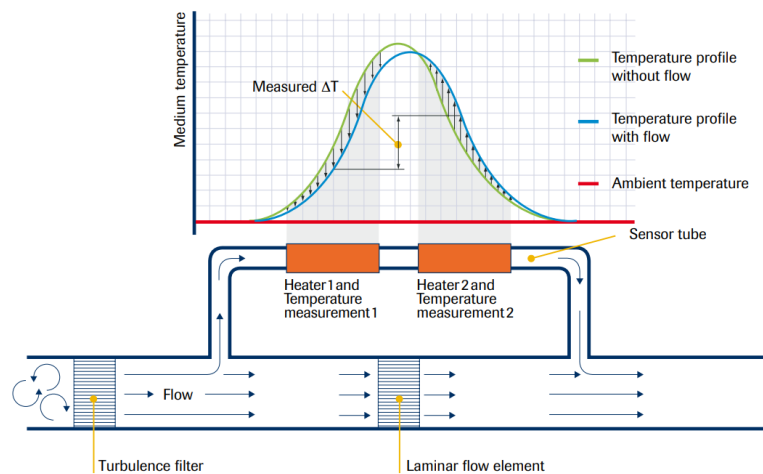


**Fig. 4.6:** Thermal sensor.

Consequently, the measured temperatures  $T_1$  and  $T_2$  separate gradually. The temperature difference is directly proportional to mass flow through the sensor. In the main channel a, patented laminar flow element is applied, consisting of a stack of stainless steel discs with precisionetched flow channels. Thanks to the perfect flow-split the sensor output is proportional to the total mass flow rate according to the following relationship:

$$\Delta T = kcp\dot{\varnothing}_m \quad (4.1)$$

Where  $\Delta T$  is the temperature difference,  $k$  is a constant,  $c_p$  is the specific heat and  $\dot{\varnothing}_m$  is the mass flow rate.

#### **4.4. Pipes and valves**

The main components of the system are connected by stainless steel pipes, produced by Swagelok. The model is SS-T6M-S-1.5M-6ME-S and is made of SS316L, with an outer and inner diameter of 6 and 3 mm respectively. They are designed so as to withstand pressures of 420 bar.

Besides, a set of ball valves made of stainless steel has been installed in order to control the operations during the experiment, load the biomass feed, isolate the reactor during the heating phase and clean the system after the experiment. The model of the valve is SS83KS6MM produced by Swagelok. They are designed to withstand a pressure of 68,9 bar at 121°C and a room pressure of 413 bar at 37°C.

Moreover, two outlet backpressure-regulated valves were installed in order to maintain the desired pressure inside the reactor and manage the collection of the products.

Eventually, in order to make the system safer, a pressure safety valve was installed in the branch upstream of the reactor and set at 300 bar.

Figure 4.7 and 4.8 show respectively the disposition of the pipes and valves, and a view section of the valve, while figure 4.9 shows the backpressure valve.



**Fig. 4.7:** Ball valves disposition.

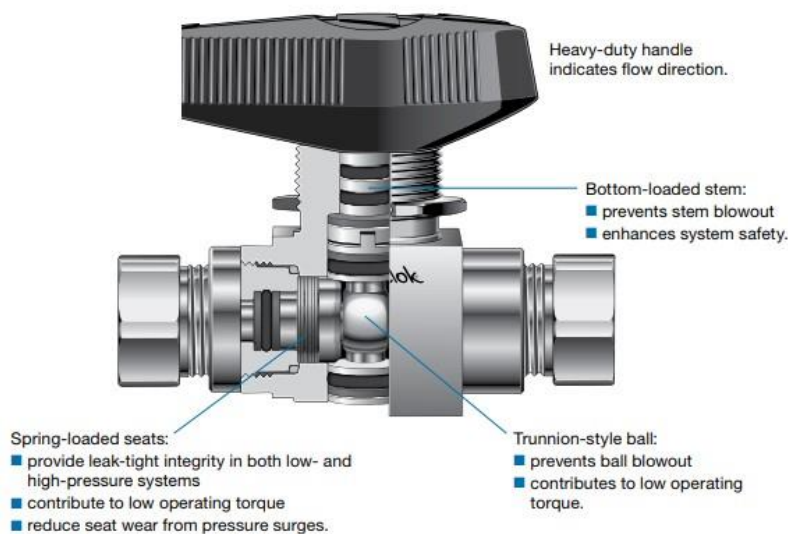


**Fig. 4.8:** View section of the valve.



**Fig. 4.9:** Backpressure valve.

#### **4.5. Pump**

The pump (figure 4.10) is a WellChrom Pneumatic Pump K-1900, produced by Knauer and designed for solvent delivery in process chemistry, column packing or preparative chromatography. It is a volumetric pump with a double piston design, powered by compressed air.



**Fig. 4.10:** Pump.

The pump is used to fill the plant and the reactor with water, before every experiment, in order to avoid feeding the empty and hot reactor which can cause thermophysical damages to the pipes and the reactor. Moreover, by doing so, the plant is pressurized and ready for the injection of the feed coming from the cylinder.

This particular device has been developed for constant pressure applications. The Pneumatic Pump K-1900 can be configured with four different pump heads (100 ml, 250 ml, 500 ml, 1000 ml) to fulfil the most pressure and flow rate requirements. Pump heads can easily be changed by loosening only four screws. In these experiments, the head of 250 ml has been used, which allows a maximum flow rate of  $500 \frac{ml}{min}$  at minimum back pressure, a minimum back pressure for solvent delivery of 670 bar and a maximum allowed air pressure of 7 bar.

Figure 4.11 shows the characteristic curve of the pump, which links the volume flow rate and the liquid flow rate at different air pressures, regulated by a knob.

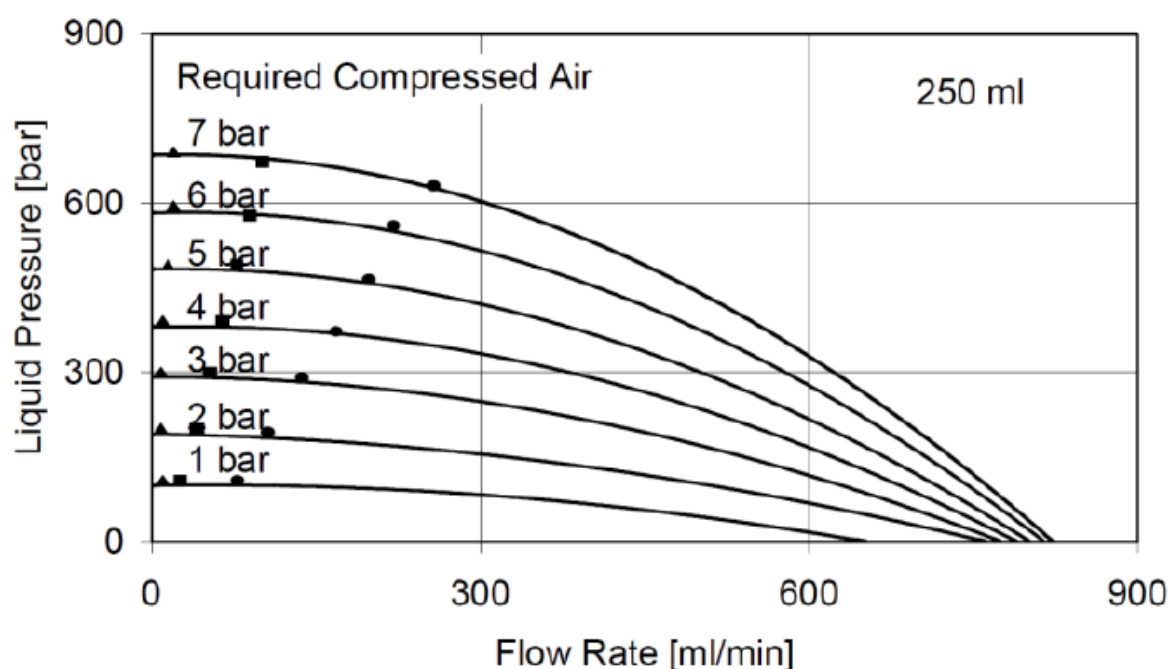


Fig. 4.11: Characteristic curve of the pump.

The delivery volume depends on the required air pressure and the loss of pressure along the column or any device that generates back pressure.

#### 4.6. Feed cylinders

The feed cylinders are a DOT-3A 5000 model produced by Swagelok (figure 4.12). They are made of stainless steel 316L, with a volume of 500 ml and can support pressures up to 344 bar at a temperature ranging from -53 °C up to 100 °C. They are equipped with a rupture disc unit, which protects sample cylinders from overpressurization by venting the cylinder contents to the atmosphere.

The main function of the feed cylinders is to ensure the feeding of the reactor avoiding the direct use of the pump, which could face many problems and issues related to plugging and corrosion phenomena.

In order to perform the experiments, one cylinder is enough, however, the second cylinder is required to test mixtures between different feedstocks. Moreover, the presence of a second cylinder facilitates eventual cleaning and start-up operations.

The experiments are performed by previously feeding the mixture in the bottom part of the cylinder by opening the bottom valve. In this phase, the venting valve is open too, in order to let the liquid mixture exit the cylinder when it is full.

Once the cylinder is filled, the top valve is open and the mixture is pushed into the reactor by the  $N_2$ . During the normal operation, only the tip valve and the feeding valves are open.

When the tests are terminated, a cleaning cycle is performed by pumping distilled water from the top, in order to remove the eventual un-reacted feed that can compromise the results of the following experiments.



**Fig. 4.12:** Feed cylinders.

## 4.7. Reactors

The experiments have been conducted by using two reactors with the same shape but made of different materials, as shown in figure 4.13.

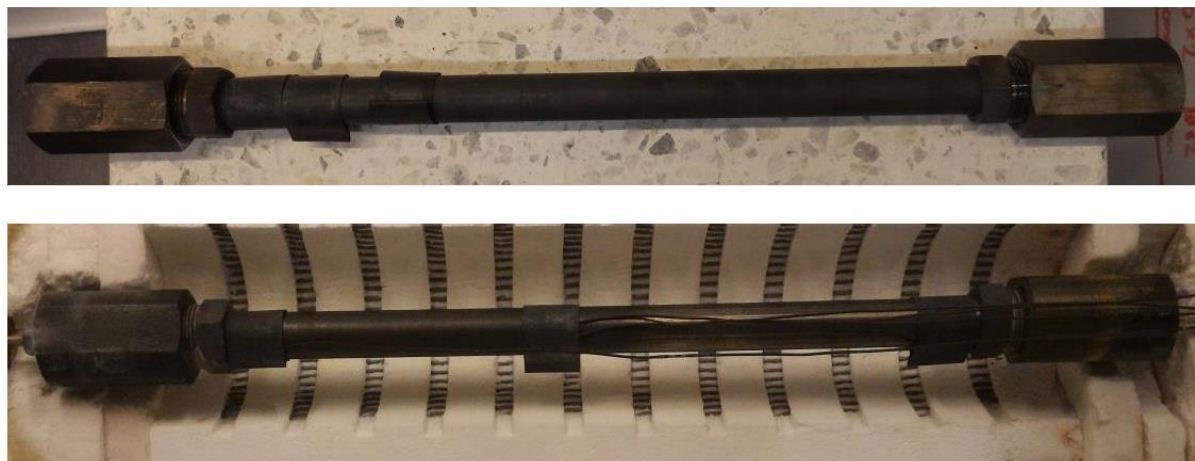


**Fig. 4.13:** Stainless steel reactor (on top) and Inconel 625 reactor (on bottom).

The first reactor is made of stainless steel 316L while the second reactor is made of Inconel 625, which is an alloy of nickel and chromium. Both of them are developed by High-Pressure Equipment Company. Stainless steel is one of the most popular manufacturing material for chemical plants. It is relatively cheap and it can bear the severe reaction conditions of these experiments (600°C and 250 bar). Inconel® 625 is a non-iron alloy made of nickel, chromium and molybdenum. Nickel-alloys are generally used in hydrothermal processes since they show great mechanical resistance to severe reaction conditions. Furthermore, they also have sufficient high chemical resistance to corrosion. However, Inconel® 625 is much more expensive than stainless steel, making its usage particularly onerous.

Even though the reactor components and the shape of the two reactors are the same, the dimensions are different. The stainless steel reactor, indeed, has a volume of 77 ml, whereas the Inconel 625 reactor has a volume of 92 ml.

Although the stainless steel reactor has a slight influence on the reactions, it will be indicated from now on as the non-catalytic reactor, while the Inconel 625 is considered as the catalytic reactor.

The section of both reactors is illustrated in figure 4.14, whereas table 4.1 reports all the components and materials.

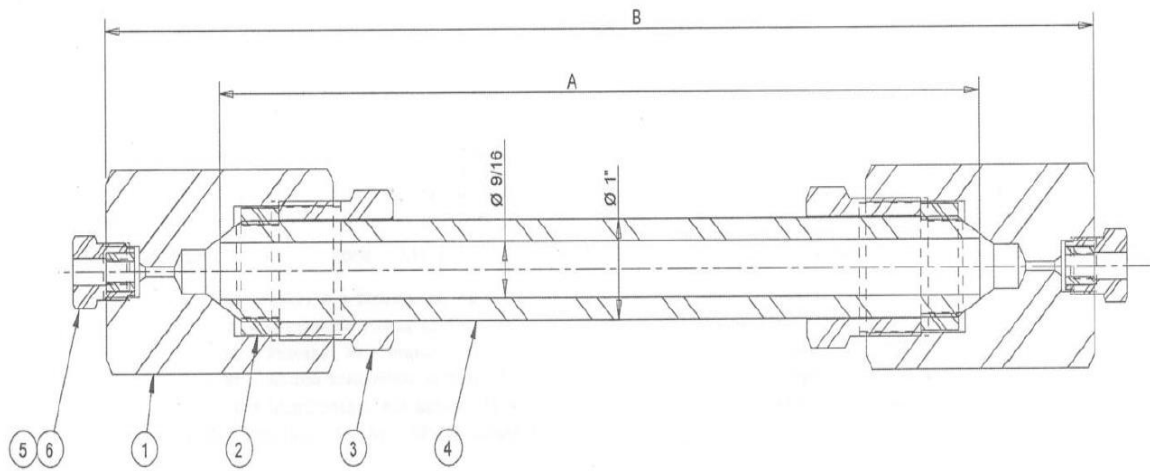


**Fig. 4.14:** Section of the reactor.

BILL OF MATERIAL				
ITEM	QTY	DESCRIPTION	PART NO.	316 SS
1	2	Coupling	20-21LF16HF4	316 SS
2	2	Collar	20-2L16	316 SS
3	2	Gland	20-2LM16	316 SS
4	1	Nipple	SEE TABLE	316 SS
5	2	Collar	60-2H4	316 SS
6	2	Gland	60-2HM4	316 SS

**Table 4.1:** Components and materials of the reactors.

The reactor is mainly constituted of a tube, where the thermochemical reactions take place, sealed at the extremities with two nuts, which open if the pressure exceeds a certain limit.

Table 4.2, finally, shows the elemental composition, features, advantages and disadvantages of stainless steel 316L and Inconel 625.

Material	Stainless steel 316	Inconel 625 (High Nickel alloy containing Chromium)
Advantages	<ul style="list-style-type: none"> <li>negligible catalytic effect;</li> <li>resistant to high pressure;</li> <li>resistant to high temperature.</li> </ul>	<ul style="list-style-type: none"> <li>Chromium increases the corrosion resistance;</li> <li>resistant to high pressure;</li> <li>resistant to high temperature;</li> <li>catalytic effect controlled [25]: <ul style="list-style-type: none"> <li>acceleration of methanol decompos. to CO and H<sub>2</sub>;</li> <li>acceleration of water shift reaction to CO<sub>2</sub> and H<sub>2</sub>;</li> <li>decrease of CO conc.</li> </ul> </li> </ul>
Disadvantages	<ul style="list-style-type: none"> <li>poor resistance to corrosion (especially in oxygen, halides or chloride presence). [26]</li> </ul>	<ul style="list-style-type: none"> <li>Loss in ductility at high temperature (600-800°C at 25MPa) [27].</li> </ul>
Treatments before shipment	<ul style="list-style-type: none"> <li>Pressure test at 134 MPa for 1 minute.</li> </ul>	<ul style="list-style-type: none"> <li>Pressure test at 93 MPa for 5 minutes.</li> <li>Heat test at 870 °C for 30 minutes.</li> </ul>
wt% C	0.01	0.037
wt% S	0.02	<0.0003
wt% Mn	1.48	0.04
wt% Si	0.65	0.07
wt% Cr	16.54	20.89
wt% Mo	2.04	8.51
wt% Co	0.14	0.1
wt% Fe	69.4	4.53
wt% Cu	0.28	0.03
wt% Ni	10.20	61.36
wt% P	0.022	0.006
wt% Ti	-	0.31
wt% Al	-	0.28
wt% B	-	0.003
wt% Zr	-	<0.01
wt% Cb	-	3.78
wt% Ta	-	<0.01
wt% W	-	0.06
wt% V	-	0.01

**Table. 4.2:** Features, advantages, disadvantages and elemental composition of stainless steel 316 and Inconel 625.

#### 4.8. Heating system

The heating system is constituted of a cylindrical insulated case with embedded electrical resistances positioned in the inner wall of the case. The reactor, as shown in figure 4.15, is placed within this structure and heated up by Joule's effect.



**Fig. 4.15:** Heating system

The model of the heating system is the Fibrothal HAS 100/500/114, produced by Kanthal. It is 50 cm long, with a resistance  $R_{20}$  of  $9,78 \Omega$  and a voltage of 115 V, for a maximum power of 2600 W.

The insulation material is a ceramic fibre able to withstand a maximum temperature of 1150 °C, with a thermal conductivity varying between 0,10-0,21W/(mK) with a temperature ranging from 400 up to 800°C.

The electronic control unit allows controlling and regulating the heating rate and maintaining a constant temperature. In this case, in order to avoid thermal shocks and deformation of the metal, the heating rate is set to  $140 \frac{^{\circ}\text{C}}{\text{h}}$ .

#### **4.9. Cooling system**

The cooling system is made of a receptacle full of water under ambient conditions. The hot flow, exiting the reactor, pass through a pipe immersed in the receptacle, as figure 4.16 shows.

There is no need for an additional heat exchanger coil since the mass flow rate is low and the amount of water at ambient conditions is enough to condensate the flow.



**Fig. 4.16:** Cooling system

#### ***4.10. Pressure and temperature sensors***

The pressure inside the plant is measured by means of a pressure sensor, placed on one of the two cylinders, as shown in figure 4.17.



**Fig. 4.17:** Pressure sensor.

The operating range of the pressure sensor is from 0 up to 400 bar, with an accuracy of  $\pm 0,5\%$  as a per cent of full scale, thus 2 bar, and with a deviation of  $\pm 0,2\%$  as a per cent of full scale on a yearly basis, which is 0,8 bar.

In order to control the temperature and check whether the reaction occurs in supercritical conditions or not, temperature measurements are necessary. They are made by using K-Type Chromel-Alumel thermocouples, with a measurement range from  $-200^{\circ}\text{C}$  up to  $1260^{\circ}\text{C}$  and with a sensitivity of  $41 \frac{\mu\text{V}}{^{\circ}\text{C}}$ .

The thermocouple junctions are attached, by means of metallic clips, to the inlet, the middle and the outlet of the reactor, as illustrated in figure 4.14.

The temperature measurement at the inlet of the reactor is the most important since the entry of the feed into the reactor causes a decrease in temperature. Therefore, it is crucial to check if the inlet temperature does not fall below the critical point.

Finally, the check and the control of temperature is made through a software called LabView, able to acquire and store both the temperature and pressure measurements. This software allows controlling directly the temperatures and the pressures during the experiment through a user-friendly graphical interface.

#### ***4.11. Collection of effluents and sampling***

The collection of the effluents is made by using a plastic bag, Tedlar<sup>®</sup>, attached to the outlet nozzle downstream the relief valve, as shown in figure 4.18.



**Fig. 4.18:** Collection system.

Afterwards, the volume of the bag and, thus, of the gas is measured and then the gas is extracted by a syringe. The liquid left in the bag is subsequently extracted for further analyses.

The way of cooling and depressurizing the effluent can modify the final composition because of the solubility of the gases in the liquid phase. Here, the collection is made at ambient conditions since at high pressure the  $CO_2$  is soluble in the liquid phase.

#### ***4.12. Energy measurement***

The electrical energy required to heat up the reactor and to keep the set-point temperature is measured by an electricity meter, as shown in figure 4.19.



**Fig. 4.19:** Electricity meter.

This instrument, placed between the socket and the power plug of the furnace, provides the energy spent in a certain period of time as well as the instantaneous power.

#### ***4.13. Monitoring system and data acquisition***

In order to monitor the heating rate, temperature and pressure of the system measured by the sensors, a dedicated software called LabView has been used, with a graphical user interface which displays data on a screen as shown in figure 4.20. The data acquisition system is the NI DAQ mix from National Instruments and the values of temperatures and pressures are automatically saved by the software.

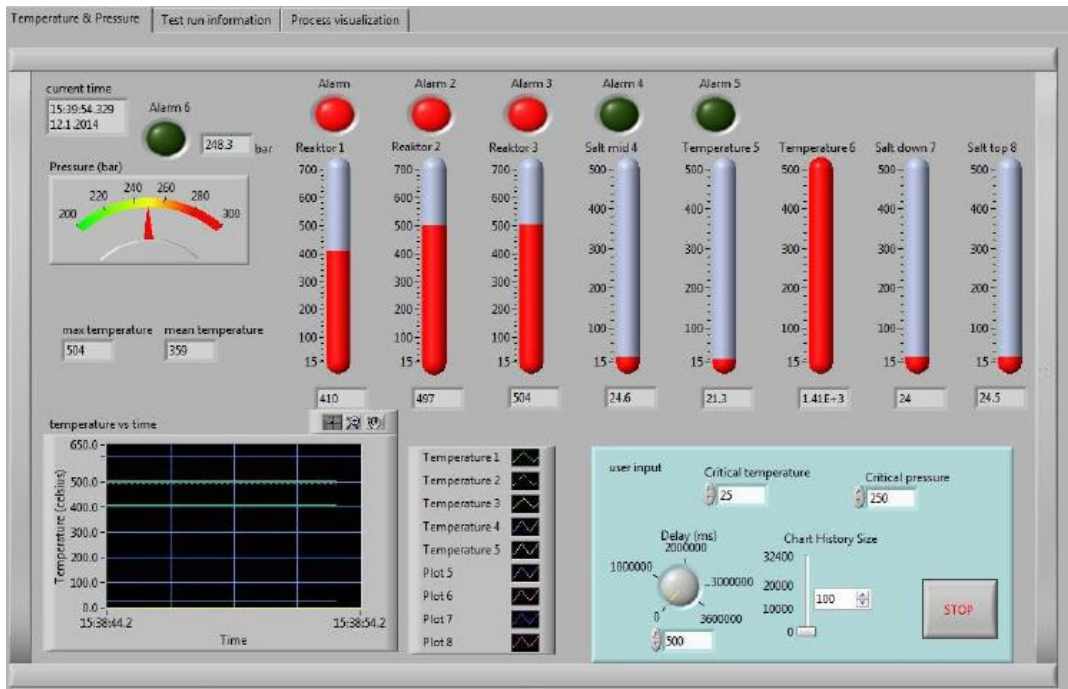


Fig. 4.20: Graphical interface for the temperature and pressure monitoring.

As can be seen, the pressure is displayed along with the inlet, middle and outlet temperatures. Additionally, an alarm and the safety valve are triggered by an increase of pressure above 300 bar.

A further software is used to regulate and monitor the volumetric flow rate of the nitrogen line. A graphical user interface, FlowView 2 V1.23, allows setting the volume flow rate, while another interface, FlowPlot V3.34, displays the set-point flow rate (in red), the degree of opening valves (in yellow) and the actual volume flow rate (in green). Figure 4.21 shows both graphical interfaces.

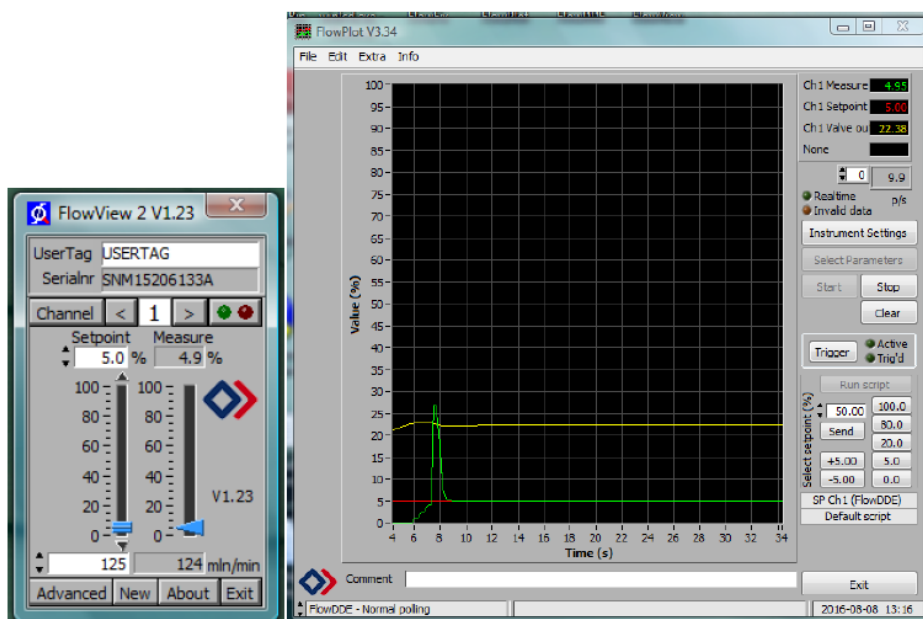


Fig. 4.21: Graphical interfaces for the regulation and control of the volume flow rate.

During the start-up phase of the system, the pressure on the nitrogen line has to be controlled and regulate by changing the volume flow rate of the nitrogen. The control is done with the help of a manometer installed close to the top valve.

## 5. Analytical equipment

The aim of this chapter is to fully describe the analytical instruments used in these experiments and present in the current experimental setup.

Firstly, a detailed description of the gas chromatograph used to analyse the composition of the final product of each experiment, is given along with the procedures for the data acquisition and the calibration of the device.

Lastly, a brief description of the other analytical instruments, present in the current setup and useful for further analysis, is provided as well.

### 5.1. Gas chromatography

The analysis of the gas product is made by using a Claurus 500 GC produced by PerkinElmer<sup>®</sup>, a fully automated gas chromatograph shown in figure 5.1.



Fig. 5.1: Claurus 500 GC gas chromatograph.

Gas Chromatography is an analytical separation technique used to analyse volatile substances in the gas phase. The main component is a narrow tube known as *column*, through which the sample flows carried out by a carrier gas, called the *mobile phase*, at different rates depending on their various chemical and physical properties and their interaction with a specific column filling, called the *stationary phase*.

The mobile phase is a chemically inert gas, such as helium, or an unreactive gas like nitrogen, necessary to carry the molecules of the sample through the column typically heated by means of an oven where the temperature of the gas can be controlled.

The stationary phase is either a solid adsorbent, termed gas-solid chromatography (GSC), or a liquid on an inert support, termed gas-liquid chromatography (GLC), inside the column.

Figure 5.2 illustrates the basic scheme of a gas chromatograph.

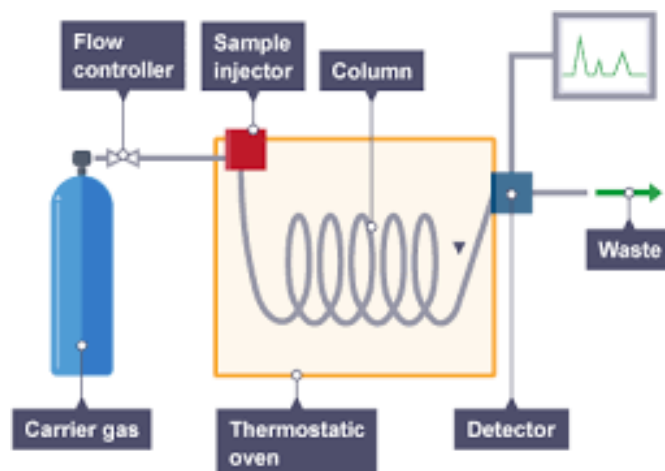


Fig. 5.2: Scheme of a typical gas chromatograph.

A solution gas sample is injected, usually using a syringe, into the head of the column through a sample injector, where the solution is vaporized. The sample then is carried by the carrier gas, which spreads the sample molecules through the column. The carrier gas used for the Claurus 500 GC in this setup is nitrogen, with a backup of a helium tank.

The absorption of the sample molecules, either on the column walls or on the packing materials in the column, inhibits its motion. The speed of progress of the gas along the column depends on the strength of absorption that, in turn, depends on the material of the stationary phase and the type of molecules.

Every compound of the sample has a different rate of progression and it is separated from the others as they advance along the column until they reach the end. The time employed by the different compounds to reach the end of the column is called retention time.

The oven is required to control the temperature of the column. It can operate in isothermal programming, where the temperature of the column is held constant throughout the entire operation, or in temperature programming, where the temperature is either increased continuously or in steps as the separation proceeds.

Finally, the gases are detected using a detector providing a quantitative measurement of the components of the mixture as they elute in combination with the carrier gas.

Every detector is characterized by the particular property of the gaseous mixture exploited for the detection. A wide choice of detectors optimized for sensitivity and selectivity is available for the Clarus 500 GC.

The Flame ionization (FID) detector is the most applicable and the most widely used. In a FID, the sample exiting the column is sent to an air-hydrogen flame. At the high temperature of the flame, the sample undergoes chemical decomposition or pyrolysis through intense heating. Pyrolyzed hydrocarbons release ions and electrons. A high-impedance picoammeter measures the current carried by the electrons to monitor the elution of the sample.

The FID detector is unaffected by flow rate, non-combustible gases and water. These properties lend FID high sensitivity and low noise. The unit is both reliable and relatively easy to use. However, this technique destroys the sample and requires flammable gas.

Another option for the Claurus 500 GC is the Electron-capture detector (ECD), a highly selective detector detecting organic compounds with moieties such as quinones, peroxides, halogens and nitro groups and gives little to no response for all other compounds. Therefore, this method is suitable for applications where traces of chemicals such as pesticides are to be detected and other chromatographic methods are unfeasible.

The advantages of ECDs are the high sensitivity and selectivity towards certain organic species with electronegative functional groups. However, the detector has a limited signal range and it is potentially dangerous because of its radioactivity. Moreover, the signal-to-noise ratio is limited by radioactive decay and the presence of  $O_2$  within the detector.

Thermal conductivity detector (TCD), the oldest detector developed for gas chromatography, is another possible option for the Claurus 500 GC. It works by measuring the change of thermal conductivity in carrier gas induced by the presence of the sample, which has a different thermal conductivity from that of the carrier gas. The moderately simple design consists of an electrically heated source that is maintained at constant power. The temperature of the source depends on the thermal conductivities of the surrounding gases, while the resistance within the wire depends on temperature, which is dependent on the thermal conductivity of the gas.

TCDs usually employ two detectors, one is used as the reference for the carrier gas and the other monitors the thermal conductivity of the carrier gas and sample mixture.

The advantages of TCDs are: broad application to inorganic and organic compounds; the simplicity of use and the ability of the sample to be collected after separation and detection. By contrast, TCD is characterized by a low sensitivity of the instrument in relation to other detection methods, in addition to flow rate and concentration dependency.

The last final example of a detector that can be used in the Claurus 500 GC is the photoionization detector (PID) which avoids the properties of chemiluminescence spectroscopy. It is a portable vapour and gas detector with a selectivity towards aromatic hydrocarbons, inorganic species, organo-heteroatom and other organic compounds. It is commonly used to detect VOCs in soil, sediment, air and water, which is often used to detect contaminants in ambient air and soil. PID is equipped with an ultraviolet lamp to emit photons that are absorbed by the compounds in an ionization chamber exiting from a GC column. A small fraction of the sample molecules is actually ionized, allowing confirmation analytical results through other detectors. Results are almost immediate.

The disadvantage is that PID is unable to detect certain hydrocarbon that has low molecular weight, such as methane and ethane.

### **5.1.1. Data elaboration**

As already mentioned above, as the sample is injected, the procedure is fully automatic. The results are provided through a chromatogram showing different peaks, with a specific area, at different times, as shown in figure 5.3.

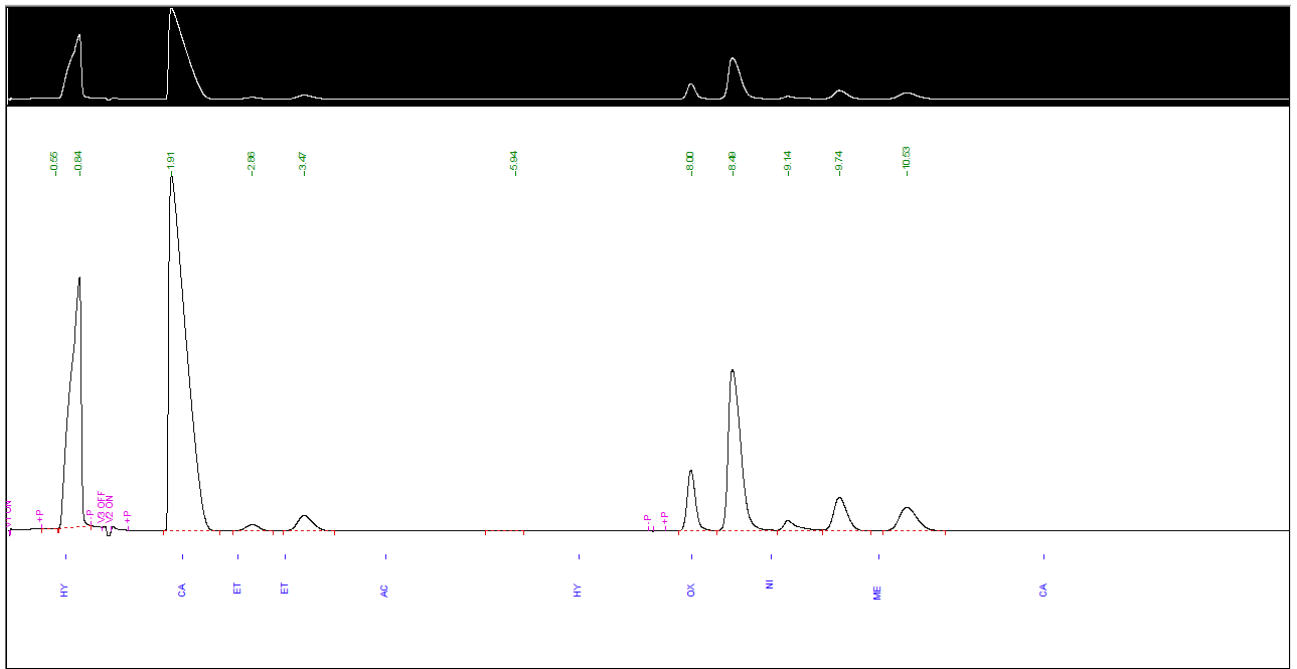


Fig. 5.3: Example of chromatogram provided by the Claurus 500 GC.

It is possible to define the particular component of the gas sample through the retention time, while the area of the peak is directly proportional to the concentration of the gas through a constant determined by calibrating the gas chromatograph. With the injection of the sample into the gas chromatograph, a small amount of air is aspirated as well. As a result, in the analysis of the final composition, the oxygen and nitrogen are subtracted.

The dedicated software shows the numerical values of time and area through which the concentration of gas is determined, as shown in figure 5.4.

DEFAULT REPORT											
Peak #	Component Name	Time [min]	Area [uV*sec]	Height [uV]	Area [%]	Norm. Area [%]	Cal. Range	Volt Range	BL	Raw Amount	Adjusted Amount
1		0.551	607.32	62.76	0.01	0.01			BB	0.0006	0.0006
2		0.836	2065592.31	237971.88	21.37	21.37			*BB	2.0656	2.0656
3	Carbondioxide	1.912	4637008.45	339358.01	47.98	47.98			BB	4.6370	4.6370
4		2.857	64890.26	6049.86	0.67	0.67			BB	0.0649	0.0649
5		3.465	179886.84	14472.72	1.86	1.86			BB	0.1799	0.1799
6		5.938	945.54	19.75	0.01	0.01			BB	0.0009	0.0009
7	Oxygen/Argon	8.001	389456.58	57787.31	4.03	4.03			BB	0.3895	0.3895
8		8.487	1545277.41	154120.16	15.99	15.99			BV	1.5453	1.5453
9	Nitrogen	9.137	110327.71	9715.53	1.14	1.14			VV	0.1103	0.1103
10		9.738	346218.42	31778.57	3.58	3.58			VB	0.3462	0.3462
11		10.528	324406.39	22580.26	3.36	3.36			BB	0.3244	0.3244
			9664617.21	873916.82	100.00	100.00				9.6646	9.6646
Missing Component Report											
Component		Expected Retention (Calibration File)									
Hydrogen		0.669									
Ethylene		2.694									
Ethane		3.244									
Acetylene		4.416									
Hydrogen Sulfide		6.680									
Methane		10.192									
Carbonmonoxide		12.131									

Fig. 5.4: Report with numerical values of time and area provided by the dedicated software.

### 5.1.2. Calibration

Calibration is an important step required to determine the proportionality constant necessary to obtain the concentrations. This procedure is made before starting the all experiments by calculating the different areas of a set of gas samples with a known concentration. As the area of the peaks is obtained, the proportionality constant is calculated as:

$$K = \frac{\text{Peak area}}{\text{Volume fraction}} \quad (5.1)$$

Table 5.1 shows the gas samples used in the laboratory for the calibration.

Bottle	Compound	Concentration
Bottle 1	$CH_4$	60%
	$CO_2$	40%
Bottle 2	$H_2$	10%
	$N_2$	90%
Bottle 3	$CO$	5%
	$N_2$	75%
	$O_2$	20%
Bottle 4	$H_2S$	0,5%
	$N_2$	99,5%
Bottle 5	$C_2H_6$	100%
Bottle 6	$C_2H_4$	1,345%
	$O_2$	20,940%
	$N_2$	77,700%

Table 5.1: Gas samples with known concentration for the calibration.

The figures below show the chromatograms obtained for the different gas samples used for the calibration.

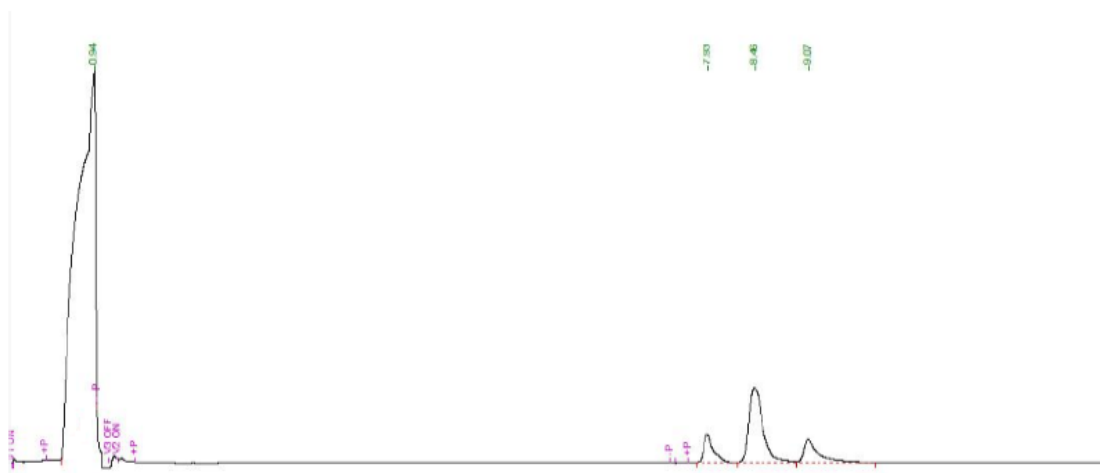


Fig. 5.5: Chromatogram of bottle 1.

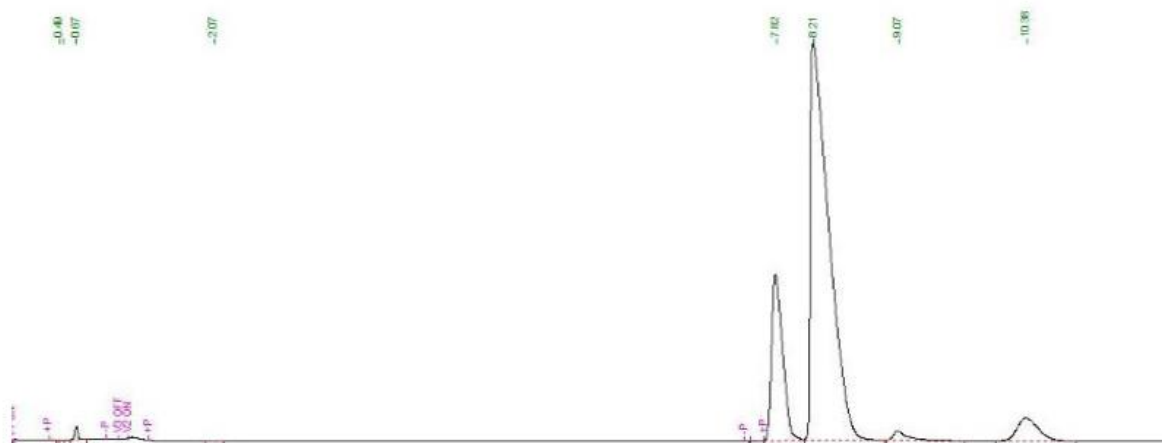


Fig. 5.6: Chromatogram of bottle 2.

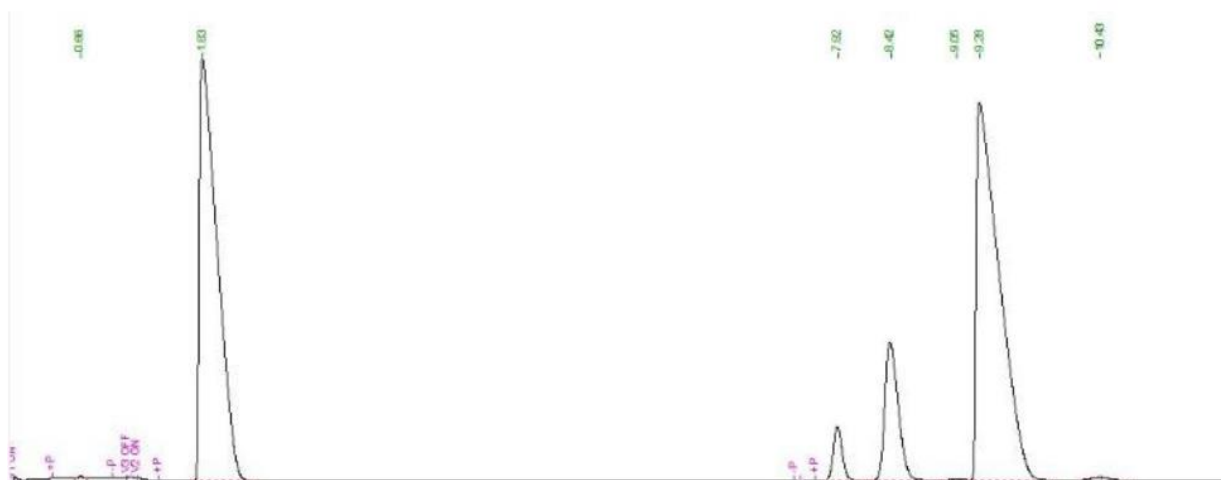


Fig. 5.7: Chromatogram of bottle 3.

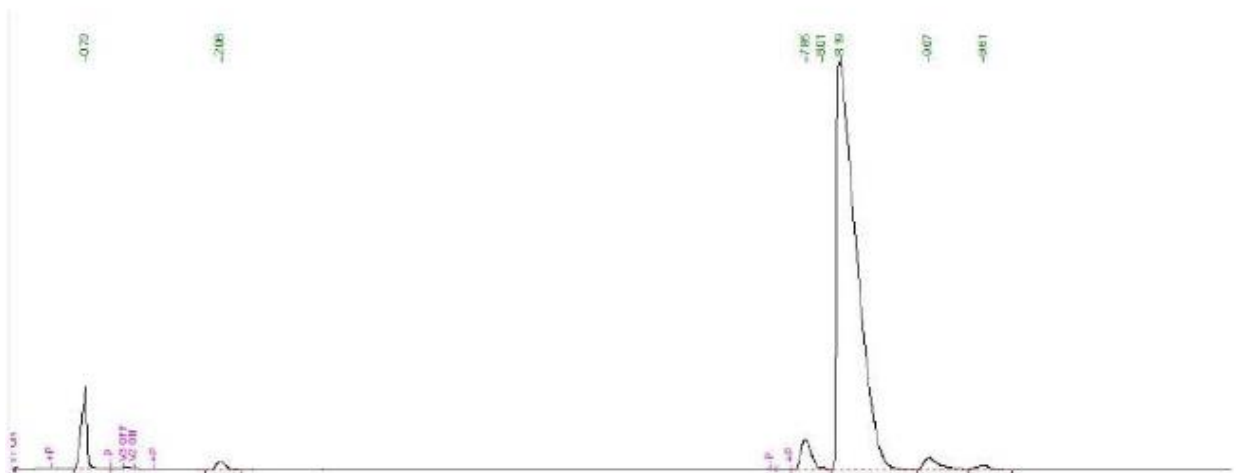


Fig. 5.8: Chromatogram of bottle 4.

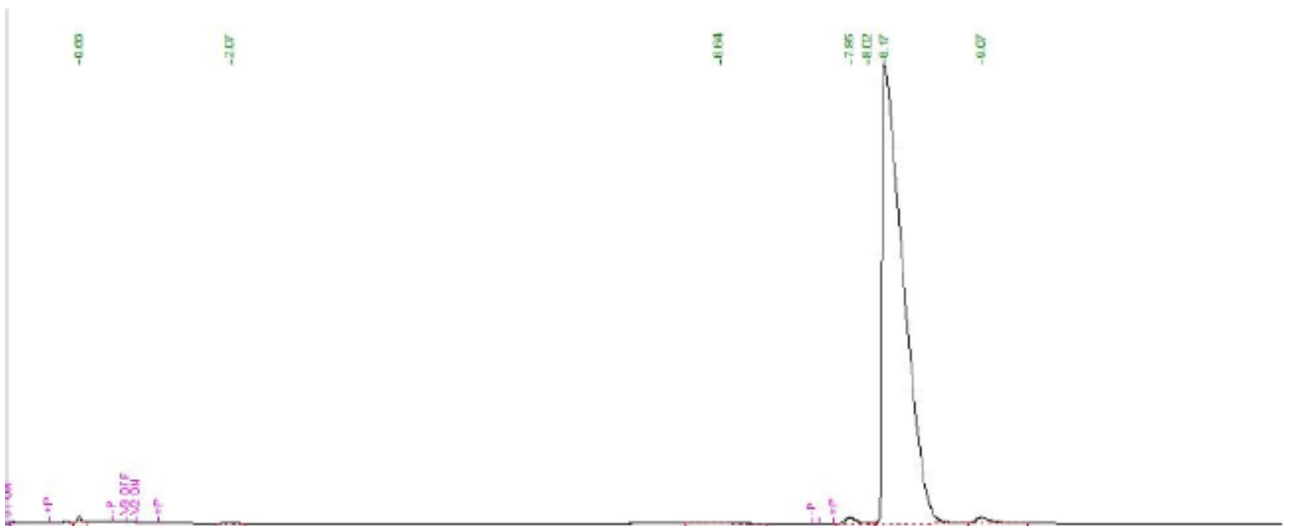


Fig. 5.9: Chromatogram of bottle 5.

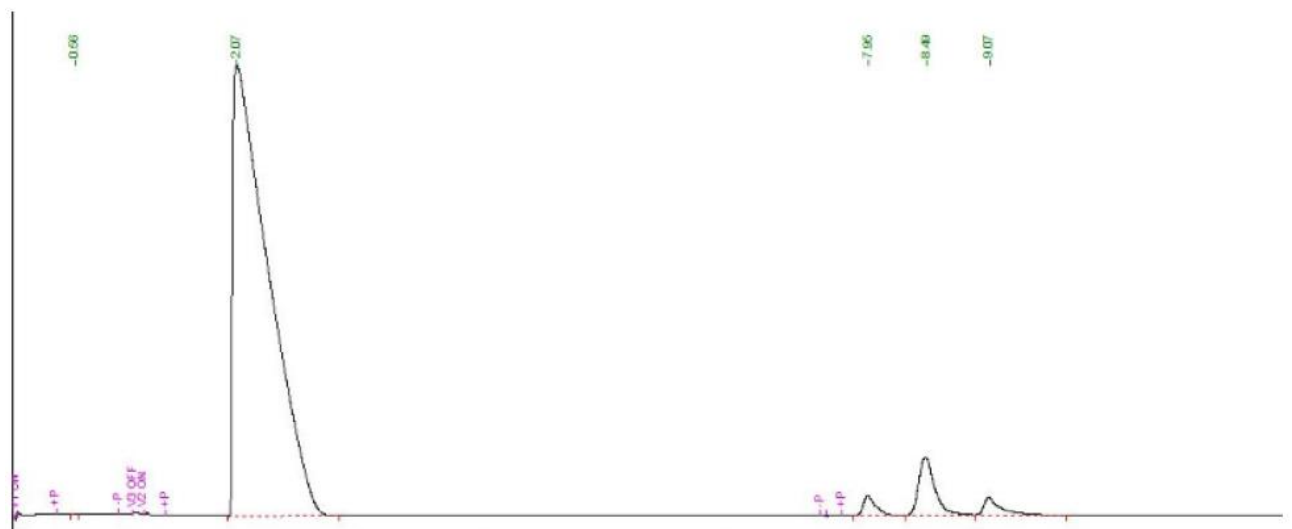


Fig. 5.10: Chromatogram of bottle 6.

While the different proportionality constant along with the known concentrations and the measured areas are reported in the following tables.

Bottle 1							
Gas	Molar concentration	Area					1/K
		Test 1	Test 2	Test 3	Test 4	Mean value	
$CH_4$	60%	3767851,76	4076432,23	4132368,6	4049358,02	4006502,653	1,498E-07
$CO_2$	40%	4515934,38	4862631,34	4941928,13	4859705,39	4795049,81	8,342E-08

**Table 5.2:** Areas and proportionality constants for bottle 1.

Bottle 2							
Gas	Molar concentration	Area					1/K
		Test 1	Test 2	Test 3	Test 4	Mean value	
$H_2$	10%	547672,02	603250,53	583959,58	657582,94	598116,2675	1,672E-07
$N_2$	90%	7759034,18	8615230,04	8299525,62	7918995,35	8316392,92	1,082E-07

**Table 5.3:** Areas and proportionality constants for bottle 2.

Bottle 3							
Gas	Molar concentration	Area					1/K
		Test 1	Test 2	Test 3	Test 4	Mean value	
$CO$	5%	410327,54	432769,22	434810,12	506607,83	446128,68	1,121E-07
$N_2$	75%	1627922,16	1743705,49	1774355,02	1798757,38	1736185,01	4,323E-07
$O_2$	20%	6492756,23	6916697,10	7023083,93	7177188,10	6902431,34	2,890E-08

**Table 5.4:** Areas and proportionality constants for bottle 3.

Bottle 4							
Gas	Molar concentration	Area					1/K
		Test 1	Test 2	Test 3	Test 4	Mean value	
$H_2S$	0,5%	37193,91	39634,36	38903,38	36619,56	38087,80	1,313E-07
$N_2$	99,5%	8406130,98	9069986,21	8900199,67	8997609,42	8843481,57	1,125E-07

**Table 5.5:** Areas and proportionality constants for bottle 4.

Bottle 5							
Gas	Molar concentration	Area					1/K
		Test 1	Test 2	Test 3	Test 4	Mean value	
$C_2H_6$	100%	10775032,4	10914410,4	10967467,8	11442944,5	11422014,4	8,755E-08

**Table 5.6:** Areas and proportionality constants for bottle 5.

Bottle 6							
Gas	Molar concentration	Area					1/K
		Test 1	Test 2	Test 3	Test 4	Mean value	
$C_2H_4$	1,345%	142904,44	141231,92	150218,61	150397,57	147948,85	9,091E-08
$O_2$	20,94%	1652256,7	1642360,69	1741135,73	1756422,7	1723897,83	1,215E-07
$N_2$	77,7%	6420206	6381613,3	6755327,47	6813275,5	6690298,26	1,161E-07

**Table 5.7:** Areas and the proportionality constants for bottle 6.

Finally, table 5.8 shows a summary of the results obtained for each compound along with the typical retention time. The  $H_2S$  is not considered as it is not a compound present in the final products of these experiments.

Compound	K	Retention time [min]
$H_2$	5981163	0,6-1
$CO_2$	11987625	1,9-2,5
$C_2H_4$	10999914	2,7-3,2
$C_2H_6$	11422014	3,2-3,9
$O_2$	34598653	7,8-8,4
$N_2$	9240437	8,4-9
$CH_4$	6677504	9,6-10,3
$CO$	8922574	10,4-11,4

**Table 5.8:** Constant of proportionality for every compound.

## 5.2. Elemental analysis

The liquid obtained from SCWG can be further analysed by the Flash EA1100 produced by ThermoQuest, shown in figure 5.11, an elemental analyser able to measure the concentration of hydrogen, nitrogen, carbon and sulphur. The detection of oxygen is also

possible but it must be done separately. The device can be used in order to analyse solids as well.

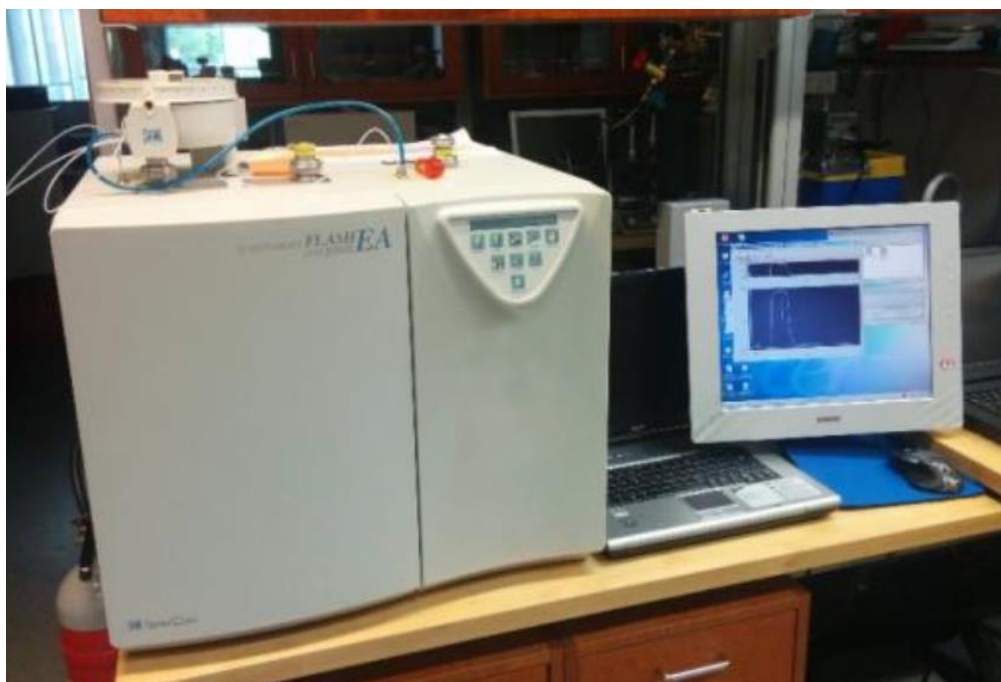


Fig. 5.11: Flash EA1100.

The analysis is made by burning the sample in a furnace, at a maximum temperature of 1100 °C, with a presence of oxygen. Afterwards, the gas produced will be sent to a chromatographic column where it will be analysed and detected through a TCD detector.

The results are provided with a plot consisting of several peaks. Similarly to the chromatograph, every peak corresponds to a specific element and the area is directly proportional to the concentration through a proportionality constant calculated at the calibration phase of the device.

As in the chromatograph, the proportionality constant is calculated by using substances with known concentrations by dividing the weight of the specific element by the area of the peak:

$$K_{element} = \frac{Weight_{element}}{Peak\ area_{element}} \quad (5.2)$$

### 5.3. Bomb calorimeter

A bomb calorimeter is a device used to measure the heat of combustion of a particular reaction. It is a sealed vessel containing a smaller container called "bomb", a combustion chamber designed to withstand high pressures.

The chemical reaction heats a quantity of water in the bomb, which contains the chemical to be analysed and enough oxygen to make sure that the sample burns completely. The bomb is plunged into a container of water and ignition wires to start the combustion, which

causes a rise in water temperature. A digital thermometer measures the change of temperature and allows calculating the value of the energy released according to the thermodynamics laws. Since the reaction takes place in a rigid, sealed container, no pressure-volume work is done by the reaction, all the energy will be released as heat, and none as work. In other words, a bomb calorimeter always measures the heat that is released by a reaction, but in this case, the heat represents not the change in enthalpy ( $\Delta H$ ), but the change in internal energy ( $\Delta U$ ).

$$\Delta H = \Delta U = -C_p \Delta T \quad (5.3)$$

The model used in the experimental setup is a 1341 Oxygen Bomb Calorimeter produced by Parr, made of an ignition unit, an electronic control unit and the insulated container, as shown in figure 5.12.

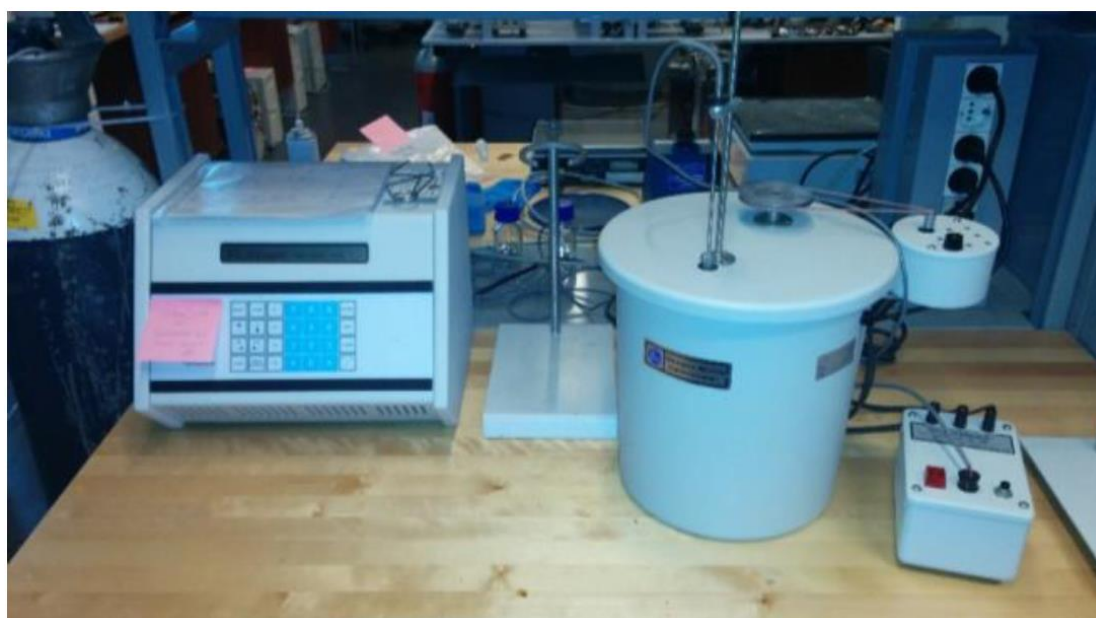


**Fig. 5.12:** 1341 Oxygen Bomb Calorimeter with the electronic control unit and the ignition unit.

The insulation is made of a fibreglass jacket with double walls, while the bomb is a stainless steel cylinder with a sealed cap at the top. The capsule containing the sample is placed in the o-ring part of the cap and pressurised with oxygen at 30 bar. The cap has, in addition, two holes for two valves and the ignition wires. The external container has a cap as well, where a high precision thermometer, submerged in water and connected to the electronic control unit, is attached. Moreover, the presence of a stirrer ensures a good homogeneous distribution of temperature during the experiments.

Figure 5.13 shows a view section of the device and the main components of a bomb calorimeter.

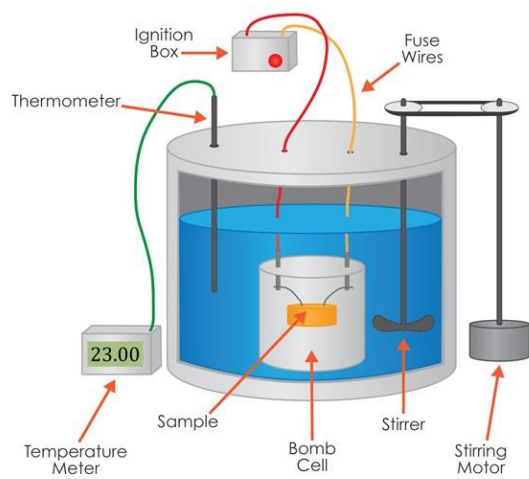


**Fig. 5.13:** Section of bomb calorimeter (left) and main components of bomb calorimeter (right).

## 6. Glycerol

The feedstock used in this thesis for its gasification with supercritical water is a glycerol solution with a concentration of 86-89% wt.

Glycerol is an organic compound with a large number of uses in food, cosmetic, industrial and pharmaceutical sectors.

In this chapter, the properties of the feedstock used in this thesis, along with the production, industrial application, purification and transformation processes to value-added products will be investigated.

Firstly, physical and chemical properties of glycerol will be examined, focusing the attention on the properties important for industrial, pharmaceutical and food purposes.

Secondly, an overview and a brief description of the main processes of production will be given, with a particular attention to the biodiesel production, the most common route for glycerol production, where it is formed as a by-product. The large availability of glycerol as a by-product of biodiesel production is constantly increasing due to the remarkable growth of the process. Moreover, most of the production processes produce crude glycerol, hard to treat as it contains many impurities such as remaining catalysts, water, soaps, salts and esters produced during the reactions. Because of the increasing availability of glycerol along with the low potential related to the crude glycerol, many purification processes to turn crude glycerol into pure glycerol have been developed. In addition, as the demand market of glycerol is tight and not able to accommodate the excess amount of glycerol produced by biodiesel production [105], transformation processes to convert glycerol into value-added products require being explored.

### ***6.1. Chemical and physical properties of glycerol***

Glycerol, also known as glycerine, glyceritol, glycyol alcohol, propane-1,2,3-triol, 1,2,3-propanetriol and 1,2,3-trihydroxypropane, is an organic compound with the chemical formula  $C_3H_8O_3$ . Glycerine is the term most often used when referring to the commercial product, which usually contains a small percentage of water.

The glycerine used in these experiments has a concentration of 86-89% wt, as shown in figure 6.1.

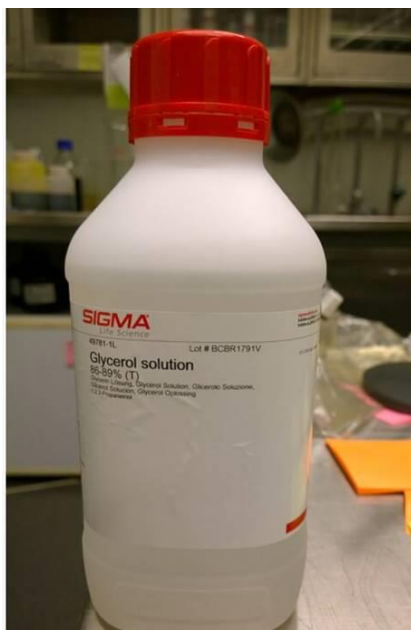


Fig. 6.1: Glycerol solution used in this thesis.

Glycerol is a colourless, odourless, viscous and hygroscopic liquid substance with a slightly sweet taste, preventing freezing and promoting long shelf life. Glycerol is a non-toxic alcohol (to both human and environment) consisting of a three-carbon chain with a hydroxyl group attached to each carbon, as shown in figure 6.2.

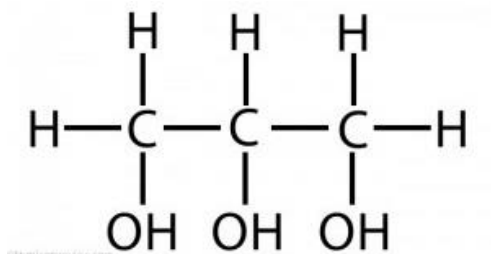


Fig. 6.2: Molecular structure of glycerol.

Nevertheless, thermal decomposition of glycerol at 28-300°C can produce poisonous acrolein, an ecological toxic substance [106].

The three hydrophilic alcoholic hydroxyl groups account for the hygroscopic property and its solubility in water.

Hygroscopicity, that is the capacity of attracting and hold moisture from the surrounding air, is one of the most valuable properties of glycerol. It is the reason for its use as humectant and conditioning agent where both glycerol itself and water, which it holds, act as plasticizers [107].

Thanks to its hydroxyl groups, glycerol has solubility characteristics similar to those of water and simple aliphatic acids. It is completely soluble in water and alcohols, slightly soluble in dioxane and ether, soluble to the extent of 5% by weight in acetone but practically insoluble in hydrocarbons, fatty oils, higher alcohols and chlorinated solvents such as

chlorobenzene, chlorhexane and chloroform. Moreover, the presence of the hydroxyl groups makes glycerol also a good solvent for many substances like bromine, iodine and phenol [108]. The solubility of glycerol in various organic solvents is summarised in table 6.1.

Solubility	Solvents
Miscible	Water; methanol; ethanol; isopropanol; n-butanol; isobutanol; 2-butanol; tert-amyl alcohol; o-cresol; diethylenetriamine; diethylformamide; diisopropylamine; triethylenetetramine; $\alpha$ -methylbenzylamine; $\alpha$ -methylbenzyl-diethanolamine; $\alpha$ -methylbenzylethanolamine; 2-methyl-5-ethylpyridine; 2-phenylethylamine; isopropanolamine; pyridine
5 wt%	Acetone
9 wt%	Ethyl acetate
Slightly soluble	Dioxane
Partially insoluble	Fatty acids, hydrocarbonate, hexane, benzene, chloroform; di-n-amyamine; di-n-butylamine
Insoluble	Ether; hydrocarbon; isoamyl acetate; n-amy cyanide; anisaldehyde; benzyl ether; cinnamaldehyde; $\alpha$ -methylbenzyl-dimethylamine; o-phenetidine; diisobutyl ketone; diethyl acetic acid; di-2-ethylhexyl amine; ethyl chloroacetate; ethyl cinnamate; ethyl ether; ethyl phenylacetate; 3-heptanol; n-heptyl acetate; n-hexyl ether; methyl isopropyl ketone; 4-methyl-n-valeric acid; o-phenetidine; salicylaldehyde; tetradecanol; tri-n-butyl phosphate

**Table 6.1:** Solubility of glycerol in various organic solvents [106].

Under atmospheric conditions, the substance is characterized by a density of  $1.261 \text{ g/cm}^3$ , a molecular weight of  $92.09 \text{ g/mol}$  and a viscosity of  $1.5 \text{ Pa.s}$ , which rises with increasing pressure [110]. The melting point, flash point and boiling point are respectively  $17.8 \text{ }^\circ\text{C}$ ,  $177 \text{ }^\circ\text{C}$  and  $290 \text{ }^\circ\text{C}$  [110]. The high viscosity and boiling point are a consequence of the extensive intermolecular hydrogen bonding [108]. Vapour pressure is lower than would be expected from its molecular weight, because of the molecular association characteristic of alcohols. The physicochemical properties and toxicity data are summarised in table 6.2.

Description	Value
Molecular formula	$\text{C}_3\text{H}_5(\text{OH})_3$
Melting point ( $^\circ\text{C}$ )	17.8
Boiling point ( $^\circ\text{C}$ )	290
Viscosity (Pa.s)	1.5
Vapor pressure at $20 \text{ }^\circ\text{C}$ (mm Hg)	< 1
Density at $20 \text{ }^\circ\text{C}$ ( $\text{g cm}^{-3}$ )	1.261
Flash point ( $^\circ\text{C}$ )	160 (closed cup)
Ethylene glycol and diethylene glycol limit (mg/ml)	$\leq 0.050$
Residue on ignition	< 0.01%
Chloride	$\leq 0.001\%$
Sulfate	$\leq 0.002\%$
Heavy metals ( $\mu\text{g/g}$ )	< 5
Chlorinated compounds	$\leq 0.003\%$
Fatty acids and esters	Not more than 1 mL of 0.5 N sodium hydroxide is consumed
Heat of fusion at $18.07 \text{ }^\circ\text{C}$ (cal/g)	47.49
Auto ignition temperature ( $^\circ\text{C}$ )	400
Critical temperature ( $^\circ\text{C}$ )	492.2
Critical pressure (atm)	42.5
Dielectric constant ( $25 \text{ }^\circ\text{C}$ )	44.38
Dipole moment ( $30\text{--}50 \text{ }^\circ\text{C}$ )	2.68 D
LD50 (oral-rat) $\text{mg kg}^{-1}$	12 600
LD50 (dermal-rabbit) $\text{mg kg}^{-1}$	> 10,000
LC50 (rat-1 h) $\text{mg m}^{-3}$	570

**Table 6.2:** Physicochemical properties and toxicity data of glycerol [106].

Under normal storage conditions, glycerol is chemically stable, but it may become explosive if in contact with strong oxidizing agents such as potassium chlorate [111].

Glycerine has been used to maintain flexibility in films and as a softener since it interrupts or breaks interchain hydrogen bonds.

Besides, in biochemistry glycerol plays a key role in stabilizing enzymes thanks to the action of polyhydric alcohol functions due to the enhancement of the structural stability of the protein by a large alteration in the hydrophilic-lipophilic balance upon clustering around the protein [112]. An important result is that glycerol protects biologicals during sol-gel entrapment in a silica-based matrix, either by direct addition to bacteria prior to the sol-gel precursors or by the formation of poly(glyceryl silicate) [113].

## 6.2. Production

Glycerol can be produced as a by-product of hydrolysis and saponification processes in oleochemical plants as well as transesterification reaction in biodiesel plants [114]. Generally, glycerol produced by biodiesel production processes and other oleochemical processes and not undergoing further chemical treatment, separation or transformation is known as crude glycerol. Crude glycerol contains many impurities such as remaining catalysts, water, soaps, salts, fatty esters, monoglycerides, diglycerides and alkali metals produced during the reactions occurring in the production processes, and its quality depends on the particular process used and materials [108]. Generally, crude glycerol is 70-80% pure and it is often purified and concentrated up to 95.5-99% for commercial sales.

### 6.2.1. Transesterification

The predominant source of glycerol is the transesterification of fat and oils (triglycerides) in biodiesel plants. Transesterification is a process where pre-treated fat or oils react chemically with alcohol (such as methanol) at a reaction temperature of 60-80 °C and with the aid of a catalyst to produce fatty acid methyl esters with glycerol as a by-product [115].

Figure 6.3 shows the schematic of a reaction where methyl-esters from triglycerides and methanol react to produce fatty esters (biodiesel) and glycerol.

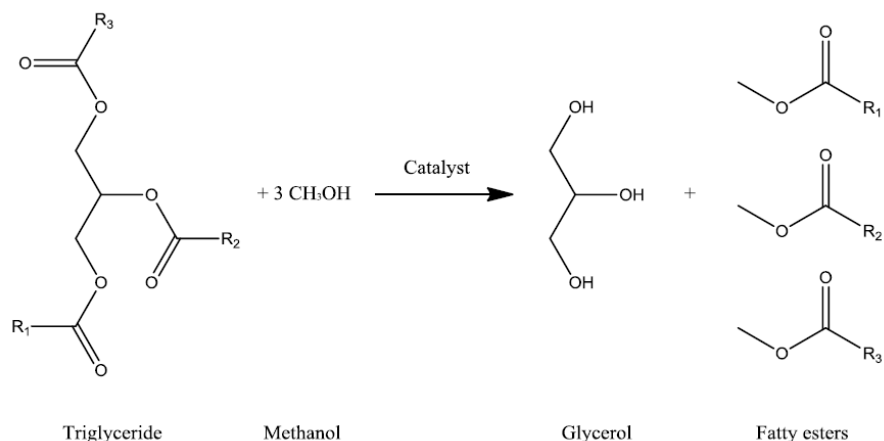


Fig. 6.3: Transesterification reaction [116].

The biodiesel production process can use both homogeneous and heterogeneous catalysts. Common catalysts for transesterification include sodium hydroxide, potassium hydroxide, and sodium methoxide, thanks to their economic importance, suitability and efficiency for the existing facilities.

Figure 6.4 shows the flow diagram of a conventional homogeneous process for biodiesel production.

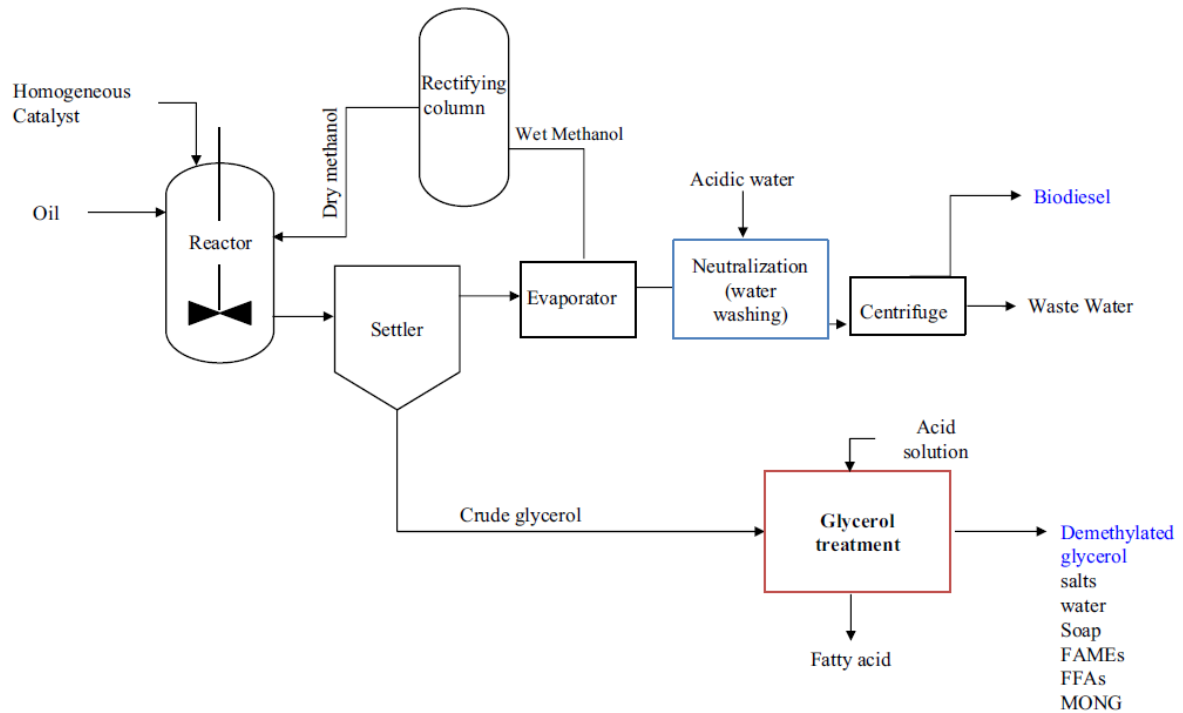


Fig. 6.4: Flow diagram of a homogeneous biodiesel production [106].

The reaction is carried out in batch or continuous reactors. As the reaction proceeds, the reaction stream is separated by a settler unit into a biodiesel-rich phase and a glycerol-rich phase. As illustrated in the figure, the crude glycerol is treated with an acid solution in order to neutralize the unreacted catalysts and soaps. After excessive water and methanol are removed, it is possible to obtain crude glycerol 50-80% pure. A further purification of the remaining contaminants, such as unreacted oil, allows obtaining 99% purity glycerol for pharmaceutical and cosmetic sectors [106].

Figure 6.5 illustrates, instead, the flow diagram of a heterogeneous process for biodiesel production.

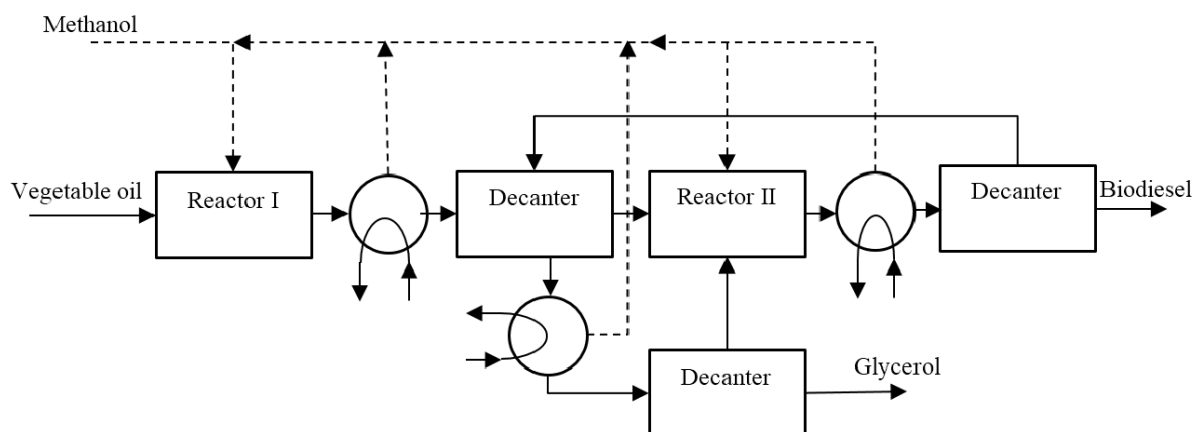


Fig. 6.5: Flow diagram of a heterogeneous process for biodiesel production [116].

Firstly, methanol and vegetable oil are introduced in the first reactor. Then, the product stream passes through a heat exchanger, where the unreacted methanol is evaporated. A decanter is required to separate non-polar (largely vegetable oil and biodiesel) and polar (most glycerol) components [116].

A second step is used in order to increase the vegetable oil conversion and, thus, to increase the biodiesel production and recover the methanol. A third heat exchanger and decanter are respectively used to recover the remaining methanol present in the mixture and separate the vegetable oil from the unreacted glycerol.

### 6.2.2. Saponification

Glycerol is produced in large quantities as a by-product of saponification of triglycerides (oils) for the production of fatty esters and free fatty acids. Saponification is the hydrolysis of fat and oils with alkali (such as sodium hydroxide or potassium hydroxide), producing salts of fatty acid and glycerol, as shown in figure 6.6.

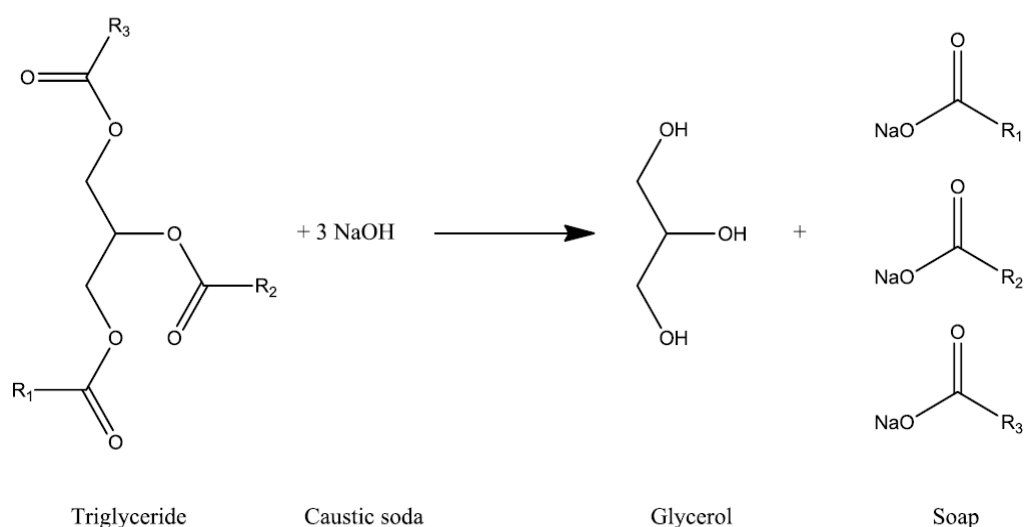


Fig. 6.6: Saponification reaction [116].

The reaction is exothermic and fast, occurring at 125°C. The alkali breaks the ester bond producing, consequently, glycerol and soap of alkali metal. Under suitable conditions of mixing and agitation, caustic alkali reacts spontaneously with free fatty acid, and soap is produced fast [117]. The soap produced is finally filtered and the filtrate contains 35% of glycerol, soluble soap, alkali, some *NaCl* and other suspended impurities.

Basically, in the process, the triglyceride mixture is boiled until the reaction is completed, as shown in figure 6.7 which illustrates a flow diagram of saponification.

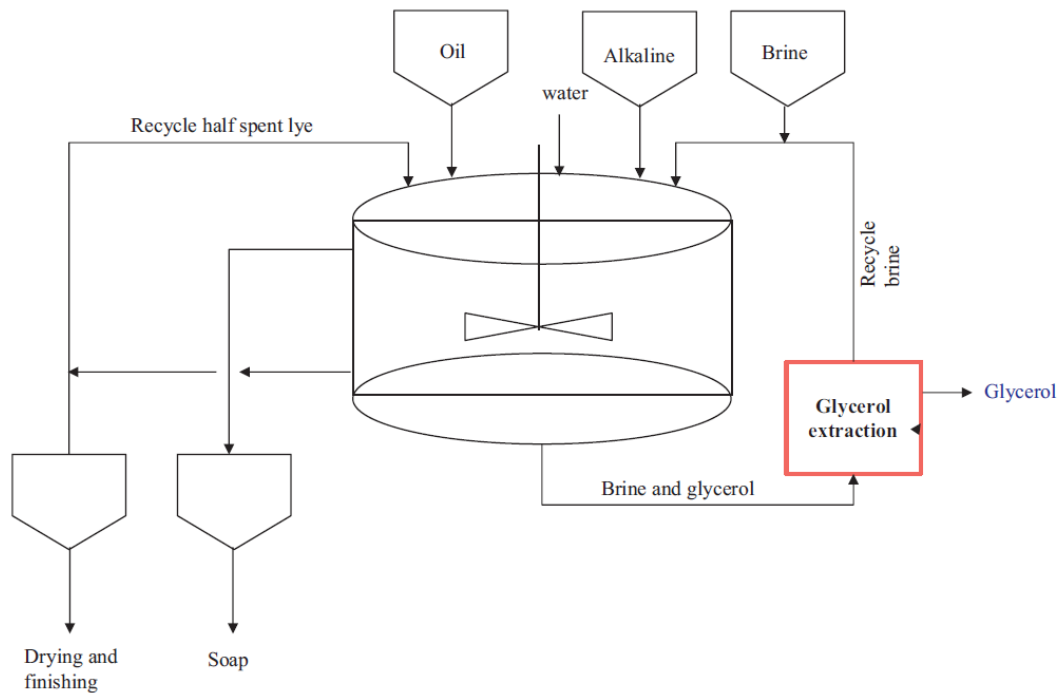


Fig. 6.7: Flow diagram of saponification process [106].

Excessive lye in a brine solution is added to the reactor in order to hydrate the soap and to enable the dissolution of glycerol. This will generate two layers: brine mixture and crude soap at the top and glycerol mixture with spent and neutral lye at the bottom. Utilization of lye allows the extraction of glycerol from the soap.

### 6.2.3. Hydrolysis

Another source of glycerol is the hydrolysis of fat and oils into fatty acid and glycerol. This reaction is similar to saponification besides that in hydrolysis triglycerides react with water to produce fatty acids and glycerine, as shown in figure 6.8.

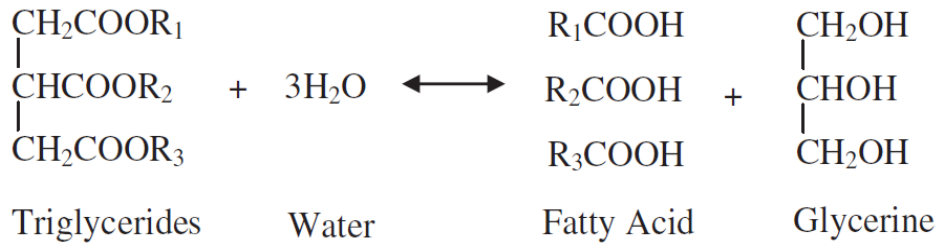


Fig. 6.8: Hydrolysis reaction [108].

The glycerol-rich solution is called *sweetwater* and it requires to be continuously removed so as the reaction is completed.

#### 6.2.4. High-pressure splitting

High-pressure splitting is a process used to obtain high-quality fatty acids in oil and fat processing industry [118]. Figure 6.9 shows the flow diagram of a splitting column.

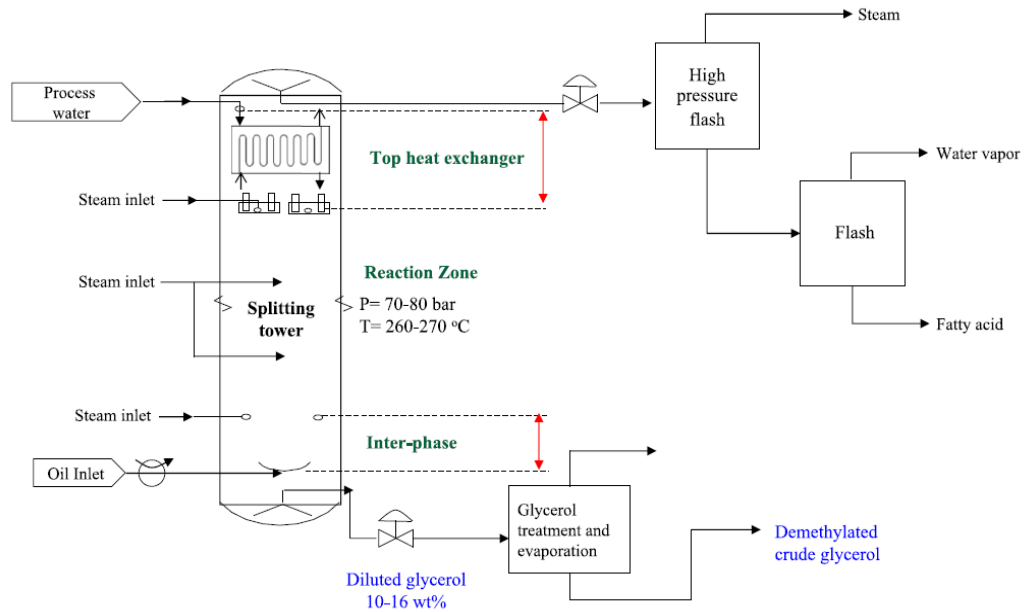


Fig. 6.9: Flow diagram of a splitting column [106].

As it is possible to see, the raw oil is fed from the bottom, while the water is introduced to the top of the column. The counter-flow guarantees a good dissolution of water droplets into the oil phase. The operating pressure is approximately of 70-80 bar, while the temperature is 260-270°C.

The diluted glycerol, with a concentration of 10-16 % in a solution of glycerol, water, fats, inorganic salts and polymers, is sent to a treatment and evaporation unit, where demethylated crude glycerol is obtained.

### 6.2.5. Glycerol via propylene

Another source of glycerol is the propylene chlorination (figure 6.10).

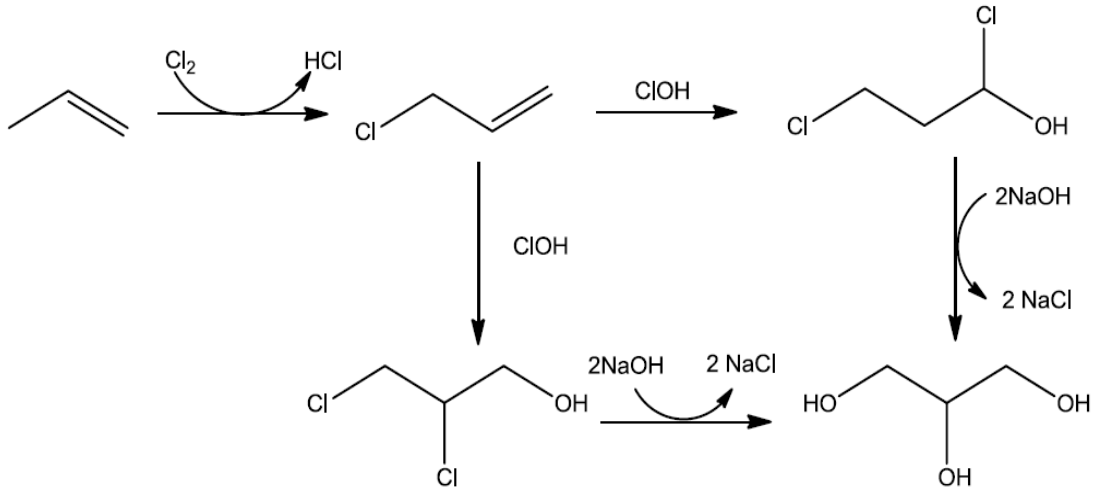


Fig. 6.10: Propylene chlorination [116].

In this reaction, allyl chloride is produced at  $510^\circ\text{C}$  with the presence of hypochlorous acid at  $38^\circ\text{C}$ . The allyl chloride reacts to produce glycerine dichlorohydrine which is hydrolysed by caustic soda in a  $\text{Na}_2\text{CO}_3$  solution at  $96^\circ\text{C}$ . Another option is to hydrolyse allyl chloride directly to glycerine by removing the epichlorohydrin in a stripping column. Finally, the epichlorohydrin is hydrated to glycerine with caustic soda [116].

Figure 6.11 illustrates two of the main pathways, involving the use of oxygen or chlorine.

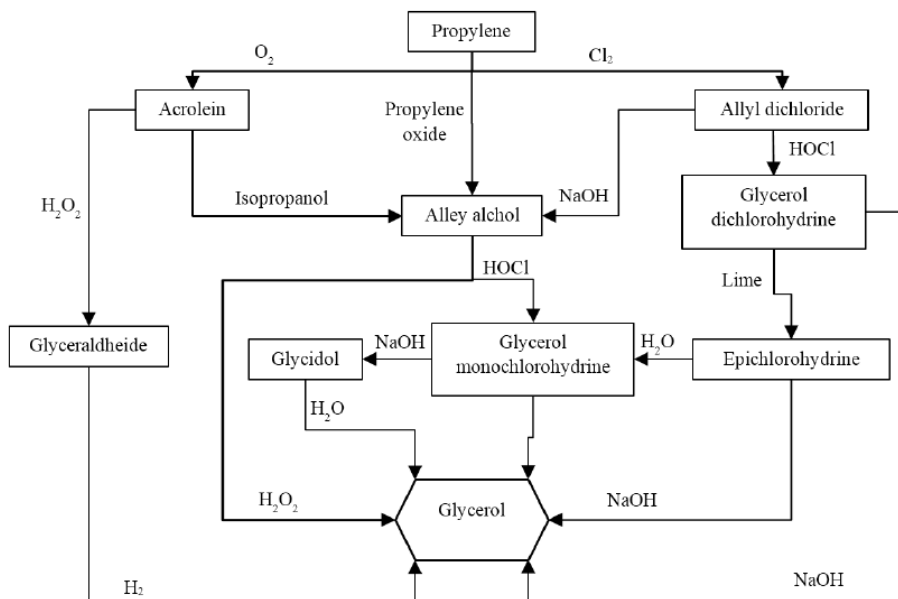


Fig. 6.11: Glycerol production via propylene [116].

### **6.3. Purification of crude glycerol**

The glycerol produced by the processes examined before is called crude glycerol and it contains many impurities such as remaining catalysts, water, soaps, salts and esters. Since this low-quality glycerol is hard to treat as it contains so many impurities, it has little applications and a low fuel value, therefore, it requires to be purified through further processes.

The different processes used for purification of crude glycerol, such as distillation, chemical treatment, filtration, adsorption with activated carbon, ion exchange with resin, decantation, extraction and crystallization, are differentiated by the particular property of glycerol that they exploit [119]. Two or more methods may be combined in order to achieve higher qualities of glycerol. The most common process is a combination of distillation for alcohol recovery, ion exchange for salt removal and adsorption using activated carbon.

Distillation, which is the absolute most common method, is based on the boiling points of the different components and it is mainly used to remove water and methanol [108]. This process is advantageous due to its small to large scale continuous operation, adaptability of the process to the different qualities of crude glycerol and the low cost of chemicals [120]

By contrast, the high specific heat capacity of glycerol, leading to a necessity of high energy for vaporization, makes distillation an energy-intensive process [121].

Ion-exchange is another method used to remove impurities, colour and odour based on ion exchanges from ion-exchange material [120]. This method does not require the vaporization of glycerol and it consumes small quantities of water for the separation of the salt from crude glycerol.

Chemical treatment (acid protonation) is a technique where crude glycerol reacts with acid to convert the fatty acid carboxylate salts to the corresponding alcohol and the alkoxide salts to the corresponding alcohol. The free fatty acid obtained can further be removed by extraction or decantation [108].

Pure glycerol, obtained by the processes mentioned above, has many industrial applications and it is an important source in food, cosmetic and pharmaceutical industries.

### **6.4. Industrial applications**

In the food and beverage industry, glycerol is used as a solvent, preservative agent and sweetener [108]. It is used as a softening agent in cakes, bread, cheese, candy and meat and it is normally ingested in extracts of tea, ginger, coffee and other vegetable substances.

Moreover, glycerol can be used in order to regulate the moisture content of tobacco, so as to eliminate the unpleasant and irritating taste and preserve its freshness.

In paper production, glycerol acts as lubricant and plasticizer, while in the textile industry it is used as lubricating, softening and sizing yarn and fabric [111].

Glycerol is also used in the manufacture of drugs and medicine since it gives humidity and increases the viscosity of liquid drugs. It is used as plasticizers for medicine capsules and in ear infection medicines and cough syrups as a carrier for antiseptics and antibiotics [122].

Glycerine is an important solvent of phenol, bromine, iodine, alkaloids, tannins and mercury chloride. In many skin and hair products, it acts as lubricant, humectant, moistener and it improves smoothness. Besides, it is the main ingredient in toothpaste, preventing hardening and drying out of the tube [123].

### 6.5. Transformation to value-added products

Another possible way to use the large amount of glycerol produced mainly by the biodiesel production process is to convert it to value-added chemicals through various types of chemical reactions [124].

The direct conversion of crude glycerol into value-added products would be very advantageous. Nevertheless, all the impurities contained in crude glycerol make the conversion tricky.

Figure 6.12 shows several glycerol derivatives produced by different reactions.

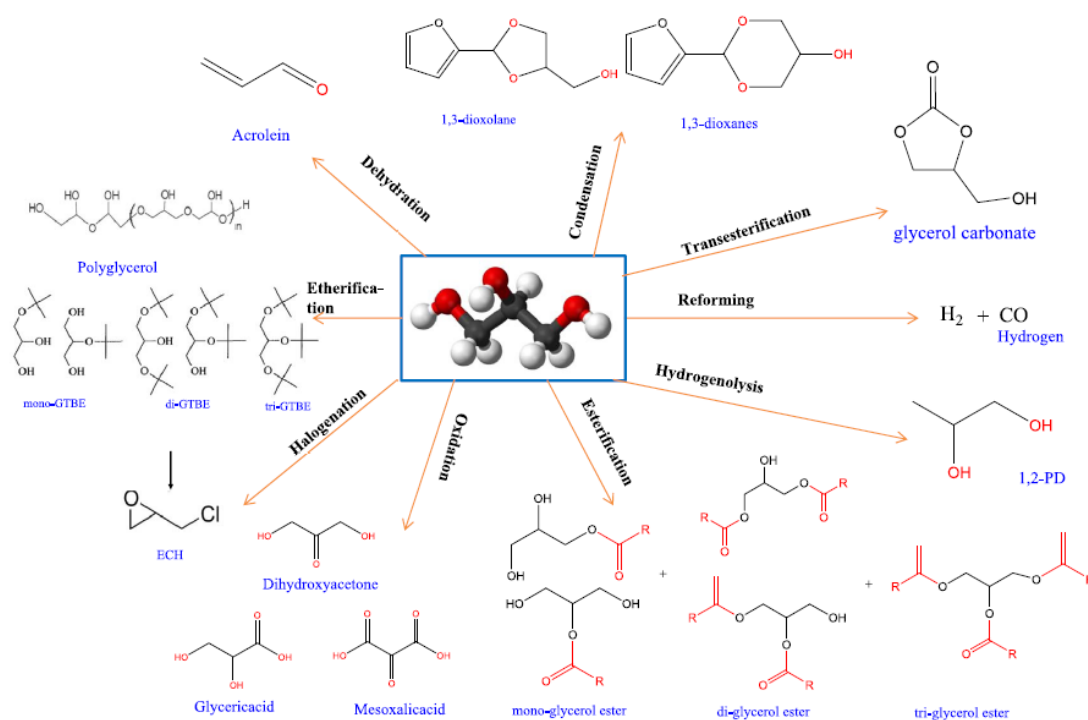


Fig. 6.12: Possible derivatives of glycerol [106].

### Hydrogen

Glycerol can be converted into hydrogen through different processes such as partial oxidation, supercritical water reforming, auto-thermal reforming, aqueous-phase reforming and catalytic-steam reforming, which is the most used technique [106].

The catalytic steam reforming is a high-temperature endothermic process carried out with the aid of a catalyst to react glycerol with water and produce hydrogen. The process consists

of three steps: glycerol dehydrogenation, CO bonded on the catalyst surface, which could undergo desorption, and water gas shift or methanation [125].

Figure 6.13 illustrates the mechanism of steam reforming of glycerol [126].

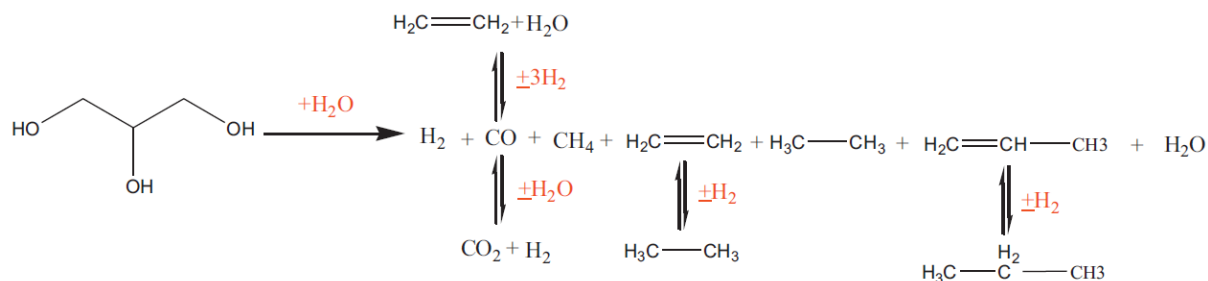


Fig. 6.13: Production of hydrogen via steam reforming of glycerol [126].

Besides hydrogen, steam reforming of glycerol in the presence of metal catalysts generates carbon monoxide, carbon dioxide and methane [127].

Partial oxidation is another process used to produce hydrogen by glycerol in which a substrate reacts with oxygen at sub-stoichiometric ratios.

### Acrolein

Acrolein, also known as acrylic aldehyde or 2-propenal, is the simplest unsaturated aldehyde [128] and it is used as a raw material of acrylic acid, a slimicide in the manufacture of paper, a microbicide in oil wells fibre treatment, methionine, medicines, fragrances and dyes. Polymers produced from acrylic acid have superabsorbent properties and they are widely employed in diapers and hygienic pads [106].

Acrolein can be produced by dehydration of glycerol with the presence of a heterogeneous acid catalyst, as shown in figure 6.14.

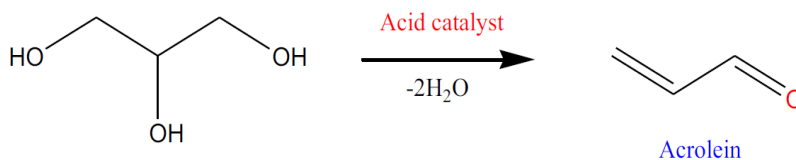


Fig. 6.14: Production of acrolein via dehydration of glycerol [126].

### Propylene glycol

Propylene glycol, also known as 1,2-propanediol, originally derived from propylene oxide through hydrolysis, is a potential replacement for ethylene glycol [129].

The process used to produce propylene glycol is a catalysed hydrogenolysis/dihydroxylation of glycerol, as shown in figure 6.15.

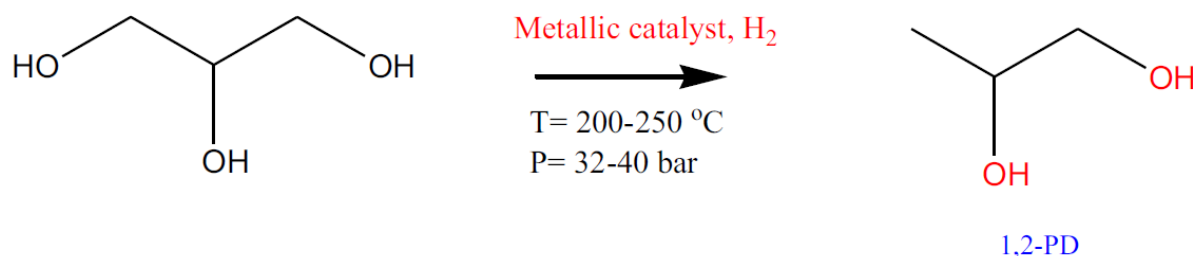


Fig. 6.15: Production of propylene glycol via hydrogenolysis of glycerol [106].

This process is normally carried out in aqueous glycerol solution at 200-250 °C and 32-40 bar.

The most common metal catalysts used are magnesium, alumina, nickel, platinum, copper, palladium, ruthenium and chopper chromite [106].

Propylene glycol can be applied to functional fluids, pharmaceuticals, unsaturated polyester resins, personal care, food, tobacco humectants, liquid detergent and animal feeds.

### Dihydroxyacetone

Dihydroxyacetone (DHA) is a substance employed in winemaking and nutritional supplement industries as well as in sunless tanning products.

It is produced by secondary alcohol catalytic oxidation of glycerol with the aid of metal catalysts such as palladium, gold, platinum and bismuth-supported palladium catalysts, where the secondary OH group of glycerol is oxidized. Usually, it is a microbiological complex oxidation with low glycerol concentration and requiring long operating hours [130].

Besides Dihydroxyacetone, oxidation of glycerol can be used to produce glyceric acid (GA) and mesoxalic acid (MA). The first is a primary OH oxidation product with no commercial applications but an essential intermediate compound for MA synthesis and tartronic acid (TA). Mesoxalic acid is produced by the oxidation of tartronic acid and it is a strong hypoglycemic agent. The general scheme of oxidation of glycerol is shown in figure 6.16.

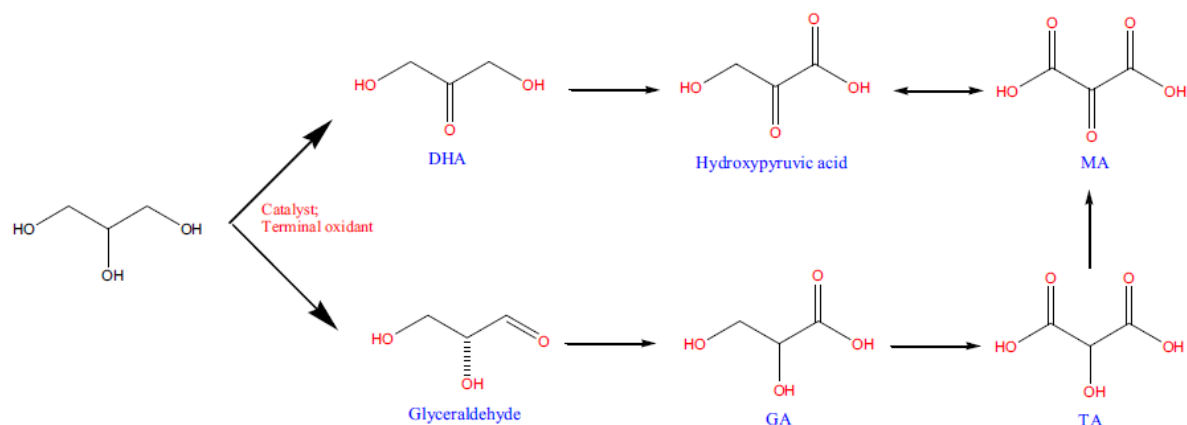


Fig. 6.16: Oxidation of glycerol [106].

### Glycerol ethers

Glycerol tertiary butyl ether (GTBE) is an oxygenated fuel. GTBE is produced by etherification of glycerol with isobutylene, as shown in figure 6.17.

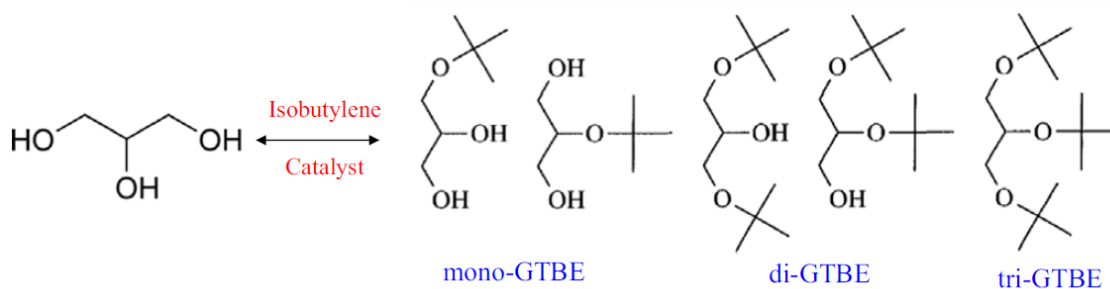


Fig. 6.17: Etherification of glycerol [106].

This fuel can potentially replace the highly toxic methyl tertiary butyl ether (MTBE) [131] and its addition in biofuels led to a decrease of particulate matters, carbon oxides, contents of fumes and carbonyl compounds in exhausts.

Etherification of glycerol is also used to produce polyglycerols, non-ionic surfactants able to stabilize suspensions and emulsions. They have different biomedical applications and are used as polymer and nutritional additives, lubricants and cosmetic ingredients [106].

### Glycerol esters

Glycerol esters are produced by esterification of glycerol, as shown in figure 6.18.

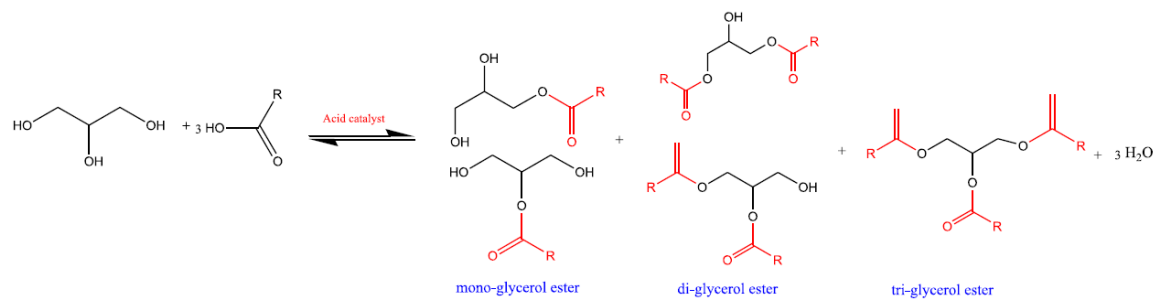


**Fig. 6.18:** Etherification of glycerol to glycerol esters [106].

In particular, triglycerides ester can be produced by esterification between glycerol and carboxylic acid [132]; mono-, di- and tri-acetin by esterification between glycerol and acetic acid and mono-, di- and tri-oleate by esterification between glycerol and oleic acid.

Tri-acetin is an excellent solvent predominantly used as a plasticizer of cellulosic polymers. It can be used, along with glyceryl diacetate, to produce bio-additives in catalytic esterification of acetic acids, since both substances act as bio-additives for liquid fuels. In particular, tri-acetin can increase the octane rating, reduce the cold point of fuels, improve viscosity and cold properties and the toxic tertiary alkyl ether [133].

Monoglycerides, instead, apply widely in food, pharmaceutical, lubricant, cosmetic and chemical industries. Their natural molecular structure and properties make them a stable emulsion [106].

## Epichlorohydrin

Epichlorohydrin (ECH) is an intermediate chemical widely used in the manufacture of elastomers, polyamide-ECH resins, epoxy resin, polyols, synthetic glycerol and glycidyl derivatives. Elastomers derived from ECH shows very good resistance to weather, fuels, oxygen and oils [134].

ECH is produced from glycerol through two steps [135]. The first step is hydrochlorination with hydrogen-chloride at 110-120 °C, 7.6 bar, 2 wt% acetic acid and 4 hours reaction time, which produces a mixture of 1,3-dichlorohydrin, 1,3-dichloropropan-2-ol and 2,3-dichlorohydrin, 2,3-dichloropropan-1-ol. This mixture is, afterwards, converted into ECH by using NaOH. Figure 6.19 shows the reaction.

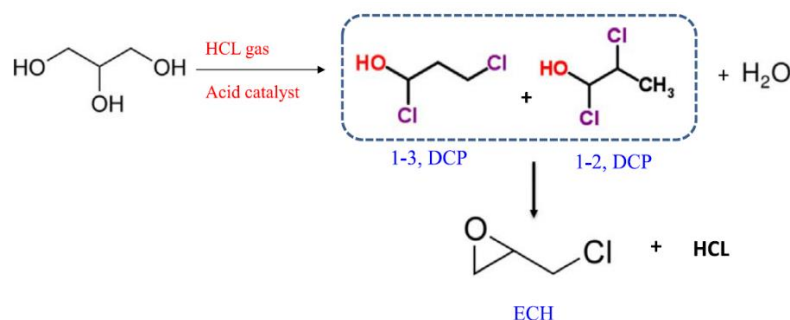


**Fig. 6.19:** Conversion of glycerol into ECH [106].

## Dioxolane and dioxane

Mixtures of furyl-1,3-dioxacyclanes made of 1,3-dioxanes and 1,3-dioxolanes are produced by acid-catalyzed condensation between glycerol and biomass derived-furfural, as shown in figure 6.20.

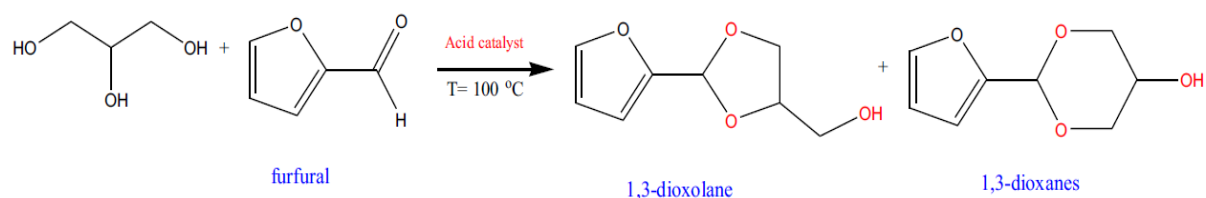


Fig. 6.20: Conversion of glycerol and furfural into dioxolane and dioxane [106].

Dioxolane and dioxane are strong aprotic solvents and important ingredients in main industrial biopolymers and some nickel pharmaceutical intermediates [136].

## Glycerol carbonate

Glycerol carbonate applies in industrial applications as a chemical intermediate in the plastic and polymeric industry, potential electrolyte in the semiconductor industry, solvent in medicine and plant-activating agent in the agriculture field.

Glycerol carbonate can be produced by catalytic (either heterogeneous or homogeneous) transesterification of glycerol with dialkyl carbonates, as shown in figure 6.21.

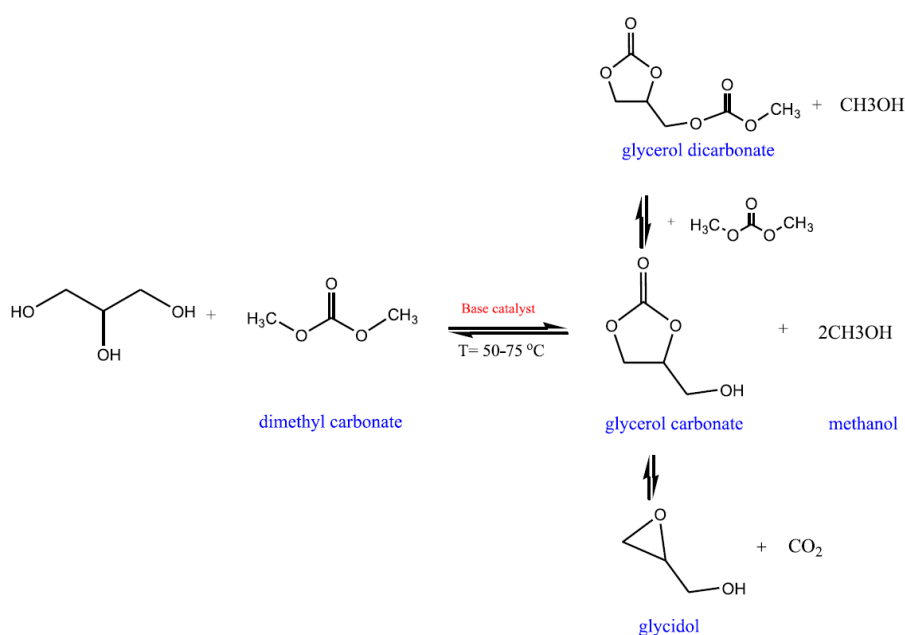


Fig. 6.21: Transesterification of glycerol with dimethyl carbonate [106].

In this thesis, a glycerol solution has been used in order to produce syngas through a supercritical water gasification process.

## 7. Data elaboration and results

This thesis is about supercritical water gasification of a glycerol solution carried out at constant temperature and pressure and at three different concentrations and residence times. The aim of the experiments is to assess the variation of the composition of the syngas produced by the supercritical water gasification of glycerol and its efficiencies and gas yields, by setting the concentration at 2.5, 5 and 10 %wt and the volumetric flow rate of the nitrogen pushing the solution into the reactor at 125, 250 and 375 ml/min.

In this chapter, all the methods for data elaboration and the results of the experiments are reported. Firstly, a detailed description of the experimental procedure adopted in the laboratory is provided. Secondly, all the methods and equations for the assessment of the composition made by means of the gas chromatograph, and the evaluation of the gas yields and efficiencies are given. Lastly, all the numerical and graphical results of the whole set of experiments are provided, making a comparison between them and between the results presented in the literature.

### 7.1. *Experimental procedure*

Before starting the experiments, as already mentioned in chapter 5, a calibration of Claurus 500 GC is necessary. The solution of glycerol and water is prepared before every experiment at the wanted concentration (2.5%, 5% and 10%) and it is left few hours with a stirrer to make it homogenous.

The first step of the procedure is aimed at reaching the thermodynamic conditions. Initially, all the valves are closed and the feed cylinder and reactor contain leftovers of water from the cleaning and washing of the last experiment. In the start-up phase, the system is filled with distilled water and put in pressure by opening the valve V2, slowly and with attention in order to avoid water hammers, for the filling of the feed cylinder, and then the valve V4 for the filling of the reactor (see figure 4.2). In order to do so, the water pump is used until all the system is full of water. The pressure is regulated by a backpressure regulator (see Figure 4.2). At this point, the valves are closed (except the BPV) and the pressure of the system is increased at about 150 bar, lower than the set-point pressure since the further heating of the system through the furnace will further increase the pressure, as shown in figure 7.1.

As it possible to see from the picture, the set-point pressure is reached when the temperature is around 100°C, so, in order to maintain the pressure constant, the BPV requires to be manually regulated.

When the set-point temperature is reached as well, the pressure is expected to remain constant since the flow maintains the BPV open, which closes when the pressure goes under a certain set value. However, as it is possible to see in figure 7.1, this does not happen since the BPV is continuously slightly moved in order to avoid clogs phenomenon, caused by tiny masses of liquid and solid residues stuck in the entrance or exit of the reactor causing sharp increases of pressure. The pressure is constantly checked through the LabView interface.

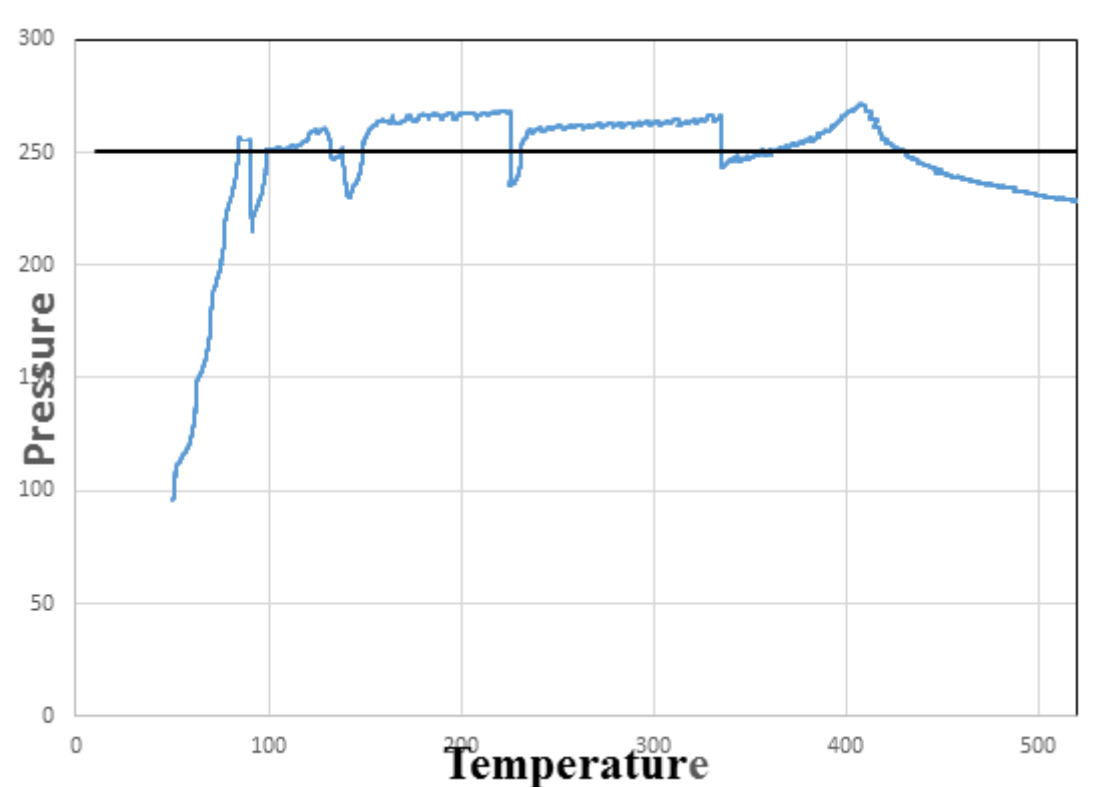


Fig. 7.1: Pressure trend as a function of temperature during the experiment.

The reason of the four sharp decreases showed by the picture may be the suction effect of the stream due to the introduction of cold feed or the release of char or tar formed during the reactions by the exit duct of the reactor.

After the start-up phase, which lasts 3.5-5 hours, the solution is injected by a syringe into the cylinder through a pipe at the bottom, with the venting valve open (see figure 4.2). When the solution exits the cylinder through a rubber tube, V3 and the venting valve are closed, while the cylinder is pressurized by nitrogen.

The main valve of the nitrogen tank is open and the output pressure is set to 280 bar by turning the black knob. The MFC is turned on and the nitrogen starts to flow toward the cylinder. The valve V1 is open and the pressure of the cylinder starts increasing. When the pressure is slightly lower than the pressure in the reactor, the MFC is turned off and a plastic bag is attached to the pipe exiting the reactor (see figure 4.17). This is done in order to have a backflow and not a forward flow which can generate uncontrolled chemical reactions that, in turn, may lead to an overproduction of flammable and toxic gases that can ignite if a leakage is present. A backflow, indeed, drags reactants to a colder zone, preventing undesired and fast reactions.

After all the thermodynamic conditions are reached, the experimental phase starts. The MFC is set initially at 375 ml/min, V1 is open and the pressure is monitored through Labview. With a flow rate of 375 ml/min, the solution reaches the reactor after about 15 minutes. Once the calculated time needed by the solution to reach the reactor passes by, the first bag is replaced and it is not considered in the calculations since it contains water and

mainly  $H_2$  produced by the water used to warm the reactor up. Every bag is replaced every 20 minutes with a flow rate of 375 ml/min, every 30 minutes with a flow rate of 250 ml/min and every 45 minutes with a flow rate of 125 ml/min.

Once the bag is full, the nitrogen flow is set to 0 ml/min, the valve V1 is closed and the bag is replaced. As the new bag is attached the MFC is turned on and the valve V1 is opened again.

The bag collected is then analysed and the gas volume is measured. The gas present in the bag is then extracted by a syringe and analysed through the gas chromatograph, while liquid products are extracted to measure the volume and collected in small vials for potential further analysis.

When a sufficient number of bags is collected the flow rate is decreased first at 250 ml/min and then at 125 ml/min, repeating all the procedure for every volumetric flow rate. When the last bag of the last flow rate is collected the MFC is turned off, the heating system is shut down and all the valves closed. The cylinder is depressurized by opening the venting valve and once the nitrogen is completely released, the unreacted solution is extracted by opening the V3 valve at the bottom part of the cylinder in order to measure its volume and weight. After all the plant is cooled down, the reactor is depressurized by opening the V5 valve, disassembled, cleaned and assembled again, ready for the next experiment. All this procedure is the same both for the Inconel and for the stainless steel reactor.

## 7.2. Data elaboration

In this paragraph, all the methods and equations used to elaborate the data acquired during the experiments, required for the calculations of the composition, gas yields, gasification conversion efficiencies and the cold gas efficiencies are investigated.

For every volume flow rate, at least three bags are collected and for every bag, three analysis of the composition of the gas are made. The chromatograph provides the results in chromatograms in form of peak areas. The values of concentrations are obtained by dividing the average area by the proportionality constant obtained during the calibration phase. Finally, the nitrogen and oxygen, composing the air unavoidably sucked by the chromatograph, are excluded by the calculations.

Other data are obtained by the measurements of volumes and masses of the gases and liquids obtained by the SCWG. The total volume of the bag is measured, along with the volume and the mass of the liquid product. For every bag, the volume and the number of moles of gas and the density of the liquid are calculated as:

$$V_{gas,j} = V_{tot,j} - V_{liq,j} - V_{bag,j} \quad (7.1)$$

$$\rho_{liq,j} = \frac{m_{liq,j}}{V_{liq,j}} \quad (7.2)$$

$$n_{gas,j} = \frac{pV_{gas,j}}{RT} \quad (7.3)$$

Where:

$V_{gas,j}$  is the gas volume of each bag [ml];

$V_{tot,j}$  is the total volume of the bag [ml];

$V_{liq,j}$  is the volume of the liquid product contained in the bag [ml];

$V_{bag,j}$  is the tare volume, i.e. the volume of the plastic bag [ml];

$\rho_{liq,j}$  is the density of the liquid product of each bag [g/ml];

$m_{liq,j}$  is the mass of the liquid product of each bag [g/ml];

$V_{liq,j}$  is the volume of the liquid product of each bag [g/ml];

$n_{gas,j}$  is the number of moles of the gas product of each bag;

$p$  is the pressure of the gas in each bag [Pa];

$R$  is the ideal gas constant [J/(mol·K)];

$T$  is the temperature of the gas in each bag [K];

The number of moles of the gas is obtained by considering the gas as a perfect gas since it is under ambient conditions. Subsequently, the number of moles of every compound of the gas is calculated as the product of its volume concentration ( $\Phi_{compound,i}$ ), obtained by the chromatograph, and the total number of moles:

$$n_{compound,i} = n_{gas,j} \Phi_{compound,i} \quad (7.4)$$

While the mass of every compound is calculated as:

$$m_{compound,i} = n_{compound,i} MW_{compound,i} \quad (7.5)$$

Where  $MW_{compound,i}$  is the molecular weight of every compound.

Finally, the total mass of the gas and liquid collected for every volume flow rate are:

$$m_{liq,tot} = \sum_j^n m_{liq,j} \quad (7.6)$$

$$m_{gas,tot} = \sum_j^n \sum_i^t m_{compound,tot,i} \quad (7.7)$$

Where:

$m_{compound,tot,i}$  is the mass of every gaseous compound in each bag [g];

$n$  is the number of bags;

$t$  is the number of compounds;

### 7.2.1. Mass balance

The previous equations are used in order to obtain the mass and the volume of the liquid and gas product, required to calculate the gas yields, efficiencies and lower heating values. For the calculation of the gas yields and efficiencies, a mass balance is required. The mass introduced into the reactor for every bag can be computed by multiplying the mass flow rate of the feed by the time spent:

$$m_{in} = \dot{m}_{sol} \Delta t_{coll} \quad (7.8)$$

Where:

$m_{in}$  is the mass of glycerol introduced into the reactor [g];

$\dot{m}_{sol}$  is the mass flow rate of the glycerol solution, pushed by nitrogen and considering that after the BPV it expands to ambient pressure [g/min];

$\Delta t_{coll}$  is the time spent for the experiment [min];

In particular  $\Delta t_{coll}$  is the sum of the intervals of time for the collection of every bag:

$$\Delta t_{coll} = \sum_{j=1}^n \Delta t_{coll,i} \quad (7.9)$$

The mass flow rate of the glycerol solution is calculated as:

$$\dot{m}_{sol} = \dot{V}_{sol} \rho_{glycerol} \quad (7.10)$$

Where:

$\dot{V}_{sol}$  is the volumetric flow rate of the glycerol solution at 25 °C and 250 bar [ml/min];

$\rho_{sol}$  is the density of the glycerol solution at 25 °C and 250 bar [g/ml];

The volumetric flow rate of glycerol is the same as the volumetric flow rate of nitrogen, which is calculated as:

$$\dot{V}_{N_2} = \dot{V}_{N_2,n,i} \frac{\rho_n}{\rho} \quad (7.11)$$

Where:

$\dot{V}_{N_2}$  is the volume flow rate in real operating conditions [ml/min];

$\dot{V}_{N_2,n,i}$  is the volume flow rate at 0°C and 1 atm [Nml/min];

$\rho_n$  is the nitrogen density at normal conditions [ $\text{kg}/\text{m}^3$ ];

$\rho$  is the nitrogen density at the operating pressure [ $\text{kg}/\text{m}^3$ ];

Another method to compute the mass of the feedstock introduced into the reactor is to consider the feedstock as completely converted into gas and liquid in the reactor. This is an approximate way for the calculation of the mass entering the reactor since in reality a small fraction of the feedstock is converted into solid (char) and liquid (tar) residues. This is done because it might be useful to compare the results with the previous method and try to understand how much feedstock has been converted in tar and char.

$$m_{feed} = m_{gas} + m_{liq} \quad (7.12)$$

### 7.2.2. Gas yield

The gas yield for every compound is calculated as the number of moles produced divided by the dry mass of the feedstock entering the system:

$$Y_i = \frac{n_{i,tot}}{m_{dry,gly}} \quad (7.12)$$

Where:

$Y_i$  is the gas yield of every compound [mol/kg];

$n_{i,tot}$  is the total number of moles of every compound [mol];

$m_{dry,gly}$  is the dry mass of feedstock entering the reactor [kg];

The total number of moles of every compound is calculated as the sum of the number of moles of every compound computed for every bag collected:

$$n_{i,tot} = \sum_{j=1}^n n_{compound,i} \quad (7.13)$$

Since the gas is considered as a perfect gas, the molar concentration is equal to the volume concentration:

$$C_{i,tot} = \frac{n_{i,tot}}{n_{gas,tot}} = \frac{V_i}{V_{gas,tot}} \quad (7.14)$$

Finally, the dry mass of the feedstock entering the reactor is calculated as the product of the total mass of the feedstock entering the system divided by the mass concentration of the solution.

$$m_{dry, gly} = m_{in} y \quad (7.15)$$

Where  $y$  is the mass concentration of the solution [%wt].

### 7.2.3. Efficiency of conversion

Conversion efficiencies are important parameters required to assess the quality of SCWG of glycerol. Conversion efficiencies are calculated for every element (C, O and H), and, considering that the gases compounds produced in these experiments are  $H_2, CO_2, C_2H_4, C_2H_6, CH_4, CO$  the general conversion efficiency is calculated as:

$$kGE = \frac{m_{k,gas}}{m_{k,feed}} \quad (7.16)$$

Where:

$k$  indicates the general element among C, H and O;

$m_{k,gas}$  is the mass of the element produced through the SCWG [g];

$m_{k,feed}$  is the mass of the element introduced into the reactor [g];

The mass of the generic element produced is calculated as:

$$m_{k,gas} = n_{k,gas,j} MW_k \quad (7.17)$$

While the total number of moles is given by the sum of the number of moles of every element calculated for every bag:

$$n_{k,gas} = \sum_{j=1}^n n_{k,gas,j} \quad (7.18)$$

For every bag, the number of moles of every compound containing the k-th atom is multiplied by the number of the atoms k presents in that particular compound. Subsequently, the results of all k atoms are summed.

$$n_{C,gas,j} = 1n_{CO_2,j} + 2n_{C_2H_4,j} + 2n_{C_2H_6,j} + 1n_{CH_4,j} + 1n_{CO,j} \quad (7.19)$$

$$n_{H,gas,j} = 2n_{H_2,j} + 4n_{C_2H_4,j} + 6n_{C_2H_6,j} + 4n_{CH_4,j} \quad (7.20)$$

$$n_{O,gas,j} = 2n_{CO_2,j} + 1n_{CO,j} \quad (7.21)$$

The mass of every element introduced into the reactor is calculated by multiplying the dry mass feedstock by the percentage amount of the atom in the glycerol solution.

$$m_{C,gly,feed} = 0.3913 \cdot m_{dry,gly} \quad (7.22)$$

$$m_{H,gly,feed} = 0.0876 \cdot m_{dry,gly} \quad (7.23)$$

$$m_{O,gly,feed} = 0.5212 \cdot m_{dry,gly} \quad (7.24)$$

#### 7.2.4. Lower and Higher Heating Values

The heating value of a substance is the amount of heat released during the combustion of a specified amount of it. In particular, the higher heating value (HHV) is determined by bringing all the products of combustion back to the original temperature before the reaction, and condensing any vapour produced, while the lower heating value (LHV) is determined by subtracting the heat of vaporization of water from the higher heating value. The energy required to vaporize the water, therefore, is not released as heat.

The lower and higher heating values of the gas product of the SCWG of the glycerol solution are calculated as:

$$LHV_{gas} = \frac{\sum_i^t m_{i,tot} LHV_i}{V_{gas}} \quad (7.25)$$

$$HHV_{gas} = \frac{\sum_i^t m_{i,tot} HHV_i}{V_{gas}} \quad (7.26)$$

Where:

$LHV_{gas}$  is the lower heating value of the gas product [MJ/m<sup>3</sup>];

$HHV_{gas}$  is the higher heating value of the gas product [MJ/m<sup>3</sup>];

$LHV_i$  is the lower heating value of the different compounds [MJ/kg];

$HHV_i$  is the higher heating value of the different compounds [MJ/kg];

$m_{i,tot}$  is the mass of the different compounds [kg];

$V_{gas}$  is the total volume of the gas produced [m<sup>3</sup>];

The lower and higher heating values of the different compounds and glycerol are available in the literature.

### 7.2.5. Cold gas efficiency

The cold gas efficiency is defined as the ratio of the energy that would be released by the combustion of the gas product, over the energy that would be released by the combustion of the feedstock.

In particular, in this thesis the cold gas efficiency of the syngas produced by the SCWG of the glycerol solution has been calculated considering the lower heating values of the different compounds that constitute the syngas and the lower heating value of the feedstock:

$$CGE_{syn} = \frac{\sum_i^t m_{i,tot} LHV_i}{LHV_{gly} y_{gly} m_{gly,feed}} \quad (7.27)$$

Where:

$CGE_{syn}$  is the cold gas efficiency of the syngas;

$LHV_{gly}$  is the lower heating value of glycerol;

$y_{gly}$  is the mass concentration of glycerol;

Table 7.1 shows all the lower heating values of the compounds found in literature.

Compound	LHV [MJ/kg]	HHV [MJ/kg]
H2	120	142,37
CO2	-	-
C2H4	50,32	53,39
C2H6	51,90	54,69
CH4	55,52	60,3
CO	10,05	10,96
$C_3H_8O_3$	17,61	-

**Table 7.1:** Lower heating values of compounds.

### 7.3. Results

Three volumetric flow rate, meaning three different residence times, for three different concentration have been tested by using both SS316 and INCONEL 625 reactors. The temperature is set at 600°C, while the pressure at 250 bar. In this paragraph, all the results obtained by the experiments are provided, summarised and analysed.

#### 7.3.1. Stainless steel 316 at 2,5 %wt and 375 ml/min

y [%wt]	2,5%
$\dot{m}_{gly}$ [g/min]	1,94
$\dot{V}_{gly,react}$ [ml/min]	27,307
Residence time [min]	2,966
$\rho_{out}$ [g/ml]	0,217

Table 7.2: Main input parameters for SS316, 2,5 %wt and 375 ml/min.

Where:

$\dot{m}_{gly}$  is the mass flow rate of the glycerol solution at ambient temperature and 250°C;

$\dot{V}_{gly,react}$  is the volume flow rate of the glycerol solution expanded inside the reactor;

$\rho_{out}$  is the density of the gas product in the pipe between the reactor and the bag.

The density of the gas product has been calculated with the Amagat's law taking into account all i-th compounds densities

$$V = \sum_{i=1}^n \bar{v}_i n_i \quad (7.28)$$

So the density is:

$$\rho_{out} = \left( \sum_{i=1}^n v_i y_i \right)^{-1} \quad (7.29)$$

Where:

$\bar{v}_i$  is the molar volume of the i-th compound [ml/mol];

$v_i$  is the mass volume of the  $i$ -th compound at 1 atm [ml/g];

$n_i$  is the number of moles [mol];

$y_i$  is the mass fraction in the mixture [%];

The mass fraction of the mixture is calculated by the composition of the total amount of gas collected within the whole single experiment:

$$y_i = \frac{n_{i,tot,coll}}{n_{tot,coll}} = \frac{\sum_{j=1}^n n_{i,j}}{\sum_{i=1}^t \sum_{j=1}^n n_{i,j}} \quad (7.30)$$

From the GC analyses, volume fractions are provided for the gas mixture that is in ambient thermodynamic conditions, whereas the mix under study is subjected to a pressure of 250bar. Therefore, the principle of mass conservation was observed considering that all compounds are in the same proportion with each other at 250bar as well as 1bar. In this way, temperature and pressure affect only the specific volume values, which have been taken from the NIST database<sup>4</sup>. Table 7.3 shows the results for all gaseous species identified by GC analyses.

	$\rho$ [g/ml]	$v$ [ml/g]
<b>H2</b>	0,018	56,625
<b>CO2</b>	0,943	1,060
<b>C2H4</b>	0,420	2,380
<b>C2H6</b>	0,436	2,292
<b>CH4</b>	0,189	5,298
<b>CO</b>	0,262	3,815

**Table 7.3:** Densities and specific volumes at 25°C and 250 bar.

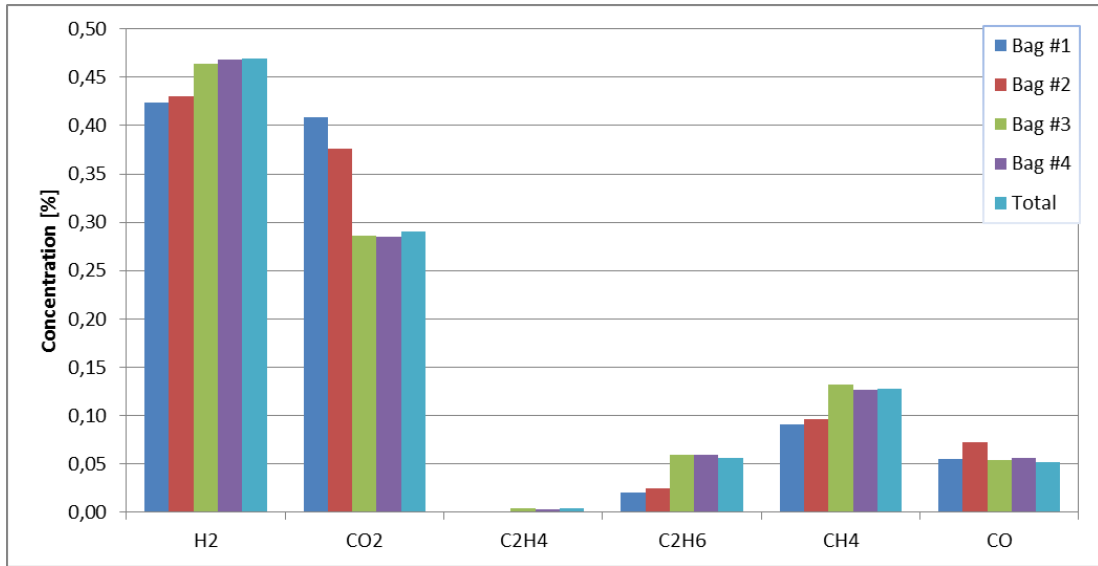


Fig. 7.2: Volumetric concentration of syngas for each bag for SS316, 2,5 %wt and 375 ml/min.

	[%vol]	m [g]	[%wt]	Yield[mol/kg]
<b>H2</b>	45,1%	0,140	4,97%	19,68
<b>CO2</b>	34,3%	1,886	67,17%	12,18
<b>C2H4</b>	0,4%	0,015	0,54%	0,15
<b>C2H6</b>	4,5%	0,249	8,87%	2,35
<b>CH4</b>	11,1%	0,303	10,79%	5,37
<b>CO</b>	4,5%	0,215	7,65%	2,18
<b>Total</b>	-	2,808	-	41,91

Table 7.4: Composition and gas yield for SS316, 2,5 %wt and 375 ml/min.

	Method 1	Method 2
<b>CCE [%]</b>	75,95%	93,81%
<b>HCE [%]</b>	86,98%	107,44%
<b>OCE [%]</b>	81,46%	100,62%
<b>CGE [%]</b>	89,26%	96,51%
<b>LHV [MJ/kg]</b>	17,60	

Table 7.5: Efficiencies and LHV for SS316, 2,5 %wt and 375 ml/min.

### 7.3.2. Stainless steel 316 at 2,5 %wt and 250 ml/min

$y$ [%wt]	2,5%
$\dot{m}_{gly}$ [g/min]	1,32
$\dot{V}_{gly, reac}$ [ml/min]	18,577
Residence time [min]	4,360
$\rho_{out}$ [g/ml]	0,216

Table 7.6: Main input parameters for SS316, 2,5 %wt and 250 ml/min.

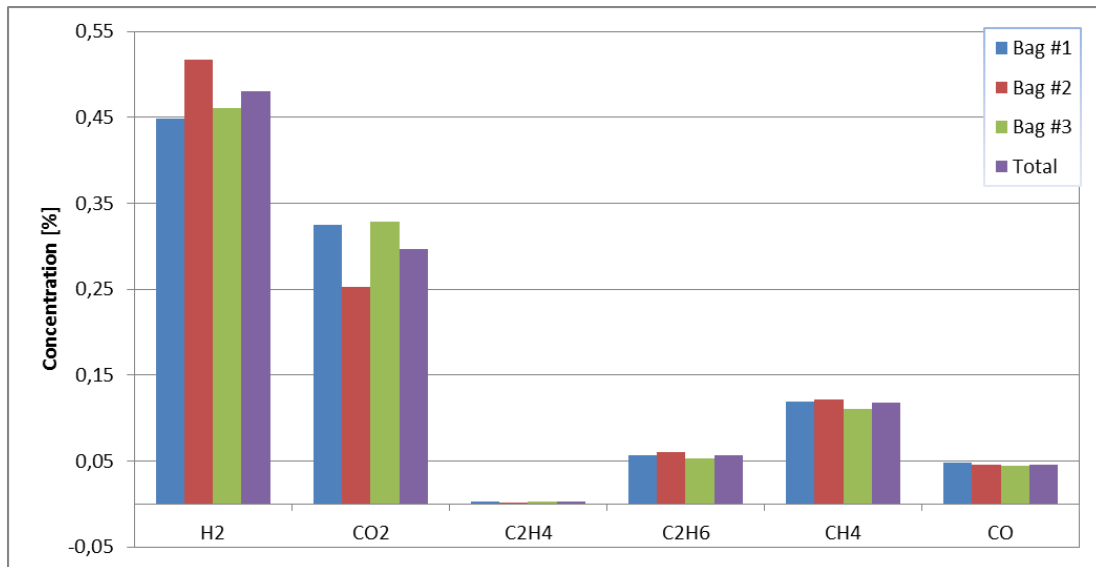


Fig. 7.3: Volumetric concentration of syngas for each bag for SS316, 2,5 %wt and 250 ml/min.

	[%vol]	m [g]	[%wt]	Yield[mol/kg]
<b>H<sub>2</sub></b>	47,5%	0,154	5,11%	24,09
<b>CO<sub>2</sub></b>	30,2%	2,066	68,73%	14,85
<b>C<sub>2</sub>H<sub>4</sub></b>	0,2%	0,010	0,35%	0,12
<b>C<sub>2</sub>H<sub>6</sub></b>	5,7%	0,272	9,03%	2,86
<b>CH<sub>4</sub></b>	11,7%	0,300	9,97%	5,91
<b>CO</b>	4,6%	0,205	6,81%	2,31
<b>Total</b>	-	3,006	-	50,13

Table 7.7: Composition and gas yield for SS316, 2,5 %wt and 250 ml/min.

	Method 1	Method 2
CCE [%]	89,06%	93,13%
HCE [%]	102,92%	107,63%
OCE [%]	98,25%	102,74%
CGE [%]	92,91%	97,15%
LHV [MJ/kg]	17,21	

Table 7.8: Efficiencies and LHV for SS316, 2,5 %wt and 250 ml/min.

### 7.3.3. Stainless steel 316 at 2,5 %wt and 125 ml/min

$y$ [%wt]	2,5%
$\dot{m}_{gly}$ [g/min]	0,77
$\dot{V}_{gly, reac}$ [ml/min]	10,901
Residence time [min]	7,430
$\rho_{out}$ [g/ml]	0,204

Table 7.9: Main input parameters for SS316, 2,5 %wt and 125 ml/min.

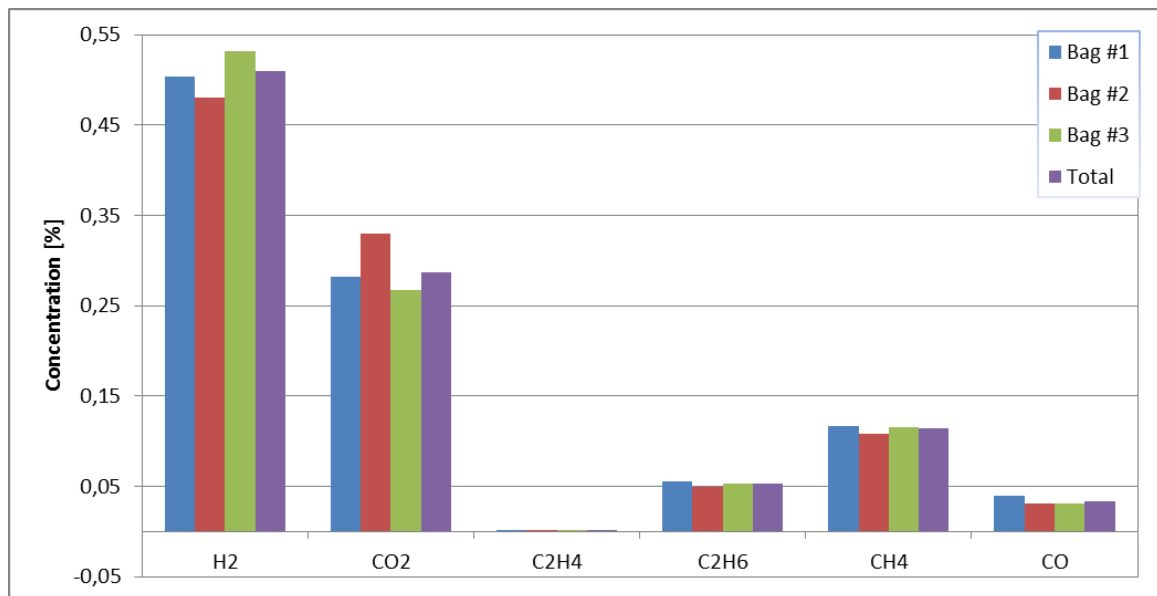


Fig. 7.4: Volumetric concentration of syngas for each bag for SS316, 2,5 %wt and 125 ml/min.

	<b>[%vol]</b>	<b>m [g]</b>	<b>[%wt]</b>	<b>Yield[mol/kg]</b>
<b>H2</b>	50,5%	0,167	5,68%	27,95
<b>CO2</b>	29,3%	2,045	69,75%	15,72
<b>C2H4</b>	0,1%	0,007	0,23%	0,08
<b>C2H6</b>	5,3%	0,262	8,92%	2,94
<b>CH4</b>	11,3%	0,297	10,14%	6,27
<b>CO</b>	3,4%	0,155	5,27%	1,87
<b>Total</b>	-	2,932	-	54,83

Table 7.10: Composition and gas yield for SS316, 2,5 %wt and 125 ml/min.

	<b>Method 1</b>	<b>Method 2</b>
<b>CCE [%]</b>	91,78%	91,88%
<b>HCE [%]</b>	113,92%	114,04%
<b>OCE [%]</b>	102,22%	102,33%
<b>CGE [%]</b>	99,81%	99,92%
<b>LHV [MJ/kg]</b>	17,72	

Table 7.11: Efficiencies and LHV for SS316, 2,5 %wt and 250 ml/min.

#### 7.3.4. Stainless steel 316 at 5 %wt and 375 ml/min

$y$ [%wt]	5%
$\dot{m}_{gly}$ [g/min]	1,95
$\dot{V}_{gly, reac}$ [ml/min]	27,307
Residence time [min]	2,966
$\rho_{out}$ [g/ml]	0,227

Table 7.12: Main input parameters for SS316, at 5 %wt and 375 ml/min.

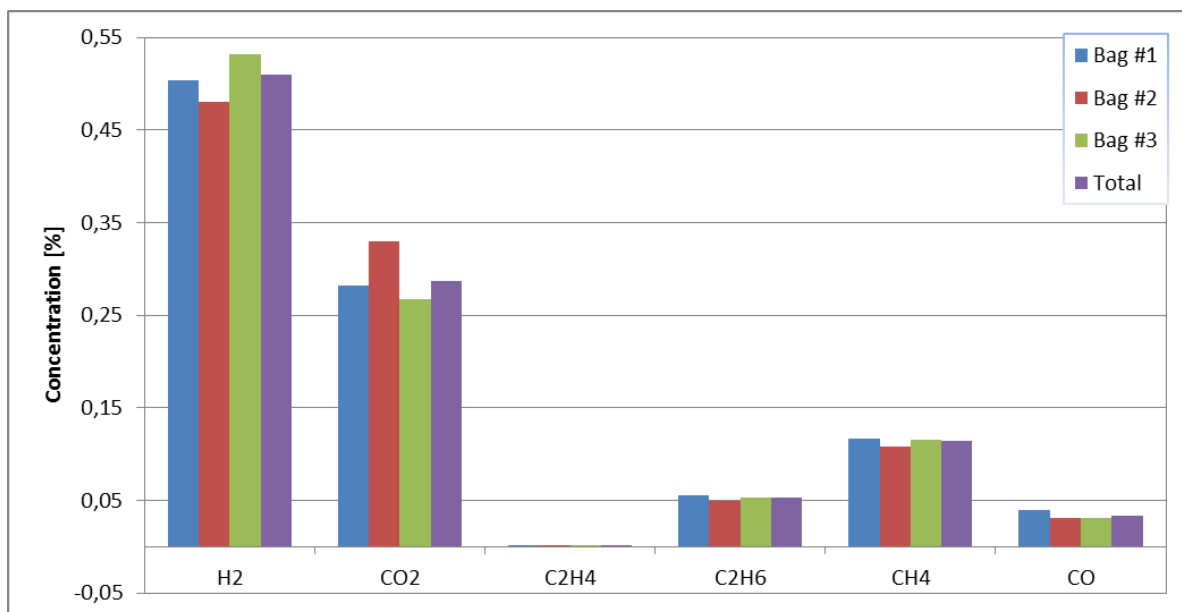


Fig. 7.5: Volumetric concentration of syngas for each bag for SS316 at 5 %wt and 375 ml/min.

	[%vol]	m [g]	[%wt]	Yield[mol/kg]
<b>H2</b>	43,9%	0,186	4,51%	16,49
<b>CO2</b>	33,3%	2,650	64,29%	10,78
<b>C2H4</b>	0,6%	0,033	0,80%	0,21
<b>C2H6</b>	5,2%	0,394	9,56%	2,34
<b>CH4</b>	10,0%	0,399	9,67%	4,45
<b>CO</b>	7,0%	0,461	11,19%	2,95
<b>Total</b>	-	4,123	-	37,22

Table 7.13: Composition and gas yield for SS316 at 5 %wt and 375 ml/min.

	Method 1	Method 2
<b>CCE [%]</b>	71,46%	72,59%
<b>HCE [%]</b>	75,60%	76,80%
<b>OCE [%]</b>	75,21%	76,40%
<b>CGE [%]</b>	72,31%	73,45%
<b>LHV [MJ/kg]</b>	17,26	

Table 7.14: Efficiencies and LHV for SS316 at 5 %wt and 375 ml/min.

### 7.3.5. Stainless steel 316 at 5 %wt and 250 ml/min

$y$ [%wt]	5%
$\dot{m}_{gly}$ [g/min]	1,33
$\dot{V}_{gly, reac}$ [ml/min]	18,577
Residence time [min]	4,360
$\rho_{out}$ [g/ml]	0,218

Table 7.15: Main input parameters for SS316, at 5 %wt and 250 ml/min.

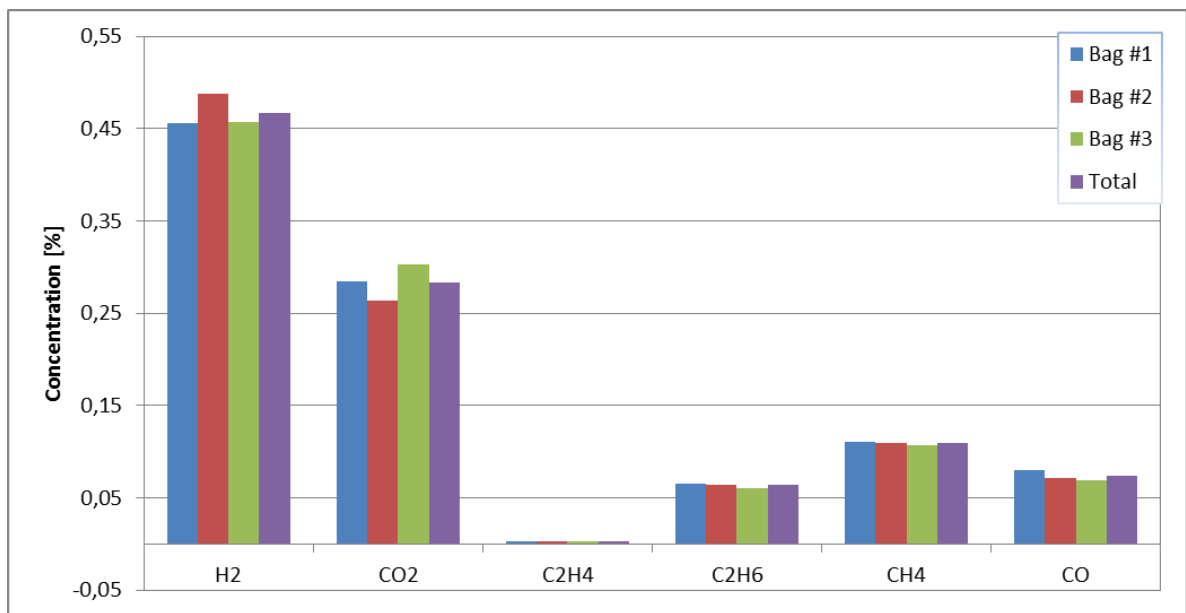


Fig. 7.6: Volumetric concentration of syngas for each bag for SS316 at 5 %wt and 250 ml/min.

	[%vol]	m [g]	[%wt]	Yield[mol/kg]
<b>H2</b>	46,7%	0,234	4,90%	20,03
<b>CO2</b>	28,4%	3,101	64,79%	12,13
<b>C2H4</b>	0,3%	0,023	0,47%	0,14
<b>C2H6</b>	6,4%	0,477	9,96%	2,73
<b>CH4</b>	10,9%	0,436	9,10%	4,68
<b>CO</b>	7,4%	0,515	10,77%	3,17
<b>Total</b>	-	4,785	-	42,87

Table 7.16: Composition and gas yield for SS316 at 5 %wt and 250 ml/min.

	Method 1	Method 2
CCE [%]	78,93%	81,04%
HCE [%]	87,15%	89,48%
OCE [%]	84,20%	86,45%
CGE [%]	81,54%	83,72%
LHV [MJ/kg]	17,43	

Table 7.17: Efficiencies and LHV for SS316 at 5 %wt and 250 ml/min.

### 7.3.6. Stainless steel 316 at 5 %wt and 125 ml/min

$y$ [%wt]	5%
$\dot{m}_{gly}$ [g/min]	0,78
$\dot{V}_{gly, reac}$ [ml/min]	10,901
Residence time [min]	7,430
$\rho_{out}$ [g/ml]	0,218

Table 7.18: Main input parameters for SS316, at 5 %wt and 125 ml/min.

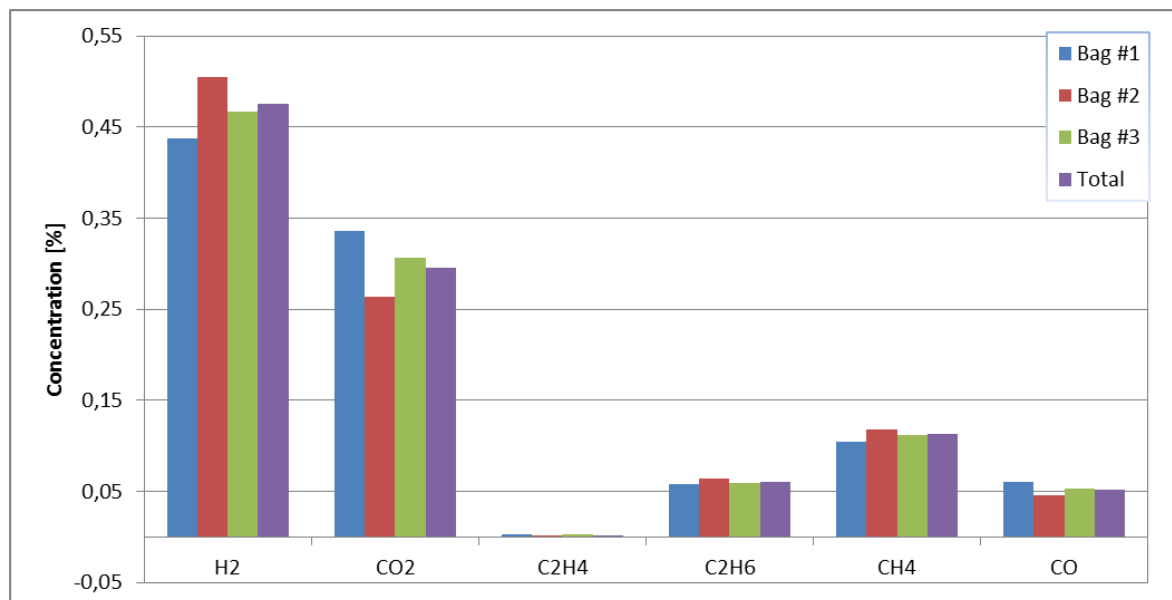


Fig. 7.7: Volumetric concentration of syngas for each bag for SS316 at 5 %wt and 125 ml/min.

	<b>[%vol]</b>	<b>m [g]</b>	<b>[%wt]</b>	<b>Yield[mol/kg]</b>
<b>H2</b>	47,0%	0,211	5,01%	18,54
<b>CO2</b>	30,2%	2,859	68,06%	11,53
<b>C2H4</b>	0,2%	0,014	0,34%	0,09
<b>C2H6</b>	6,0%	0,403	9,59%	2,38
<b>CH4</b>	11,2%	0,397	9,46%	4,39
<b>CO</b>	5,3%	0,317	7,54%	2,01
<b>Total</b>	-	4,200	-	38,93

Table 7.19: Composition and gas yield for SS316 at 5 %wt and 125 ml/min.

	<b>Method 1</b>	<b>Method 2</b>
<b>CCE [%]</b>	70,17%	84,49%
<b>HCE [%]</b>	79,74%	96,01%
<b>OCE [%]</b>	76,93%	92,62%
<b>CGE [%]</b>	72,68%	87,51%
<b>LHV [MJ/kg]</b>	17,17	

Table 7.20: Efficiencies and LHV for SS316 at 5 %wt and 125 ml/min.

### 7.3.7. *Stainless steel 316 at 10 %wt and 375 ml/min*

$y$ [%wt]	10%
$\dot{m}_{gly}$ [g/min]	1,97
$\dot{V}_{gly, reac}$ [ml/min]	27,307
Residence time [min]	2,966
$\rho_{out}$ [g/ml]	0,239

Table 7.21: Main input parameters for SS316, at 10 %wt and 375 ml/min.

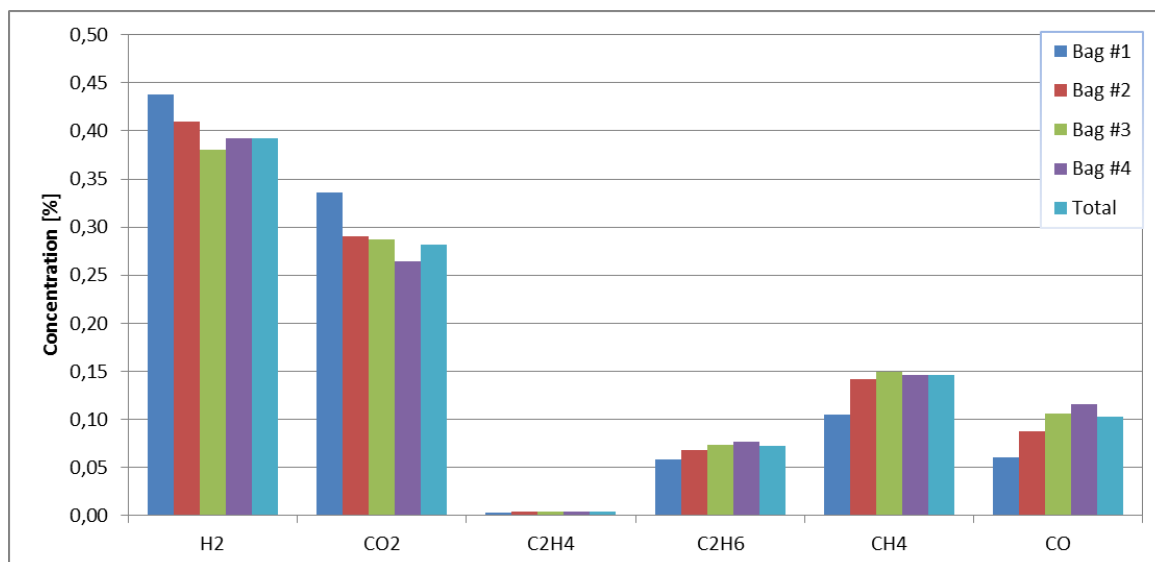


Fig. 7.8: Volumetric concentration of syngas for each bag for SS316 at 10 %wt and 375 ml/min.

	<b>[%vol]</b>	<b>m [g]</b>	<b>[%wt]</b>	<b>Yield[mol/kg]</b>
<b>H2</b>	40,7%	0,228	3,82%	12,94
<b>CO2</b>	28,2%	3,577	59,85%	9,28
<b>C2H4</b>	0,4%	0,034	0,57%	0,14
<b>C2H6</b>	6,8%	0,630	10,55%	2,39
<b>CH4</b>	13,9%	0,677	11,32%	4,82
<b>CO</b>	10,1%	0,830	13,89%	3,38
<b>Total</b>	-	5,976	-	32,96

Table 7.22: Composition and gas yield for SS316 at 10 %wt and 375 ml/min.

	<b>Method 1</b>	<b>Method 2</b>
<b>CCE [%]</b>	69,22%	69,22%
<b>HCE [%]</b>	69,15%	69,16%
<b>OCE [%]</b>	67,36%	67,37%
<b>CGE [%]</b>	69,88%	69,89%
<b>LHV [MJ/kg]</b>	18,03	

Table 7.23: Efficiencies and LHV for SS316 at 10 %wt and 375 ml/min.

### 7.3.8. Stainless steel 316 at 10 %wt and 250 ml/min

$y$ [%wt]	10%
$\dot{m}_{gly}$ [g/min]	1,34
$\dot{V}_{gly, reac}$ [ml/min]	18,577
Residence time [min]	4,360
$\rho_{out}$ [g/ml]	0,239

Table 7.24: Main input parameters for SS316, at 10 %wt and 250 ml/min.

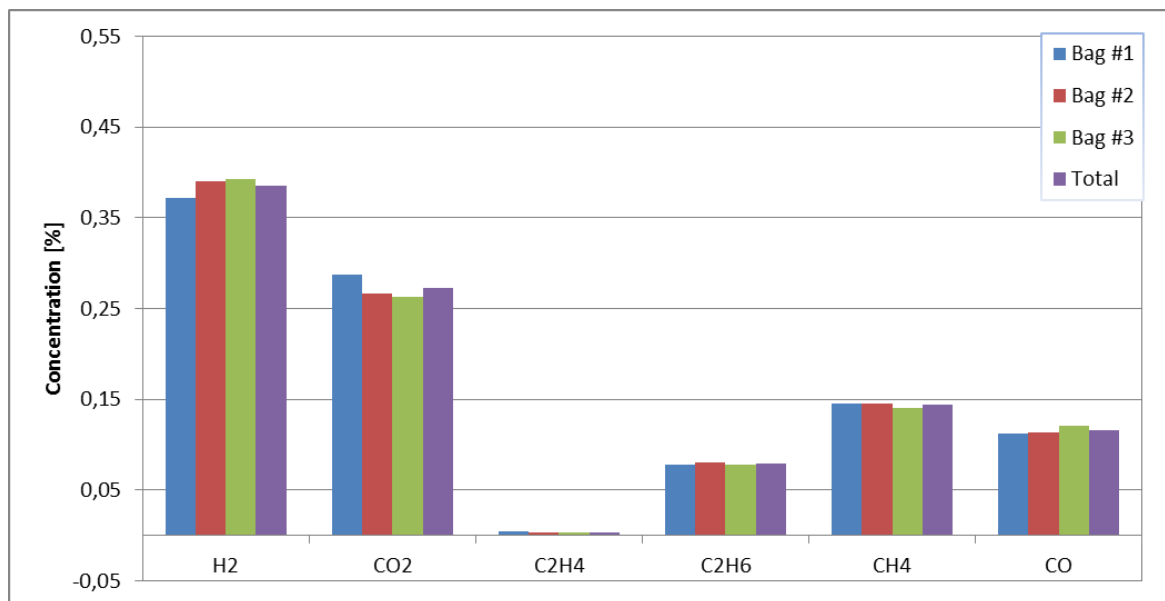


Fig. 7.9: Volumetric concentration of syngas for each bag for SS316 at 10 %wt and 250 ml/min.

	[%vol]	m [g]	[%wt]	Yield[mol/kg]
<b>H2</b>	38,5%	0,247	3,74%	13,18
<b>CO2</b>	27,3%	3,810	57,69%	9,32
<b>C2H4</b>	0,4%	0,033	0,49%	0,13
<b>C2H6</b>	7,9%	0,753	11,41%	2,70
<b>CH4</b>	14,4%	0,732	11,09%	4,92
<b>CO</b>	11,6%	1,029	15,58%	3,96
<b>Total</b>	-	6,604	-	34,19

Table 7.25: Composition and gas yield for SS316 at 10 %wt and 250 ml/min.

	Method 1	Method 2
CCE [%]	73,18%	80,21%
HCE [%]	72,18%	79,12%
OCE [%]	69,37%	76,04%
CGE [%]	74,20%	81,32%
LHV [MJ/kg]	18,37	

Table 7.26: Efficiencies and LHV for SS316 at 10 %wt and 250 ml/min.

### 7.3.9. Stainless steel 316 at 10 %wt and 125 ml/min

y [%wt]	10%
$\dot{m}_{gly}$ [g/min]	0,79
$\dot{V}_{gly, reac}$ [ml/min]	10,901
Residence time [min]	7,430
$\rho_{out}$ [g/ml]	0,237

Table 7.27: Main input parameters for SS316, at 10 %wt and 125 ml/min.

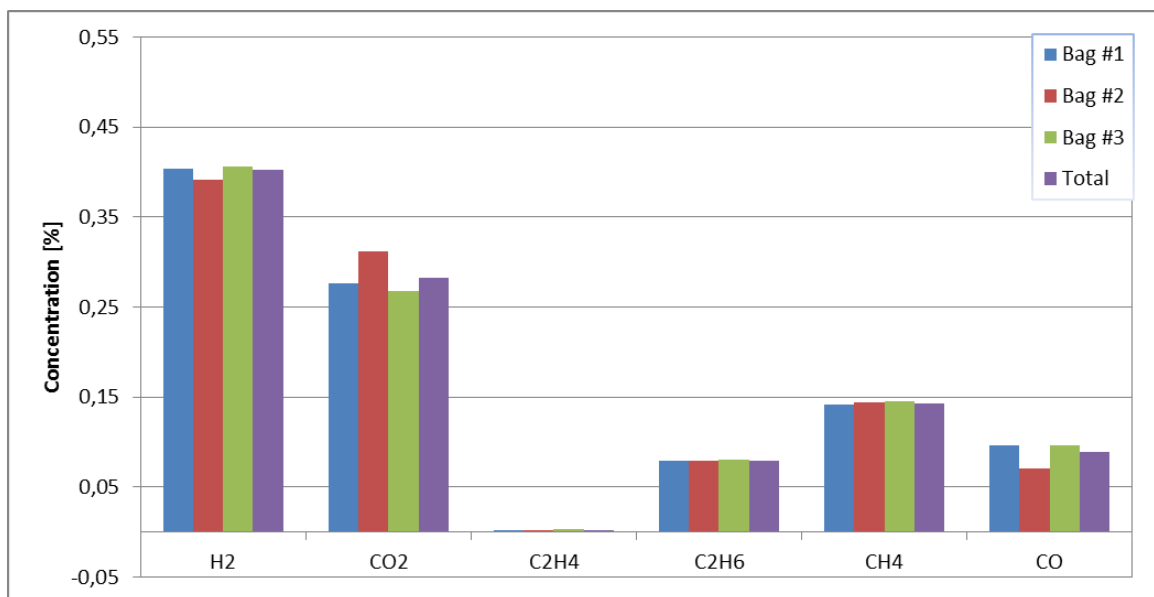


Fig. 7.10: Volumetric concentration of syngas for each bag for SS316 at 10 %wt and 125 ml/min.

	<b>[%vol]</b>	<b>m [g]</b>	<b>[%wt]</b>	<b>Yield[mol/kg]</b>
<b>H2</b>	40,1%	0,269	3,95%	12,60
<b>CO2</b>	28,6%	4,131	60,59%	8,86
<b>C2H4</b>	0,3%	0,024	0,35%	0,08
<b>C2H6</b>	8,0%	0,795	11,67%	2,50
<b>CH4</b>	14,4%	0,765	11,22%	4,50
<b>CO</b>	8,8%	0,833	12,22%	2,81
<b>Total</b>	-	6,818	-	31,34

Table 7.28: Composition and gas yield for SS316 at 10 %wt and 125 ml/min.

	<b>Method 1</b>	<b>Method 2</b>
<b>CCE [%]</b>	65,45%	77,77%
<b>HCE [%]</b>	67,36%	80,03%
<b>OCE [%]</b>	63,00%	74,85%
<b>CGE [%]</b>	67,34%	80,01%
<b>LHV [MJ/kg]</b>	18,43	

Table 7.29: Efficiencies and LHV for SS316 at 10 %wt and 125 ml/min.

### 7.3.10. INCONEL 625 at 2,5 %wt and 375 ml/min

$y$ [%wt]	2,5%
$\dot{m}_{gly}$ [g/min]	1,94
$\dot{V}_{gly, reac}$ [ml/min]	27,307
Residence time [min]	3,369
$\rho_{out}$ [g/ml]	0,249

Table 7.30: Main input parameters for INCONEL 625, at 2.5 %wt and 375 ml/min.

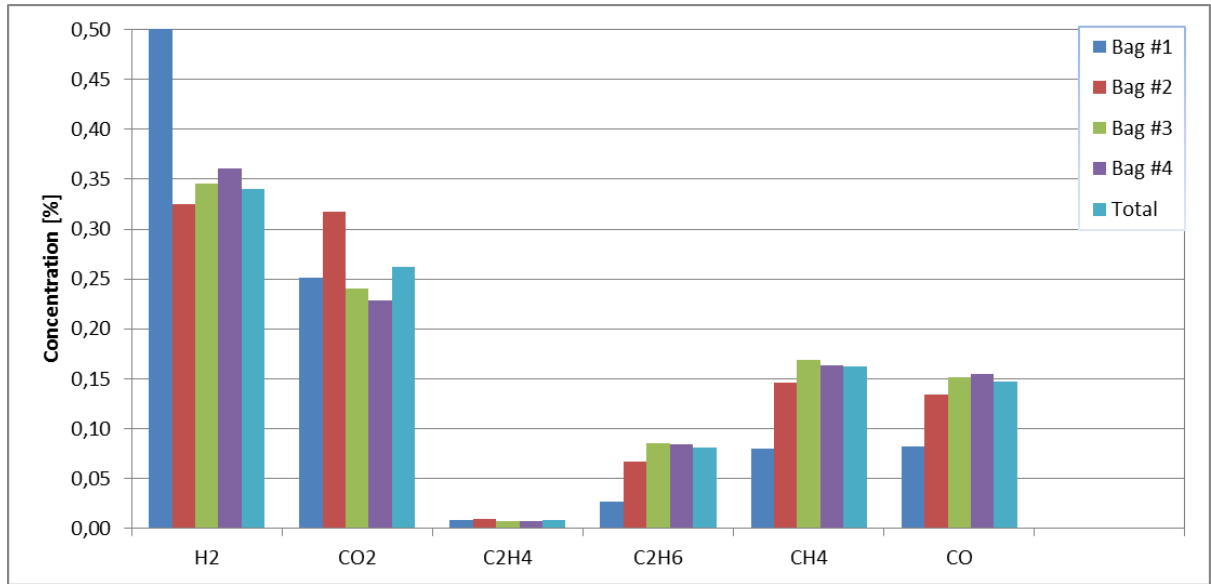


Fig. 7.11: Volumetric concentration of syngas for each bag for INCONEL 625 at 2.5 %wt and 375 ml/min.

	[%vol]	m [g]	[%wt]	Yield[mol/kg]
<b>H<sub>2</sub></b>	39,6%	0,074	3,18%	11,10
<b>CO<sub>2</sub></b>	25,9%	1,238	53,38%	8,54
<b>C<sub>2</sub>H<sub>4</sub></b>	0,8%	0,024	1,04%	0,26
<b>C<sub>2</sub>H<sub>6</sub></b>	6,6%	0,260	11,23%	2,63
<b>CH<sub>4</sub></b>	13,9%	0,280	12,06%	5,29
<b>CO</b>	13,1%	0,443	19,10%	4,80
<b>Total</b>	-	2,319	-	32,63

Table 7.31: Composition and gas yield for INCONEL 625 at 2.5 %wt and 375 ml/min.

	Method 1	Method 2
<b>CCE [%]</b>	74,95%	75,59%
<b>HCE [%]</b>	69,30%	69,90%
<b>OCE [%]</b>	67,16%	67,73%
<b>CGE [%]</b>	75,10%	75,74%
<b>LHV [MJ/kg]</b>	18,79	

Table 7.32: Efficiencies and LHV for INCONEL 625 at 2.5 %wt and 375 ml/min.

### 7.3.11. INCONEL 625 at 2,5 %wt and 250 ml/min

$y$ [%wt]	2,5%
$\dot{m}_{gly}$ [g/min]	1,32
$\dot{V}_{gly, reac}$ [ml/min]	18,577
Residence time [min]	4,952
$\rho_{out}$ [g/ml]	0,240

Table 7.33: Main input parameters for INCONEL 625, at 2.5 %wt and 250 ml/min.

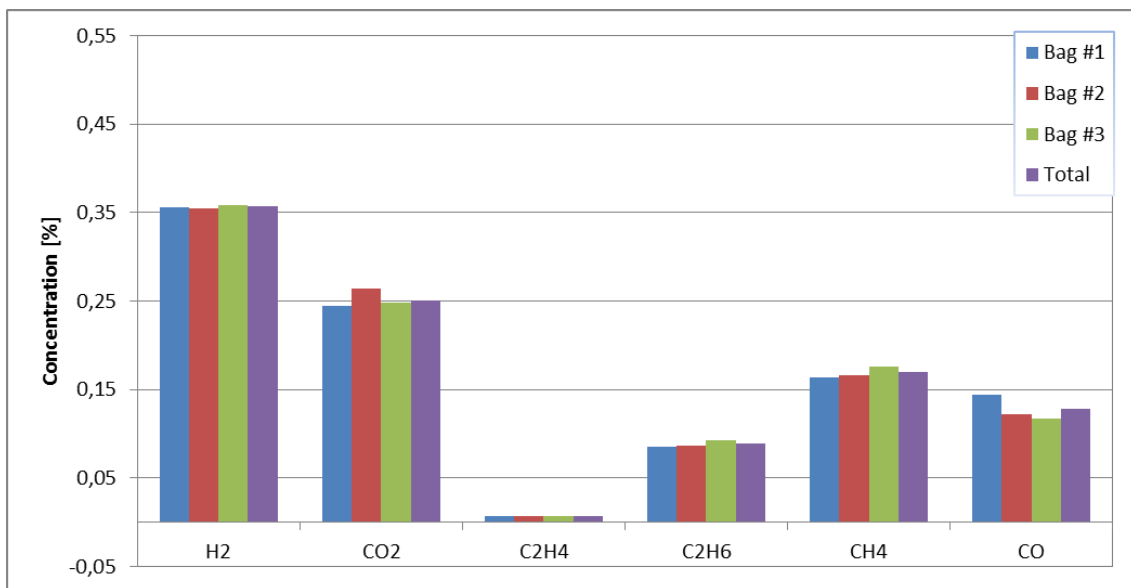


Fig. 7.12: Volumetric concentration of syngas for each bag for INCONEL 625 at 2.5 %wt and 250 ml/min.

	[%vol]	m [g]	[%wt]	Yield[mol/kg]
<b>H<sub>2</sub></b>	35,7%	0,083	3,44%	13,82
<b>CO<sub>2</sub></b>	25,2%	1,278	52,80%	9,71
<b>C<sub>2</sub>H<sub>4</sub></b>	0,6%	0,021	0,87%	0,25
<b>C<sub>2</sub>H<sub>6</sub></b>	8,8%	0,308	12,73%	3,42
<b>CH<sub>4</sub></b>	16,9%	0,315	13,00%	6,56
<b>CO</b>	12,8%	0,415	17,15%	4,95
<b>Total</b>	-	2,420	-	38,71

Table 7.34: Composition and gas yield for INCONEL 625 at 2.5 %wt and 250 ml/min.

	Method 1	Method 2
CCE [%]	87,71%	93,63%
HCE [%]	86,82%	92,68%
OCE [%]	74,80%	79,86%
CGE [%]	92,43%	9867,66%
LHV [MJ/kg]	20,12	

Table 7.35: Efficiencies and LHV for INCONEL 625 at 2.5 %wt and 250 ml/min.

### 7.3.12. INCONEL 625 at 2,5 %wt and 125 ml/min

$y$ [%wt]	2,5%
$\dot{m}_{gly}$ [g/min]	0,77
$\dot{V}_{gly, reac}$ [ml/min]	10,901
Residence time [min]	8,439
$\rho_{out}$ [g/ml]	0,259

Table 7.36: Main input parameters for INCONEL 625, at 2.5 %wt and 125 ml/min.

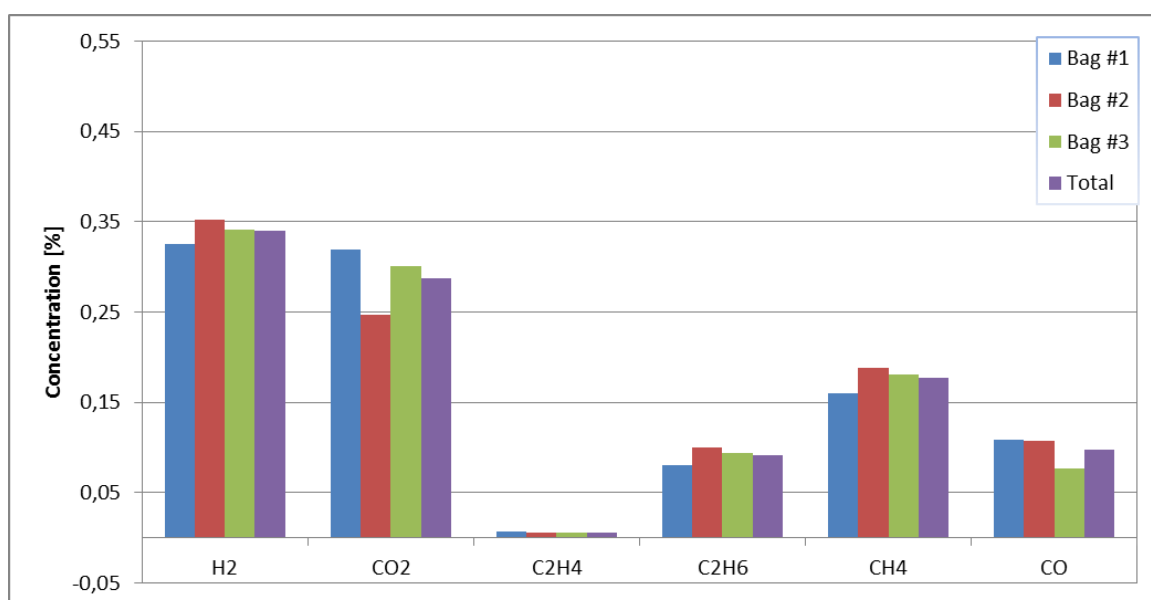


Fig. 7.13: Volumetric concentration of syngas for each bag for INCONEL 625 at 2.5 %wt and 125 ml/min.

	<b>[%vol]</b>	<b>m [g]</b>	<b>[%wt]</b>	<b>Yield[mol/kg]</b>
<b>H2</b>	33,9%	0,063	3,14%	11,50
<b>CO2</b>	28,9%	1,167	57,90%	9,71
<b>C2H4</b>	0,6%	0,016	0,78%	0,21
<b>C2H6</b>	9,1%	0,255	12,67%	3,11
<b>CH4</b>	17,6%	0,262	13,00%	5,98
<b>CO</b>	9,8%	0,252	12,51%	3,30
<b>Total</b>	-	2,015	-	33,80

Table 7.37: Composition and gas yield for INCONEL 625 at 2.5 %wt and 125 ml/min.

	<b>Method 1</b>	<b>Method 2</b>
<b>CCE [%]</b>	78,64%	87,15%
<b>HCE [%]</b>	76,43%	84,71%
<b>OCE [%]</b>	69,73%	77,28%
<b>CGE [%]</b>	80,52%	89,23%
<b>LHV [MJ/kg]</b>	19,21	

Table 7.38: Efficiencies and LHV for INCONEL 625 at 2.5 %wt and 125 ml/min.

### 7.3.13. INCONEL 625 at 5 %wt and 375 ml/min

$y$ [%wt]	5%
$\dot{m}_{gly}$ [g/min]	1,95
$V_{gly, reac}$ [ml/min]	27,307
Residence time [min]	3,369
$\rho_{out}$ [g/ml]	0,274

Table 7.39: Main input parameters for INCONEL 625, at 5 %wt and 375 ml/min.

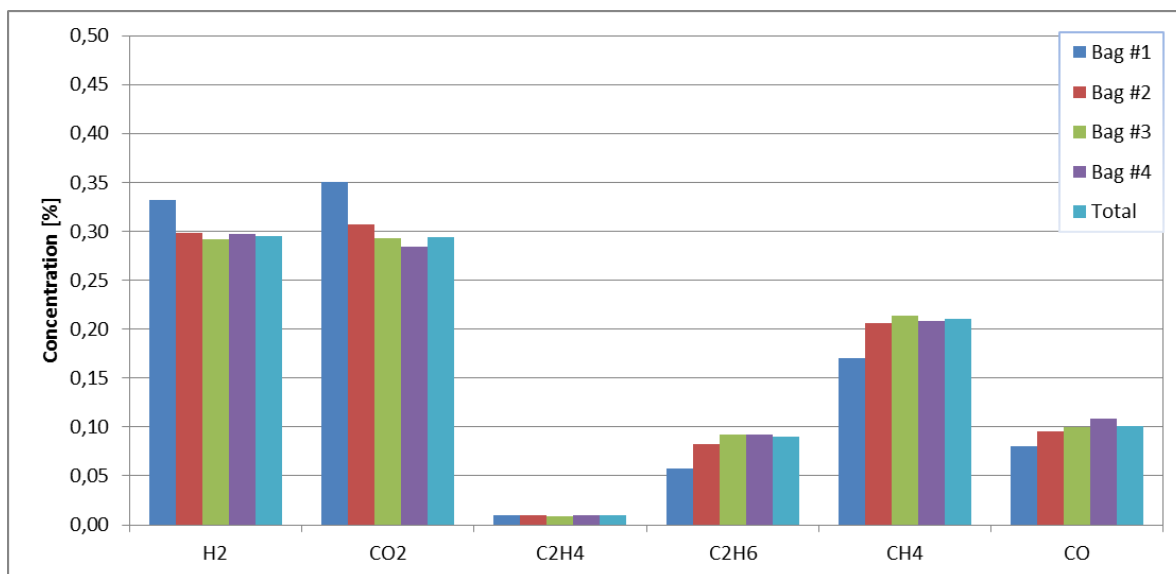


Fig. 7.14: Volumetric concentration of syngas for each bag for INCONEL 625 at 5 %wt and 375 ml/min.

	<b>[%vol]</b>	<b>m [g]</b>	<b>[%wt]</b>	<b>Yield[mol/kg]</b>
<b>H<sub>2</sub></b>	30,5%	0,118	2,62%	9,77
<b>CO<sub>2</sub></b>	30,9%	2,567	57,04%	9,74
<b>C<sub>2</sub>H<sub>4</sub></b>	1,0%	0,052	1,15%	0,31
<b>C<sub>2</sub>H<sub>6</sub></b>	8,1%	0,534	11,86%	2,96
<b>CH<sub>4</sub></b>	19,9%	0,668	14,83%	6,95
<b>CO</b>	9,6%	0,563	12,50%	3,35
<b>Total</b>	-	4,500	-	33,07

Table 7.40: Composition and gas yield for INCONEL 625 at 5 %wt and 375 ml/min.

	<b>Method 1</b>	<b>Method 2</b>
<b>CCE [%]</b>	81,57%	85,59%
<b>HCE [%]</b>	76,35%	80,11%
<b>OCE [%]</b>	70,06%	73,51%
<b>CGE [%]</b>	82,62%	86,70%
<b>LHV [MJ/kg]</b>	19,37	

Table 7.41: Efficiencies and LHV for INCONEL 625 at 5 %wt and 375 ml/min.

### 7.3.14. INCONEL 625 at 5 %wt and 250 ml/min

$y$ [%wt]	5%
$\dot{m}_{gly}$ [g/min]	1,33
$\dot{V}_{gly, reac}$ [ml/min]	18,577
Residence time [min]	4,952
$\rho_{out}$ [g/ml]	0,275

Table 7.42: Main input parameters for INCONEL 625, at 5 %wt and 250 ml/min.

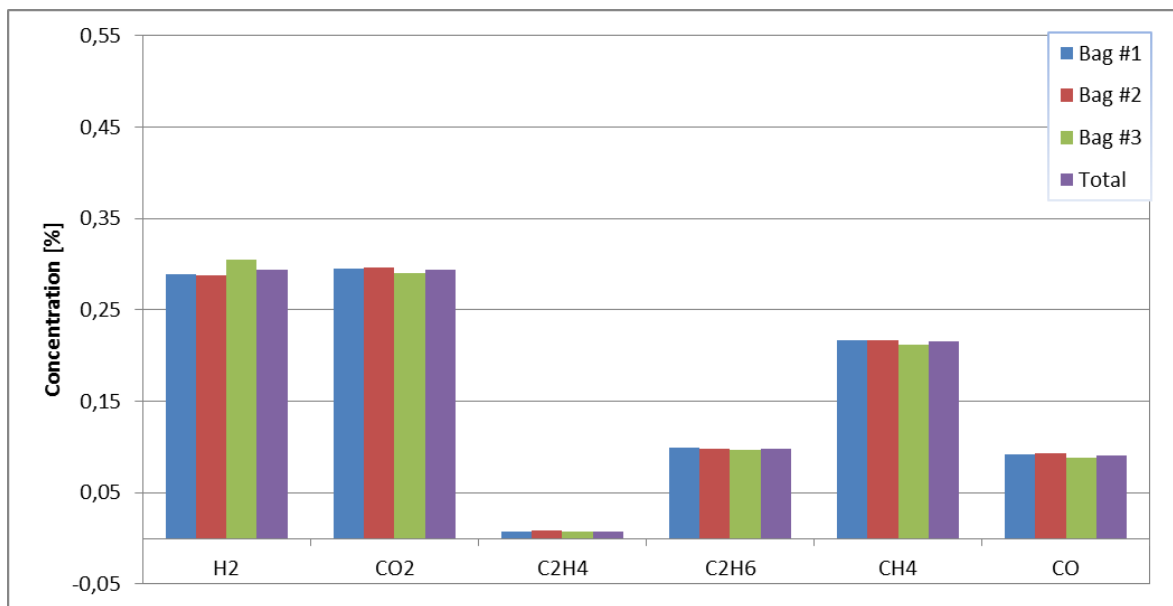


Fig. 7.15: Volumetric concentration of syngas for each bag for INCONEL 625 at 5 %wt and 250 ml/min.

	[%vol]	m [g]	[%wt]	Yield[mol/kg]
<b>H2</b>	29,4%	0,127	2,61%	9,99
<b>CO2</b>	29,4%	2,759	56,94%	9,98
<b>C2H4</b>	0,8%	0,046	0,96%	0,26
<b>C2H6</b>	9,8%	0,631	13,02%	3,34
<b>CH4</b>	21,5%	0,737	15,22%	7,31
<b>CO</b>	9,1%	0,545	11,25%	3,10
<b>Total</b>	-	4,845	-	33,99

Table 7.43: Composition and gas yield for INCONEL 625 at 5 %wt and 250 ml/min.

	Method 1	Method 2
CCE [%]	84,70%	90,12%
HCE [%]	80,96%	86,14%
OCE [%]	70,76%	75,28%
CGE [%]	87,37%	92,96%
LHV [MJ/kg]	19,95	

Table 7.44: Efficiencies and LHV for INCONEL 625 at 5 %wt and 250 ml/min.

### 7.3.15. INCONEL 625 at 5 %wt and 125 ml/min

y [%wt]	5%
$\dot{m}_{gly}$ [g/min]	0,78
$\dot{V}_{gly, reac}$ [ml/min]	10,901
Residence time [min]	8,439
$\rho_{out}$ [g/ml]	0,281

Table 7.45: Main input parameters for INCONEL 625, at 5 %wt and 125 ml/min.

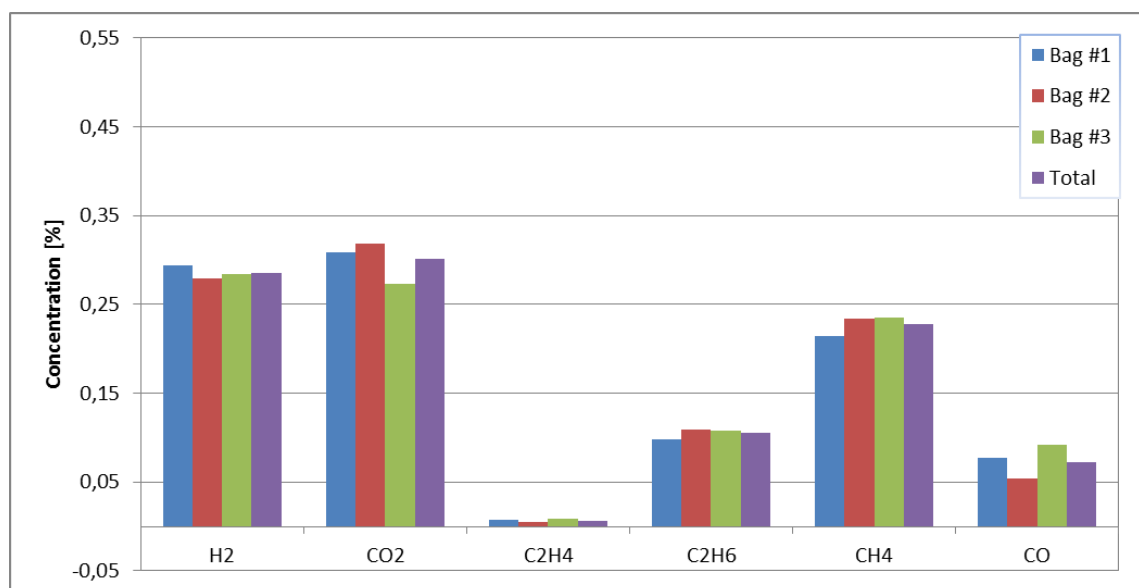


Fig. 7.16: Volumetric concentration of syngas for each bag for INCONEL 625 at 5 %wt and 125 ml/min.

	<b>[%vol]</b>	<b>m [g]</b>	<b>[%wt]</b>	<b>Yield[mol/kg]</b>
<b>H2</b>	28,6%	0,090	2,51%	8,37
<b>CO2</b>	30,0%	2,074	57,96%	8,84
<b>C2H4</b>	0,7%	0,030	0,83%	0,20
<b>C2H6</b>	10,5%	0,495	13,82%	3,09
<b>CH4</b>	22,8%	0,572	15,99%	6,69
<b>CO</b>	7,4%	0,318	8,88%	2,13
<b>Total</b>	-	3,578	-	29,33

Table 7.46: Composition and gas yield for INCONEL 625 at 5 %wt and 125 ml/min.

	<b>Method 1</b>	<b>Method 2</b>
<b>CCE [%]</b>	74,40%	91,70%
<b>HCE [%]</b>	72,34%	89,16%
<b>OCE [%]</b>	60,83%	74,97%
<b>CGE [%]</b>	77,71%	95,78%
<b>LHV [MJ/kg]</b>	20,38	

Table 7.47: Efficiencies and LHV for INCONEL 625 at 5 %wt and 125 ml/min.

### 7.3.16. INCONEL 625 at 10 %wt and 375 ml/min

$y$ [%wt]	10%
$\dot{m}_{gly}$ [g/min]	1,97
$\dot{V}_{gly, reac}$ [ml/min]	27,307
Residence time [min]	3,369
$\rho_{out}$ [g/ml]	0,270

Table 7.48: Main input parameters for INCONEL 625, at 10 %wt and 375 ml/min.

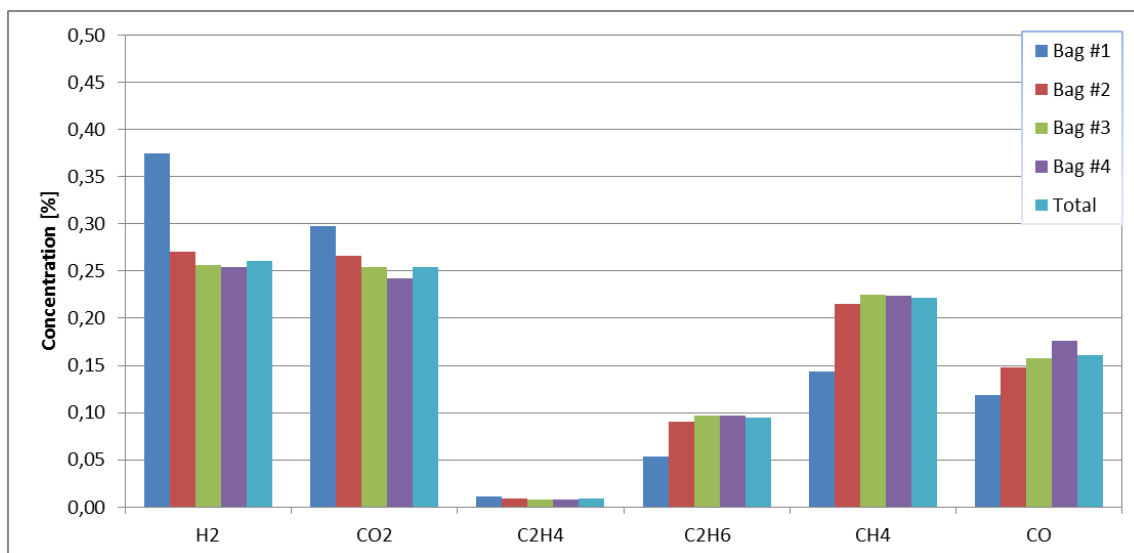


Fig. 7.17: Volumetric concentration of syngas for each bag for INCONEL 625 at 10 %wt and 375 ml/min.

	[%vol]	m [g]	[%wt]	Yield[mol/kg]
<b>H2</b>	28,9%	0,168	2,29%	7,07
<b>CO2</b>	26,5%	3,580	48,87%	6,89
<b>C2H4</b>	0,9%	0,078	1,06%	0,24
<b>C2H6</b>	8,4%	0,915	12,49%	2,58
<b>CH4</b>	20,2%	1,138	15,53%	6,01
<b>CO</b>	15,0%	1,446	19,75%	4,38
<b>Total</b>	-	7,324	-	27,16

Table 7.49: Composition and gas yield for INCONEL 625 at 10 %wt and 375 ml/min.

	Method 1	Method 2
<b>CCE [%]</b>	70,32%	70,98%
<b>HCE [%]</b>	62,83%	63,42%
<b>OCE [%]</b>	55,75%	56,28%
<b>CGE [%]</b>	71,83%	72,51%
<b>LHV [MJ/kg]</b>	20,38	

Table 7.50: Efficiencies and LHV for INCONEL 625 at 10 %wt and 375 ml/min.

### 7.3.17. INCONEL 625 at 10 %wt and 250 ml/min

$y$ [%wt]	2,5
$\dot{m}_{gly}$ [g/min]	1,82
$\dot{V}_{gly, reac}$ [ml/min]	25,573
Residence time [min]	3,167
$\rho_{out}$ [g/ml]	0,217

Table 7.51: Main input parameters for INCONEL 625, at 10 %wt and 250 ml/min.

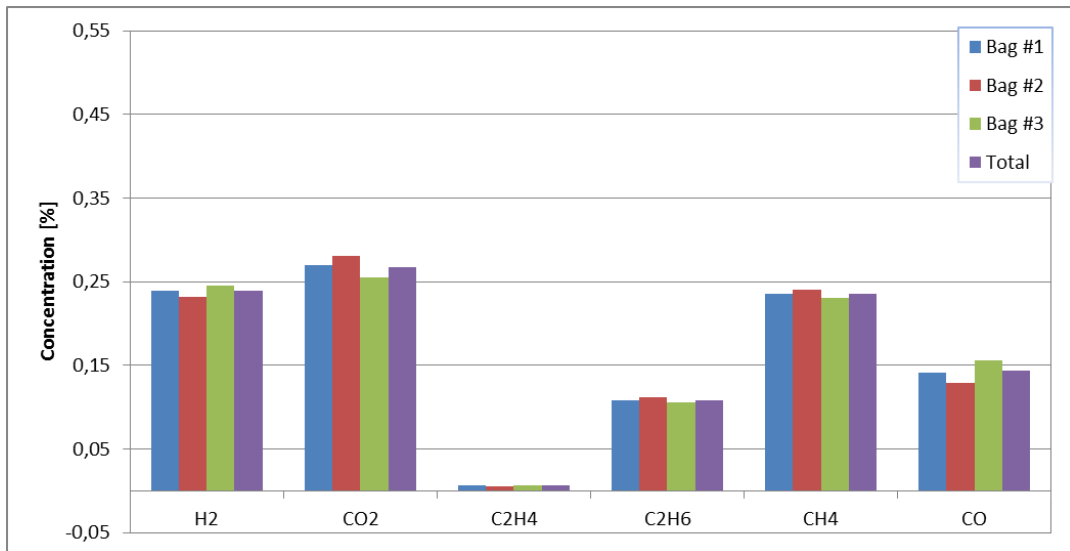


Fig. 7.18: Volumetric concentration of syngas for each bag for INCONEL 625 at 10 %wt and 250 ml/min.

	[%vol]	m [g]	[%wt]	Yield[mol/kg]
<b>H2</b>	23,9%	0,158	2,05%	6,16
<b>CO2</b>	26,9%	3,864	50,19%	6,90
<b>C2H4</b>	0,6%	0,057	0,74%	0,16
<b>C2H6</b>	10,9%	1,069	13,89%	2,80
<b>CH4</b>	23,5%	1,235	16,05%	6,06
<b>CO</b>	14,2%	1,315	17,08%	3,69
<b>Total</b>	-	7,698	-	25,77

Table 7.52: Composition and gas yield for INCONEL 625 at 10 %wt and 250 ml/min.

	Method 1	Method 2
CCE [%]	69,26%	71,94%
HCE [%]	62,12%	64,52%
OCE [%]	53,71%	55,79%
CGE [%]	71,06%	73,80%
LHV [MJ/kg]	20,67	

Table 7.53: Composition and gas yield for INCONEL 625 at 10 %wt and 250 ml/min.

### 7.3.18. INCONEL 625 at 10 %wt and 125 ml/min

$y$ [%wt]	10%
$\dot{m}_{gly}$ [g/min]	0,79
$\dot{V}_{gly, reac}$ [ml/min]	10,901
Residence time [min]	8,439
$\rho_{out}$ [g/ml]	0,286

Table 7.54: Main input parameters for INCONEL 625, at 10 %wt and 125 ml/min.

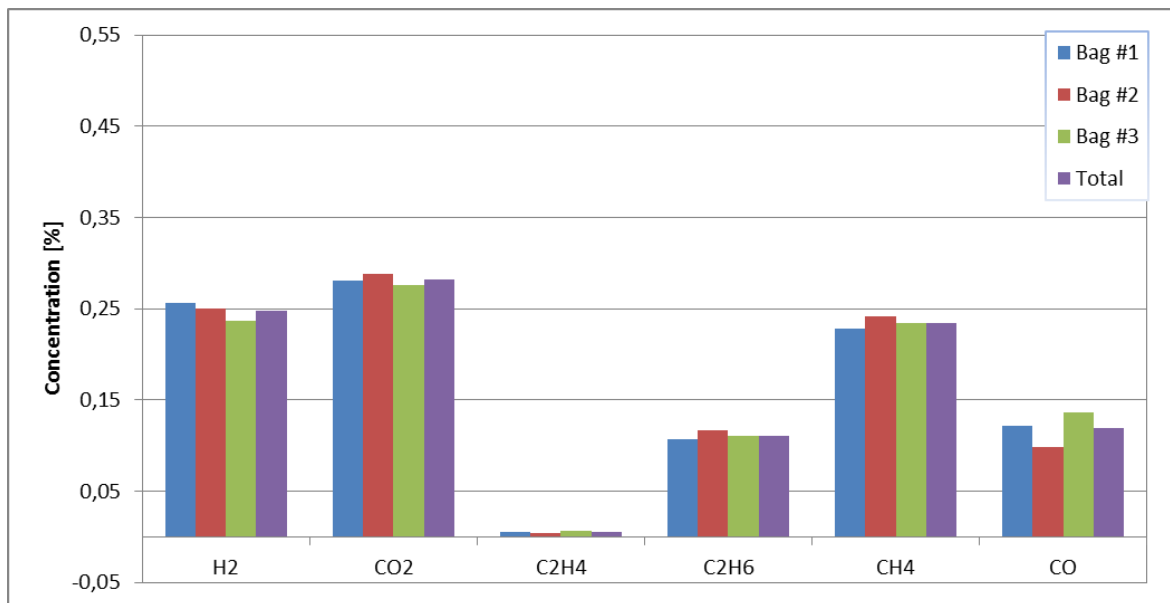


Fig. 7.19: Volumetric concentration of syngas for each bag for INCONEL 625 at 10 %wt and 125 ml/min.

	<b>[%vol]</b>	<b>m [g]</b>	<b>[%wt]</b>	<b>Yield[mol/kg]</b>
<b>H2</b>	24,8%	0,127	2,12%	6,56
<b>CO2</b>	28,2%	3,158	52,71%	7,47
<b>C2H4</b>	0,5%	0,038	0,64%	0,14
<b>C2H6</b>	11,1%	0,853	14,23%	2,95
<b>CH4</b>	23,5%	0,960	16,02%	6,23
<b>CO</b>	11,9%	0,856	14,28%	3,18
<b>Total</b>	-	5,992	-	26,52

**Table 7.55:** Composition and gas yield for INCONEL 625 at 10 %wt and 125 ml/min.

	<b>Method 1</b>	<b>Method 2</b>
<b>CCE [%]</b>	70,78%	78,77%
<b>HCE [%]</b>	64,80%	72,11%
<b>OCE [%]</b>	55,61%	61,89%
<b>CGE [%]</b>	72,86%	81,09%
<b>LHV [MJ/kg]</b>	20,58	

**Table 7.56:** Composition and gas yield for INCONEL 625 at 10 %wt and 125 ml/min.

#### **7.4. Effect of concentration**

The effect of concentration of the feedstock has been studied by setting three levels of concentration: 2.5%, 5% and 10%.

Figure 7.20 shows the effect of concentration on the final composition of the syngas for both reactors at fixed concentrations.

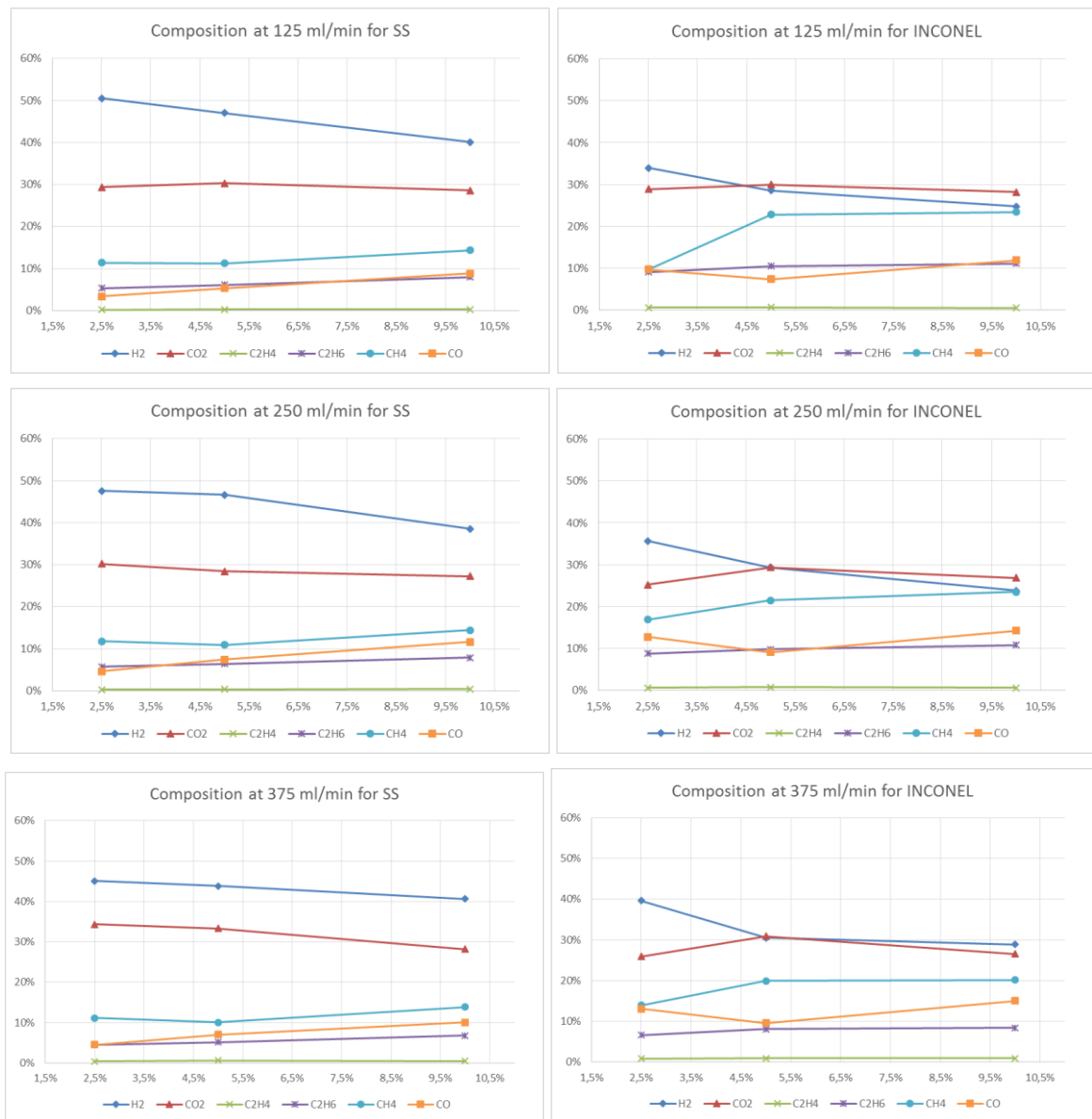


**Fig. 7.20:** Composition of syngas as a function of concentrations and at fixed volume flow rate for SS316 and INCONEL 625.

As it is possible to notice from the pictures, the general trend of  $H_2$  for both reactors is decreasing as the concentration of the feedstock increases, while the  $CH_4$  is increasing. The general decrease of  $H_2$  can be attributed to the deceleration of water-gas shift reaction, which can also be the reason of the slight decrease of  $CO_2$  for the SS316 reactor. For all the three residence times with the INCONEL 625 reactor, instead, it is possible to observe a first increase of  $CO_2$  concentration from 125 to 250 ml/min followed by a decrease at 375 ml/min, a phenomenon that can be subject of further studies as reactions leading to coke formation can occur.



Another possible reason is that, above 250 ml/min, Sabatier reactions occur, i.e. the  $H_2$  reacts with the  $CO_2$  producing  $CH_4$  and  $H_2O$  in presence of a nickel catalyst. Moreover, at higher concentrations, methanation reactions are preferred leading to the consumption of  $H_2$ ,  $CO_2$  and  $CO$  and a production of  $CH_4$ . Finally, even if the concentration of  $C_2H_4$  is very low, it is possible to observe a slight increase of both  $C_2H_4$  and  $C_2H_6$  in both reactors.

Figure 7.21 shows the effects of concentration on the gas yield for both reactors at fixed residence time.

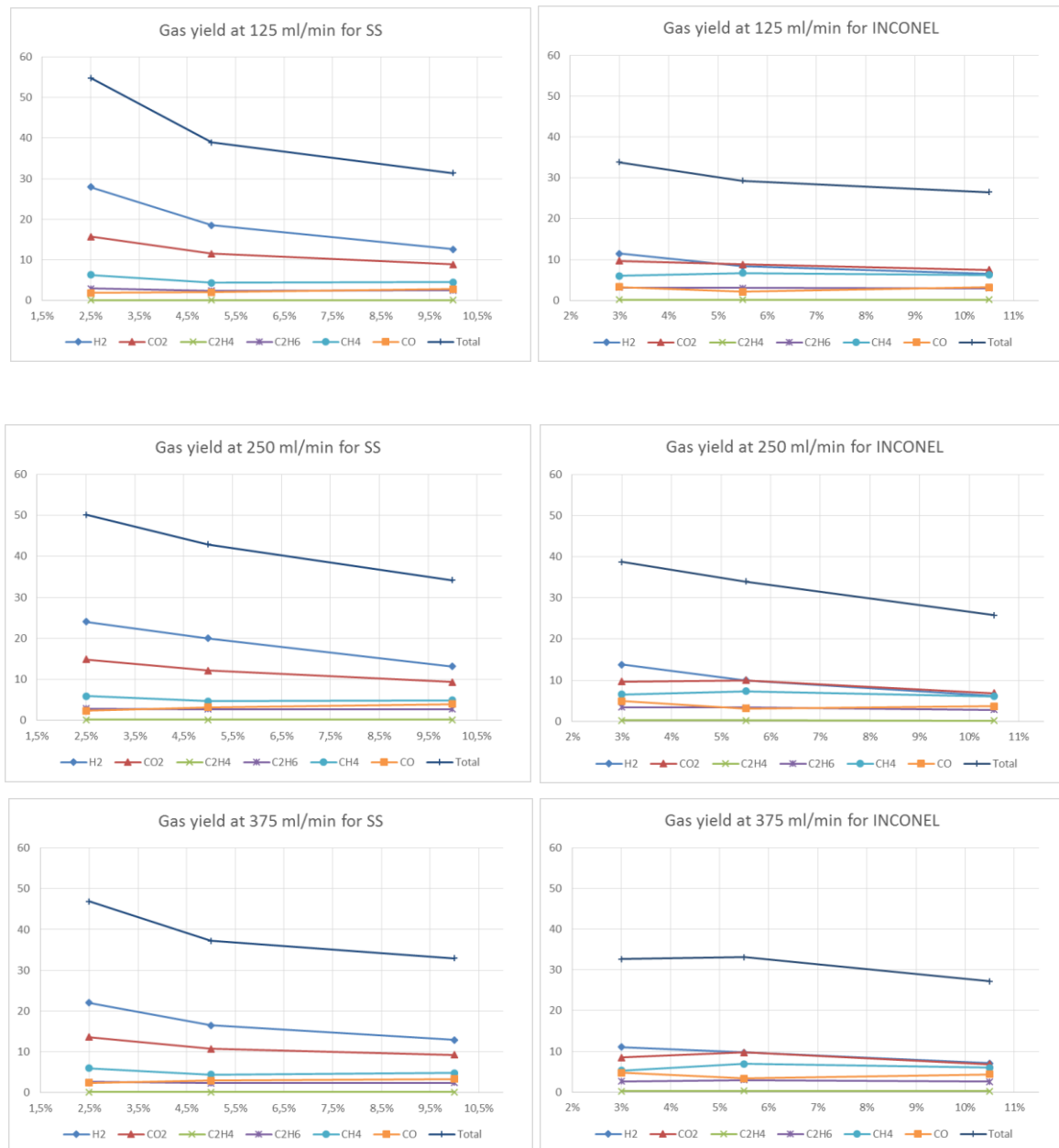
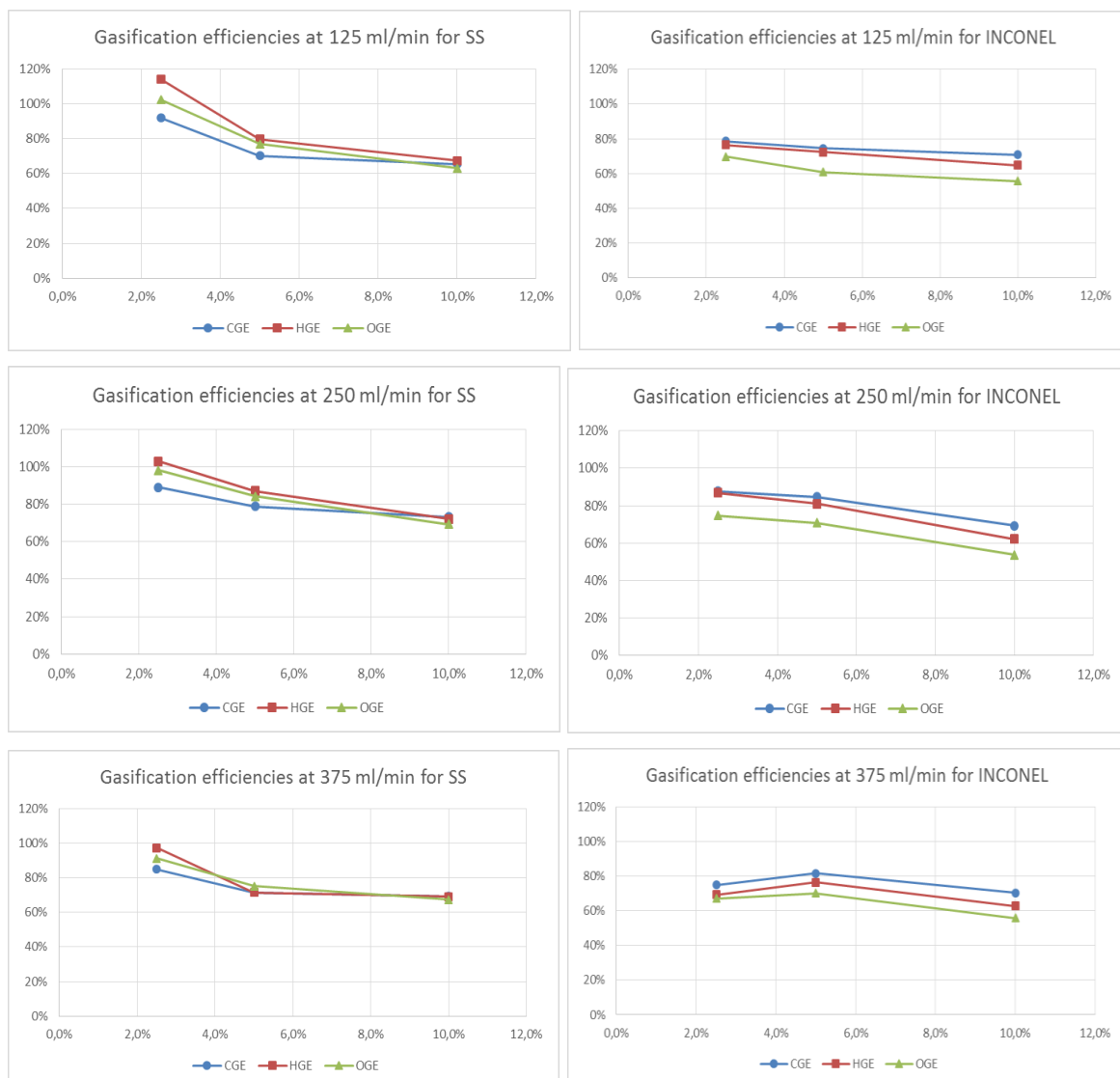


Fig. 7.21: Gas yield as a function of concentrations and at fixed volume flow rate for SS316 and INCONEL 625.

These pictures show that the increase of the feed concentration has a negative impact on the total gas yield. All the reactions involving water as a reactant like water gas-shift, hydrocarbon reforming and intermediate reforming, are retarded due to the decrease in water molecules with the increase in feed molecules at higher feed concentrations. In particular, as the volume concentration of  $H_2$ , also its gas yield decreases for both reactors as the concentration of the feedstock increases.

Even here, for the INCONEL 625 reactor, it is possible to observe a first increase of  $CO_2$  followed by a decrease at 375 ml/min, while for the SS 316 it is decreasing as the concentration increases. Finally, it is possible to notice that the feedstock concentration has a less influence on the gas yields of or  $CH_4$ ,  $C_2H_4$ ,  $C_2H_6$  and  $CO$ . These gases originate from pyrolysis and reforming reactions [57]. Since water does not influence the pyrolysis reaction,  $CH_4$ ,  $C_2H_4$ ,  $C_2H_6$  and  $CO$  yields increase at the expense of  $CO_2$  and  $H_2$ . This explains the decrease in the total gas yield. In conclusion, from these experiments has been found that operating at high concentrations is not suitable for high-yield productions. Figure 7.22 illustrates the effect of the feed concentration on the gasification efficiencies.



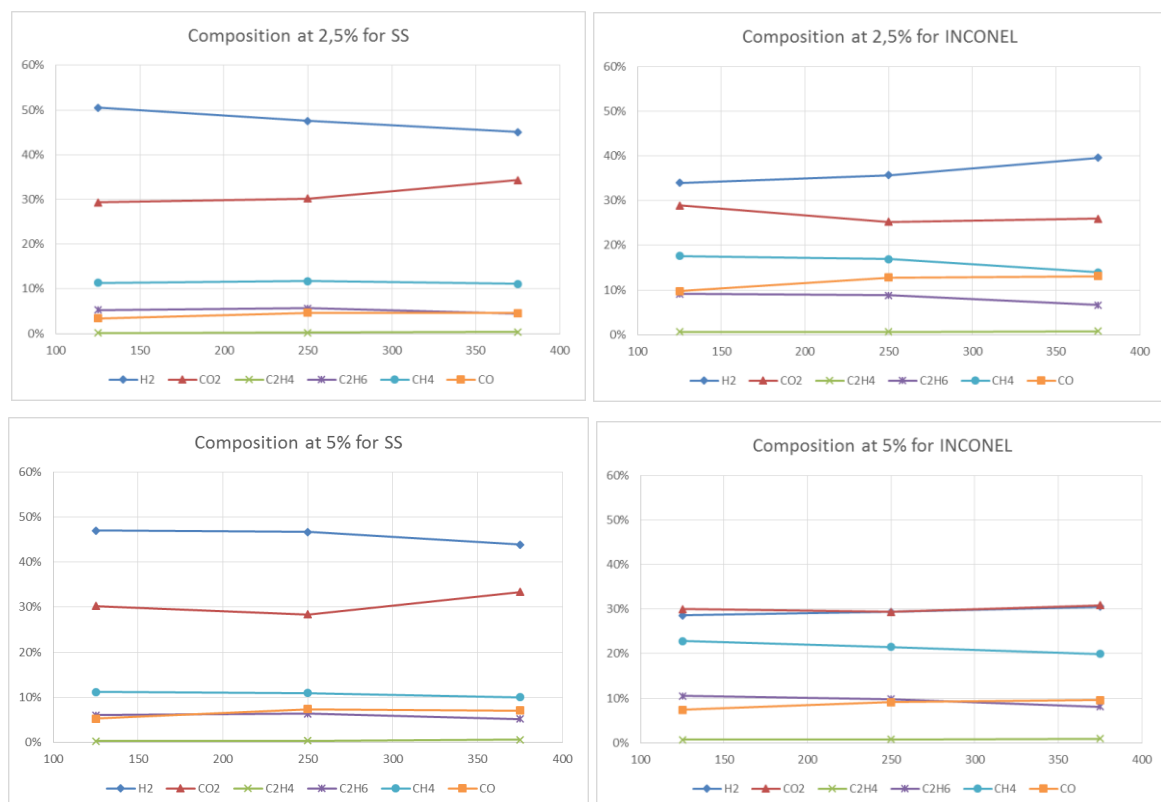
**Fig. 7.22:** Gasification efficiencies as a function of concentrations and at fixed volume flow rate for SS316 and INCONEL 625.

As it is possible to notice from the pictures above, the general trend of the efficiencies is decreasing as the concentration increases. A particular case which can be subject of further studies is the first increase of all the efficiencies as the feed concentration is switched from 2.5% to 5%, followed by a decrease at 10%, which can be explained by the fact that the  $CO_2$  follows the same trend. The decrease of the CGE for the SS316 reactor is caused, instead, by the formation of a lower amount of  $CO$  and  $CO_2$  at the high concentration. It is important to notice that the gasification efficiencies of oxygen and hydrogen might exceed 100%. This means that, in the gaseous products, there is more oxygen and hydrogen with respect to the dry feed. This indicates that water participates to the gasification reactions so it is not only the medium in which the reaction take place.

Normally, higher feed concentration can lead to further dehydration or polymerization of liquid intermediates into tar/char formation. Complex interactions between liquid products and char/tar formation are kinetically driven and most likely influenced by concentration as well [137].

### 7.5. Effect of residence time

Figure 7.23 shows the composition of the syngas as a function of the volumetric flow rate expressed in normal ml/min, and, thus, of the residence time, at a fixed concentration.



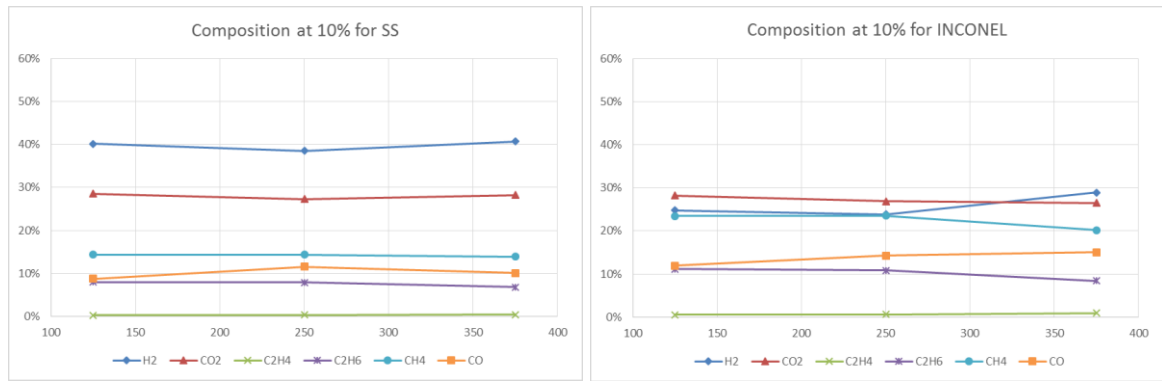
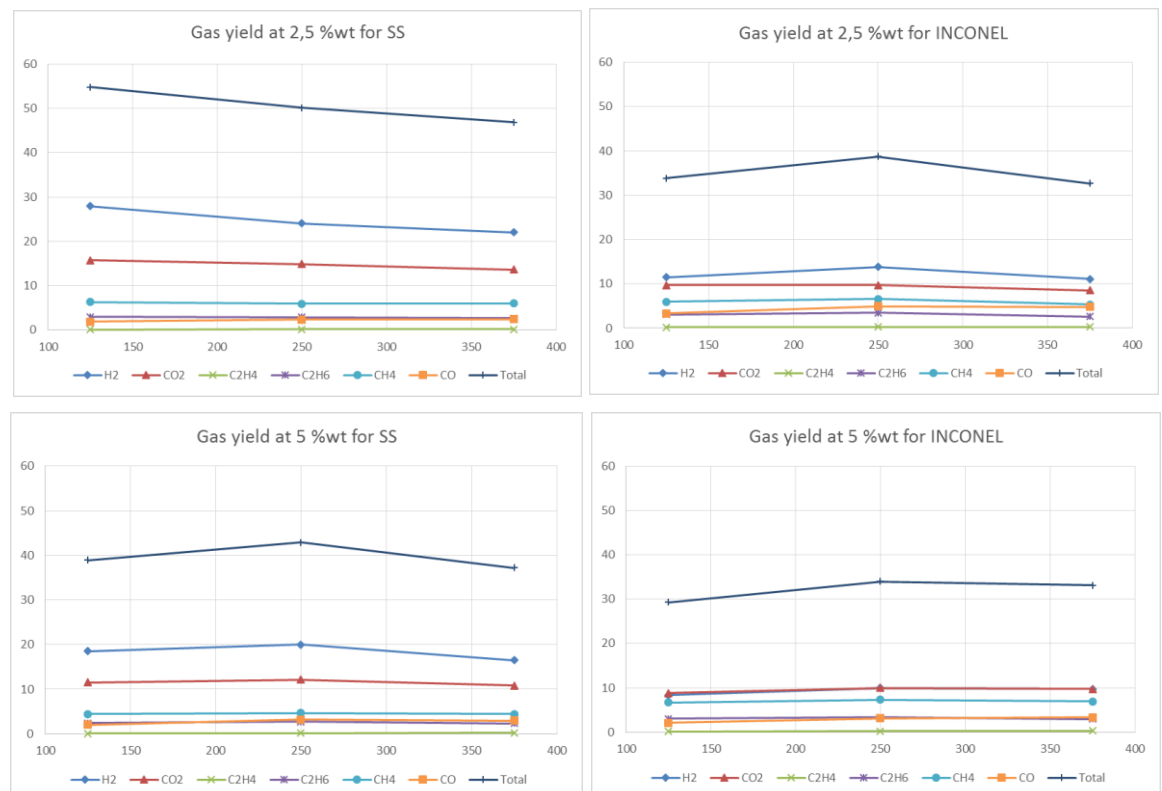


Fig. 7.23: Composition of syngas as a function of volume flow rates at fixed concentration for SS316 and INCONEL 625.

The figures show a general decrease in  $H_2$  for SS 316 as the residence time decrease. This decrease is less marked as the concentration increases until it remains almost constant for a concentration of 10%. By contrast, with INCONEL, has been observed that the volume fraction of  $H_2$  increases as the residence time decreases. By using SS 316, the  $CO_2$  fraction increased with the volume flow rate for low concentrations, while it evolved steadily for a concentration of 10 %wt. Moreover, although  $CO$  presents a slight increase for both reactors, it seems that the residence time does not remarkably affect the volume fraction of  $CH_4$ ,  $C_2H_4$  and  $C_2H_6$  for the SS 316 reactor. On the other hand, the residence time appears to affect in a stronger way the volume fraction of  $CH_4$ , decreasing as the residence time increases, and of  $C_2H_4$ , increasing with the residence time.

Figure 7.24 illustrates the effects of residence time on the gas yield for both reactors at a fixed concentration.



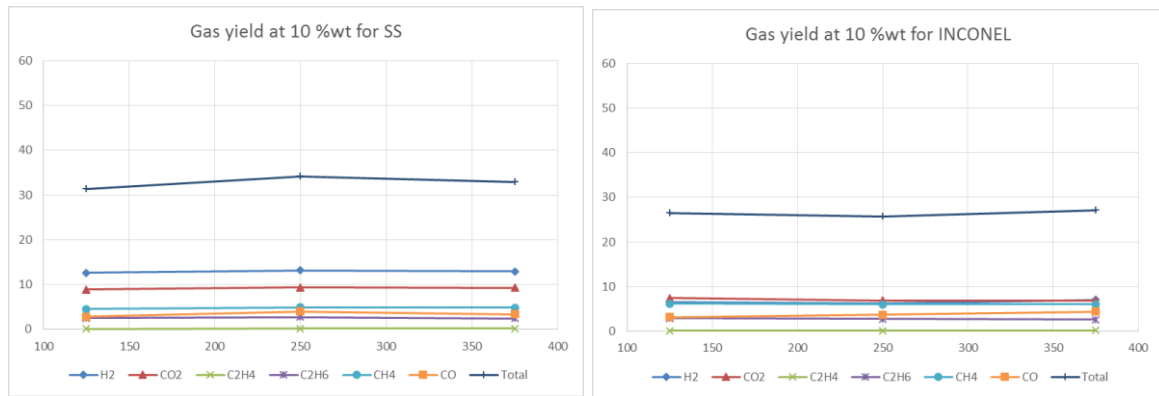
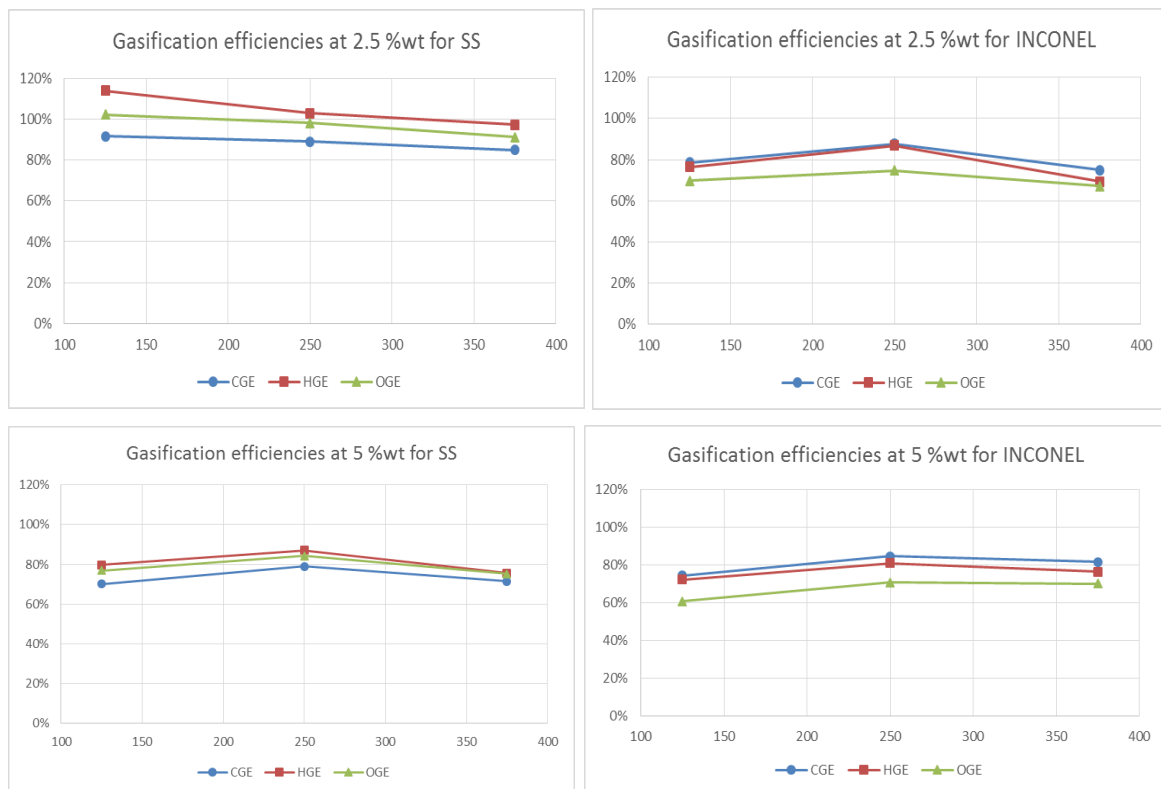
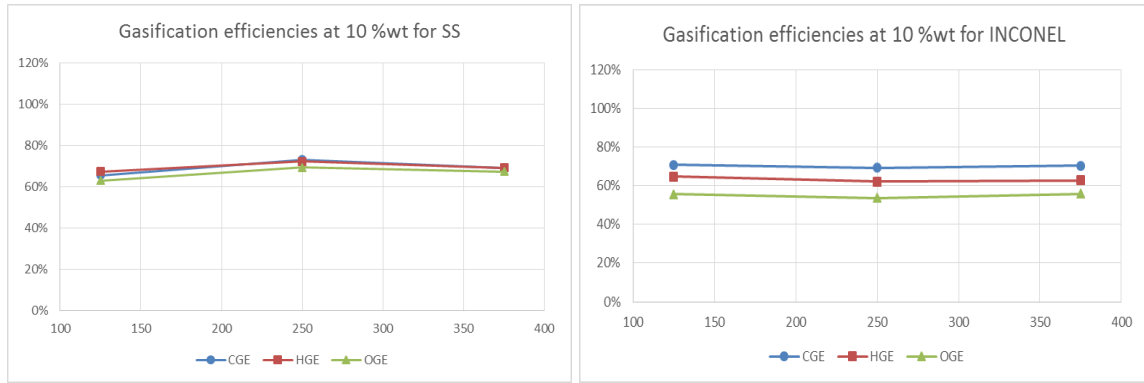


Fig. 7.24: Gas yield of syngas as a function of volume flow rates at fixed concentration for SS316 and INCONEL 625.

The figures show that at the lowest concentration the total gas yield is increasing as the residence time increases, while at higher concentrations it is possible to observe a first increase followed by a decrease at 10 %wt. The same trend is present for INCONEL, except at 10 %wt where the total gas yield slightly decreases to 5 %wt and then slightly increases to 10 %wt. In conclusion, the variation of the gas yields is almost imperceptible for all of the cases, especially for  $CH_4$ ,  $C_2H_4$  and  $C_2H_6$  which are almost constant. As a consequence of these results, it is possible to claim that the residence time has little effect on the gas yields.

Figure 7.24 illustrates the effects of the residence time on the gasification efficiencies for both reactors at a fixed concentration.





**Fig. 7.25:** Gasification efficiencies as a function of volume flow rates at fixed concentration for SS316 and INCONEL 625.

The figures above have the same trend of the gas yield. The gasification efficiencies are increasing as the residence time increases for SS at the lowest feed concentration, while they are first increasing and then decreasing again for the INCONEL at 2.5 %wt. With other concentrations, the influence of the residence time is less marked and the efficiencies are almost constant.

Finally, figure 7.26 and 7.27 show the variation of the Cold Gas Efficiency and the Lower Heating Value for both SS 316 and INCONEL 625.

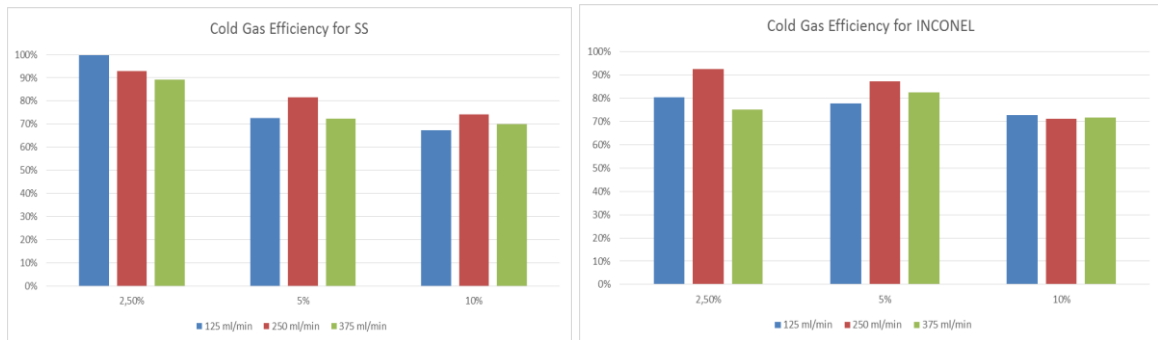


**Fig. 7.26:** Cold Gas Efficiency for SS316 and INCONEL 625.

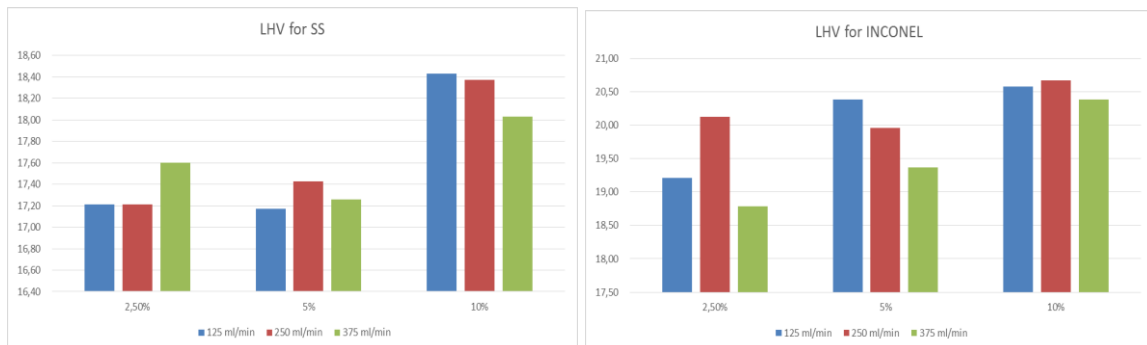


**Fig. 7.27:** LHV for SS316 and INCONEL 625.

The cold gas efficiency is decreasing as the concentration increases for both reactors, except at 375 ml/min for INCONEL, where the cold gas efficiency is first increasing and then decreasing. A consequence of these results is, thus, that the process is generally more efficient with low feed concentrations. For what concern the residence time, except the case at 2.5 % for SS where the efficiency is increasing as the residence time increases, the general Cold Gas Efficiency is first increasing and then decreasing again. There seems to be a maximum at 250 ml/min. The higher efficiency for the SS reactor is of 99.8%, reached at 2.5 %wt and with a residence time of 7.43 minutes. For INCONEL the higher Cold Gas Efficiency is of 92.4 %, reached 2.5 %wt and a residence time of 4.95 minutes.

Finally, the LHV is extremely varying at the different settings. The maximum LHV is reached when the volume flow rate is set at 250 ml/min and the concentration is 10 %wt.

## **7.6. *Effect of catalyst***

As far as the composition of the syngas obtained is concerned, the usage of the catalysed reactor leads to lower volume concentrations of  $H_2$  and higher volume concentrations of  $CH_4$ , while the volume fractions of the other component is comparable for both reactors.

The same result can also be observed by looking at the gas yields for both reactors, noticing in particular that the total gas yield is lower if the catalysed reactor is used. The maximum gas yield reached is of 54,83 mol/kg at a feed concentration of 2.5 %wt and a residence time of 7.43 minutes for the SS 316 reactor and of 38.71 mol/kg at a feed concentration of 2.5 %wt and a residence time of 4.95 minutes for the INCONEL reactor.

Concerning the carbon gasification efficiencies, there are not substantial differences among the two reactors. The highest efficiency is of 91.78%, reached the lowest concentration and the highest residence time with the SS 316 reactor.

However, as regards the cold gas efficiency it is possible to notice a general decrease as the catalysed reactor is used. An efficiency of 99.8 % is reached at the lowest concentration and the highest residence time if the SS 316 reactor is used.

## 8. Design of experiments

In the previous chapter, it was possible to see how the compositions, efficiencies and gas yields are affected by the residence time and the feed concentration. In particular, the gas yields and the efficiencies showed a non-linear behaviour as the residence time and the feed concentration changed. Nevertheless, the volume concentration of  $H_2$  appears to depend linearly on this two variables.

The aim of this last chapter is to introduce a design of experiments with two levels and two quantitative and continuous factors (feed concentration and residence time), in order to analyse how both variables affect the volume concentration of  $H_2$  (response variable), so as to try to predict the outcome of SCWG of glycerol in terms of  $H_2$  production. Unfortunately, costs and time did not allow repeating all the experiments in such a way that inherent variations in the process are reduced and a complete statistical study could be performed.

Therefore, the following study is a merely qualitative analysis in order to assess how the feed concentration and residence time affect the volume concentration of  $H_2$  and which factor is more critical. Further studies on SCWG of glycerol can be useful to perform a complete design of experiments and to analyse the non-linear behaviour of the efficiencies and gas yields.

### 8.1. Effects for the SS 316 reactor

The first part of a design of experiments is constituted of a factor selection, the setting of levels and contingent randomizations of the order of performance [138]. The factors selected in this thesis are the feed concentration and the residence time. The chosen output measure, called *response variable*, is the volume concentration of  $H_2$ , as it shows a linear trend as the factors change. This could be useful if SCWG of glycerol is used with the aim to produce a gas mainly composed of  $H_2$ . Further analysis of the non-linear behaviour of other outputs can be carried out subsequently, along with a complete statistical study with a repetition of each experiment. Considering two factors and two levels for each variable (2.5 and 10 %wt and 3 and 7.4 minutes) the responses obtained are shown in table 8.1.

		A. Residence time [min]	
		3 (Low)-	7,4 (High)+
B. Feed concentration [%]	2.5 %wt (Low)-	46,95%	50,98%
	10 %wt (High)+	39,27%	40,20%

Table 8.1: Data for SS316.

The minus and plus signs identify respectively the low and the high level. The main effects of the variables are defined as the difference in the average response between the high and the low levels of a factor [138].

$$E(A) = \bar{Y}_{A+} - \bar{Y}_{A-} = \frac{40.2+50.98}{2} - \frac{39.27+46.95}{2} = 2.48\% \quad (8.1)$$

$$E(B) = \bar{Y}_{B+} - \bar{Y}_{B-} = \frac{39.27+40.2}{2} - \frac{46.95+50.98}{2} = -9.23\% \quad (8.2)$$

Where:

E(A) is the effect of the residence time;

E(B) is the effect of the concentration;

$\bar{Y}_{A+}$  is the average of the response at high residence time;

$\bar{Y}_{A-}$  is the average of the response at low residence time;

$\bar{Y}_{B+}$  is the average of the response at high concentration;

$\bar{Y}_{B-}$  is the average of the response at low concentration;

The main effect of 2.48% means that the average  $H_2$  volume concentration at high residence time (7.4 minutes) is 2.48% higher than the average of  $H_2$  volume concentration at low residence time (3 minutes). As far as the feed concentration is concerned, the main effect of -9.23% means that the average  $H_2$  volume concentration at high feed concentration (10 %wt) is 9.23% lower than the average of  $H_2$  volume concentration at low feed concentration (2.5 %wt). Figures 8.1 shows the direction of influence for the factors.

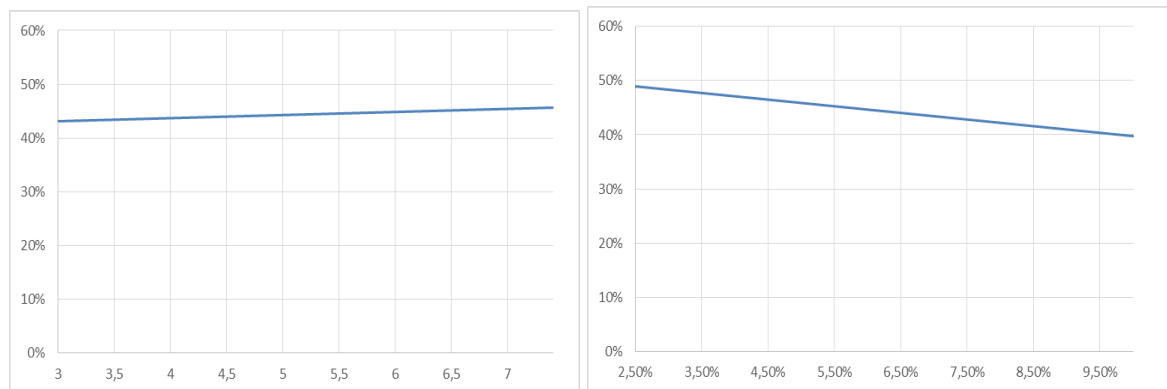


**Fig. 8.1:** Effect of residence time (left) and feed concentration (right) on  $H_2$  volume concentration.

As it is possible to notice, the feed concentration has a stronger effect on the  $H_2$  volume concentration than the residence time, which has a very little influence.

Another important effect is the interaction that may occur between the two factors and have an important and unexpected effect. The interaction *residence time-feed concentration* is

defined as one-half of the difference between the effect of A at the high level of B and the effect of A at the low level of B [138]:

$$E(AB) = \frac{1}{2} [(\bar{Y}_{A+} - \bar{Y}_{A-})_{B+} - (\bar{Y}_{A+} - \bar{Y}_{A-})_{B-}] \quad (8.3)$$

$$E(AB) = \frac{1}{2} [(40.2 - 39.27) - (50.98 - 46.95)] = -1.55\% \quad (8.4)$$

The joint effect between the two factors increases or decreases the main effect of the experiment by 1.55%. For example, the main effect of residence time is 2.48%, nevertheless, when 2.5 %wt of feed concentration is used, the effect of the residence time is actually 0.93% (40.2 - 39.27). On the contrary, when 10% of feed concentration is used, the residence time effect is 4.03% (50.98 - 46.95).

The interaction *feed concentration-residence time* is defined, instead, as one-half of the difference between the effect of B at the high level of A and the effect of B at the low level of A:

$$E(BA) = \frac{1}{2} [(\bar{Y}_{B+} - \bar{Y}_{B-})_{A+} - (\bar{Y}_{B+} - \bar{Y}_{B-})_{A-}] \quad (8.3)$$

$$E(BA) = \frac{1}{2} [(40.2 - 50.98) - (39.27 - 46.95)] = -1.55\% \quad (8.4)$$

It is possible to notice that  $H_2$  volume concentrations are obtained when the feed concentration is lower. This result was already evident by looking at the table 8.1.

A final conclusion for SS 316 is that interactions between the two factors are not significant. Figure 8.2 illustrates the interaction between the two factors.

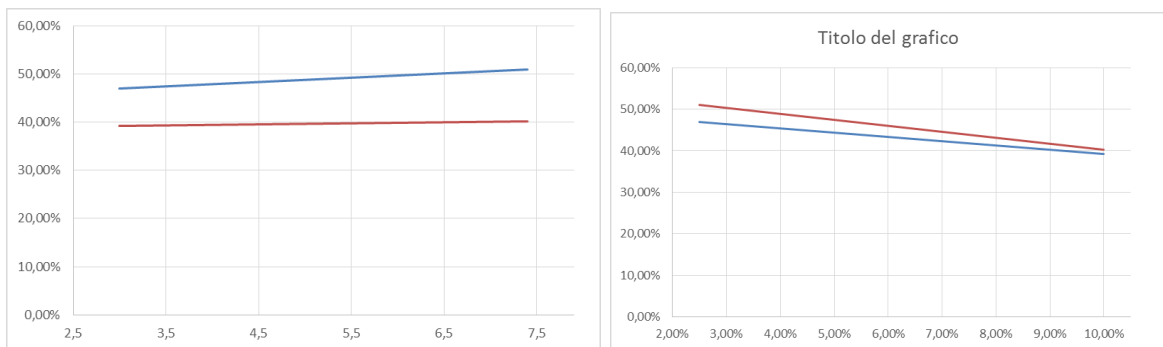


**Fig. 8.2:** Residence time-feed concentration interaction (left) and feed concentration-residence time interaction (right) for SS316.

In order to show the relative importance of the effects, a Pareto chart of the absolute values of the effects is shown in figure 8.3.

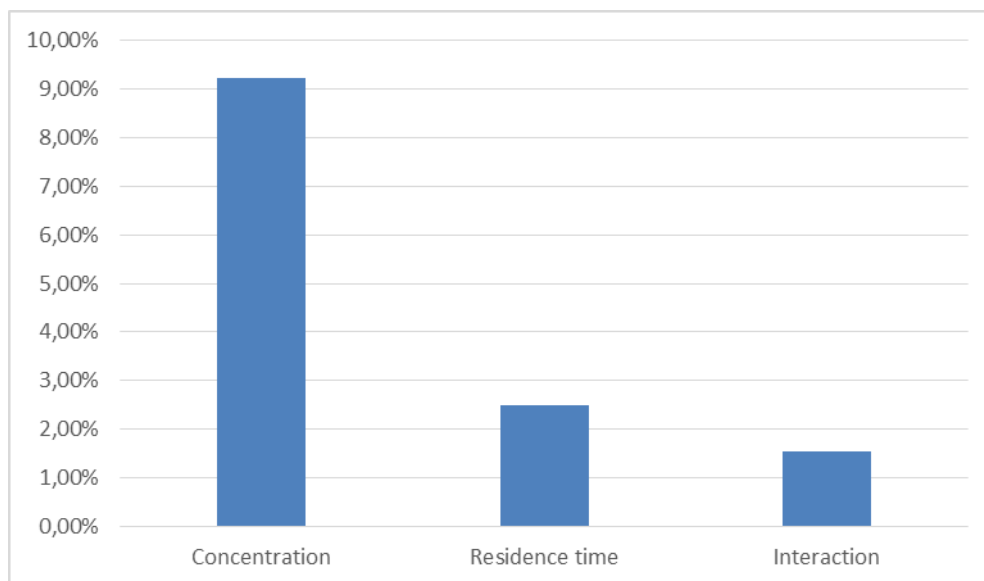


Fig. 8.3: Pareto chart of effects of SS316.

The graph shows that the concentration has the highest effect on the  $H_2$  volume concentrations compared to the residence time and the join effects.

## 8.2. Effects for the INCONEL 625 reactor

The same procedure is done for the experiments with the INCONEL reactor. The chosen factors and the output variable are the same, as well as the levels. The aim of this analysis is to investigate the effects of residence time and feed concentrations even for the INCONEL 625 reactor and compare the results with the previous case.

Table 8.2 shows the responses obtained from the experiments.

		A. Residence time [min]	
		3 (Low)-	7,4 (High)+
B. Feed concentration [%]	2.5 %wt (Low)-	34,03%	34,02%
	10 %wt (High)+	26,02%	24,73%

Table 8.2: Data for INCONEL 625.

The main effects of the variables are:

$$E(A) = \bar{Y}_{A+} - \bar{Y}_{A-} = \frac{24.73+34.02}{2} - \frac{26.02+34.03}{2} = -0.65\% \quad (8.1)$$

$$E(B) = \bar{Y}_{B+} - \bar{Y}_{B-} = \frac{26.02+24.73}{2} - \frac{34.03+34.02}{2} = -8.65\% \quad (8.2)$$

The main effect of -0.65% means that the residence time has a very little effect on the  $H_2$  volume concentration which remains basically constant as the residence time increases. As far as the feed concentration is concerned, the main effect of -8.65%. The difference between the two effects is more marked in the case of INCONEL. Figure 8.4 shows the direction of influence for the factors.

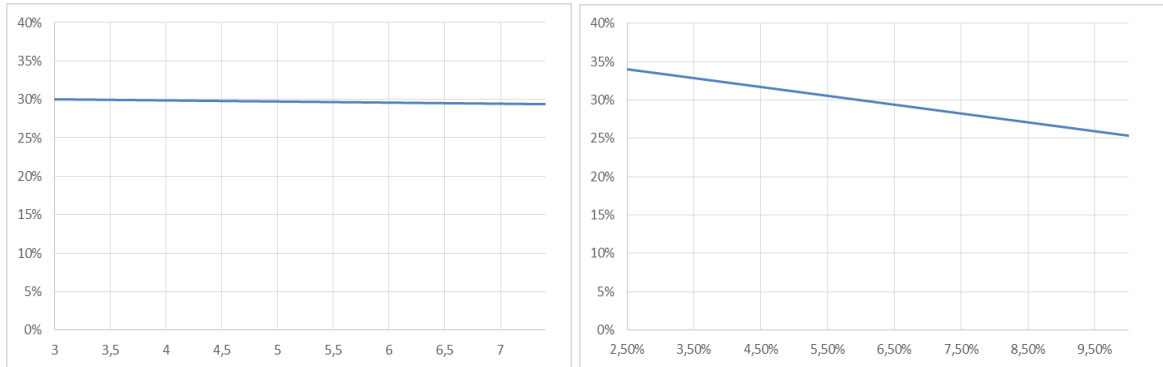


Fig. 8.4: Effect of residence time (left) and feed concentration (right) on  $H_2$  volume concentration.

The interaction *residence time-feed concentration* is:

$$E(AB) = \frac{1}{2}[(\bar{Y}_{A+} - \bar{Y}_{A-})_{B+} - (\bar{Y}_{A+} - \bar{Y}_{A-})_{B-}] \quad (8.3)$$

$$E(AB) = \frac{1}{2}[(24.73 - 26.02) - (34.02 - 34.03)] = -0.64\% \quad (8.4)$$

A point worth noting, which can be subject of further studies, is that, unlike the SS316 reactor, in the INCONEL 625 reactor the  $H_2$  volume concentration decreases as the residence time increases. Moreover, it is possible to notice that even the interaction between the two factors has a very little effect.

Figure 8.5 illustrates the interaction between the two factors, while a Pareto chart of the absolute values of the effects is shown in figure 8.6.

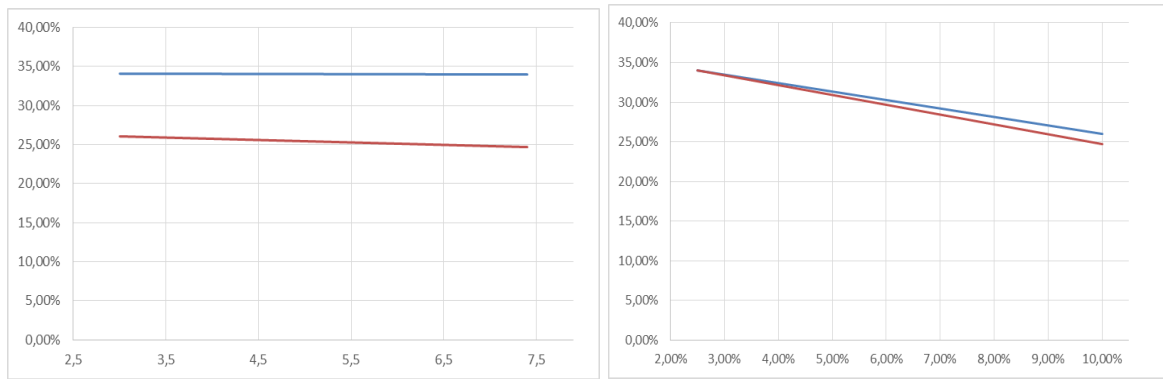


**Fig. 8.5:** Residence time-feed concentration interaction (left) and feed concentration-residence time interaction (right) for INCONEL.

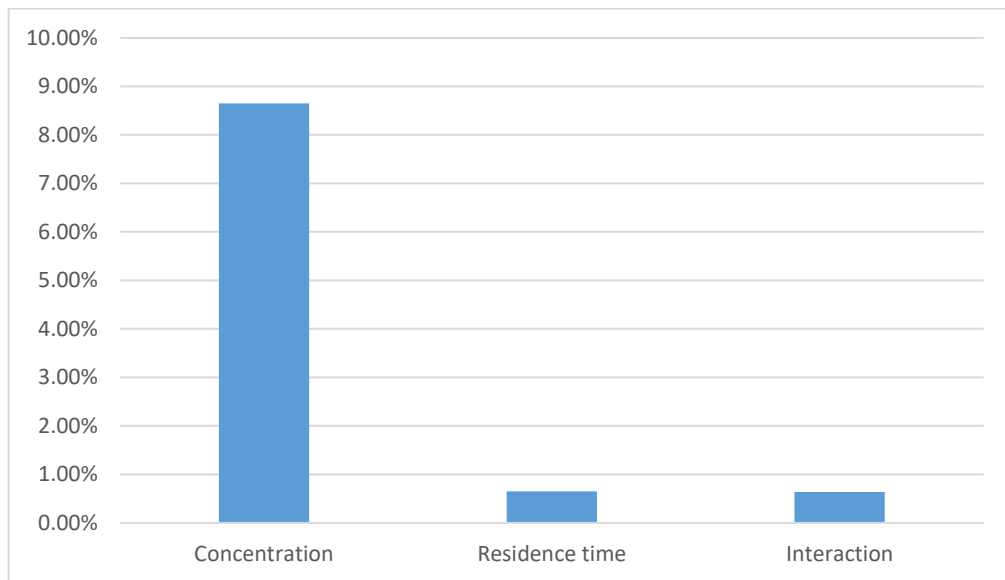


**Fig. 8.6:** Pareto chart of effects of INCONEL.

The graph shows more clearly that the difference between the feed concentration effect and the residence time effect is more significant in the case of INCONEL 625.

## 9. Conclusions

SCWG is a very promising process which benefits from the special properties of supercritical water. It, therefore, may become an important technology to convert biomass or organic waste to a medium calorific value gas with high hydrogen content.

In particular, SCWG of glycerol appeared to be an efficient way of conversion of glycerol to syngas. This is an interesting technology as the large availability of glycerol is constantly increasing due to the remarkable growth of the biodiesel production process. Moreover, as the demand market of glycerol is tight and not able to accommodate the excess amount of glycerol produced by biodiesel production, transformation processes to convert glycerol into value-added products require being explored [105].

Unfortunately, this technology is still at an experimental stage, as it presents many challenges, and some optimizations of the process could appear contradicting. High heating rates, for example, are positive for the chemical process but cannot be reached by conventional heat exchangers. Alkali salts are important to reach high hydrogen yields but might cause corrosion, fouling or plugging. The next step towards technical application is, thus, to overcome these challenges.

The aim of this thesis was to evaluate the influence of concentration and residence time on the efficiencies and gas yields of SCWG of glycerol. Tests were carried out at a fixed temperature of 600 °C and a fixed pressure of 250 bar. Glycerol has been tested at different residence times and feed concentrations by using a stainless steel and an INCONEL reactor.

The design of experiments proved that feed concentration affects the efficiencies and gas yields of the process, while the residence time hardly influences them. In particular, the increase of the feed concentration seems to have a negative impact on the total gas yield and on the efficiencies for both reactors. By contrast, an increase of the residence time, which do not lead to a significant change in the gas yields and efficiencies, shows a non-linear trend. It seems, therefore, that temperature is a more critical variable than residence time and feed concentration, as many studies in the literature have proved and as Simonetti [100] observed by gasifying black liquor and sucrose at different temperatures and pressures with the same setup.

In addition, the usage of the INCONEL reactor led to lower volume concentrations of  $H_2$  and higher volume concentrations of  $CH_4$ , while the volume fractions of the other component is comparable for both reactors. This means that, if the SCWG of glycerol is addressed to a production of  $H_2$ , the SS 316 reactor should be the choice.

As far as the gas yield is concerned, the catalysed reactor showed a lower total gas yield, while there are no substantial differences between the two reactors if the carbon efficiency is taken into account. However, as regards the cold gas efficiency, it is possible to notice a general decrease as the catalysed reactor is used. Therefore, the SS 316 reactor, which is less expensive than the INCONEL reactor, provided better results, leading apparently to a legit preference of the non-catalysed reactor.

After having summarised all the results obtained from these experiments, the following paragraph aims to investigate all the potential further analysis related to SCWG of glycerol that could be carried out.

### ***9.1. Future analysis***

This work could lay the foundation for a much wider set of studies, which might investigate the reason why the gas yields and efficiencies have a different behaviour whether the residence time or the feed concentrations are varied.

A further analysis of the liquid and solid products obtained by SCWG of glycerol could be worth the attention as well. It indeed would allow greater precision regarding the quantification of the final products, through a mass balance which takes into account the material deposited along the walls of the reactor. In order to do so, a first test on the elemental composition of C, H, N and O can be made by other instruments present in the laboratory such as the Elementar Analysensysteme GmbH, which can be joined with the spectrometer Spectro Arcos SOP ICP.

Another important study would be the examination of disposal methods of liquid products and the possibility of an energy recover from them.

In addition, could be interesting to perform a complete design of experiments by repeating all the experiments at 600°C and 250 bar in order to decrease the influence of the inherent variables and evaluate all the statistical variables. Another potentially intriguing study could be the statistical analysis of the non-linear behaviour of the gas yields and the efficiencies.

Eventually, an accurate economic and energy analysis, with proper software, could help to evaluate the feasibility of an industrial application of such technology.

# Bibliography

[1] BP, British Petroleum, 2017, Statistical review of world energy, 66<sup>th</sup> edition, available online at <https://www.bp.com/content/dam/bp/en/corporate/pdf/energy-economics/statistical-review-2017/bp-statistical-review-of-world-energy-2017-full-report.pdf>

[2] European commission, Energy strategy and Energy Union, available online at <https://ec.europa.eu/energy/en/topics/energy-strategy-and-energy-union>

[3] European commission, 2015, Report from the commission to the European parliament and the council, Assessment of the progress made by Member States towards the national energy efficiency targets for 2020 and towards the implementation of the Energy Efficiency Directive 2012/27/EU as required by Article 24 (3) of Energy Efficiency Directive 2012/27/EU.

[4] European commission, EU energy in figures, statistical pocketbook 2017, available online at [https://ec.europa.eu/energy/sites/ener/files/documents/pocketbook\\_energy\\_2017\\_web.pdf](https://ec.europa.eu/energy/sites/ener/files/documents/pocketbook_energy_2017_web.pdf)

[5] Directorate-General of the European Commission (Eurostat), available online at <http://ec.europa.eu/eurostat/web/environmental-data-centre-on-natural-resources/natural-resources/energy-resources/energy-from-biomass>

[6] Bracmort K., 2015, Biomass: comparison of definitions in legislation. *Congressional research service*.

[7] Tekin K., Karagöz S. and Bektaş S., 2014, A review of hydrothermal biomass processing. *Renewable and sustainable energy reviews* **40**, 673-687.

[8] Jenkins B.M., Baxter L.L. and Koppejan J., 2011, Biomass combustion, in “*Thermochemical processing of biomass: conversion into fuels*”, (Brown R.C., Ed.), Chap. 2. Chichester, UK, pp. 13–46.

[9] Kumar S. and Gupta R.B., 2008, Hydrolysis of microcrystalline cellulose in subcritical and supercritical water in a continuous flow reactor. *Ind Eng Chem Res* **47**, 9321-9.

[10] European commission, Archive: Energy from renewable sources, available online at

[http://ec.europa.eu/eurostat/statistics-explained/index.php/Energy\\_from\\_renewable\\_sources](http://ec.europa.eu/eurostat/statistics-explained/index.php/Energy_from_renewable_sources)

[11] European commission, 2017, Report from the commission to the European parliament, the council the European economic and social committee and the committee of the regions, Renewable energy progress report.

[12] Küçük M.M. and Demirbaş A., 1997, Biomass conversion processes. *Energy Convers. Mgmt* **38** (2), 151-165.

[13] Grassi G., 1997, “*Renewable Energy and the Environment*”, (Sayigh A.A.M., Ed.), Vol. 3. Pergamon Press, New York, p. 1255.

[14] Yokoyama S. and Matsumura Y., 2008, The Asian biomass handbook. Tokyo: The Japan of energy, 21-135.

[15] Savage P.E., Levine R.B. and Huelsman C.M., 2010, Hydrothermal processing of biomass, in “*Thermochemical conversion of biomass liquid fuels and chemicals*”, (Crocker M, Ed.), Chap. 8. Cambridge, UK, pp. 192-215.

[16] Elliott D.C., 2011, Hydrothermal processing, in “*Thermochemical processing of biomass: conversion into fuels*”, (Brown R.C., Ed.), Chap. 7. Chichester, UK, pp. 200–31.

[17] Zhang L., Xu C. and Champagne P., 2010, Overview of recent advances in thermochemical conversion of biomass. *Energy Conver. Manag.* **51**, 969-82.

[18] Karagöz S., Bhaskar T., Muto A., Sakata Y. and Uddin M.A., 2004, Low-temperature hydrothermal treatment of biomass: effect of reaction parameters on products and boiling point distributions. *Energy fuels* **18**, 234-41.

[19] Gollakota A.R., Kishor N. and Sai Gu, 2017, A review on hydrothermal liquefaction of biomass, *Renewable and Sustainable Energy Reviews.*

[20] Peterson A.A., Vogel F., Lachance R.P., Fröling Jr.M., Antal M.J. and Tester J.W., 2008, Thermochemical biofuel production in hydrothermal media: a review of sub- and supercritical water technologies. *Energy Environm Sci* **1**, 32-65.

[21] Shah Y.T., 2015, Energy and fuel systems integration. Boca Raton, Florida: Taylor and Francis Group.

- [22] Kruse A., 2009, Hydrothermal biomass gasification. *The Journal of supercritical fluids* **47**, 391-399.
- [23] Cortright R.D., Davda R.R. and Dumesic J.A., 2002, Hydrogen from catalytic reforming of biomass-derived hydrocarbons in liquid water. *Nature* **418**, 964-967.
- [24] Elliott D.C., 2008, Catalytic hydrothermal gasification of biomass. *Biofuels, Bioproducts and Biorefining* **2**, 254-265.
- [25] Antal M.J., Allen S.G., Schulman D., Xu X.D. and Divilio R.J., 2000, Biomass gasification in supercritical water. *Industrial & Engineering Chemistry Research* **39**, 4040-4053.
- [26] Savage P.E., 2009, A perspective on catalysis in sub- and supercritical water. *The Journal of supercritical fluids* **47**, 407-414.
- [27] Pioro I and Mokry, 2011, Thermophysical Properties at Critical and Supercritical Pressures, in “*Heat Transfer – Theoretical Analysis, Experimental Investigations and Industrial Systems*”, (Prof. Aziz Belmiloudi, Ed.), ISBN: 978-953-307-226-5, In Tech, available online at <https://www.intechopen.com/books/heat-transfer-theoretical-analysis-experimental-investigations-and-industrial-systems/thermophysical-properties-at-critical-and-supercritical-pressures>
- [28] Meyer C.A., McClintock R.B., Silvestri G.J. and Spencer R.C., 1992, Steam Tables – Thermodynamic and Transport Properties of Steam.
- [29] Franck E.U., Rosenzweig S. and Christoforakos M., Calculation of dielectric constant of water to 1000 °C and very high pressures. *Berichte der Bunsengesellschaft für Physikalische Chemie* **94**, 199-203.
- [30] Kruse A. and Dinjus E., 2007, Hot compressed water as reaction medium and reactant Properties and synthesis reactions. *The Journal of Supercritical Fluids* **39**, 362-380.
- [31] Akiya N. and Savage P.E., 2002, Roles of Water for Chemical Reactions in High-Temperature Water. *Chem. Rev.* **102**, 2725-2750.
- [32] Weingärtner H. and Franck E.U., 2005, Supercritical water as a Solvent. *Angew. Chem. Int.* **44**, 2672-2692.

- [33] Kalinichev A.G., 2001, Molecular simulations of liquid and supercritical water: thermodynamics, structure and hydrogen bonding, in “*Molecular Modeling Theory: Applications in the Geoscience*”, (Cygan R.T., Dubicki J.D., Eds.), p.93.
- [34] Hippler H., 1997, Elementary reactions in supercritical fluids, in “*Proceedings of the Fourth Italian Conference on Supercritical Fluids and their Applications*”, (Reverchon E., Ed.), p. 279.
- [35] Ederer H.J., Kruse A., Mas C. and Ebert K.H., 1999, Modelling of the pyrolysis of tert-butylbenzene in supercritical water. *The Journal of Supercritical Fluids* **15**, 191-204.
- [36] Guillot B., 2002, A reappraisal of what we have learnt during three decades of computer simulations on water. *Journal of molecular liquids* **101**, 219-260.
- [37] Ved' O.V., Gurina L., Antipova M.L. and Petrenko V.E., 2010, Hydrogen Bond and Dipole Moment in Sub- and Supercritical Water Close to the Saturation Curve. *Russian Journal of Physical Chemistry* **84**, 1359-1363.
- [38] Ikushima Y., Hatakeda K., Sato O., Yokoyama T. and Arai M., 1999, Noncatalytic Organic Synthesis Using Supercritical Water : The Peculiarity Near the Critical Point. *Angewandte Chemie* **38**, 2910-2914.
- [39] Kritzer P., 2004, Corrosion in high-temperature and supercritical water and aqueous solutions: a review. *The Journal of Supercritical Fluids* **29**, 1-29.
- [40] Kaul C., Vogel H. and Exner H.E., 1999, Corrosion behaviour of inorganic materials in subcritical and supercritical aqueous solutions. *Materialwissenschaft und Werkstofftechnik* **30**, 326-331.
- [41] Kruse A. and Dinjus E., 2007, Hot compressed water as reaction medium and reactant 2. Degradation reactions. *The Journal of Supercritical Fluids* **41**, 361-379.
- [42] Kruse A., 2008, Review: Supercritical water gasification. *Biofuels, Bioproducts and Biorefining* **2**, 415-437.
- [43] Xu X., Matsumura Y., Stenberg J. and Antal Jr M.J., 1996, Carbon-Catalyzed Gasification of Organic Feedstocks in Supercritical Water. *Ind Eng Chem Res* **35**, 2522-2530.
- [44] Boukis N., Diem V., Habicht W. and Dinjus E., 2003, Methanol Reforming in Supercritical Water. *Ind. Eng. Chem. Res.* **42**, 728-735.

- [45] Di Leo G.J. and Savage P.E., 2006, Catalysis during methanol gasification in supercritical water. *The Journal of Supercritical Fluids* **39**, 228-232.
- [46] Arita T., Nakahara K., Nagami K. And Kajimoto O., 2003, Hydrogen generation from ethanol in supercritical water without catalyst. *Tetrahedron Lett.* **44**, 1083-1086.
- [47] Kabyemela B.M., Takigawa M., Adschiri T., Malaluan R.M. and Arai K., 1998, Mechanism and Kinetics of Cellobiose Decomposition in Sub- and Supercritical Water. *Ind. Eng. Chem. Res.* **37**, 357.
- [48] Kabyemela B.M., Adschiri T., Malaluan R.M. and Arai K., 1999, Glucose and Fructose Decomposition in Subcritical and Supercritical Water: Detailed Reaction Pathway, Mechanisms, and Kinetics. *Ind. Eng. Chem. Res.* **38**, 2888.
- [49] Kabyemela B.M., Adschiri T., Malaluan R.M. and Arai K., 1997, Degradation Kinetics of Dihydroxyacetone and Glyceraldehyde in Subcritical and Supercritical Water. *Ind. Eng. Chem. Res.* **36**, 2025.
- [50] Promdej C. and Matsumura Y., 2011, Temperature Effect on Hydrothermal Decomposition of Glucose in Sub- and Supercritical Water. *Ind. Eng. Chem. Res.* **50**, 8492.
- [51] Jing Q. L. and Lü X., 2007, Kinetics of Non-Catalyzed Decomposition of D-Xylose in High Temperature Liquid Water. *Chin. J. Chem. Eng.* **15**, 666.
- [52] Goodwin A.K. and Rorrer G.L., 2010, Reaction Rates for Supercritical Water Gasification of Xylose in a Micro-Tubular Reactor. *Chem. Eng. J.* **163**, 10.
- [53] Yong T.L.K. and Matsumura Y., 2013, Kinetic Analysis of Lignin Hydrothermal Conversion in Sub- and Supercritical Water. *Ind. Eng. Chem. Res.* **52**, 5626.
- [54] Yakaboylu O., Yapar G., Recalde M., Harinck J., Smit K.G., Martelli E. and de Jong W., 2015, Supercritical Water Gasification of Biomass: An Integrated Kinetic Model for the Prediction of Product Compounds. *Ind. Eng. Chem. Res.*
- [55] Rodriguez Correa C. and Kruse A., 2017, Supercritical water gasification of biomass for hydrogen production – Review. *The journal of Supercritical Fluids*, <https://doi.org/10.1016/j.supflu.2017.09.019>
- [56] Kruse A. and Dinjus E., 2005, Influence of salts during hydrothermal biomass gasification: the role of the catalyzed water-gas shift reaction. *Zeitschrift Fur Phys. Chemie* **219**, 341-366.

- [57] Guo S., Guo L., Yin J. and Jin H., 2013, Supercritical water gasification of glycerol: Intermediates and kinetics. *The Journal of Supercritical Fluids* **78**, 95-102.
- [58] May A., Salvado J., Torras C. and Montane D., 2010, Catalytic gasification of glycerol in supercritical water. *Chemical Engineering Journal* **160**, 751-759.
- [59] Buhler W., Dinjus E., Ederer H.J., Kruse A. and Mas C., 2002, Ionic reactions and pyrolysis of glycerol as competing reaction pathways in near- and supercritical water. *The Journal of Supercritical Fluids* **22**, 37-53.
- [60] Yoshida T., Matsumura Y., 2001, Gasification of cellulose xylan, and lignin mixtures in supercritical water. *Ind. Eng. Chem. Res.* **40**, 5469-5474.
- [61] Kruse A., Krupka A., Schwarzkopf V., Camard C. and Henningsen T., 2005, Influence of proteins on the hydrothermal gasification and liquefaction of biomass. 1. Comparison of different feedstocks. *Ind. Eng. Chem. Res.* **44**, 3013-3020.
- [62] Holliday R.L., King J.W. and List G.R., 1997, Hydrolysis of vegetable oils in sub- and supercritical water. *Ind. Eng. Chem. Res.* **36**, 932-935.
- [63] Matsumura Y., Minowa T., Potic B., Kersten S.R.A., Prins W., van Swaaij W.P.M. et al., 2005, Biomass gasification in near- and supercritical water: Status and prospects. *Biomass Bioener.* **29**, 269-292.
- [64] Watanabe M., Inomata H., Smith J., Arai K., Sato T., Kruse A. et al., 2004, Chemical reactions of C1 compounds in near-critical and supercritical water. *Chem. Rev.* **104**, 5803-5821.
- [65] Peterson A.A., Vogel F., Lachance R.P., Froling M., Antal M.J. Jr. and Tester J.W., 2008, Thermochemical biofuel production in hydrothermal media: a review of sub- and supercritical water technologies. *Energy & Environmental Science* **1**, 32-65.
- [66] Loppinet-Serani A., Aymonier C. and Casell F., 2008, Current and foreseeable applications of supercritical water for energy and the environment. *ChemSusChem* **1**, 486-503.
- [67] Minowa T. and Ogi T., 1998, Hydrogen production from cellulose using a reduced nickel catalyst. *Catalysis Today* **45**, 411-416.

[68] Kruse A. and Gawlik A., 2003, Biomass conversion in water at 330-410 °C and 30-50 MPa. Identification of Key Compounds for Indicating Different Chemical Reaction Pathways. *Ind. Eng. Chem. Res.* **42**, 267-279.

[69] Matsumura Y., Sasaki M., Okuda K., Takami S., Ohara S., Umetsu M. and Adschiri T., 2006, Supercritical water treatment of biomass for energy and material recovery. *Combustion Sci. Technol.* **178**, 509-536.

[70] Matsumura Y., Minowa T., Potic B., Kersten S.R.A., Prins W., van Swaaij W.P.M., van de Beld B., Elliott D.C., Neuenschwander G.G., Kruse A. and Antal Jr M.J., 2005, Biomass gasification in near- and supercritical water: Status and prospects. *Biomass Bioenergy* **29**, 269-292.

[71] Watanabe M., Inomata H. and Arai K., 2002, Catalytic hydrogen generation from biomass (glucose and cellulose) with ZrO<sub>2</sub> in supercritical water. *Biomass Bioenergy* **22**, 405-410.

[72] Yoshida T., Oshima Y. and Matsumura Y., 2004, Gasification of biomass model compounds and real biomass in supercritical water. *Biomass Bioenergy* **26**, 71-78.

[73] Yoshida T. and Oshima Y., 2004, Partial Oxidative and Catalytic Biomass Gasification in Supercritical Water: A Promising Flow Reactor System. *Ind. Eng. Chem. Res.* **43**, 4097-4014.

[74] Li S., Guo L., Zhu C. and Lu Y., 2013, Co-precipitated Ni-Mg-Al catalysts for hydrogen production by supercritical water gasification of glucose. *Int. J. Hydrogen Energy* **38**, 9688-9700.

[75] Elliott D.C., Neuenschwander G.G., Hart T.R., Butner R.S., Zacher A.H., Engelhard M.H., Young J.S. and McCready D.E., 2004, Chemical processing in high-pressure aqueous environments. 7. Process development for catalytic gasification of wet biomass feedstocks. *Ind. Eng. Chem. Res.* **43**, 199-2004.

[76] Azadi P., Khan S., Strobel F., Azadi F. and Farnood R., 2012, Hydrogen production from cellulose, lignin, bark and model carbohydrates in supercritical water using nickel and ruthenium catalysts. *Appl. Catal. B Environ.* **117-118**, 330-338.

[77] Osada M., Sato O., Watanabe M., Arai K. And Shirai M., 2006, Water Density Effect on Lignin Gasification over Supported Noble Metal Catalysts in Supercritical Water. *Energy Fuels* **20**, 930-935.

[78] Osada M., Sato T., Watanabe M., Adschiri T. and Arai K., 2004, Low-Temperature Catalytic Gasification of Lignin and Cellulose with a Ruthenium Catalyst in Supercritical Water. *Energy Fuels* **18**, 327-333.

[79] Chakinala A., Brillman D., Van Swaaij W. and Kersten S., 2010, Catalytic and Non-catalytic Supercritical Water Gasification of Microalgae and Glycerol. *Industrial and Engineering Chemistry Research* **43**, no. 3, 1113-1122.

[80] Lu Y., Guo L., Zhang X. and Yan Q., 2007, Thermodynamic modeling and analysis of biomass gasification for hydrogen production in supercritical water. *Chem. Eng. J.* **131**, 233-244.

[81] Fang Z., Minowa T., Smith Jr. R.L., Ogi T. and Kozinski J.A., 2004, Liquefaction and gasification of Cellulose with Na<sub>2</sub>CO<sub>3</sub> and Ni in Subcritical water at 350 °C. *Ind. Eng. Chem. Res.* **43**, 2454-2463.

[82] Kruse A. and Dahmen N., 2015, Water – A magic solvent for biomass conversion. *The Journal of Supercritical Fluids* **96**, 36-45.

[83] Sato T., Osada M., Watanabe M., Shirai M. and Arai K., 2003, Gasification of Alkylphenols with Supported Noble Metal Catalysts in Supercritical Water. *Ind. Eng. Chem. Res.* **42**, 4277-4282.

[84] Kruse A., Henningsen T. and Sinağ A., Pfeitter J., 2003, Biomass gasification in supercritical water: influence of the dry matter content and the formation of phenols. *Ind. Eng. Chem. Res.* **42**, 3711-3717.

[85] Cortright R.D., Davda R.R. and Dumesic J.A., 2002, Hydrogen from catalytic reforming of biomass-derived hydrocarbons in liquid water. *Nature* **418**, 964-967.

[86] Waldner M.H. and Vogel F., 2005, Renewable Production of Methane from Woody Biomass by Catalytic Hydrothermal Gasification. *Ind. Eng. Chem. Res.* **44**, 4543-4551.

[87] Ondze F., Boutin O., Ruiz J.C., Ferrasse J.H. and Charton F., 2015, Supercritical water gasification of beet residues: From batch to continuous reactor. *Chemical Engineering Science* **123**, 350-358.

[88] Yu D., Aihara M. and Antal M.J., 1993, Hydrogen production by steam reforming glucose in supercritical water. *Energy Fuels* **7**, 574-577.

- [89] Bjerre A.B. and Soerensen E., 1992, Thermal decomposition of dilute aqueous formic acid solutions. *Ind. Eng. Chem. Res.* **31**, 1574-1577.
- [90] Yu J.L. and Savage P.E., 1998, Decomposition of formic acid under hydrothermal conditions. *Ind. Eng. Chem. Res.* **37**, 2-10.
- [91] Castello D., Kruse A. and Fiori L., 2013, Biomass gasification in supercritical and subcritical water: the effect of the reactor material. *Chem. Eng. J.* **228**, 535-544.
- [92] Richard T., Poirier J., Reverte C., Aymonier C., Loppinet-Serani A., Iskender G., Pablo E.B. and Marias F., 2012, Corrosion of ceramics for vinasse gasification in supercritical water. *J. Eur. Ceram. Soc.* **32**, 2219-2233.
- [93] Hosseini S.E., Abdul Wahid M., Jamil M.M., Azli A.A.M. and Misbah M.F., 2015, A review on biomass-based hydrogen production for renewable energy supply. *Int. J. Energy Res.* **39**, 1597-1615.
- [94] Wan W., 2016, An innovative system by integrating the gasification unit with the supercritical water unit to produce clean syngas for solid oxide fuel cell (SOFC): System performance assessment. *Int. J. Hydrogen Energy* **41**, 22695-22710.
- [95] Molino A., Giordano G., Migliori M., Lauro V., Santarcangelo G., Marino T., Larocca V. and Tarquini P., 2016, Process innovation via supercritical water gasification to improve the conventional plants performance in treating highly humid biomass. *Waste Biomass Valorization* **7**, 1289-1295.
- [96] Boukis N., Galla U., Müller H. and Dinjus E., 2008, Biomass gasification in supercritical water. Experimental progress achieved with the VERENA pilot plant. 15<sup>th</sup> European Conference & Exhibition, May 7, Berlin, Germany, pp. 1013-1016.
- [97] Kritzer P., Boukis N. and Dinjus E., 2000, Transpassive dissolution of alloy 625, chromium, nickel and molybdenum in high-temperature solutions containing hydrochloric acid and oxygen. *Corrosion* **56**, 265-272.
- [98] Kawasaki S.I., Oe T., Itoh S., Suzuki A., Sue K. and Arai K., 2007, Flow characteristics of aqueous salt solutions for applications in supercritical water oxidation. *The Journal of Supercritical Fluids* **42**, 241-254.
- [99] Kruse A., Forchheim D., Gloede M., Ottinger F. and Zimmermann J., 2010, Brines in supercritical biomass gasification: 1. Salt extraction by salts and the influence on glucose conversion. *The Journal of Supercritical Fluids* **53**, 64-71.

- [100] Simonetti M., 2016, Theoretical and experimental studies on Supercritical Water Gasification of biomass with technical assessment of a newly development system. Senior Thesis, Politecnico di Torino.
- [101] Lucca G., 2014, Supercritical water gasification of wet biomass: experiments conducted in stainless steel and Inconel (Nickel-Chromium-Molybdenum Catalyst) reactors in a laboratory scale experimental setup. Senior Thesis, Politecnico di Torino.
- [102] Magnano A., 2015, Supercritical Water Gasification (SCWG) of Black Liquor: Thermodynamic Analysis and Experimental Tests in a Plug Flow Reactor. Senior Thesis, Politecnico di Torino.
- [103] Saqlain M., 2015, Process modeling of Supercritical Water Gasification equipment based on pure water for design of continuous feeding system. Senior Thesis, Aalto University School of Chemical Technology.
- [104] De Blasio C., Lucca G., Özdenkci K., Mulas M., Lundqvist K., Koskinen J., Santarelli M., Westerlund T. and Järvinen M., A study on supercritical water gasification of black liquor conducted in stainless steel and nickel-chromium-molybdenum reactors. *J. Chem. Technol. Biotechnol.* **91**, 2664-2678.
- [105] Johnson D.T. and Taconi K.A., 2007, The glycerine glut: options for the value-added conversion of crude glycerol resulting from biodiesel production. *Environmental Progress and Sustainable Energy* **26**, 338-48.
- [106] Kong P.S., Aroua M.K. and Daud W.M.A.W., 2016, Conversion of crude and pure glycerol into derivatives: A feasibility evaluation. *Renewable and Sustainable Energy Reviews* **63**, 533-555.
- [107] Physical properties of glycerine and its solution, (Glycerine Producers' Association, Ed.), New York, 1963.
- [108] Tan H.W., Abdul Aziz A.R. and Aroua M.K., 2013, Glycerol production and its applications as a raw material: A review. *Renewable and Sustainable Energy Reviews* **27**, 118-127.
- [109] Pagliaro M. and Rossi M., 2010, The future of glycerol: Edition 2, (Royal Society of Chemistry, Ed.), London.
- [110] Speight J.R., 2002, Chemical process and design handbook, (McGraw-Hill Professional, Ed.), United States.

- [111] Glycerine: an overview. The soap and detergent association, 1990.
- [112] Grandori R., Matecko I., Mayr P. and Müller N., 2001, Probing protein stabilization by glycerol using electrospray mass spectrometry. *J. Mass Spectrom.* **36**, 918.
- [113] Pagliaro M. and Rossi M., 2008, Glycerol: Properties and Production, in “*The Future of Glycerol: New uses of a Versatile Raw Material*”, (RSC Green Chemistry Mook Series, Ed.), Chap. 1.
- [114] Ueoka H. and Katayama T., 2001, Process for preparing glycerol, United States Patent 6288287.
- [115] Wang Y., Wang X., Liu Y., Ou S., Tan Y. and Tang S., 2009, Refining of biodiesel by ceramic membrane separation. *Fuel Processing Technology* **90**, 422-7.
- [116] Bagnato G., Iulianelli A., Sanna A. and Basile A., 2017, Glycerol Production and Transformation: A Critical Review with Particular Emphasis on Glycerol Reforming Reaction for Producing Hydrogen in Conventional and Membrane Reactors. *Membranes* **7**, **17**, 1-31.
- [117] Bonato J.A., headridge J.B. and Morrison R.J., 1987, Chemistry serves the South Pacific. USP Library Cataloguing in Publication Data.
- [118] Bernardini C.M., Process technology for Oleo Chemistry. Spec Engineers & Consultants Pvt. Ltd.
- [119] Stamatelatou K., 2011, Advanced oil crop biorefineries, (RSC Publishing, Ed.), Cambridge.
- [120] Miserlis C.D. and Mukaddam W.A., 1991, Refining if natural glycerine derived from palm kernel or palm oil for a new high-grade product, in “*Proceedings of the World conference on oleochemicals: into 21<sup>st</sup> century*”, pp. 305-10.
- [121] Yong K.C., Ooi T.L., Dzulkefly K., Wan Yunus W.M.Z. and Hazimah A.H., 2001, Refining of crude glycerol recovered from glycerol residue by simple vacuum distillation. *Journal of Oil Palm Research* **19**, 39-44.

- [122] Ampaitepin S. and Tetsuo T.A., 2010, A perspective on incorporation of glycerine purification process in biodiesel plants using waste cooking oil as feedstock. *Energy* **35**, 2493-504.
- [123] Donkin Shawn S., 2008, Glycerol from biodiesel production: the new corn for diary cattle. *Revista Brasileira de Zootecnia* **37**, 280-6.
- [124] Brandner A., Lehnert K., Bienhonz A., Lucas M. and Claus P., 2009, Production of biomass-derived chemicals and energy: chemocatalytic conversion of glycerol. *Topics in Catalysis* **52**, 278-87.
- [125] Watanabe M., Iida T., Aizawa T.M. and Inomata H., 2007, Acrolein synthesis from glycerol in hot-compressed water. *Biosource Technology* **98**, 1285-90.
- [126] van Bennekom J.G., Venderborsch R.H., Assink D. and Heeres H.J., 2011, Reforming of methanol and glycerol in supercritical water. *The Journal of Supercritical Fluids* **58**, 99-113.
- [127] Adhikari S., Fernando S.D. and Haryanto A., 2008, Hydrogen production from glycerin by steam reforming over nickel catalysts. *Renew Energy* **33**, 1097-100.
- [128] Painter R.M., Pearson D.M. and Waymouth R.M., 2010, Selective catalytic oxidation of glycerol to dihydroxyacetone. *Angew. Chem. Int. Ed.* **49**, 9456-9.
- [129] Barbelli M.L., Santori G.F. and Nichio N.N., 2012, Aqueous phase hydrogenolysis of glycerol to bio-propylene over Pt-Sn catalysts. *Bioresour. Technol.* **111**, 500-3.
- [130] Kwon Y., Birdja Y., Spanos I., Rodriguez P. and Koper M.T.M., 2012, Highly selective electro-oxidation of glycerol to dihydroxyacetone on platinum in the presence of bismuth. *ACS Catal.* **2**, 759-64.
- [131] González M.D., Cesteros Y., Llorca J. And Salagre P., 2012, Boosted selectivity toward high glycerol tertiary butyl ethers by microwave-assisted sulfonic acid-functionalization of SBA-15 and beta-zeolite. *J. Catal.* **290**, 202-9.
- [132] Kong P.S., Aroua M.K. and Ashri W.D.W.M., 2015, Catalytic esterification of bioglycerol to value-added products. *Rev. Chem. Eng.* **31**, 437.
- [133] Rahmat N., Abdullah A.Z. and Mohamed A.R., 2010, Recent progress on innovative and potential technologies for glycerol transformation into fuel additives: a critical review. *Renew. Sustain. Energy. Rev.* **14**, 987-1000.

[134] Solvay. Applications of epichlorohydrin. Belgium, 2002.

[135] Bell B., Briggs J.R., Campbell R., Chambers S.M., Gaarenstroom P.D., Hippler J.G. et al., 2008, Glycerine as a renewable feedstock for epichlorohydrin production. *GTE Process Clean: Soil, Air, Water* **36**, 657-61.

[136] BASF.1,3-Dioxolaner, 2015, available at <http://www.intermediates.basf.com/chemicals/web/en/content/products-and-industries/performance-materials/high-performance-solvents/dioxolane>

[137] Dianningrum L.W., Choi H., Kim Y., Jung K.D., Susanti R., Kim J. and Sang B.I., 2014, Hydrothermal gasification of pure and crude glycerol in supercritical water: A comparative study, *Internation Journal of Hydrogen Energy* **39**, 1262-1273.

[138] Barrentine L.B., 1999, An introduction to Design of Experiments: A simplified Approach, (ASQ Quality Press, Ed.).